USDA
United States Department of Agriculture

Forest Health Monitoring: National Status, Trends, and Analysis 2019

Editors Kevin M. Potter Barbara L. Conkling

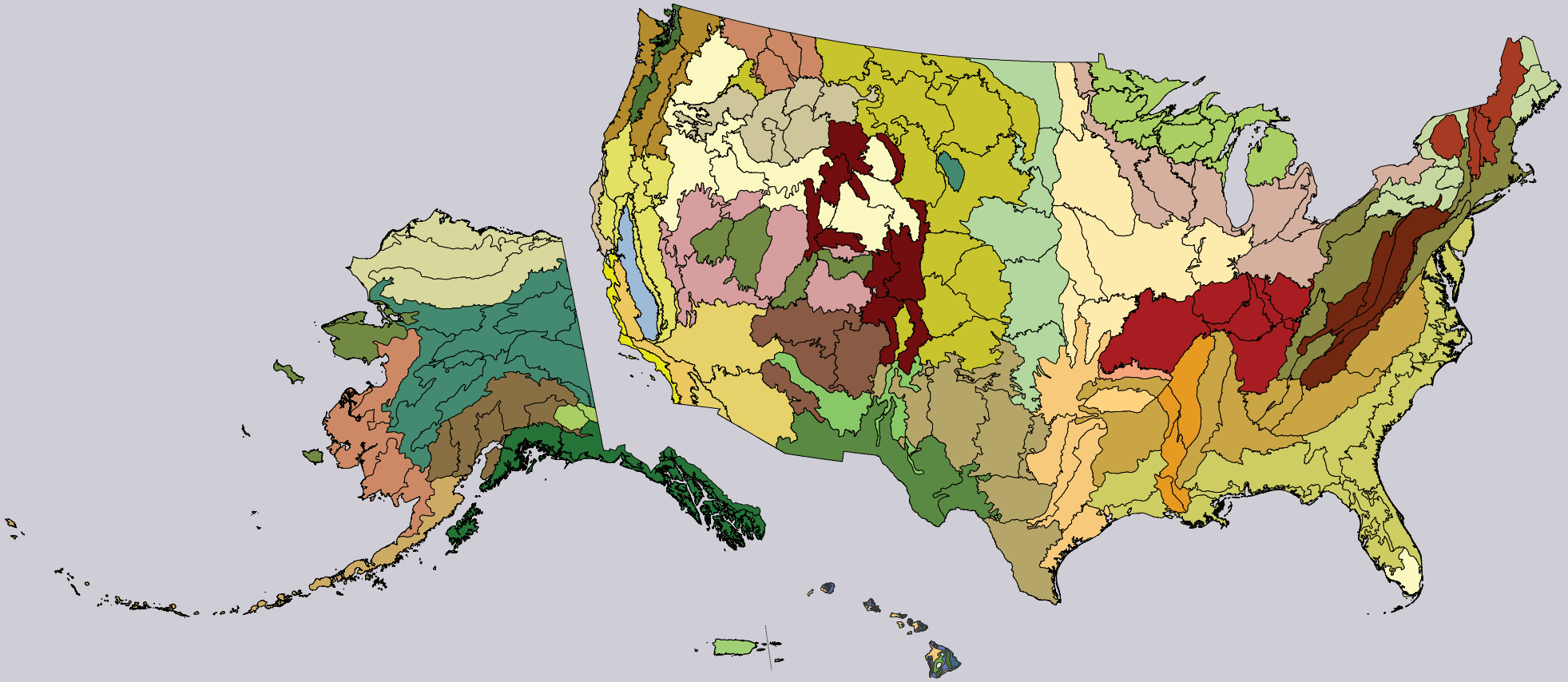

Forest Service
Research & Development
Southern Research Station
General Technical Report SRS-250
June 2020

Front cover map:
Ecoregion provinces and ecoregion sections for the conterminous United States (Cleland and others 2007) and for Alaska (Spencer and others 2002), and ecoregions within the islands of Hawaii, along with Puerto Rico and the U.S. Virgin Islands, for which no corresponding ecoregion treatments exist.

Back cover maps:
Tree canopy cover (green) for the conterminous 48 States, Hawaii, Puerto Rico, and the U.S. Virgin Islands based on data from a cooperative project between the Multi-Resolution Land Characteristics Consortium and the U.S. Department of Agriculture Forest Service, Geospatial Technology and Applications Center (GTAC) using the 2011 National Land Cover Database. Forest and shrubland cover for Alaska derived from the 2011 National Land Cover Database.

June 2020

Southern Research Station
200 W.T. Weaver Blvd.
Asheville, NC 28804

www.srs.fs.usda.gov

Forest Health Monitoring:

National Status, Trends, and Analysis 2019

Editors

Kevin M. Potter, Research Professor, North Carolina State University, Department of Forestry and Environmental Resources, Raleigh, NC 27695

Barbara L. Conkling, Research Assistant Professor, North Carolina State University, Department of Forestry and Environmental Resources, Raleigh, NC 27695

ABSTRACT

The annual national report of the Forest Health Monitoring (FHM) program of the Forest Service, U.S. Department of Agriculture, presents forest health status and trends from a national or multi-State regional perspective using a variety of sources, introduces new techniques for analyzing forest health data, and summarizes results of recently completed Evaluation Monitoring projects funded through the FHM national program. In this 19th edition in a series of annual reports, national survey data are used to identify recent geographic patterns of insect and disease activity. Satellite data are employed to detect geographic patterns of forest fire occurrence. Recent drought and moisture surplus conditions are compared across the conterminous United States. Data collected by the Forest Inventory and Analysis (FIA) program are employed to detect regional differences in tree mortality. Twenty years of national Insect and Disease Survey data are used to provide a retrospective medium-term analysis of insect and disease damage to forests across the United States. A new measure is described for detecting forest disturbance using high-frequency satellite data. Two recently completed Evaluation Monitoring projects are summarized, addressing forest health concerns at smaller scales.

Keywords—Change detection, drought, fire, forest health, forest insects and disease, tree canopy, tree mortality.

CONTENTS

SECTION 3.

CHAPTER 8.

CHAPTER 9.

LIST OF FIGURES

Figures, cont.

LIST OF TABLES

Tables, cont.

EXECUTIVE SUMMARY

Healthy ecosystems are those that are stable and sustainable, able to maintain their organization and autonomy over time while remaining resilient to stress (Costanza 1992). Healthy forests are vital to our future (Edmonds and others 2011), and consistent, large-scale, and long-term monitoring of key indicators of forest health status, change, and trends is necessary to identify forest resources deteriorating across large regions (Riitters and Tkacz 2004). The Forest Health Monitoring (FHM) program of the Forest Service, U.S. Department of Agriculture, with cooperating researchers within and outside the Forest Service and with State partners, quantifies status and trends in the health of U.S. forests (ch. 1). The analyses and results outlined in sections 1 and 2 of this FHM annual national report offer a snapshot of the current condition of U.S. forests from a national or multi-State regional perspective, incorporating baseline investigations of forest ecosystem health, examinations of change over time in forest health metrics, and assessments of developing threats to forest stability and sustainability. For datasets collected on an annual basis, analyses are presented from 2018 data. For datasets collected over several years, analyses are presented at a longer temporal scale. Finally, section 3 of this report presents summaries of results from recently completed Evaluation Monitoring (EM) projects that have been funded through the FHM national program to determine the extent, severity, and/or causes of specific forest health problems (FHM 2018).

Monitoring the occurrence of forest pest and pathogen outbreaks is important at regional scales because of the significant impact insects and disease can have on forest health across landscapes (ch. 2). National Insect and Disease Survey data collected in 2018 by the Forest Health Protection program of the Forest Service and partners in State agencies identified 56 different mortality-causing agents and complexes on 2.13 million ha and 56 defoliating agents and complexes on approximately 1.72 million ha in the conterminous United States. In the Western States, bark beetles (especially fir engraver, spruce beetle, mountain pine beetle, and western pine beetle) were the primary cause of geographic hot spots of forest mortality. In the Eastern States, emerald ash borer infestation resulted in several geographic hot spots of mortality. Hot spots of defoliation were associated with western spruce budworm, Swiss needle cast, pandora moth, and Douglas-fir tussock moth in the West, and with baldcypress leafroller, forest tent caterpillar, gypsy moth, spruce budworm, and browntail moth in the East. In Alaska, spruce beetle was by far the most widely detected mortality agent, and aspen leafminer and birch leafminer were the most commonly found defoliators. In Hawaii, surveyors identified approximately 46 000 ha of mortality, much of which may have been caused by rapid ʻōhiʻa death.

Forest fire occurrence outside the historic range of frequency and intensity can result in extensive economic and ecological impacts. The

detection of regional patterns of fire occurrence density can allow for the identification of areas at greatest risk of significant impact and for the selection of locations for more intensive analysis (ch. 3). In 2018, the number of satellite-detected forest fire occurrences recorded for the conterminous States was very close to the average for the previous 17 years of data collection. Ecoregion sections in northwestern California/southwestern Oregon, northeastern Nevada, and north-central Washington had the highest forest fire occurrence density per 100 km^2 of forested area. Geographic hot spots of high fire occurrence density were detected in these same areas, as well as in the Sierra Nevada and north-central Utah. Ecoregion sections in northwestern California/southwestern Oregon, western Wyoming, northern and eastern Utah, northwestern and south-central Colorado, northeastern New Mexico, and southern Florida experienced greater fire occurrence density than normal compared to the previous 17-year mean and accounting for variability over time. Alaska experienced low fire occurrence densities across the State. The eastern edge of the Big Island of Hawai'i had a relatively high fire occurrence density because of a dramatic volcanic eruption. Fire occurrence density in Puerto Rico was slightly less than in the 17 preceding years.

Most U.S. forests experience droughts, with varying degrees of intensity and duration between and within forest ecosystems. Arguably, the duration of a drought event is more critical than its intensity. A standardized drought and moisture surplus indexing approach was applied to monthly climate data from 2018 and prior years to map drought conditions and surplus moisture availability across the conterminous United States at a fine scale (ch. 4). From the Rocky Mountains westward, a majority of forested areas experienced at least mild drought in 2018, but contiguous areas of severe to extreme drought were limited in number and geographic extent. Meanwhile, 2018 drought conditions in the Eastern United States were largely confined to northern New England and southern Florida. Analyses of longer term (3-year and 5-year) conditions underscore dramatic differences between the East and the West, showing almost no areas of severe to extreme moisture surplus west of the Rocky Mountains but a nearly continuous swath of severe to extreme moisture surplus across much of the East. Nearly all forested areas in the Western United States have experienced moderate or worse drought conditions that have persisted over multiple consecutive years, which has undeniable implications for long-term forest health.

Mortality is a natural process in all forested ecosystems, but high levels of mortality at large scales may indicate that the health of forests is declining. Phase 2 data collected by the Forest Inventory and Analysis (FIA) program of the Forest Service offer tree mortality information on a relatively spatially intense basis of approximately one plot per 6,000 acres (ch. 5). An analysis of FIA plots from all the Central and Eastern States found that, in most areas, tree mortality is low relative to tree growth,

while the areas of highest mortality occurred on the margins of land suitable for forest growth, particularly in the Great Plains region, as a result of drought combined with a variety of other stressors. Additionally, two ecoregion sections in Indiana, Ohio, and Michigan had extremely high mortality as a result of emerald ash borer. Preliminary analyses of FIA data from the Western States show that mortality is very high as a percent of standing live tree volume in northern and central parts of the Interior West, and that several West Coast ecoregion sections have high mortality levels relative to growth. These are all areas that have experienced insect outbreaks, fire, and/or severe drought. These three mortality-causing agents are related in that drought stresses trees, making them more susceptible to insect attack, while both drought and insect-killed trees create conditions favorable for wildfires.

Although the annual FHM reports address annual spatial extent and patterns of insect and disease detections, there has been no comprehensive long-term analysis of Insect and Disease Survey (IDS) data in the FHM reports. To examine medium-term trends in insect and disease damage to the forests of the United States, we organized and analyzed 20 years of IDS data, then produced an assessment of trends in forest area exposed to insects and disease in multiple timeframes and within four Resources Planning Act (RPA) Assessment regions (ch. 6). We found that the tree canopy area affected by mortality agents has been consistently large across the three most recent 5-year assessment periods, with regional differences in temporal patterns of area exposed to mortality. Insects have been much more widespread agents of mortality than diseases, with bark beetles consistently the most important mortality agents across regions and over time, especially in the West. Nationally, the tree canopy area affected by nonnative invasive agents of mortality and defoliation has remained relatively consistent over time, though these agents have had a larger relative impact on forests in the North. Tree canopy area affected by defoliation agents has remained relatively consistent over time and has usually exceeded or equaled the area affected by mortality agents. Evaluating trends in these threats at a national scale provides context to managers attempting to understand the implications and scope of current forest health threats.

The role of remote sensing in forest monitoring is evolving, with satellite imagery now systematically used to recognize and track forest disturbances in near-real time (ch. 7). High-frequency monitoring is important as much observed forest change is ephemeral, lasting less than a season. Meanwhile, more consequential impacts to forest structure can be hard to recognize or track except immediately after a disturbance event occurs or during select seasons. A new measure of forest disturbance combines two aspects of vegetation phenology change, its magnitude and duration, to isolate locations with substantive and sustained disturbance impacts across the conterminous United States. This approach was

used to generate three seamless maps of the conterminous United States that show where substantive and sustained summer disturbance occurred during 2016, 2017, and 2018. These maps reveal summer patterns of stress and decline from all causes that had a substantive and sustained impact on forest canopies. This change includes mid- to large-sized patchy tree mortality, defoliation, and decline caused by logging, development, mining, insects and disease, fire, wind, hail, and drought somewhat indiscriminately, though not inclusively, as the resolution of the data (Moderate Resolution Imaging Spectroradiometer [MODIS] Normalized Difference Vegetation Index [NDVI]) is ill-suited for resolving low-density declines in mixed stands.

Finally, two recently completed Evaluation Monitoring (EM) projects address a wide variety of forest health concerns at a scale smaller than the national or multi-State regional analyses included in the first sections of the report. These EM projects (funded by the FHM program):

- Monitored the health of black walnut (*Juglans nigra*) trees in Ohio and Indiana with symptoms of thousand cankers disease and assessed the roles of *Geosmithia morbida*, the causal agent of the disease, and other fungal pathogens in affecting walnut tree health (ch. 8)
- Characterized woodborer activity in 16 sites in the Sierra Nevada region encompassing 11 burned sites and five sites that experienced bark beetle outbreaks, with a goal of informing forest management strategies designed to maintain processes dependent on woodborers (ch. 9)

The FHM program, in cooperation with forest health specialists and researchers inside and outside the Forest Service, continues to investigate a broad range of issues relating to forest health using a wide variety of data and techniques. This report presents some of the latest results from ongoing national-scale detection monitoring and smaller scale environmental monitoring efforts by FHM and its cooperators. For more information about efforts to determine the status, changes, and trends in indicators of the condition of U.S. forests, please visit the FHM website at https://www.fs.fed.us/foresthealth/protecting-forest/forest-health-monitoring.

LITERATURE CITED

Costanza, R. 1992. Toward an operational definition of ecosystem health. In: Costanza, R.; Norton, B.G.; Haskell, B.D., eds. Ecosystem health: new goals for environmental management. Washington, DC: Island Press: 239–256.

Edmonds, R.L.; Agee, J.K.; Gara, R.I. 2011. Forest health and protection. Long Grove, IL: Waveland Press, Inc. 667 p.

Forest Health Monitoring (FHM). 2018. Program description. Forest Health Monitoring fact sheet series. https://www.fhm.fs.fed.us/fact/. [Date accessed: September 20, 2018].

Riitters, K.H.; Tkacz, B. 2004. The U.S. Forest Health Monitoring program. In: Wiersma, G.B., ed. Environmental monitoring. Boca Raton, FL: CRC Press: 669–683.

CHAPTER 1.
Introduction

Kevin M. Potter

Forests cover a vast area of the United States, 304 million ha or approximately one-third of the Nation's land area (Smith and others 2009). These forests possess the capacity to provide a broad range of goods and services to current and future generations, to safeguard biological diversity, and to contribute to the resilience of ecosystems, societies, and economies (USDA Forest Service 2011). Their ecological roles include supplying large and consistent quantities of clean water, preventing soil erosion, and providing habitat for a broad diversity of plant and animal species. Their socioeconomic benefits include wood products, nontimber goods, recreational opportunities, and pleasing natural beauty. Both the ecological integrity and the continued capacity of these forests to provide ecological and economic goods and services are of concern, however, in the face of a long list of threats, including insect and disease infestation, fragmentation and forest conversion to other land uses, catastrophic fire, invasive species, and the effects of climate change.

Natural and anthropogenic stresses vary among biophysical regions and local environments; they also change over time and interact with each other. These and other factors make it challenging to establish baselines of forest health and to detect important departures from normal forest ecosystem functioning (Riitters and Tkacz 2004). Monitoring the health of forests is a critically important task, however, reflected within the Criteria and Indicators for the Conservation and Sustainable Management of Temperate and Boreal Forests (Montréal Process Working Group 1995), which the Forest Service, U.S. Department of Agriculture (USDA), uses as a forest sustainability assessment framework (USDA Forest Service 2004, 2011). The primary objective of such monitoring is to identify ecological resources whose condition is deteriorating in subtle ways over large regions in response to cumulative stresses, a goal that requires consistent, large-scale, and long-term monitoring of key indicators of forest health status, change, and trends (Riitters and Tkacz 2004). This is best accomplished through the participation of multiple Federal, State, academic, and private partners.

Although the concept of a healthy forest has universal appeal, forest ecologists and managers have struggled with how exactly to define forest health (Teale and Castello 2011), and there is no universally accepted definition. Most definitions of forest health can be categorized as representing an ecological or an utilitarian perspective (Kolb and others 1994). From an ecological perspective, the current understanding of ecosystem dynamics suggests that healthy ecosystems are those that are able to maintain their organization and autonomy over time while remaining resilient to stress (Costanza 1992), and that evaluations of forest health should emphasize factors that affect the inherent processes and resilience of forests (Edmonds and others 2011, Kolb and others 1994, Raffa and others 2009). On the other hand, the utilitarian perspective holds that a forest is healthy if management objectives are met, and that a forest is unhealthy if these objectives are not met (Kolb and others 1994). Although this definition

may be appropriate when a single, unambiguous management objective exists, such as the production of wood fiber or the maintenance of wilderness attributes, it is too narrow when multiple management objectives are required (Edmonds and others 2011, Teale and Castello 2011). Teale and Castello (2011) incorporate both ecological and utilitarian perspectives into their two-component definition of forest health: first, a healthy forest must be sustainable with respect to its size structure, including a correspondence between baseline and observed mortality; second, a healthy forest must meet the landowner's objectives, provided that these objectives do not conflict with sustainability.

This national report, the 19th in an annual series sponsored by the Forest Health Monitoring (FHM) program of the Forest Service, attempts to quantify the status of, changes to, and trends in a wide variety of broadly defined indicators of forest health. The indicators described in this report encompass forest insect and disease activity, wildland fire occurrence, drought, tree mortality, and vegetation phenology change, among others. The previous reports in this series are Ambrose and Conkling (2007, 2009), Conkling (2011), Conkling and others (2005), Coulston and others (2005a, 2005b, 2005c), and Potter and Conkling (2012a, 2012b, 2013a, 2013b, 2014, 2015a, 2015b, 2016, 2017, 2018, 2019). Visit https://www.fs.fed.us/foresthealth/publications/fhm/fhm-annual-national-reports.shtml for links to each of these reports in their entirety and for searchable lists of links to chapters included in the reports.

This report has three specific objectives. The first is to present information about forest health from a national perspective, or from a multi-State regional perspective when appropriate, using data collected by the Forest Health Protection (FHP) and Forest Inventory and Analysis (FIA) programs of the Forest Service, as well as from other sources available at a wide extent. The chapters that present analyses at a national scale, or multi-State regional scale, are divided between section 1 and section 2 of the report. Section 1 presents results from the analyses of forest health data that are available on an annual basis. Such repeated analyses of regularly collected indicator measurements allow for the detection of trends over time and help establish a baseline for future comparisons (Riitters and Tkacz 2004). Section 2 presents longer term forest health trends, in addition to describing new techniques for analyzing forest health data at national or regional scales (the second objective of the report). While in-depth interpretation and analysis of specific geographic or ecological regions are beyond the scope of these parts of the report, the chapters in sections 1 and 2 present information that can be used to identify areas that may require investigation at a finer scale.

The second objective of the report is to present new techniques for analyzing forest health data as well as new applications of established techniques, often applied to longer timescales, presented in selected chapters of section 2. Examples in this report are chapters 6 and 7. Chapter 6 presents the results of analyses

of 20 years of national Insect and Disease Survey data providing a retrospective long-term analysis of insect and disease damage to forests across the United States. Chapter 7, meanwhile, describes a new measure of forest disturbance that combines the magnitude and duration of satellite-detected vegetation phenology change to isolate locations with substantive and sustained disturbance impacts across the conterminous United States.

The third objective of the report is to present results of recently completed Evaluation Monitoring (EM) projects funded through the FHM national program. These project summaries, presented in section 3, determine the extent, severity, and/or cause of forest health problems (FHM 2019), generally at a finer scale than that addressed by the analyses in sections 1 and 2. Each of the two chapters in section 3 contains an overview of an EM project, key results, and contacts for more information.

When appropriate throughout this report, authors use the Forest Service revised ecoregions for the conterminous United States and Alaska (Cleland and others 2007, Spencer and others 2002) as a common ecologically based spatial framework for their forest health assessments (fig. 1.1). Specifically, when the spatial scale of the data and the expectation of an identifiable pattern in the data are appropriate, authors use ecoregion sections or provinces as assessment units for their analyses. Bailey's hierarchical system bases the two broadest ecoregion scales, domains and divisions, on large ecological climate zones, while each division is broken into provinces based on vegetation macro features (Bailey 1995). Provinces are further divided into sections, which may be thousands of km^2 in area and are expected to encompass regions similar in their geology, climate, soils, potential natural vegetation, and potential natural communities (Cleland and others 1997). This hierarchical system does not address either Hawaii or Puerto Rico beyond including each in a unique, single ecoregion province (Bailey 1995). Previous FHM reports have summarized forest health indicators at the island level in these jurisdictions, and/or by county council district for the Big Island of Hawai'i. A set of Hawaii ecoregions based on moisture and elevational characteristics was developed for use in this and future FHM national reports because a finer scale and ecologically oriented spatial assessment framework was needed to estimate the impacts of a destructive forest disease (ch. 2) and of forest fires associated with volcanic eruptions (ch. 3) (fig. 1.2, box 1.1).

(A)

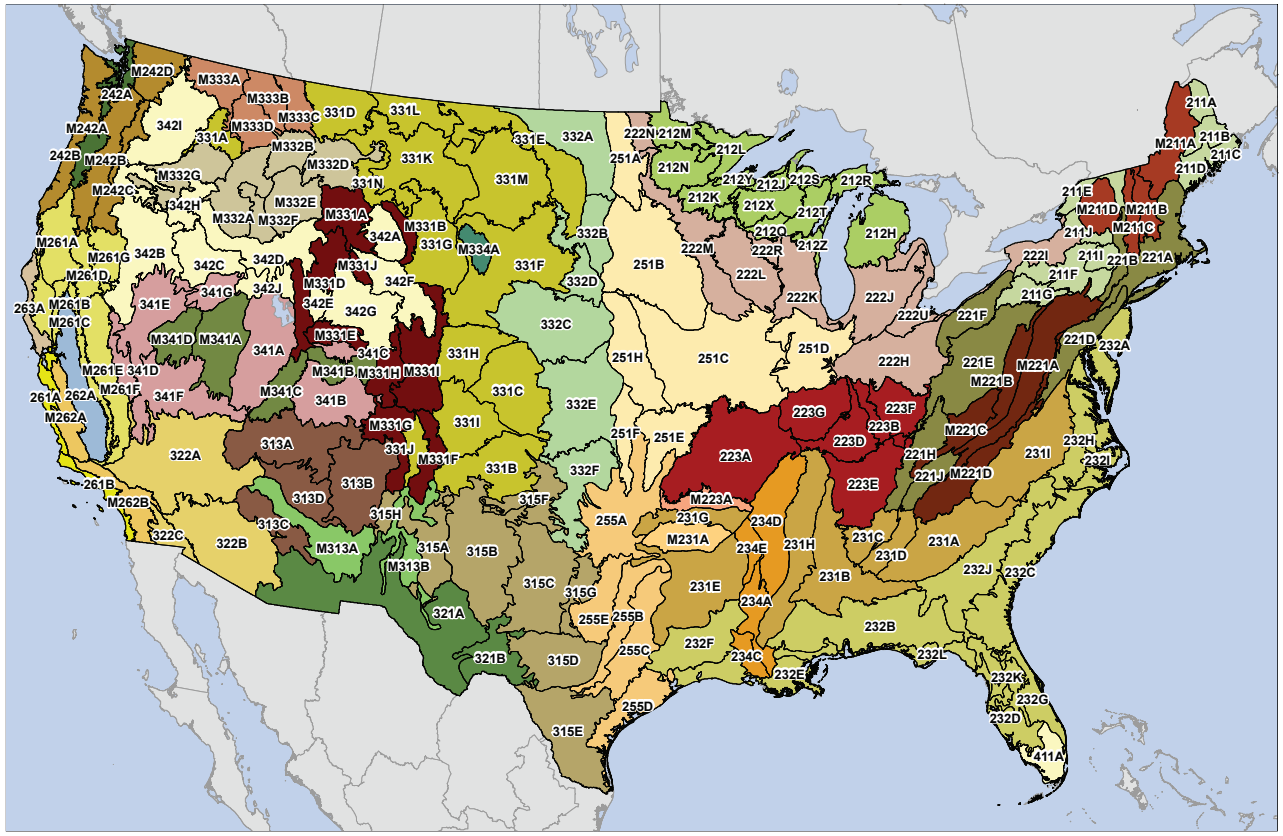

(B)

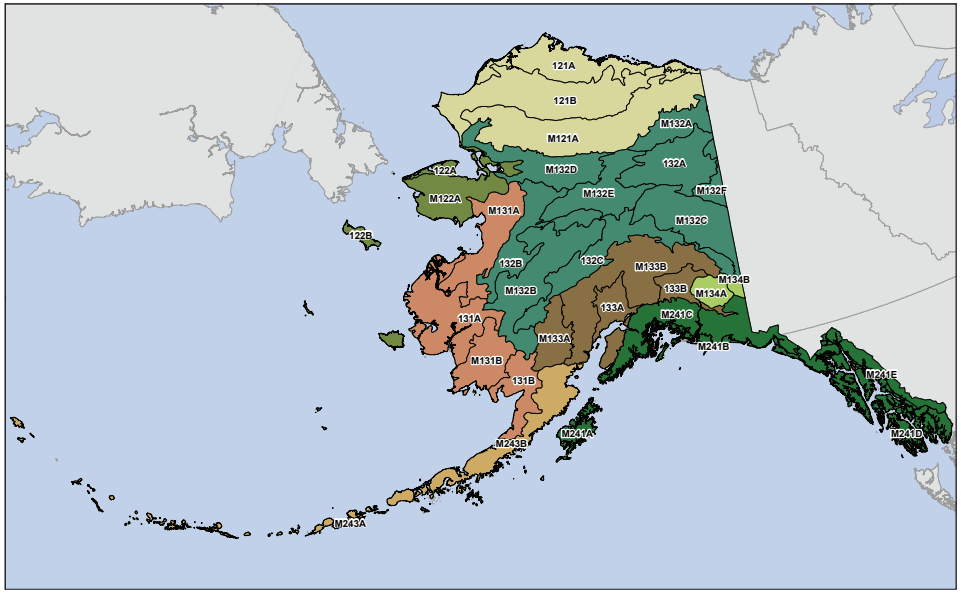

Figure 1.1—Ecoregion provinces and sections for (A) the conterminous United States (Cleland and others 2007) and (B) Alaska (Spencer and others 2002). Ecoregion sections within each ecoregion province are shown in the same color.

Conterminous States ecoregion provinces

- 211: Northeastern Mixed Forest
- M211: Adirondack-New England Mixed Forest—Coniferous Forest—Alpine Meadow
- 212: Laurentian Mixed Forest
- 221: Eastern Broadleaf Forest
- M221: Central Appalachian Broadleaf Forest—Coniferous Forest—Meadow
- 222: Midwest Broadleaf Forest
- 223: Central Interior Broadleaf Forest
- M223: Ozark Broadleaf Forest
- 231: Southeastern Mixed Forest
- M231: Ouachita Mixed Forest—Meadow
- 232: Outer Coastal Plain Mixed Forest
- 234: Lower Mississippi Riverine Forest
- 242: Pacific Lowland Mixed Forest
- 251: Prairie Parkland (Temperate)
- 255: Prairie Parkland (Subtropical)
- M242: Cascade Mixed Forest—Coniferous Forest—Alpine Meadow
- 261: California Coastal Chaparral Forest and Shrub
- M261: Sierran Steppe—Mixed Forest—Coniferous Forest—Alpine Meadow
- 262: California Dry Steppe
- M262: California Coastal Range Open Woodland—Shrub—Coniferous Forest—Meadow
- 263: California Coastal Steppe—Mixed Forest—Redwood Forest
- 313: Colorado Plateau Semi-Desert
- M313: Arizona-New Mexico Mountains Semi-Desert—Open Woodland—Coniferous Forest—Alpine Meadow
- 315: Southwest Plateau and Plains Dry Steppe and Shrub
- 321: Chihuahuan Semi-Desert
- 322: American Semi-Desert and Desert
- 331: Great Plains—Palouse Dry Steppe
- M331: Southern Rocky Mountain Steppe—Open Woodland—Coniferous Forest—Alpine Meadow
- 332: Great Plains Steppe
- M332: Middle Rocky Mountain Steppe—Coniferous Forest—Alpine Meadow
- M333: Northern Rocky Mountain Forest-Steppe—Coniferous Forest—Alpine Meadow
- M334: Black Hills Coniferous Forest
- 341: Intermountain Semi-Desert and Desert
- M341: Nevada-Utah Mountains Semi-Desert—Coniferous Forest—Alpine Meadow
- 342: Intermountain Semi-Desert
- 411: Everglades

Alaska ecoregion provinces

- 121: Arctic Tundra
- M122: Bering Tundra
- M131: Bering Taiga
- M132: Intermontane Boreal
- 133: Alaska Range Transition
- M134: Coastal Mountains Transition
- M241: Coastal Rainforest
- M243: Aleutian Meadows

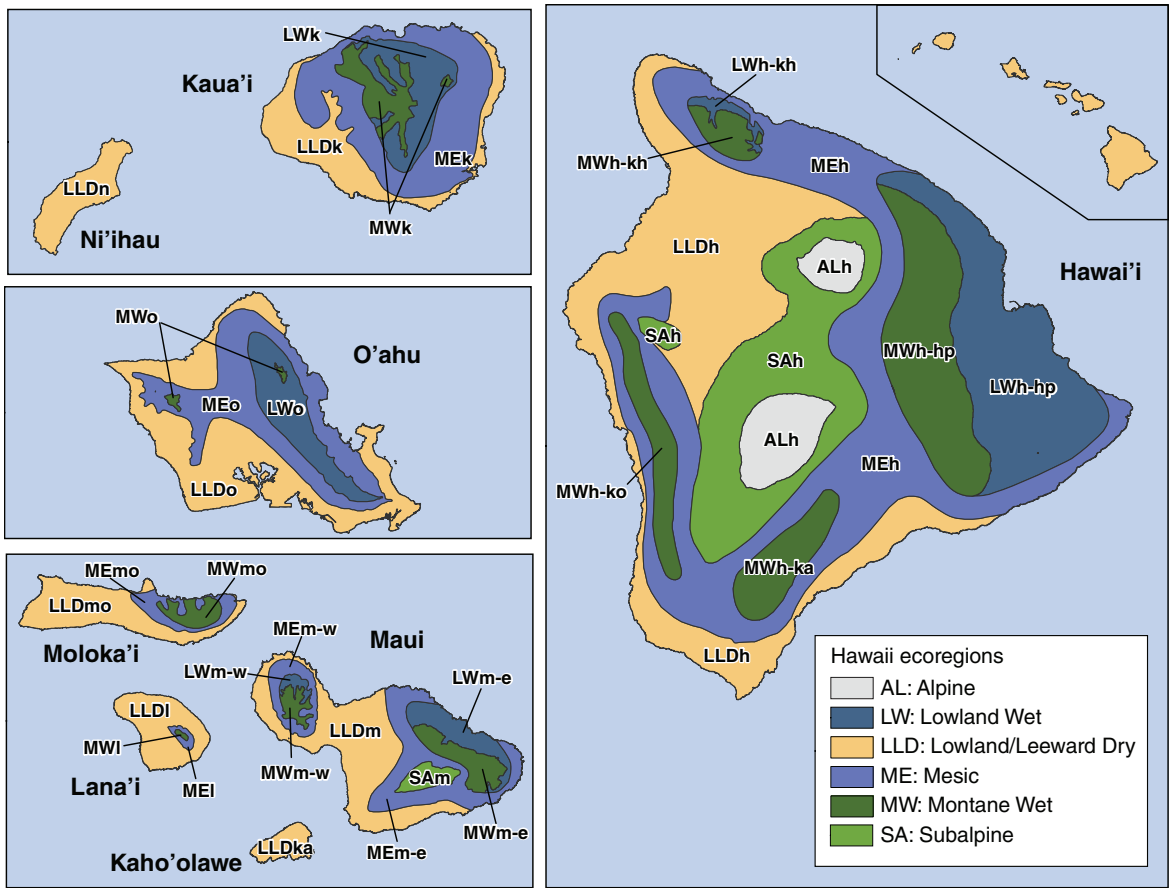

Figure 1.2—Ecoregions, and within-island ecoregion units, for Hawaii, developed based on moisture zones and elevation (see box 1.1). Within-island ecoregion units are shown in the same color by ecoregion. See the table in box 1.1 for the names of the within-island ecoregion units listed on the map.

Box 1.1

The Hawaiian archipelago encompasses a great deal of variation in several ecological factors, including climate, elevation, and natural communities, and possesses a unique flora with some of the highest levels of endemism in the world (Ziegler 2002). Monitoring assessments that aggregate and summarize data to islands within the archipelago, as done in previous Forest Health Monitoring (FHM) national reports, are not accounting for ecological variation within the islands that could affect the spatial occurrence of forest health indicators. A delineation of ecoregions within the State of Hawaii was therefore an important improvement for the FHM national reports. This delineation, described here, is based on the two environmental factors most important for grouping major natural native vegetation zones in Hawaii: moisture regime and elevation (Cuddihy 1989).

The moisture regime data are from Price and others (2007), which encompass seven moisture zones determined based on a moisture availability index (MAI), calculated as the difference between median annual precipitation (MAP) and potential evapotranspiration (PET). The moisture zones range from arid to very wet. For the delineation of Hawaii ecoregions, the seven moisture zones were combined into three: dry (Arid, Very Dry, and Moderately Dry), mesic (Seasonal Mesic and Moist Mesic), and wet (Moderately Wet and Very Wet). Dry areas are those where PET exceeds MAP (MAI <0), and the breakpoint between mesic and wet is MAI = 1661 mm (Price and others 2007).

The elevational data are polygons of 500-foot range contours for the islands of Hawai‘i, Kaua‘i, Maui, Moloka‘i, and O‘ahu, and 100-foot contours for Lāna‘i and Kaho‘olawe, derived from U.S. Geological Survey digital elevation models (State of Hawaii, Office of Planning 2019). For the delineation of Hawaiian ecoregions, four elevation zones were created: lowland (0–2,500 feet), montane (2,501–6,000 feet), subalpine (6,001–10,500 feet), and alpine (>10,500 feet). These elevational ranges correspond with broad vegetational zones (Cuddihy 1989). The original dataset did not include Ni‘ihau, but this arid island is relatively low-lying, so it was classified as lowland.

The moisture zones and elevational zones were intersected using ArcMap® (ESRI 2015). The resulting mesic lowland and mesic montane combinations were grouped into a single Mesic ecoregion, while the lowland dry and montane dry combinations were grouped into a single Lowland/Leeward Dry ecoregion. There were six final ecoregions: Lowland Wet (LW), Lowland/Leeward Dry (LLD), Mesic (ME), Montane Wet (MW), Subalpine (SA), and Alpine (AL) (fig. 1.2). The Alpine ecoregion encompasses the volcanic summits of Mauna Loa and Mauna Kea on the Big Island of Hawai‘i, while the Subalpine ecoregion occurs only on the Big Island and on Maui. The Lowland/Leeward Dry ecoregion is present on all eight major islands, while the Mesic and Montane Wet ecoregions are present on all but the two lowest-elevation islands (Kaho‘olawe and Ni‘ihau). The Lowland Wet ecoregion occurs on the four largest islands (Hawai‘i, Maui, O‘ahu, and Kaua‘i). The largest ecoregion is Lowland/Leeward Dry, which is about 551 000 ha in extent and has about 26.7 percent tree canopy cover (see table). The Montane Wet and Lowland Wet ecoregions have 94.8 percent and 93.9 percent tree canopy cover, respectively. The Mesic ecoregion has 60.9 percent canopy cover, while the percent of tree canopy cover in the Subalpine and Alpine ecoregions is extremely small to almost nonexistent.

continued to next page

Forest health monitoring efforts require assessing the status of forest resources within ecoregion units on individual islands, so the six broad ecoregions were intersected with the Hawaiian Islands in ArcMap® (ESRI 2015). Different shapefiles of the same ecoregion on each island were merged into single polygons, with a few exceptions. On the Big Island, there were four separate large Montane Wet ecoregion parts (Hilo-Puna [MWh-hp], Kaʻū [MWh-ka], Kohala-Hāmākua [MWh-kh], and Kona [MWh-ko]) and two large Lowland Wet parts (Hilo-Puna [LWh-hp] and Kohala-Hāmākua [LWh-kh]), each separated within their larger ecoregions by at least 10 km. These were kept as separate subunits because of the size of the island and the need to assess forest health indicators in different areas of the island. Maui similarly has two sets each of Mesic, Lowland Wet, and Montane wet ecoregion subunits, each at the western and eastern ends of the island. These too were kept and labeled accordingly. The result was a set of 34 ecoregion subunits (see table, fig. 1.2).

The six ecoregions and 34 ecoregion subunits for the State of Hawaii, including total area, area of forest canopy cover, and percent of total area with tree canopy cover

Ecoregion	Subunit	Area	Canopy area	Percent canopy
		ha	*ha*	
AL: Alpine	Alh: Alpine-Hawai'i	48 911.2	11.5	0.0
LW: Lowland Wet	LWh-hp: Lowland Wet-Hawai'i-Hilo-Puna	133 282.8	121 000.8	90.8
	LWh-kh: Lowland Wet-Hawai'i-Kohala-Hāmākua	5105.4	5063.8	99.2
	LWk: Lowland Wet-Kaua'i	27 192.0	27 166.6	99.9
	LWm-e: Lowland Wet-Maui-East	19 239.9	18 977.0	98.6
	LWm-w: Lowland Wet-Maui-West	3355.2	3343.7	99.7
	LWo: Lowland Wet-O'ahu	25 085.2	24 759.7	98.7
	All subunits	213 260.7	200 311.6	93.9
LLD: Lowland/Leeward Dry	LLDh: Lowland/Leeward Dry-Hawai'i	254 722.5	28 740.4	11.3
	LLDka: Lowland/Leeward Dry-Kaho'olawe	11 352.2	342.1	3.0
	LLDk: Lowland/Leeward Dry-Kaua'i	36 877.7	22 237.6	60.3
	LLDl: Lowland/Leeward Dry-Lāna'i	33 593.8	4963.7	14.8
	LLDm: Lowland/Leeward Dry-Maui	76 990.3	21 795.3	28.3

continued

(continued) The six ecoregions and 34 ecoregion subunits for the State of Hawaii, including total area, area of forest canopy cover, and percent of total area with tree canopy cover

Ecoregion	Subunit	Area	Canopy area	Percent canopy
		ha	*ha*	
	LLDmo: Lowland/Leeward Dry-Moloka'i	45 596.8	11 610.4	25.5
	LLDn: Lowland/Leeward Dry-Ni'ihau	18 719.3	14 058.5	75.1
	LLDo: Lowland/Leeward Dry-O'ahu	73 476.6	43 520.2	59.2
	All subunits	551 329.2	147 268.2	26.7
ME: Mesic	MEh: Mesic-Hawai'i	286 566.1	135 893.5	47.4
	MEk: Mesic-Kaua'i	64 682.6	56 249.4	87.0
	MEl: Mesic-Lāna'i	2117.0	1646.3	77.8
	MEm-e: Mesic-Maui-East	44 143.3	24 745.6	56.1
	MEm-w: Mesic-Maui-West	13 373.4	12 142.7	90.8
	MEmo: Mesic-Moloka'i	12 407.5	11 407.3	91.9
	MEo: Mesic-O'ahu	55 141.8	49 492.9	89.8
	All subunits	478 431.7	291 577.7	60.9
MW: Montane Wet	MWh-hp: Montane Wet-Hawai'i-Hilo-Puna	96 224.2	90 116.8	93.7
	MWh-ka: Montane Wet-Hawai'i-Ka'	30 543.8	28 738.9	94.1
	MWh-kh: Montane Wet-Hawai'i-Kohala-Hāmākua	11 971.9	11 527.8	96.3
	MWh-ko: Montane Wet-Hawai'i-Kona	29 949.6	27 133.7	90.6
	MWk: Montane Wet-Kaua'i	14 759.4	14 759.4	100.0
	MWl: Montane Wet-Lāna'i	490.6	462.4	94.3
	MWm-e: Montane Wet-Maui-East	16 953.8	16 940.7	99.9
	MWm-w: Montane Wet-Maui-West	5724.8	5718.1	99.9
	MWmo: Montane Wet-Moloka'i	9212.8	9124.5	99.0
	MWo: Montane Wet-O'ahu	996.8	996.8	100.0
	All subunits	216 827.6	205 519.0	94.8
SA: Subalpine	SAh: Subalpine-Hawai'i	145 342.8	6202.2	4.3
	SAm: Subalpine-Maui	8405.7	65.4	0.8
	All subunits	153 748.5	6267.5	4.1

THE FOREST HEALTH MONITORING PROGRAM

The national FHM program is designed to determine the status, changes, and trends in indicators of forest condition on an annual basis and covers all forested lands through a partnership encompassing the Forest Service, State foresters, and other State and Federal agencies and academic groups (FHM 2019). The FHM program utilizes data from a wide variety of data sources, both inside and outside the Forest Service, and develops analytical approaches for addressing forest health issues that affect the sustainability of forest ecosystems. The FHM program has four major components (fig. 1.3):

- Detection Monitoring—nationally standardized aerial and ground surveys to evaluate status and change in condition of forest ecosystems (sections 1 and 2 of this report)

- Evaluation Monitoring—projects to determine the extent, severity, and causes of undesirable changes in forest health identified through Detection Monitoring (section 3 of this report)

- Research on Monitoring Techniques—work to develop or improve indicators, monitoring systems, and analytical techniques, such as urban and riparian forest health monitoring, early detection of invasive species, multivariate analyses of forest health indicators, and spatial scan statistics (section 2 of this report)

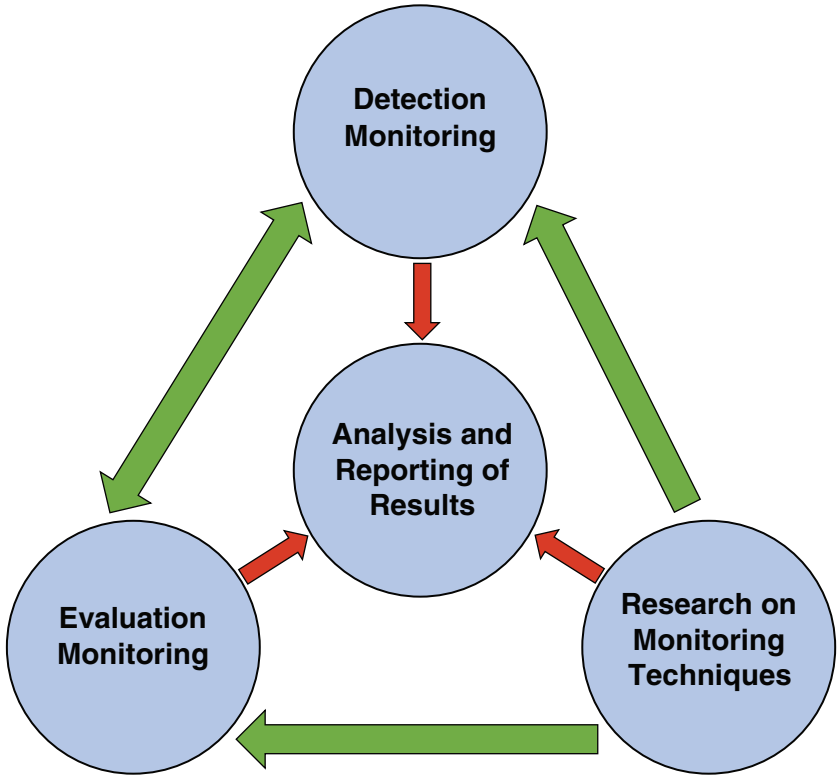

Figure 1.3—The design of the Forest Health Monitoring Program (FHM 2003).

- Analysis and Reporting—synthesis of information from various data sources within and external to the Forest Service to produce issue-driven reports on status and change in forest health at national, regional, and State levels (sections 1, 2, and 3 of this report)

The FHM program, in addition to national reporting, generates regional and State reports, often in cooperation with FHM partners, both within the Forest Service and in State forestry and agricultural departments. For example, the FHM regions cooperate with their respective State partners to produce the annual Forest Health Highlights report series, available on the FHM website at https://www.fs.fed.us/foresthealth/protecting-forest/forest-health-monitoring/monitoring-forest-highlights.shtml. Other examples include Steinman (2004) and Harris and others (2011).

The FHM program and its partners also produce reports and journal articles on monitoring techniques and analytical methods (see https://www.fs.fed.us/foresthealth/publications/fhm/fhm-publications.shtml). The emphases of these publications include forest health data (Potter and others 2016, Siry and others 2018, Smith and Conkling 2004); soils as an indicator of forest health (O'Neill and others 2005); urban forest health monitoring (Bigsby and others 2014; Cumming and others 2006, 2007; Lake and others 2006); remote sensing of forest disturbances (Chastain and others 2015, Rebbeck and others 2015); health conditions in national forests (Morin and others 2006); crown conditions (Morin and others 2015; Randolph 2010a, 2010b, 2013; Randolph and Moser 2009; Schomaker and others 2007); indicators of regeneration (McWilliams and others 2015); vegetation diversity and structure (Schulz and Gray 2013, Schulz and others 2009, Simkin and others 2016); forest lichen communities (Jovan and others 2012, Root and others 2014); downed woody materials in forests (Woodall and others 2012, 2013); drought (Vose and others 2016); ozone monitoring (Rose and Coulston 2009); patterns of nonnative invasive plant occurrence (Guo and others 2015, 2017; Iannone and others 2015, 2016a, 2016b, 2018; Jo and others 2018; Oswalt and others 2015; Riitters and others 2018a, 2018b); assessments of forest risk or tree species vulnerability to exotic invasive forest insects and diseases (Koch and others 2011, 2014; Krist and others 2014; Potter and others 2019a, 2019b; Vogt and Koch 2016; Yemshanov and others 2014); spatial patterns of landcover and forest fragmentation (Guo and others 2018; Riitters 2011; Riitters and Costanza 2018; Riitters and Wickham 2012; Riitters and others 2012, 2016, 2017); impacts of deer browse on forest structure (Russell and others 2017); broad-scale assessments of forest biodiversity (Guo and others 2019; Potter 2018; Potter and Koch 2014; Potter and Woodall 2012, 2014); predictions and indicators of climate change effects on forests and forest tree species (Fei and others 2017, Heath and others 2015, Potter and Hargrove 2013); and the overall forest health indicator program (Woodall and others 2010).

For more information about the FHM program, visit the FHM website at https://www.fs.fed.us/foresthealth/protecting-forest/forest-health-monitoring/. Among other resources,

this website includes links to all past national forest health reports (https://www.fs.fed.us/foresthealth/publications/fhm/fhm-annual-national-reports.shtml), information about funded EM projects (https://www.fs.fed.us/foresthealth/fhm/em), and annual State Forest Health Highlights reports (https://www.fs.fed.us/foresthealth/protecting-forest/forest-health-monitoring/monitoring-forest-highlights.shtml).

DATA SOURCES

Forest Service data sources in this edition of the FHM national report include FIA annualized Phase 2 survey data (Bechtold and Patterson 2005, Burrill and others 2018, Woodall and others 2010); FHP national Insect and Disease Survey forest mortality and defoliation data for 2018 (FHP 2019); Moderate Resolution Imaging Spectroradiometer (MODIS) Active Fire Detections for the United States data for 2018 (USDA Forest Service 2019); tree canopy cover data generated from the 2011 National Land Cover Database (NLCD) (Homer and others 2015) through a cooperative project between the Multi-Resolution Land Characteristics Consortium and Forest Service Geospatial Technology and Applications Center (GTAC) (Coulston and others 2012); and FIA's publicly available Environmental Monitoring and Assessment Program (EMAP) hexagons (Brand and others 2000). Other sources of data include Parameter-elevation Regression on Independent Slopes Model (PRISM) climate mapping system data (PRISM Climate Group 2019), twice-daily MODIS Normalized Difference Vegetation Index (NDVI) data from the Terra and Aqua satellites provided by NASA's Global Inventory Monitoring and Modeling Studies (GIMMS) Global Agricultural Monitoring (GLAM) system, and Alaskan forest and shrub cover derived from the 2011 NLCD. For more information about the FIA program, which is a major source of data for several FHM analyses, see box 1.2.

FHM REPORT PRODUCTION

This FHM national report, the 19th in a series of such annual documents, is produced by forest health monitoring researchers at the Eastern Forest Environmental Threat Assessment Center (EFETAC) in collaboration with North Carolina State University cooperators. A unit of the Southern Research Station of the Forest Service, EFETAC was established under the Healthy Forests Restoration Act of 2003 to generate the knowledge and tools needed to anticipate and respond to environmental threats. For more information about the research team and about threats to U.S. forests, please visit https://www.forestthreats.org/about.

Box 1.2

The Forest Inventory and Analysis (FIA) program collects forest inventory information across all forest land ownerships in the United States and maintains a network of more than 130,000 permanent forested ground plots across the conterminous United States, Hawaii, and southeastern Alaska, with a sampling intensity of approximately one plot/2428 ha (one plot per 6,000 acres). Forest Inventory and Analysis Phase 2 encompasses the annualized inventory measured on plots at regular intervals, with each plot surveyed every 5 to 7 years in most Eastern States, but with plots in the Rocky Mountain and Pacific Northwest regions surveyed once every 10 years (Reams and others 2005). The standard 0.067-ha plot (see figure) consists of four 7.315-m (24-foot) radius subplots (approximately 168.6 m^2 or 1/24th acre), on which field crews measure trees at least 12.7 cm (5 inches) in diameter. Within each of these subplots is nested a 2.073-m (6.8-foot) radius microplot (approximately 13.48 m^2 or 1/300th acre), on which crews measure trees smaller than 12.7 cm (5 inches) in diameter. A core-optional variant of the standard design includes four "macroplots," each with a radius of 17.953 m or 58.9 feet (approximately 0.1012 ha or 1/4 acre) that originates at the center of each subplot (Burrill and others 2018).

Forest Inventory and Analysis Phase 3 plots have represented a subset of these Phase 2 plots, with one Phase 3 plot for every 16 standard FIA Phase 2 plots. In addition to traditional forest inventory measurements, data for a variety of important ecological indicators have been collected from Phase 3 plots, including tree crown condition, lichen communities, downed woody material, soil condition, and vegetation structure and diversity, whereas data on ozone bioindicator plants are collected on a separate grid of plots (Woodall and others 2010, 2011). Most of these additional forest health indicators were measured as part of the Forest Health Monitoring Detection Monitoring ground plot system prior to 2000[1] (Palmer and others 1991).

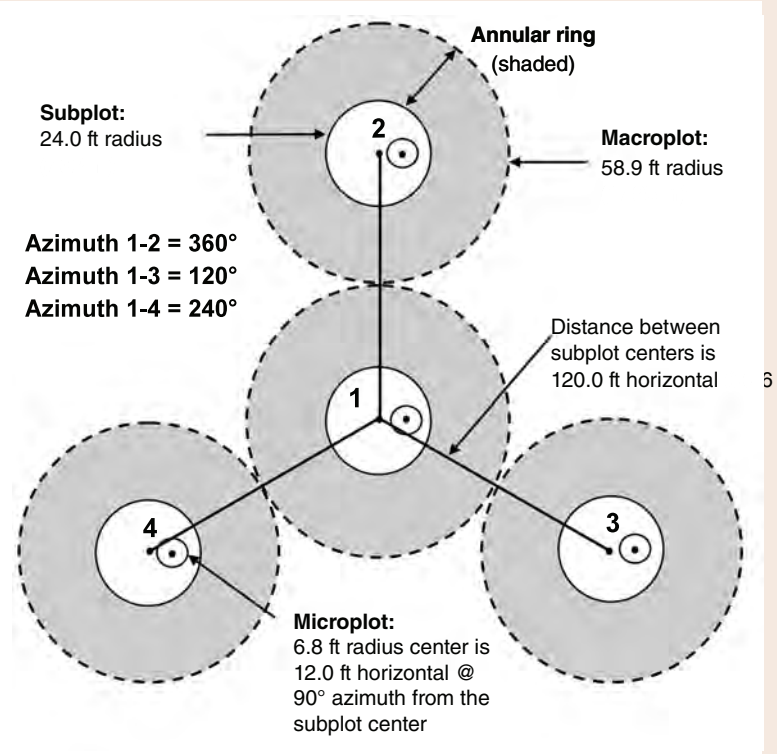

The Forest Inventory and Analysis mapped plot design. Subplot 1 is the center of the cluster with subplots 2, 3, and 4 located 120 feet away at azimuths of 360°, 120°, and 240°, respectively (Burrill and others 2018).

[1] U.S. Department of Agriculture Forest Service. 1998. Forest Health Monitoring 1998 field methods guide. Research Triangle Park, NC: U.S. Department of Agriculture Forest Service, Forest Health Monitoring program. 473 p. On file with: Forest Health Monitoring program, 3041 Cornwallis Rd., Research Triangle Park, NC 27709.

LITERATURE CITED

Ambrose, M.J.; Conkling, B.L., eds. 2007. Forest Health Monitoring 2005 national technical report. Gen. Tech. Rep. SRS-104. Asheville, NC: U.S. Department of Agriculture Forest Service, Southern Research Station. 76 p.

Ambrose, M.J.; Conkling, B.L., eds. 2009. Forest Health Monitoring 2006 national technical report. Gen. Tech. Rep. SRS-117. Asheville, NC: U.S. Department of Agriculture Forest Service, Southern Research Station. 118 p.

Bailey, R.G. 1995. Descriptions of the ecoregions of the United States. 2d ed. Miscellaneous Publication No. 1391. Washington, DC: U.S. Department of Agriculture Forest Service. 108 p. Map; presentation scale 1:7,500,000.

Bechtold, W.A.; Patterson, P.L., eds. 2005. The enhanced Forest Inventory and Analysis program—national sampling design and estimation procedures. Gen. Tech. Rep. SRS-80. Asheville, NC: U.S. Department of Agriculture Forest Service, Southern Research Station. 85 p.

Bigsby, K.M.; Ambrose, M.J.; Tobin, P.C.; Sills, E.O. 2014. The cost of gypsy moth sex in the city. Urban Forestry & Urban Greening. 13(3): 459–468.

Brand, G.J.; Nelson, M.D.; Wendt, D.G.; Nimerfro, K.K. 2000. The hexagon/panel system for selecting FIA plots under an annual inventory. In: McRoberts, R.E.; Reams, G.A.; Van Deusen, P.C., eds. Proceedings of the first annual Forest Inventory and Analysis symposium. Gen. Tech. Rep. NC-213. St. Paul, MN: U.S. Department of Agriculture Forest Service, North Central Research Station: 8–13.

Burrill, E.A.; Wilson, A.M.; Turner, J.A. [and others]. 2018. The Forest Inventory and Analysis Database: database description and user guide version 8.0 for Phase 2. U.S. Department of Agriculture Forest Service. 946 p. http://www.fia.fs.fed.us/library/database-documentation/. [Date accessed: August 23, 2019].

Chastain, R.A.; Fisk, H.; Ellenwood, J.R. [and others]. 2015. Near-real time delivery of MODIS-based information on forest disturbances. In: Lippitt, C.D.; Stow, D.A.; Coulter, L.L., eds. Time sensitive remote sensing. New York, NY: Springer: 147–164.

Cleland, D.T.; Avers, P.E.; McNab, W.H. [and others]. 1997. National hierarchical framework of ecological units. In: Boyce, M.S.; Haney, A., eds. Ecosystem management applications for sustainable forest and wildlife resources. New Haven, CT: Yale University Press: 181–200.

Cleland, D.T.; Freeouf, J.A.; Keys, J.E. [and others]. 2007. Ecological subregions: sections and subsections for the conterminous United States. Gen. Tech. Rep. WO-76D. Washington, DC: U.S. Department of Agriculture Forest Service. Map; Sloan, A.M., cartographer; presentation scale 1:3,500,000; colored. Also on CD-ROM as a GIS coverage in ArcINFO format or at http://data.fs.usda.gov/geodata/edw/datasets.php. [Date accessed: July 20, 2015].

Conkling, B.L., ed. 2011. Forest Health Monitoring 2007 national technical report. Gen. Tech. Rep. SRS-147. Asheville, NC: U.S. Department of Agriculture Forest Service, Southern Research Station. 159 p.

Conkling, B.L.; Coulston, J.W.; Ambrose, M.J., eds. 2005. Forest Health Monitoring 2001 national technical report. Gen. Tech. Rep. SRS-81. Asheville, NC: U.S. Department of Agriculture Forest Service, Southern Research Station. 204 p.

Costanza, R. 1992. Toward an operational definition of ecosystem health. In: Costanza, R.; Norton, B.G.; Haskell, B.D., eds. Ecosystem health: new goals for environmental management. Washington, DC: Island Press: 239–256.

Coulston, J.W.; Riitters, K.H.; Conkling, B.L., eds. 2005a. Forest Health Monitoring 2002 national technical report. Gen. Tech. Rep. SRS-84. Asheville, NC: U.S. Department of Agriculture Forest Service, Southern Research Station. 97 p.

Coulston, J.W.; Ambrose, M.J.; Riitters, K.H. [and others], eds. 2005b. Forest Health Monitoring 2003 national technical report. Gen. Tech. Rep. SRS-85. Asheville, NC: U.S. Department of Agriculture Forest Service, Southern Research Station. 97 p.

Coulston, J.W.; Ambrose, M.J.; Riitters, K.H.; Conkling, B.L., eds. 2005c. Forest Health Monitoring 2004 national technical report. Gen. Tech. Rep. SRS-90. Asheville, NC: U.S. Department of Agriculture Forest Service, Southern Research Station. 81 p.

Coulston, J.W.; Moisen, G.G.; Wilson, B.T. [and others]. 2012. Modeling percent tree canopy cover: a pilot study. Photogrammetric Engineering and Remote Sensing. 78(7): 715–727.

Cuddihy, L.W. 1989. Vegetation zones of the Hawaiian Islands. In: Stone, C.P.; Stone, D.B., eds. Conservation biology in Hawai'i. Honolulu, HI: University of Hawaii Press: 27–37.

Cumming, A.B.; Nowak, D.J.; Twardus, D.B. [and others]. 2007. Urban forests of Wisconsin: pilot monitoring project 2002. NA-FR-05-07. Newtown Square, PA: U.S. Department of Agriculture Forest Service, Northeastern Area State and Private Forestry. 33 p. Low resolution: http://www.na.fs.fed.us/pubs/fhm/pilot/pilot_study_wisconsin_02_lr.pdf. High resolution: http://www.na.fs.fed.us/pubs/fhm/pilot/pilot_study_wisconsin2_02_hr.pdf. [Date accessed: October 19, 2007].

Cumming, A.B.; Twardus, D.B.; Smith, W.D. 2006. National Forest Health Monitoring program, Maryland and Massachusetts street tree monitoring pilot projects. NA-FR-01-06. Newtown Square, PA: U.S. Department of Agriculture Forest Service, Northeastern Area State and Private Forestry. 23 p.

Edmonds, R.L.; Agee, J.K.; Gara, R.I. 2011. Forest health and protection. Long Grove, IL: Waveland Press, Inc. 667 p.

ESRI. 2015. ArcMap® 10.3. Redlands, CA: Environmental Systems Research Institute.

Fei, S.; Desprez, J.M.; Potter, K.M. [and others]. 2017. Divergence of species responses to climate change. Science Advances. 3(5): e1603055. DOI: 10.1126/sciadv.1603055.

Forest Health Monitoring (FHM). 2003. Forest Health Monitoring: a national strategic plan. 7 p. http://fhm.fs.fed.us/annc/strategic_plan03.pdf. [Date accessed: August 23, 2019].

Forest Health Monitoring (FHM). 2019. Program description. Forest Health Monitoring fact sheet series. https://www.fs.fed.us/foresthealth/protecting-forest/forest-health-monitoring/. [Date accessed: August 23, 2019].

Forest Health Protection (FHP). 2019. Insect and Disease Detection Survey Database (IDS). [Online database]. Fort Collins, CO: U.S. Department of Agriculture Forest Service, Forest Health Technology Enterprise Team. https://www.fs.fed.us/foresthealth/applied-sciences/mapping-reporting/gis-spatial-analysis/detection-surveys.shtml#idsdownloads. [Date accessed: July 17, 2019].

Guo, Q.; Fei, S.; Dukes, J.S. [and others]. 2015. A unified approach to quantify invasibility and degree of invasion. Ecology. 95(10): 2613–2621.

Guo, Q.; Fei, S.; Potter, K.M. [and others]. 2019. Tree diversity regulates forest pest invasion. Proceedings of the National Academy of Sciences. 116(15): 7382–7386.

Guo, Q.; Iannone, B.V.; Nunez-Mir, G.C. [and others]. 2017. Species pool, human population, and global vs. regional invasion patterns. Landscape Ecology. 32(2): 229–238.

Guo, Q.; Riitters, K.H.; Potter, K.M. [and others]. 2018. A subcontinental analysis of forest fragmentation and pest invasion. Forests. 9(12): 744.

Harris, J.L., comp.; Region 2 Forest Health Protection staff. 2011. Forest health conditions, 2009–2010: Rocky Mountain Region (R2). R2-11-RO-31. Golden, CO: U.S. Department of Agriculture Forest Service, Renewable Resources, Forest Health Protection, Rocky Mountain Region. 108 p.

Heath, L.S.; Anderson, S.; Emery, M.R. [and others]. 2015. Indicators for climate change impacts for forests: National Climate Assessment indicators. Gen. Tech. Rep. NRS-155. Newtown Square, PA: U.S. Department of Agriculture Forest Service, Northern Research Station. 143 p.

Homer, C.G.; Dewitz, J.A.; Yang, L. [and others]. 2015. Completion of the 2011 National Land Cover Database for the conterminous United States: representing a decade of land cover change information. Photogrammetric Engineering and Remote Sensing. 81(5): 345–354.

Iannone, B.V.; Oswalt, C.M.; Liebhold, A.M. [and others]. 2015. Region-specific patterns and drivers of macroscale forest plant invasions. Diversity and Distributions. 21: 1181–1192.

Iannone, B.V.; Potter, K.M.; Guo, Q. [and others]. 2016a. Biological invasion hotspots: a trait-based perspective reveals new sub-continental patterns. Ecography. 39: 961–969.

Iannone, B.V.; Potter, K.M.; Guo, Q. [and others]. 2018. Environmental harshness drives spatial heterogeneity in biotic resistance. NeoBiota. 40: 87–105.

Iannone, B.V.; Potter, K.M.; Hamil, K.-A.D. [and others]. 2016b. Evidence of biotic resistance to invasions in forests of the Eastern USA. Landscape Ecology. 31: 85–99.

Jo, I.; Potter, K.M.; Domke, G.; Fei, S. 2018. Dominant forest tree mycorrhizal type mediates understory plant invasions. Ecology Letters. 21: 217–224.

Jovan, S.; Riddell, J.; Padgett, P.E.; Nash, T.H., III. 2012. Eutrophic lichens respond to multiple forms of N: implications for critical levels and critical loads research. Ecological Applications. 22(7): 1910–1922.

Koch, F.H.; Yemshanov, D.; Colunga-Garcia, M. [and others]. 2011. Potential establishment of alien-invasive forest insect species in the United States: where and how many? Biological Invasions. 13: 969–985.

Koch, F.H.; Yemshanov, D.; Haack, R.A.; Magarey, R.D. 2014. Using a network model to assess risk of forest pest spread via recreational travel. PLOS ONE. 9(7): e102105.

Kolb, T.E.; Wagner, M.R.; Covington, W.W. 1994. Concepts of forest health: utilitarian and ecosystem perspectives. Journal of Forestry. 92: 10–15.

Krist, F.J., Jr.; Ellenwood, J.R.; Woods, M.E. [and others]. 2014. 2012–2027 national insect and disease forest risk assessment. FHTET-14-01. U.S. Department of Agriculture Forest Service, Forest Health Technology Enterprise Team. 199 p. http://www.fs.fed.us/foresthealth/technology/pdfs/2012_RiskMap_Report_web.pdf. [Date accessed: July 24, 2014].

Lake, M.; Marshall, P.; Mielke, M. [and others]. 2006. National Forest Health Monitoring program monitoring urban forests in Indiana: pilot study 2002, part 1. Analysis of field methods and data collection. NA-FR-06-06. Newtown Square, PA: U.S. Department of Agriculture Forest Service, Northeastern Area State and Private Forestry. http://www.fhm.fs.fed.us/pubs/ufhm/indianaforests02/indianaforests02.html. [Date accessed: November 6, 2007].

McWilliams, W.H.; Westfall, J.A.; Brose, P.H. [and others]. 2015. A regeneration indicator for Forest Inventory and Analysis: history, sampling, estimation, analytics, and potential use in the Midwest and Northeast United States. Gen. Tech. Rep. NRS-148. Newtown Square, PA: U.S. Department of Agriculture Forest Service, Northern Research Station. 74 p.

Montréal Process Working Group. 1995. Criteria and indicators for the conservation and sustainable management of temperate and boreal forests. http://www.montrealprocess.org/. [Date accessed: March 4, 2015].

Morin, R.S.; Liebhold, A.M.; Gottschalk, K.W. [and others]. 2006. Analysis of Forest Health Monitoring surveys on the Allegheny National Forest (1998–2001). Gen. Tech. Rep. NE-339. Newtown Square, PA: U.S. Department of Agriculture Forest Service, Northeastern Research Station. 102 p. http://www.fs.fed.us/ne/newtown_square/publications. [Date accessed: November 6, 2007].

Morin, R.S.; Randolph, K.C.; Steinman, J. 2015. Mortality rates associated with crown health for eastern forest tree species. Environmental Monitoring and Assessment. 187(3): 87.

O'Neill, K.P.; Amacher, M.C.; Perry, C.H. 2005. Soils as an indicator of forest health: a guide to the collection, analysis, and interpretation of soil indicator data in the Forest Inventory and Analysis program. Gen. Tech. Rep. NC-258. St. Paul, MN: U.S. Department of Agriculture Forest Service, North Central Research Station. 53 p.

Oswalt, C.M.; Fei, S.; Guo, Q. [and others]. 2015. A subcontinental view of forest plant invasions. NeoBiota. 24: 49–54.

Palmer, C.J.; Riitters, K.H.; Strickland, T. [and others]. 1991. Monitoring and research strategy for forests—Environmental Monitoring and Assessment Program (EMAP). EPA/600/4-91/012. Washington, DC: U.S. Environmental Protection Agency. 189 p.

Potter, K.M. 2018. Do United States protected areas effectively conserve forest tree rarity and evolutionary distinctiveness? Biological Conservation. 224: 34–46.

Potter, K.M.; Conkling, B.L., eds. 2012a. Forest Health Monitoring 2008 national technical report. Gen. Tech. Rep. SRS-158. Asheville, NC: U.S. Department of Agriculture Forest Service, Southern Research Station. 179 p.

Potter, K.M.; Conkling, B.L., eds. 2012b. Forest Health Monitoring 2009 national technical report. Gen. Tech. Rep. SRS-167. Asheville, NC: U.S. Department of Agriculture Forest Service, Southern Research Station. 252 p.

Potter, K.M.; Conkling, B.L., eds. 2013a. Forest Health Monitoring: national status, trends, and analysis 2010. Gen. Tech. Rep. SRS-176. Asheville, NC: U.S. Department of Agriculture Forest Service, Southern Research Station. 162 p.

Potter, K.M.; Conkling, B.L., eds. 2013b. Forest Health Monitoring: national status, trends, and analysis 2011. Gen. Tech. Rep. SRS-185. Asheville, NC: U.S. Department of Agriculture Forest Service, Southern Research Station. 149 p.

Potter, K.M.; Conkling, B.L., eds. 2014. Forest Health Monitoring: national status, trends, and analysis 2012. Gen. Tech. Rep. SRS-198. Asheville, NC: U.S. Department of Agriculture Forest Service, Southern Research Station. 192 p.

Potter, K.M.; Conkling, B.L., eds. 2015a. Forest Health Monitoring: national status, trends, and analysis 2013. Gen. Tech. Rep. SRS-207. Asheville, NC: U.S. Department of Agriculture Forest Service, Southern Research Station. 199 p.

Potter, K.M.; Conkling, B.L., eds. 2015b. Forest Health Monitoring: national status, trends, and analysis 2014. Gen. Tech. Rep. SRS-209. Asheville, NC: U.S. Department of Agriculture Forest Service, Southern Research Station. 190 p.

Potter, K.M.; Conkling, B.L., eds. 2016. Forest Health Monitoring: national status, trends, and analysis 2015. Gen. Tech. Rep. SRS-213. Asheville, NC: U.S. Department of Agriculture Forest Service, Southern Research Station. 199 p.

Potter, K.M.; Conkling, B.L., eds. 2017. Forest Health Monitoring: national status, trends, and analysis 2016. Gen. Tech. Rep. SRS-222. Asheville, NC: U.S. Department of Agriculture Forest Service, Southern Research Station. 195 p.

Potter, K.M.; Conkling, B.L., eds. 2018. Forest Health Monitoring: national status, trends, and analysis 2017. Gen. Tech. Rep. SRS-233. Asheville, NC: U.S. Department of Agriculture Forest Service, Southern Research Station. 190 p.

Potter, K.M.; Conkling, B.L., eds. 2019. Forest Health Monitoring: national status, trends, and analysis 2018. Gen. Tech. Rep. SRS-239. Asheville, NC: U.S. Department of Agriculture Forest Service, Southern Research Station. 168 p.

Potter, K.M.; Escanferla, M.E.; Jetton, R.M.; Man, G. 2019a. Important insect and disease threats to United States tree species and geographic patterns of their potential impacts. Forests. 10(4): 304.

Potter, K.M.; Escanferla, M.E.; Jetton, R.M. [and others]. 2019b. Prioritizing the conservation needs of United States tree species: evaluating vulnerability to forest insect and disease threats. Global Ecology and Conservation. 18: e00622.

Potter, K.M.; Hargrove, W.W. 2013. Quantitative metrics for assessing predicted climate change pressure on North American tree species. Mathematical and Computational Forestry and Natural Resources Sciences. 5(2): 151–169.

Potter, K.M.; Koch, F.H. 2014. Phylogenetic community structure of forests across the conterminous United States: regional ecological patterns and forest health implications. Forest Science. 60(5): 851–861.

Potter, K.M.; Koch, F.H.; Oswalt, C.M.; Iannone, B.V. 2016. Data, data everywhere: detecting spatial patterns in fine-scale ecological information collected across a continent. Landscape Ecology. 31: 67–84.

Potter, K.M.; Woodall, C.W. 2012. Trends over time in tree and seedling phylogenetic diversity indicate regional differences in forest biodiversity change. Ecological Applications. 22(2): 517–531.

Potter, K.M.; Woodall, C.W. 2014. Does biodiversity make a difference? Relationships between species richness, evolutionary diversity, and aboveground live tree biomass across U.S. forests. Forest Ecology and Management. 321: 117–129.

Price, J.P.; Gon, S.M., III; Jacobi, J.D.; Matsuwaki, D. 2007. Mapping plant species ranges in the Hawaiian Islands: developing a methodology and associated GIS layers. Technical Report HCSU-008. Hilo, HI: University of Hawai'i at Hilo, Hawai'i Cooperative Studies Unit. 58 p.

PRISM Climate Group. 2019. 2.5-arcmin (4 km) gridded monthly climate data. http://www.prism.oregonstate.edu. [Date accessed: August 1, 2019].

Raffa, K.F.; Aukema, B.; Bentz, B.J. [and others]. 2009. A literal use of "forest health" safeguards against misuse and misapplication. Journal of Forestry. 107: 276–277.

Randolph, K.C. 2010a. Equations relating compacted and uncompacted live crown ratio for common tree species in the South. Southern Journal of Applied Forestry. 34(3): 118–123.

Randolph, K.C. 2010b. Comparison of the arithmetic and geometric means in estimating crown diameter and crown cross-sectional area. Southern Journal of Applied Forestry. 34(4): 186–189.

Randolph, K.C. 2013. Development history and bibliography of the U.S. Forest Service crown-condition indicator for forest health monitoring. Environmental Monitoring and Assessment. 185(6): 4977–4993.

Randolph, K.C.; Moser, W.K. 2009. Tree crown condition in Missouri, 2000–2003. Gen. Tech. Rep. SRS-113. Asheville, NC: U.S. Department of Agriculture Forest Service, Southern Research Station. 11 p.

Reams, G.A.; Smith, W.D.; Hansen, M.H. [and others]. 2005. The Forest Inventory and Analysis sampling frame. In: Bechtold, W.A.; Patterson, P.L., eds. The enhanced Forest Inventory and Analysis program—national sampling design and estimation procedures. Asheville, NC: U.S. Department of Agriculture Forest Service, Southern Research Station: 11–26.

Rebbeck, J.; Kloss, A.; Bowden, M. [and others]. 2015. Aerial detection of seed-bearing female *Ailanthus altissima*: a cost-effective method to map an invasive tree in forested landscapes. Forest Science. 61: 1068–1078.

Riitters, K.H. 2011. Spatial patterns of land cover in the United States: a technical document supporting the Forest Service 2010 RPA assessment. Gen. Tech. Rep. SRS-136. Asheville, NC: U.S. Department of Agriculture Forest Service, Southern Research Station. 64 p.

Riitters, K.; Costanza, J. 2018. The landscape context of family forests in the United States: anthropogenic interfaces and forest fragmentation from 2001 to 2011. Landscape and Urban Planning. 188: 64–71.

Riitters, K.H.; Costanza, J.K.; Buma, B. 2017. Interpreting multiscale domains of tree cover disturbance patterns in North America. Ecological Indicators. 80: 147–152.

Riitters, K.H.; Coulston, J.W.; Wickham, J.D. 2012. Fragmentation of forest communities in the Eastern United States. Forest Ecology and Management. 263: 85–93.

Riitters, K.; Potter, K.M.; Iannone, B.V. [and others]. 2018a. Exposure of protected forest to plant invasions in the Eastern United States. Forests. 9(11): 723.

Riitters, K.; Potter, K.M.; Iannone, B.V. [and others]. 2018b. Landscape correlates of forest plant invasions: a high-resolution analysis across the Eastern United States. Diversity and Distributions. 24: 274–284.

Riitters, K.H.; Tkacz, B. 2004. The U.S. Forest Health Monitoring program. In: Wiersma, G.B., ed. Environmental monitoring. Boca Raton, FL: CRC Press: 669–683.

Riitters, K.H.; Wickham, J.D. 2012. Decline of forest interior conditions in the conterminous United States. Scientific Reports. 2: 653. 4 p. DOI: 10.1038.srep00653.

Riitters, K.H.; Wickham, J.D.; Costanza, J.K.; Vogt, P. 2016. A global evaluation of forest interior area dynamics using tree cover data from 2000 to 2012. Landscape Ecology. 31: 137–148.

Root, H.T.; McCune, B.; Jovan, S. 2014. Lichen communities and species indicate climate thresholds in southeast and south-central Alaska, USA. The Bryologist. 117(3): 241–252.

Rose, A.K.; Coulston, J.W. 2009. Ozone injury across the Southern United States, 2002–06. Gen. Tech. Rep. SRS-118. Asheville, NC: U.S. Department of Agriculture Forest Service, Southern Research Station. 25 p.

Russell, M.B.; Woodall, C.W.; Potter, K.M. [and others]. 2017. Interactions between white-tailed deer density and the composition of forest understories in the Northern United States. Forest Ecology and Management. 384: 26–33.

Schomaker, M.E.; Zarnoch, S.J.; Bechtold, W.A. [and others]. 2007. Crown-condition classification: a guide to data collection and analysis. Gen. Tech. Rep. SRS-102. Asheville, NC: U.S. Department of Agriculture Forest Service, Southern Research Station. 78 p.

Schulz, B.K.; Bechtold, W.A.; Zarnoch, S.J. 2009. Sampling and estimation procedures for the vegetation diversity and structure indicator. Gen. Tech. Rep. PNW-781. Portland, OR: U.S. Department of Agriculture Forest Service, Pacific Northwest Research Station. 53 p.

Schulz, B.K.; Gray, A.N. 2013. The new flora of Northeastern USA: quantifying introduced plant species occupancy in forest ecosystems. Environmental Monitoring and Assessment. 185: 3931–3957.

Simkin, S.M.; Allen, E.B.; Bowman, W.D. [and others]. 2016. Conditional vulnerability of plant diversity to atmospheric nitrogen deposition across the United States. Proceedings of the National Academy of Sciences. 113: 4086–4091.

Siry, J.; Cubbage, F.W.; Potter, K.M.; McGinley, K. 2018. Current perspectives on sustainable forest management: North America. Current Forestry Reports. 4(3): 138–149.

Smith, W.B.; Miles, P.D.; Perry, C.H.; Pugh, S.A. 2009. Forest resources of the United States, 2007. Gen. Tech. Rep. WO-78. St. Paul, MN: U.S. Department of Agriculture Forest Service, Washington Office. 336 p.

Smith, W.D.; Conkling, B.L. 2004. Analyzing forest health data. Gen. Tech. Rep. SRS-077. Asheville, NC: U.S. Department of Agriculture Forest Service, Southern Research Station. 33 p. http://www.srs.fs.usda.gov/pubs/gtr/gtr_srs077.pdf. [Date accessed: November 6, 2007].

Spencer, P.; Nowacki, G.; Fleming, M. [and others]. 2002. Home is where the habitat is: an ecosystem foundation for wildlife distribution and behavior. Arctic Research of the United States. 16: 6–17.

State of Hawaii, Office of Planning. 2019. USGS elevational ranges. http://planning.hawaii.gov/gis/download-gis-data/. [Date accessed: January 18, 2019].

Steinman, J. 2004. Forest Health Monitoring in the Northeastern United States: disturbances and conditions during 1993–2002. NA-TP-01-04. Newtown Square, PA: U.S. Department of Agriculture Forest Service, Northeastern Area State and Private Forestry. 46 p. http://fhm.fs.fed.us/pubs/tp/dist_cond/dc.shtml. [Date accessed: December 8, 2009].

Teale, S.A.; Castello, J.D. 2011. The past as key to the future: a new perspective on forest health. In: Castello, J.D.; Teale, S.A., eds. Forest health: an integrated perspective. New York: Cambridge University Press: 3–16.

U.S. Department of Agriculture (USDA) Forest Service. 2004. National report on sustainable forests—2003. FS-766. Washington, DC: U.S. Department of Agriculture Forest Service. 139 p.

U.S. Department of Agriculture (USDA) Forest Service. 2011. National report on sustainable forests—2010. FS-979. Washington, DC: U.S. Department of Agriculture Forest Service. 134 p.

U.S. Department of Agriculture (USDA) Forest Service. 2019. MODIS active fire mapping program: fire detection GIS data. https://fsapps.nwcg.gov/afm/gisdata.php. [Date accessed: May 7, 2019].

Vogt, J.T.; Koch, F.H. 2016. The evolving role of Forest Inventory and Analysis data in invasive insect research. American Entomologist. 62(1): 46–58.

Vose, J.M.; Clark, J.S.; Luce, C.H.; Patel-Weynand, T., eds. 2016. Effects of drought on forests and rangelands in the United States: a comprehensive science synthesis. Gen. Tech. Rep. WO-93b. Washington, DC: U.S. Department of Agriculture Forest Service, Washington Office. 289 p.

Woodall, C.W.; Amacher, M.C.; Bechtold, W.A. [and others]. 2011. Status and future of the forest health indicators program of the USA. Environmental Monitoring and Assessment. 177: 419–436.

Woodall, C.W.; Conkling, B.L.; Amacher, M.C. [and others]. 2010. The Forest Inventory and Analysis database version 4.0: database description and users manual for Phase 3. Gen. Tech. Rep. NRS-61. Newtown Square, PA: U.S. Department of Agriculture Forest Service, Northern Research Station. 180 p.

Woodall, C.W.; Walters, B.F.; Oswalt, S.N. [and others]. 2013. Biomass and carbon attributes of downed woody materials in forests of the United States. Forest Ecology and Management. 305: 48–59.

Woodall, C.W.; Walters, B.F.; Westfall, J.A. 2012. Tracking downed dead wood in forests over time: development of a piece matching algorithm for line intercept sampling. Forest Ecology and Management. 277: 196–204.

Yemshanov, D.; Koch, F.H.; Lu, B. [and others]. 2014. There is no silver bullet: the value of diversification in planning invasive species surveillance. Ecological Economics. 104: 61–72.

Ziegler, A.C. 2002. Hawaiian natural history, ecology, and evolution. Honolulu, HI: University of Hawai'i Press. 512 p.

SECTION 1.

Analyses of Short-Term Forest Health Data

CHAPTER 2.

Large-Scale Patterns of Insect and Disease Activity in the Conterminous United States, Alaska, and Hawaii from the National Insect and Disease Survey, 2018

Kevin M. Potter
Jeanine L. Paschke
Frank H. Koch
Erin M. Berryman

INTRODUCTION

Forest insects and diseases are having widespread ecological and economic impacts on the forests of the United States and may represent the most serious threats to the Nation's forests (Logan and others 2003, Lovett and others 2016, Tobin 2015). Insects and diseases cause changes in forest structure and function, species succession, and biodiversity, which may be considered negative or positive depending on management objectives (Edmonds and others 2011). Nearly all native tree species of the United States are affected by at least one injury-causing insect or disease agent, with exotic agents on average considerably more severe than native ones (Potter and others 2019a). Additionally, the genetic integrity of several native tree species is highly vulnerable to exotic diseases and insects (Potter and others 2019b).

An important task for forest managers, pathologists, and entomologists is recognizing and distinguishing between natural and excessive mortality, a task that relates to ecologically based or commodity-based management objectives (Teale and Castello 2011). The impacts of insects and diseases on forests vary from natural thinning to extraordinary levels of tree mortality, but insects and diseases are not necessarily enemies of the forest because they kill trees (Teale and Castello 2011). If disturbances, including insects and diseases, are viewed in their full ecological context, then some amount can be considered "healthy" to sustain the structure of the forest (Manion 2003, Zhang and others 2011) by causing tree mortality that culls weak competitors and releases resources that are needed to support the growth of surviving trees (Teale and Castello 2011).

Analyzing patterns of forest insect infestations, disease occurrences, forest declines, and related biotic stress factors is necessary to monitor the health of forested ecosystems and their potential impacts on forest structure, composition, biodiversity, and species distributions (Castello and others 1995). Introduced nonnative insects and diseases, in particular, can extensively damage the biodiversity, ecology, and economy of affected areas (Brockerhoff and others 2006, Mack and others 2000). Few forests remain unaffected by invasive species, and their devastating impacts in forests are undeniable, including, in some cases, wholesale changes to the structure and function of an ecosystem (Parry and Teale 2011).

Examining insect pest occurrences and related stress factors from a landscape-scale perspective is useful, given the regional extent of many infestations and the large-scale complexity of interactions between host distribution, stress factors, and the development of insect pest outbreaks (Holdenrieder and others 2004, Liebhold and others 2013). One such landscape-scale approach is detecting geographic patterns of disturbance, which allows for the identification of areas at greater risk of significant ecological and economic impacts and for the selection of locations for more intensive monitoring and analysis.

METHODS

Data

Forest Health Protection (FHP) national Insect and Disease Survey (IDS) data (FHP 2019) consist of information from low-altitude aerial survey and ground survey efforts by FHP and partners in State agencies. These data can be used to identify forest landscape-scale patterns associated with geographic hot spots of forest insect and disease activity in the conterminous 48 States and to summarize insect and disease activity by regions in the conterminous United States, Alaska, and Hawaii (Potter 2012, 2013; Potter and Koch 2012; Potter and Paschke 2013, 2014, 2015a, 2015b, 2016, 2017; Potter and others 2018, 2019).

The IDS data identify areas of mortality and defoliation caused by insect and disease activity, although some important forest insects (such as emerald ash borer [*Agrilus planipennis*] and hemlock woolly adelgid [*Adelges tsugae*]), diseases (such as laurel wilt [*Raffaelea lauricola*], Dutch elm disease [*Ophiostoma novo-ulmi*], white pine blister rust [*Cronartium ribicola*], and thousand cankers disease [*Geosmithia morbida*]), and mortality complexes (such as oak decline) are not easily detected or thoroughly quantified through aerial detection surveys. Such pests may attack hosts that are widely dispersed throughout forests with high tree species diversity or may cause mortality or defoliation that is otherwise difficult to detect. A pathogen or insect might be considered a mortality-causing agent in one location and a defoliation-causing agent in another, depending on the level of damage to the forest in a given area and the convergence of other stress factors such as drought. In some cases, the identified agents of mortality or defoliation are actually complexes of multiple agents summarized under an impact label related to a specific host tree species (e.g., "beech bark disease complex" or "yellow-cedar decline"). Additionally, differences in data collection, attribute recognition, and coding procedures among States and regions can complicate data analysis and interpretation of the results.

In 2018, IDS surveys of the conterminous United States covered about 211.34 million ha of both forested and unforested area (fig. 2.1), of which approximately 147.27 million ha encompassed areas with tree canopy cover (about 46.6 percent of the total 315.99-million-ha tree canopy area of the conterminous States). Nearly the entirety of this area was surveyed using the Digital Mobile Sketch Mapping (DMSM) approach, which is replacing the legacy Digital Aerial Sketch Mapping (DASM) approach (Berryman and McMahan 2019). In Alaska, roughly 13.65 million ha were surveyed in 2018, of which 9.9 million ha were forest or shrubland, about 12.7 percent of the total forest and shrubland area of the State. For Hawaii, about 933 000 ha were surveyed in 2018, with 598 000 of those in areas with tree canopy cover, approximately 69.4 percent of the State's total tree canopy area.

Digital Mobile Sketch Mapping includes tablet hardware, software, and data support processes that allow trained aerial surveyors

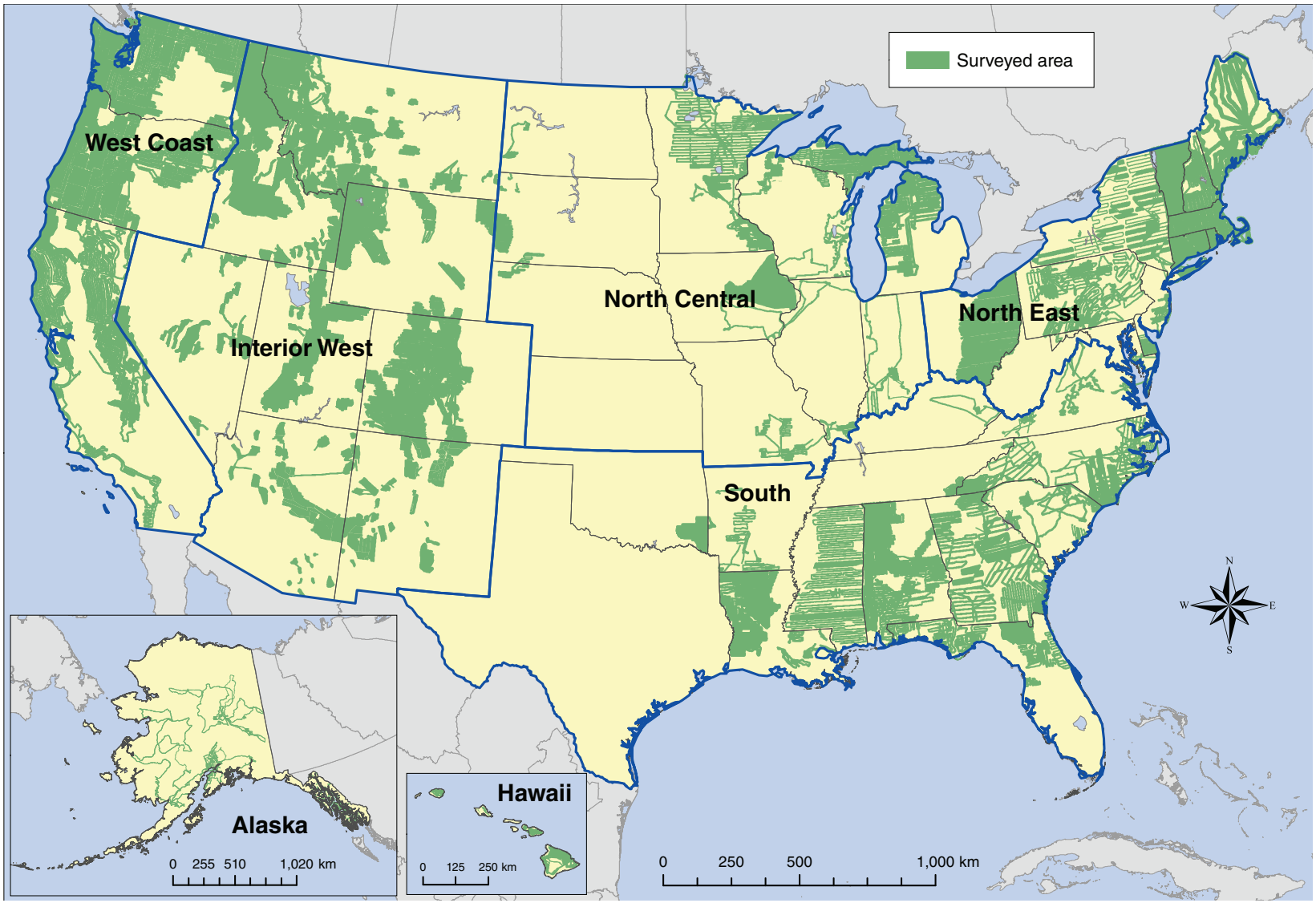

Figure 2.1—The extent of surveys for insect and disease activity conducted in the conterminous United States and Alaska in 2018. The blue lines delineate Forest Health Monitoring regions. Note: Alaska and Hawaii are not shown to scale with map of the conterminous United States. (Data source: U.S. Department of Agriculture Forest Service, Forest Health Protection)

in light aircraft, as well as ground observers, to record forest disturbances and their causal agents. Digital Mobile Sketch Mapping enhances the quality and quantity of forest health data while having the potential to improve safety by integrating with programs such as operational remote sensing (ORS), which uses satellite imagery to monitor disturbances in areas of higher aviation risk (FHP 2016). Geospatial data collected with DMSM are stored in the national IDS database. Digital Mobile Sketch Mapping includes both polygon geometry, used for damage areas where boundaries are discrete and obvious from the air, and point geometry, used for small clusters of damage where the size and shape of the damage are less important than recording the location of damage, such as for sudden oak death (caused by the pathogen *Phytophthora ramorum*), southern pine beetle (*Dendroctonus frontalis*), and some types of bark beetle damage in the West. For the 2018 data, these points were assigned an area of 0.8 ha (about 2 acres). Additionally, DMSM allows for the use of grid cells (240-, 480-, 960-, or 1920-m resolution) to estimate the percent of trees affected by damages that may be widespread and diffuse, such as those associated with European gypsy moth (*Lymantria dispar dispar*) and emerald ash borer. When calculating the total areas affected by each damage agent, we used the entire areas of these grid cells (e.g., 240-m cell = 5.76 ha).

Analyses

To estimate the extent of damaging insect and disease agents in 2018, we conducted two types of analyses. In the first, we reported the most widely detected mortality and defoliation agents in a series of tables. Specifically, the 2018 mortality and defoliation polygons were used to identify the select mortality and defoliation agents and complexes causing damage on >5000 ha of forest in the conterminous United States in that year. Similarly, we listed the five most widely reported mortality and defoliation agents and complexes within each of five Forest Health Monitoring (FHM) regions within the conterminous United States (West Coast, Interior West, North Central, North East, and South), as well as for Alaska and Hawaii where data were available.

Because of the insect and disease aerial sketch-mapping process (i.e., digitization of polygons by a human interpreter aboard the aircraft), all quantities are approximate "footprint" areas for each agent or complex, delineating areas of visible damage within which the agent or complex is present. Unaffected trees may exist within the footprint, and the amount of damage within the footprint is not reflected in the estimates of forest area affected. The sum of areas affected by all agents and complexes is not equal to the total affected area as a result of reporting multiple agents per polygon in some situations.

In our second set of analyses, we used the IDS data for 2018 to more directly estimate the impacts of insect- and disease-related mortality and defoliation on U.S. forests. These results are reported in a set of figures describing (1) the percent of surveyed tree canopy cover

area with insect- and disease-related mortality or defoliation within ecoregions across the United States and (2) geographic hot spots of insect- and disease-related mortality or defoliation across the conterminous 48 States and within the five FHM regions.

As an indicator of the extent of damaging insect and disease agents, we summarized the percent of surveyed tree canopy cover area experiencing mortality or defoliation for ecoregions within the conterminous 48 States and Hawaii, and for surveyed forest and shrubland in Alaska ecoregions. This is a change from previous FHM reports, in which we reported on the percent of regions *exposed to* mortality and defoliating agents based only on the footprint of mortality or defoliation polygon boundaries (masked by forest cover) because information on the percent of damage within polygons was not yet completely available. The new DMSM approach, however, allows surveyors to both define the extent of an area experiencing damage and to estimate a percent range of the area within the polygon that is affected (specifically 1–3 percent, 4–10 percent, 11–29 percent, 30–50 percent, and >50 percent). By multiplying the area of damage within each polygon (after masking by tree canopy cover) by the midpoint of the estimated range of percent affected, it is possible to generate an adjusted estimate of the area affected by each mortality or defoliation agent detection (Berryman and McMahan 2019). These individual estimates can be summed for all the polygons (intersected and dissolved) within an ecoregion and divided by the total surveyed tree canopy cover area within the ecoregion to generate an estimate of the percent of its canopy cover area affected by defoliating or mortality-causing agents. (Digital Mobile Sketch Mapping point data are also included in this estimate. Surveyors have the option to estimate the number of trees affected at a point and are required to assign an area value associated with each point [e.g., 1 acre {0.405 ha}], which is assumed to be 100 percent affected by its mortality or defoliation agent. These areas for all the points in an ecoregion are then added to the polygon-adjusted affected area estimates for the ecoregion.)

For the conterminous States, percent of surveyed tree canopy area with mortality or defoliation was calculated within each of 190 ecoregion sections (Cleland and others 2007). Similarly, the mortality and defoliation data were summarized for each of the 32 ecoregion sections in Alaska (Spencer and others 2002). In Hawaii, the percent of surveyed tree canopy area affected by mortality agents was calculated by ecoregions on each of the major islands of the archipelago (see ch. 1 for a description of these ecoregions). Statistics were not calculated for analysis regions in the conterminous United States or Hawaii with <5 percent of the tree canopy cover area surveyed, nor in Alaska with <2.5 percent of the forest and shrubland area surveyed.

The tree canopy data used for the conterminous States and Hawaii were resampled to 240 m from a 30-m raster dataset that

estimates percent tree canopy cover (from 0 to 100 percent) for each grid cell; this dataset was generated from the 2011 National Land Cover Database (NLCD) (Homer and others 2015) through a cooperative project between the Multi-Resolution Land Characteristics Consortium and the U.S. Department of Agriculture Forest Service, Geospatial Technology and Applications Center (GTAC) (Coulston and others 2012). For our purposes, we treated any cell with >0 percent tree canopy cover as forest. Comparable tree canopy cover data were not available for Alaska, so we instead created a 240-m-resolution layer of forest and shrub cover from the 2011 NLCD. (This is a change from previous Forest Health Monitoring national reports, for which the mortality and defoliation polygons were masked using a forest cover map [1-km resolution] derived from Moderate Resolution Imaging Spectroradiometer [MODIS] imagery by the Forest Service GTAC [USDA Forest Service 2008].)

Additionally, we used the Spatial Association of Scalable Hexagons (SASH) analytical approach to identify statistically significant geographic hot spots of mortality or defoliation in the conterminous 48 States. This method identifies locations where ecological phenomena occur at greater or lower frequency than expected by random chance and is based on a sampling frame optimized for spatial neighborhood analysis, adjustable to the appropriate spatial resolution, and applicable to multiple data types (Potter and others 2016). Specifically, it consists of dividing an analysis area into scalable equal-area hexagonal cells within which data are aggregated, followed by identifying statistically significant geographic clusters of hexagonal cells within which mean values are greater or less than those expected by chance. To identify these clusters, we employed a Getis-Ord (G_i^*) hot spot analysis (Getis and Ord 1992) in ArcMap® 10.3 (ESRI 2015). We conducted two sets of hot spot analyses for both mortality-causing and defoliation-causing agents: one for the conterminous 48 States in their entirety, and one for each of the five FHM regions within the conterminous States. The low density of survey data in 2018 from Alaska and the small spatial extent of Hawaii (fig. 2.1) precluded the use of Getis-Ord G_i^* hot spot analyses for these States.

The units of analysis were 9,810 hexagonal cells, each approximately 834 km^2 in area, generated in a lattice across the conterminous United States using intensification of the Environmental Monitoring and Assessment Program (EMAP) North American hexagon coordinates (White and others 1992). These coordinates are the foundation of a sampling frame in which a hexagonal lattice was projected onto the conterminous United States by centering a large base hexagon over the region (Reams and others 2005, White and others 1992). This base hexagon can be subdivided into many smaller hexagons, depending on sampling needs, and serves as the basis of the plot sampling frame for the Forest Inventory and Analysis (FIA) program (Reams and others 2005). Importantly, the hexagons maintain equal areas across the study region regardless of the degree of intensification of the EMAP

hexagon coordinates. In addition, the hexagons are compact and uniform in their distance to the centroids of neighboring hexagons, meaning that a hexagonal lattice has a higher degree of isotropy (uniformity in all directions) than does a square grid (Shima and others 2010). These are convenient and highly useful attributes for spatial neighborhood analyses. These scalable hexagons also are independent of geopolitical and ecological boundaries, avoiding the possibility of different sample units (such as counties, States, or watersheds) encompassing vastly different areas (Potter and others 2016). We selected hexagons 834 km^2 in area because this is a manageable size for making monitoring and management decisions in analyses that are national in extent (Potter and others 2016).

The Getis-Ord G_i^* statistic was then used to identify clusters of hexagonal cells in which the percent of surveyed tree canopy area with mortality or defoliation was higher than expected by chance. This statistic allows for the decomposition of a global measure of spatial association into its contributing factors, by location, and is therefore particularly suitable for detecting instances of nonstationarity in a dataset, such as when spatial clustering is concentrated in one subregion of the data (Anselin 1992). Hexagons were excluded if they contained <5 percent tree canopy cover or if <1 percent of the tree canopy cover was surveyed in 2018.

The Getis-Ord G_i^* statistic for each hexagon summed the differences between the mean values in a local sample, determined by a moving window consisting of the hexagon and its 18 first- and second-order neighbors (the 6 adjacent hexagons and the 12 additional hexagons contiguous to those 6) and a global mean. Our first analysis encompassed a global mean of all the forested hexagonal cells in the conterminous 48 States, while we conducted another set of analyses separately within each of the five FHM regions. The G_i^* statistic was standardized as a *z*-score with a mean of 0 and a standard deviation of 1, with values >1.96 representing significant (p <0.025) local clustering of high values and values <-1.96 representing significant clustering of low values (p <0.025), since 95 percent of the observations under a normal distribution should be within approximately two (exactly 1.96) standard deviations of the mean (Laffan 2006). In other words, a G_i^* value of 1.96 indicates that the local mean of the percentage of forest exposed to mortality-causing or defoliation-causing agents for a hexagon and its 18 neighbors is approximately two standard deviations greater than the mean expected in the absence of spatial clustering, while a G_i^* value of -1.96 indicates that the local mortality or defoliation mean for a hexagon and its 18 neighbors is approximately two standard deviations less than the mean expected in the absence of spatial clustering. Values between -1.96 and 1.96 have no statistically significant concentration of high or low values. In other words, when a hexagon has a G_i^* value between -1.96 and 1.96, mortality or defoliation damage within it and its 18 neighbors is not statistically different from a normal

expectation. As described in Laffan (2006), it is calculated as:

$$G_i^*(d) = \frac{\sum_j w_{ij}(d)\,x_j - W_i^* \bar{x}^*}{s^* \sqrt{\frac{(n s_{1i}^*) - W_i^{*2}}{n-1}}}$$

where

G_i^* = the local clustering statistic (in this case, for the target hexagon)

i = the center of local neighborhood (the target hexagon)

d = the width of local sample window (the target hexagon and its first- and second-order neighbors)

x_j = the value of neighbor j

w_{ij} = the weight of neighbor j from location i (all the neighboring hexagons in the moving window were given an equal weight of 1)

n = number of samples in the dataset (the 4,303 hexagons containing >5 percent tree cover and with at least 1 percent of the canopy cover surveyed)

W_i^* = the sum of the weights

s_{1i}^* = the number of samples within d of the central location (19: the focal hexagon and its 18 first- and second-order neighbors)

$\bar{x}^*$ = mean of whole dataset (in this case, the 4,303 hexagons)

s^* = the standard deviation of whole dataset (for the 4,303 hexagons)

It is worth noting that the -1.96 and 1.96 threshold values are not exact because the correlation of spatial data violates the assumption of independence required for statistical significance (Laffan 2006). The Getis-Ord approach does not require that the input data be normally distributed because the local G_i^* values are computed under a randomization assumption, with G_i^* equating to a standardized z-score that asymptotically tends to a normal distribution (Anselin 1992). The z-scores are reliable, even with skewed data, as long as the distance band used to define the local sample around the target observation is large enough to include several neighbors for each feature (ESRI 2015).

RESULTS AND DISCUSSION

Conterminous United States Mortality

The national IDS survey data identified 56 different mortality-causing agents and complexes on approximately 2.13 million ha across the conterminous United States in 2018, slightly less than the combined land area of New Jersey and Rhode Island. By way of comparison, forests are estimated to cover approximately 252 million ha of the conterminous 48 States (Smith and others 2009). Twenty-two of the agents were detected on >5000 ha.

Fir engraver (*Scolytus ventralis*) was the most widespread mortality agent in 2018, detected on approximately 786 000 ha (table 2.1), or about 37 percent of the total mortality area, followed by emerald ash borer, which was identified on about 338 000 ha. Four other mortality agents

Table 2.1—Mortality agents and complexes affecting >5000 ha in the conterminous United States during 2018

Agents/complexes causing mortality, 2018	Area
	ha
Fir engraver	785 581
Emerald ash borer	337 618
Spruce beetle	143 342
Unknown bark beetle[a]	134 310
Mountain pine beetle	124 236
Western pine beetle	115,689
Eastern larch beetle	73 671
Douglas-fir beetle	56 390
Balsam woolly adelgid	48 072
Unknown	46 492
Sudden oak death	42 771
Jeffrey pine beetle	40 109
Flatheaded fir borer	31 088
Oak decline	24 260
Root disease and beetle complex	23 585
Twolined chestnut borer	22 689
Gypsy moth	22 187
Beech bark disease complex	16 629
Western balsam bark beetle	16 386
Pinyon ips	10 932
Southern pine beetle	9572
Ips engraver beetles	5689
Other (34)	21 802
Total, all mortality agents	**2 126 526**

Note: All values are "footprint" areas for each agent or complex. The sum of the individual agents is not equal to the total for all agents due to the reporting of multiple agents per polygon.

[a] In the Interior West, this is primarily damage on ponderosa pines. The group of bark beetles is known and varied, but not distinguishable from the air. Regions have characterized it as "Southwest bark beetle complex" consisting mainly of damage caused by roundheaded pine beetle, western pine beetle, and ips beetles.

and complexes were detected on >100 000 ha: spruce beetle (*D. rufipennis*) on 143 000 ha, unknown bark beetle on 134 000 ha (mostly damage on ponderosa pines [*Pinus ponderosa*] in the Interior West by a list of different bark beetles that are not possible to distinguish from the air), mountain pine beetle (*D. ponderosae*) on 124 000 ha, and western pine beetle (*D. brevicomis*) on 116 000 ha. Mortality from the western bark beetle group, which encompasses 16 different agents in the IDS data (table 2.2), was detected on approximately 1.43 million ha in 2018, representing about two-thirds of the total area on which mortality was recorded across the conterminous States.

The FHM West Coast region had the largest area on which mortality agents and complexes were detected, about 1.08 million ha (table 2.3). Approximately two-thirds of this area (721 000 ha) was exposed to fir engraver mortality. Twenty-two other mortality-causing agents and complexes were recorded, with the most widespread being western pine beetle (10.3 percent of the mortality area), mountain pine beetle (8.0 percent), sudden oak death (3.9 percent), and Jeffrey pine beetle (*D. jeffreyi*, 3.7 percent).

When estimating the amount of mortality occurring within the footprint of mortality in the West Coast region, we found that mortality was detected on 1.98 percent of the surveyed tree canopy area in the M261E–Sierra Nevada ecoregion section in California (fig. 2.2) as a result of infestation by fir engraver in red fir

Table 2.2—Beetle taxa included in the "western bark beetle" group

Western bark beetle mortality agents	
Common name	Scientific name
Cedar and cypress bark beetles	*Phloeosinus* spp.
Douglas-fir beetle	*Dendroctonus pseudotsugae*
Douglas-fir engraver	*Scolytus unispinosus*
Fir engraver	*Scolytus ventralis*
Ips engraver beetles	*Ips* spp.
Jeffrey pine beetle	*Dendroctonus jeffreyi*
Mountain pine beetle	*Dendroctonus ponderosae*
Pine engraver	*Ips pini*
Pinyon ips	*Ips confuses*
Root disease and beetle complex	N/A
Roundheaded pine beetle	*Dendroctonus adjunctus*
Silver fir beetle	*Pseudohylesinus sericeus*
Spruce beetle	*Dendroctonus rufipennis*
Unknown bark beetle	N/A
Western balsam bark beetle	*Dryocoetes confuses*
Western pine beetle	*Dendroctonus brevicomis*

(*Abies magnifica*) and white fir (*A. concolor*), and to a lesser degree by Jeffrey pine beetle, mountain pine beetle, and western pine beetle in pine species. The same agents resulted in 0.86 and 0.78 percent of surveyed canopy cover mortality in two ecoregion sections immediately north of the Sierra Nevada, M261D–Southern Cascades and M261G–Modoc Plateau, respectively. In the hot spot analysis encompassing the entire conterminous United States, a geographic hot spot of high mortality was detected in M261E–Sierra Nevada, while hot spots of moderate mortality were identified in neighboring ecoregions, including M261D–Southern Cascades and M261G–Modoc Plateau (fig. 2.3A). Similar hot spots were identified in the analysis limited to the West Coast FHM region (fig. 2.3B).

Elsewhere in the West Coast region, the M332G–Blue Mountains ecoregion section of northeastern Oregon had mortality on 0.66 percent of the surveyed tree canopy cover, as a result of fir engraver, western pine beetle, mountain pine beetle, and Douglas-fir beetle (*D. pseudotsugae*). Moderate-mortality hot spots were identified in this ecoregion section, both in the analyses of the conterminous States and of the West Coast FHM region.

Sudden oak death in tanoak (*Notholithocarpus densiflorus*), as well as some flatheaded fir borer (*Phaenops drummondi*) in Douglas-fir, resulted in 0.65 percent mortality of surveyed canopy area in 263A–Northern California Coast. Sudden oak death, along with a suite of bark beetles, was also an important mortality agent in 261A–Central California Coast (0.43 percent mortality) and M261B–Northern California Coast Ranges (0.40 percent mortality). A moderate-mortality hot spot associated with sudden oak death was detected in these ecoregion sections. Meanwhile, mountain pine beetle in lodgepole pine (*P. contorta*) was the primary factor in the respective 0.46 and 0.29 percent mortality in the surveyed canopy areas of M333A–Okanogan Highland and M242D–Northern Cascades in northern Washington. A variety of pine beetles, especially pinyon ips (*Ips confusus*) in singleleaf

Table 2.3—The top five mortality agents or complexes for each Forest Health Monitoring region, and for Alaska and Hawaii, in 2018

Mortality agents and complexes, 2018	Area
	ha
Interior West	
Spruce beetle	142 872
Unknown bark beetle[a]	133 036
Fir engraver	64 328
Balsam woolly adelgid	43 625
Douglas-fir beetle	37 791
Other mortality agents (19)	100 464
Total, all mortality agents and complexes	**517 183**
North Central	
Emerald ash borer	323 707
Eastern larch beetle	73 671
Oak decline	23 713
Beech bark disease complex	16 629
Unknown	1528
Other mortality agents (10)	2181
Total, all mortality agents and complexes	**440 926**
North East	
Twolined chestnut borer	22 280
Gypsy moth	22 187
Emerald ash borer	11 271
Southern pine beetle	5214
Unknown	2409
Other mortality agents (16)	6969
Total, all mortality agents and complexes	**70 060**
South	
Southern pine beetle	4358
Ips engraver beetles	4163
Emerald ash borer	2639
Unknown	2062
Unknown bark beetle	166
Other mortality agents (1)	<1
Total, all mortality agents and complexes	**13 365**

Mortality agents and complexes, 2018	Area
	ha
West Coast	
Fir engraver	721 252
Western pine beetle	111 946
Mountain pine beetle	86 702
Sudden oak death	42 771
Jeffrey pine beetle	40 107
Other mortality agents (18)	103 057
Total, all mortality agents and complexes	**1 084 994**
Alaska	
Spruce beetle	239 799
Yellow-cedar decline	7171
Unknown canker	2287
Northern spruce engraver	661
Western balsam bark beetle	45
Other mortality agents (2)	16
Total, all mortality agents and complexes	**249 976**
Hawaii	
Unknown	46 054
Total, all mortality agents and complexes	**46 054**

Note: The total area affected by other agents is listed at the end of each section. All values are "footprint" areas for each agent or complex. The sum of the individual agents is not equal to the total for all agents due to the reporting of multiple agents per polygon.

[a] In the Interior West, this is primarily damage on ponderosa pines. The group of bark beetles is known and varied, but not distinguishable from the air. Regions have characterized it as "Southwest bark beetle complex" consisting mainly of damage caused by roundheaded pine beetle, western pine beetle, and ips beetles.

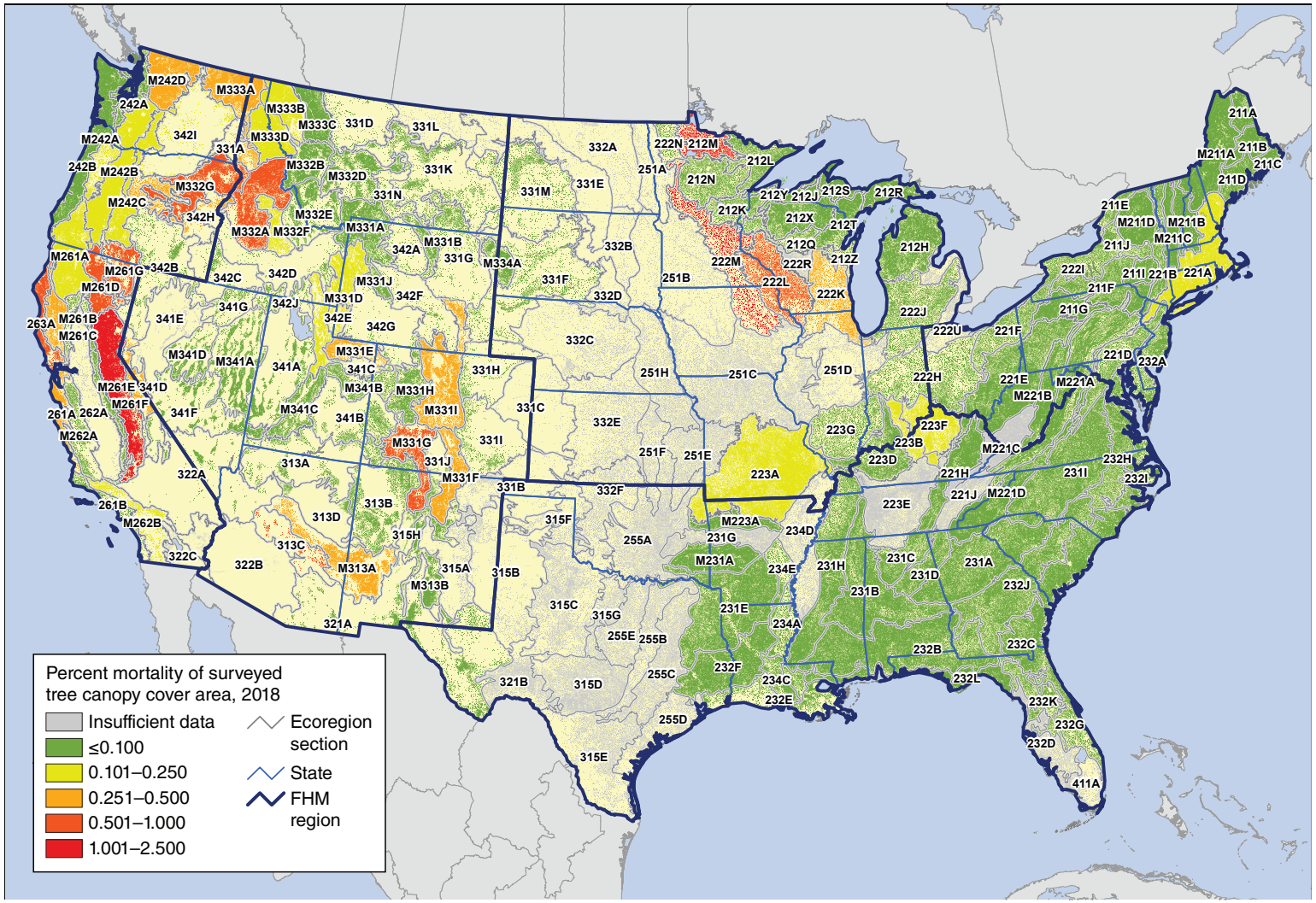

Figure 2.2—The percent of surveyed tree canopy cover area with insect and disease mortality, by ecoregion section within the conterminous 48 States, for 2018. The gray lines delineate ecoregion sections (Cleland and others 2007). The 240-m tree canopy cover is based on data from a cooperative project between the Multi-Resolution Land Characteristics Consortium (Coulston and others 2012) and the Forest Service Geospatial Technology and Applications Center using the 2011 National Land Cover Database. (Data source: U.S. Department of Agriculture Forest Service, Forest Health Protection)

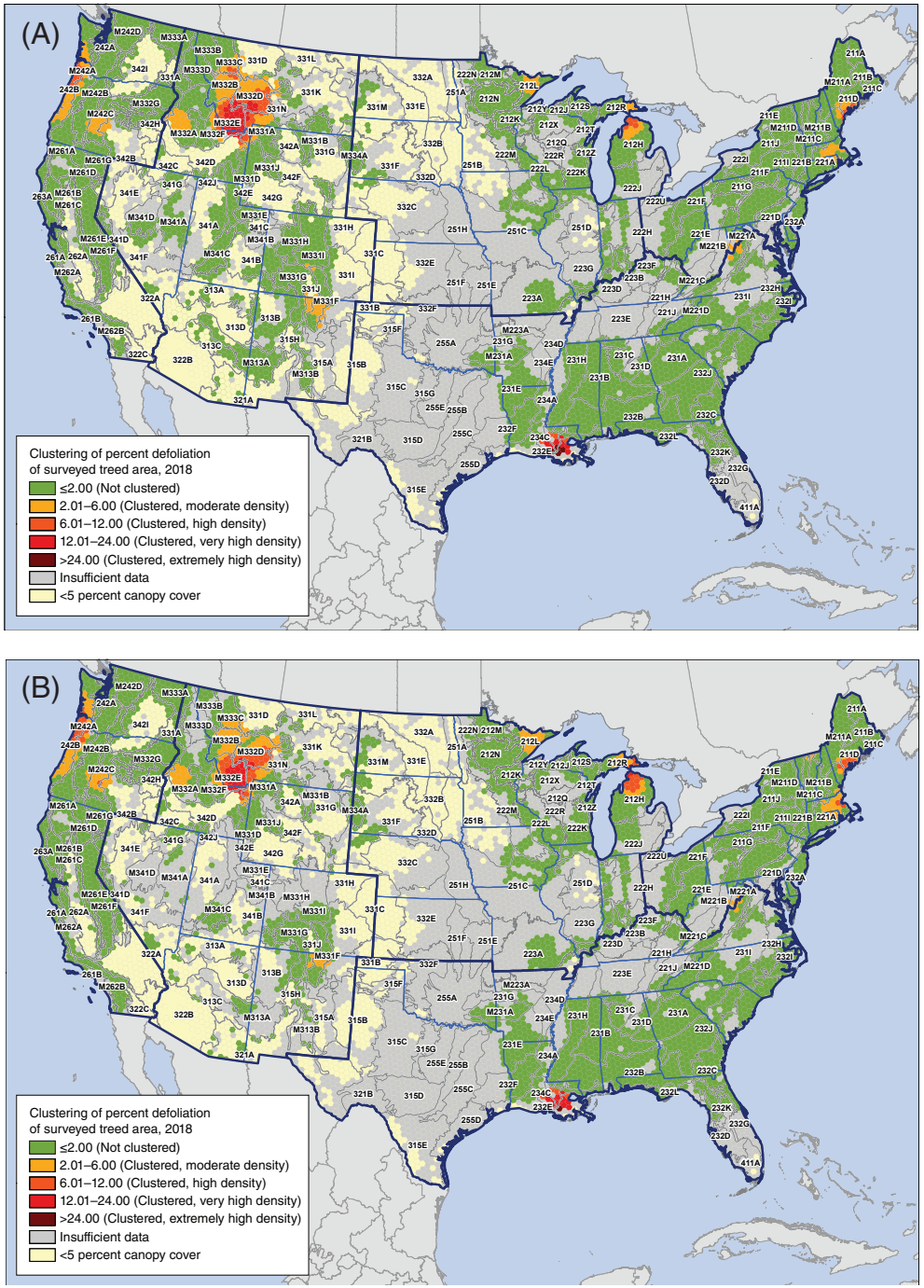

Figure 2.3—Hot spots of percent of surveyed tree canopy cover area with insect and disease mortality in 2018 for (A) the conterminous 48 States and (B) for separate Forest Health Monitoring regions, by hexagons containing >5 percent tree canopy cover. Values are Getis-Ord Gi* *scores, with values >2 representing significant clustering of high mortality occurrence densities and values <-2 representing significant clustering of low mortality occurrence densities. The gray lines delineate ecoregion sections (Cleland and others 2007), and blue lines delineate Forest Health Monitoring regions. Tree canopy cover is based on data from a cooperative project between the Multi-Resolution Land Characteristics Consortium (Coulston and others 2012) and the Forest Service Geospatial Technology and Applications Center using the 2011 National Land Cover Database. (Data source: U.S. Department of Agriculture Forest Service, Forest Health Protection)*

pinyon (*P. monophylla*), caused the 0.26 percent mortality of surveyed canopy area in 341D–Mono in east-central California.

Twenty-four mortality-causing agents and complexes were detected across 517 000 ha of the FHM Interior West region in 2018 (table 2.3). Of this mortality footprint, about 28 percent was attributed to spruce beetle (143 000 ha) and 26 percent to unknown bark beetles (133 000 ha). Other widespread mortality agents were fir engraver detected on 64 000 ha (12.4 percent), balsam woolly adelgid (*Adelges piceae*) on 44 000 ha (8.4 percent), and Douglas-fir beetle on 38 000 ha (7.3 percent) (table 2.3).

The estimate of the percent of mortality within the mortality footprint of the region, meanwhile, indicated that three ecoregion sections in the Interior West experienced 0.501 to 1 percent of mortality of surveyed tree canopy cover (fig. 2.2). In central Arizona, the 313C–Tonto Transition ecoregion section had 0.74 percent mortality, mostly caused by an unknown bark beetle infesting ponderosa pine. The M332A–Idaho Batholith ecoregion section in central Idaho experienced 0.52 percent mortality of surveyed tree cover as a result of spruce beetle mortality in Engelmann spruce (*Picea engelmannii*), mountain pine beetle mortality in lodgepole pine, Douglas-fir beetle mortality in Douglas-fir, and balsam woolly adelgid and root disease and beetle complex in subalpine fir (*Abies lasiocarpa*). Finally, the mortality detected in M331G–South-Central Highlands in southwestern Colorado and north-central New Mexico (>0.50 percent) was caused mostly by spruce beetle in Engelmann spruce and Douglas-fir beetle in Douglas-fir.

The conterminous States hot spot analysis revealed three moderate-mortality hot spots in the region: M332A–Idaho Batholith in central Idaho, M331G–South-Central Highlands in Colorado and New Mexico, and 313C–Tonto Transition in Arizona (fig. 2.3A). In the regional analysis, each of these was a high-mortality hot spot, with additional moderate hot spots found in Colorado (M331I–Northern Parks and Ranges; spruce beetle and western balsam bark beetle), Utah (M331E–Uinta Mountains and M331D–Overthrust Mountains; spruce beetle and root disease and beetle complex), and Arizona (322A–Mojave Desert; pinyon ips and unknown bark beetle) (fig. 2.3B).

In 2018, surveyors recorded approximately 441 000 ha with damage in the FHM North Central region, with approximately three-fourths of the mortality attributed to emerald ash borer (324 000 ha) (table 2.3). Of the other 14 mortality agents recorded, eastern larch beetle (*Dendroctonus simplex*) was the most widespread (16.7 percent of the mortality area), followed by oak decline (5.4 percent), and beech bark disease complex (3.8 percent).

The ecoregion section with the greatest mortality of surveyed tree canopy cover was 212M–Northern Minnesota and Ontario, where eastern larch beetle resulted in 2.05 percent mortality of surveyed tree canopy cover

(fig. 2.2). Emerald ash borer was the most important mortality agent in 222M–Minnesota and Northeast Iowa Morainal-Oak Savannah (1.39 percent mortality), 222L–North Central U.S. Driftless and Escarpment (0.73 percent mortality), and 222K–Southwestern Great Lakes Morainal (0.43 percent). Oak decline was relatively widely detected in south-central Indiana (223B–Interior Low Plateau-Transition Hills and 223D–Interior Low Plateau) and southern Missouri (223A–Ozark Highlands).

In the analysis of the conterminous States, three geographic hot spots of very high mortality associated with emerald ash borer were detected in 251C–Central Dissected Till Plains of southeastern Iowa; 222M–Minnesota and Northeast Iowa Morainal-Oak Savannah of northeastern Iowa; and 222L–North Central U.S. Driftless and Escarpment of southwestern Wisconsin, northeastern Iowa, and southeastern Minnesota (fig. 2.3A). A hot spot of high mortality, meanwhile, was associated with eastern larch beetle in 212M–Northern Minnesota and Ontario. The same hot spots were revealed in the analysis focusing on the North Central FHM region but were of lower intensity (fig. 2.3B).

In the North East FHM region, mortality in 2018 was recorded on approximately 70 000 ha, attributed to 21 mortality agents and complexes (table 2.3). Two agents, twolined chestnut borer (*Agrilus bilineatus*) and gypsy moth, accounted for a nearly identical amount of this mortality (approximately 31 percent each), while emerald ash borer was associated with 16.1 percent.

The only ecoregion in the North East FHM region with >0.1 percent mortality of its surveyed treed area (0.13 percent) was 221A–Lower New England, where twolined chestnut borer in red oak stands was detected in Rhode Island, emerald ash borer was found in Connecticut, and gypsy moth was identified in Connecticut and Massachusetts (fig. 2.2). No mortality hot spots were revealed in the region in the analysis encompassing the conterminous States (fig. 2.3A), but a hot spot in the regional analysis spanned Long Island Sound, including the gypsy moth and emerald ash borer mortality in Connecticut to the north and southern pine beetle mortality in pitch pine (*P. rigida*) on Long Island to the south (fig. 2.3B).

In the South FHM region, surveyors identified 13 000 ha of mortality from six agents (table 2.3). Southern pine beetle was the most commonly detected agent, on 4400 ha (32.6 percent), followed closely by ips engraver beetles (4200 ha, 31.6 percent). Emerald ash borer was found on an additional 2600 ha (19.7 percent).

No ecoregions in the South had mortality exceeding 0.1 percent as a result of mortality within the region (fig. 2.2). (Three ecoregions exceeded this threshold because of mortality in the neighboring North Central region.) No mortality hot spots were identified in the analysis of the conterminous States (fig. 2.3A), but several were detected in the regional hot spot analysis (fig. 2.3B). Three of these hot spots were associated with southern pine beetle, in south-central Mississippi (231B–Coastal Plains-Middle and 232B–Gulf Coastal Plains and Flatwoods);

southwestern Mississippi and eastern Louisiana (231H–Coastal Plains-Loess); and western North Carolina (M221D–Blue Ridge Mountains). A hot spot in central Arkansas (M231A–Ouachita Mountains and 231G–Arkansas Valley) was caused by ips engraver beetles, while another in northern Kentucky (223F–Interior Low Plateau-Bluegrass and 221E–Southern Unglaciated Allegheny Plateau) was the result of emerald ash borer infestation. Finally, the agent or agents causing a hot spot in northeastern North Carolina and southeastern Virginia (232I–Northern Atlantic Coastal Flatwoods) were reported as unknown by surveyors.

Conterminous United States Defoliation

In 2018, the national IDS survey identified 56 defoliation agents and complexes affecting approximately 1.72 million ha across the conterminous United States (table 2.4), an area similar to the land area of Connecticut and Delaware combined. The most widespread defoliation agent was western spruce budworm (*Choristoneura freemani*), detected on approximately 654 000 ha, or 38 percent of the total area with defoliation. Five other agents were also detected on >100 000 ha each: forest tent caterpillar (*Malacosoma disstria*) on 289 000 ha, Swiss needle cast on 199 000 ha, gyspy moth on 156 000 ha, and baldcypress leafroller (*Archips goyerana)* on 137 000 ha (table 2.4).

In 2018, the Interior West was the FHM region with the largest area on which defoliation agents were detected, with 20 defoliators identified on approximately 774 000 ha (table 2.5). Of this area, 84.2 percent

Table 2.4—Defoliation agents and complexes affecting >5000 ha in the conterminous United States in 2018

Agents/complexes causing defoliation, 2018	Area
	ha
Western spruce budworm	654 521
Forest tent caterpillar	289 136
Swiss needle cast	199 143
Gypsy moth	155 871
Baldcypress leafroller	136 741
Spruce budworm	90 474
Pandora moth	58 894
Browntail moth	55 130
Douglas-fir tussock moth	49 433
Unknown defoliator	46 203
White pine needle damage	19 267
Balsam woolly adelgid	14 613
Pinyon needle scale	10 835
Unknown	8417
Walkingstick	7857
Larch casebearer	7814
Spruce aphid	7355
Marssonina blight	7147
Scarlet oak sawfly	6843
Other (37)	24 167
Total, all defoliation agents	**1 722 675**

Note: All values are "footprint" areas for each agent or complex. The sum of the individual agents is not equal to the total for all agents due to the reporting of multiple agents per polygon.

Table 2.5—The top five defoliation agents or complexes for each Forest Health Monitoring region and for Alaska in 2018

Defoliation agents and complexes, 2018	Area
	ha
Interior West	
Western spruce budworm	651 491
Unknown defoliator	45 855
Douglas-fir tussock moth	44 883
Pinyon needle scale	10 824
Spruce aphid	7355
Other defoliation agents (15)	14 852
Total, all defoliation agents and complexes	**774 191**
North Central	
Forest tent caterpillar	119 128
Spruce budworm	90 474
Larch casebearer	6920
Unknown	4106
Gypsy moth	2671
Other defoliation agents (8)	3444
Total, all defoliation agents and complexes	**226 743**
North East	
Gypsy moth	143 361
Browntail moth	55 130
Forest tent caterpillar	32 805
White pine needle damage	19 267
Cherry scallop shell moth	2823
Other defoliation agents (11)	4565
Total, all defoliation agents and complexes	**257 861**

Defoliation agents and complexes, 2018	Area
	ha
South	
Forest tent caterpillar	136 802
Baldcypress leafroller	136 741
Gypsy moth	9839
Walkingstick	7857
Scarlet oak sawfly	6843
Other defoliation agents (2)	2241
Total, all defoliation agents and complexes	**170 680**
West Coast	
Swiss needle cast	199 143
Pandora moth	58 894
Balsam woolly adelgid	14 613
Douglas-fir tussock moth	4550
Larch needle cast	3932
Other defoliation agents (20)	8452
Total, all defoliation agents and complexes	**293 200**
Alaska	
Aspen leafminer	97 058
Birch leafminer	43 951
Unknown defoliator	25 590
Hemlock sawfly	19 655
Willow leaf blotchminer	14 473
Other defoliation agents (6)	4289
Total, all defoliation agents and complexes	**201 200**

Note: The total area affected by other agents is listed at the end of each section. All values are "footprint" areas for each agent or complex. The sum of the individual agents is not equal to the total for all agents due to the reporting of multiple agents per polygon.

was affected by western spruce budworm (651 000 ha). No other agent accounted for >6 percent of the total defoliated area in the region.

Ecoregion sections in the northern Rockies were particularly affected by western spruce budworm in 2018, with 7.1 percent of surveyed tree canopy area defoliated in M332E–Beaverhead Mountains in central Idaho and southwestern Montana, and with 3.9 percent of the M332D–Belt Mountains and 2.7 percent of the M332B–Northern Rockies and Bitterroot Valley, respectively, defoliated in western Montana (fig. 2.4). This outbreak in stands of subalpine fir and Douglas-fir was reflected in a hot spot of very high defoliation in the analyses both for the entire conterminous States (fig. 2.5A) and for the Interior West region (fig. 2.5B). Farther south, in south-central Colorado and northern New Mexico, western spruce budworm was the source of hot spots of moderate defoliation in M331F–Southern Parks and Rocky Mountain Range.

In west-central Idaho, meanwhile, Douglas-fir tussock moth (*Orgyia pseudotsugata*) was the source of a hot spot of moderate defoliation in M332A–Idaho Batholith (fig. 2.5), where 1.6 percent of surveyed tree canopy area was defoliated (fig. 2.4).

The West Coast FHM region recorded 25 defoliating agents on 293 000 ha (table 2.5). Swiss needle cast (caused by the fungus *Phaeocryptopus gaeumannii*) was the most widely reported, encompassing 68 percent of the total defoliated area (199 000 ha). Other widespread defoliation agents included pandora moth (*Coloradia pandora*) (59 000 ha, 20.1 percent) and balsam woolly adelgid (15 000 ha, 5.0 percent).

As a result of Swiss needle cast, a native disease that defoliates Douglas-fir, a hot spot of high defoliation was detected along the coast of Oregon and Washington (M242A–Oregon and Washington Coast Ranges) (fig. 2.5), an ecoregion section that experienced 3.6 percent defoliation of surveyed tree canopy area (fig. 2.4). An additional hot spot in central Oregon in the M242C–Eastern Cascades ecoregion section (of moderate defoliation in both the conterminous States and West Coast region analysis) was caused by an outbreak of pandora moth in ponderosa and lodgepole pine stands.

In the North East region, gypsy moth was the most widely identified defoliation agent among the 16 detected across 258 000 ha in 2018 (table 2.5). It was found on approximately 143 000 ha (55.6 percent of the total defoliated area), followed by browntail moth (*Euproctis chrysorrhoea*) on 55 000 ha (21.4 percent), forest tent caterpillar on 33 000 ha (12.7 percent), and white pine needle damage on 19 000 ha (7.5 percent).

The 211D–Central Maine Coastal Embayment ecoregion section had the highest defoliation of surveyed tree cover in the region (2.9 percent), as a result of browntail moth infestation of northern red oak (*Quercus rubra*) (fig. 2.4). Defoliation was 1.1 percent of surveyed canopy cover area, meanwhile, in neighboring 221A–Lower New England, where gypsy moth

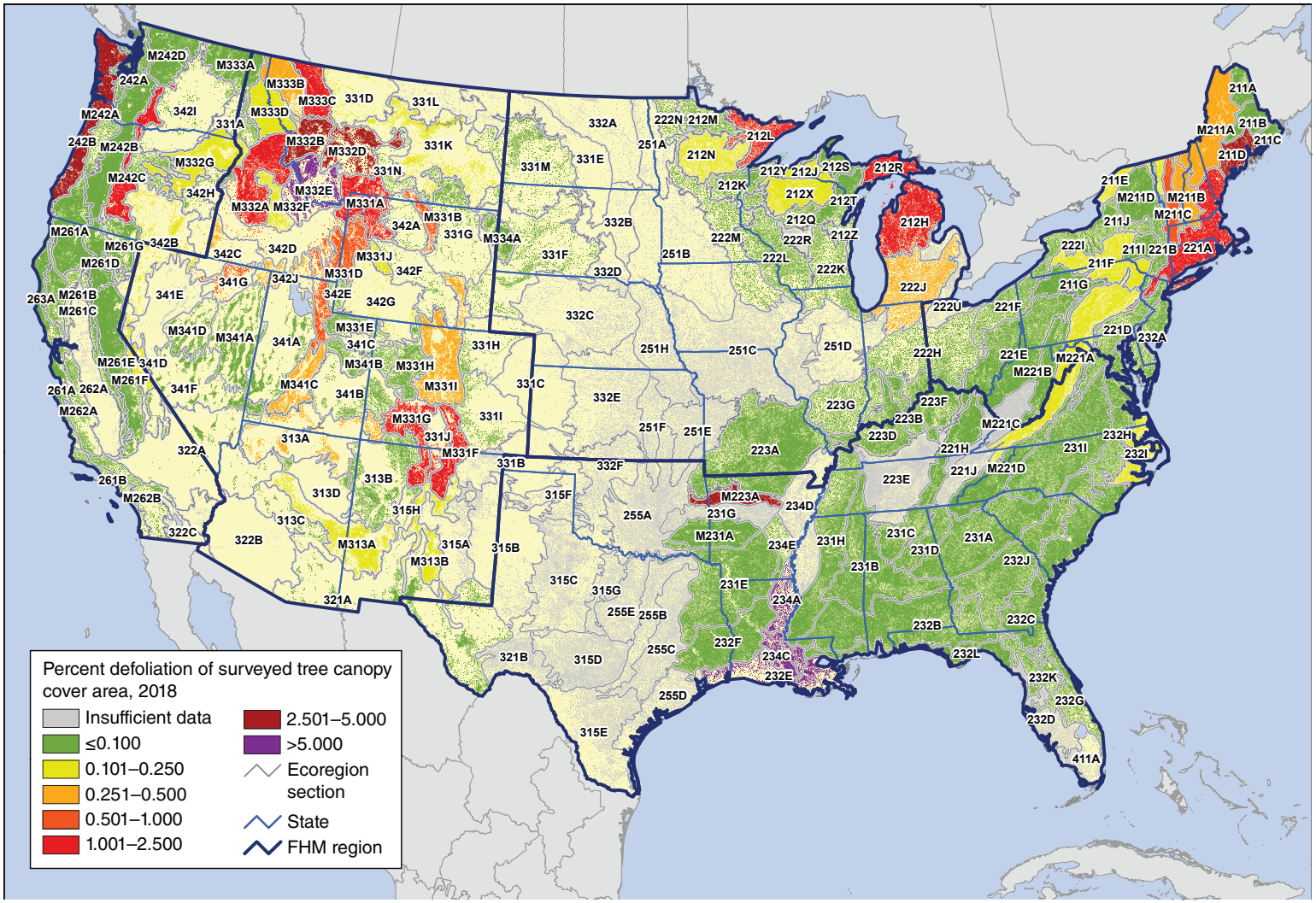

Figure 2.4—The percent of surveyed tree canopy cover area with insect and disease defoliation, by ecoregion section within the conterminous 48 States, for 2018. The gray lines delineate ecoregion sections (Cleland and others 2007). The 240-m tree canopy cover is based on data from a cooperative project between the Multi-Resolution Land Characteristics Consortium (Coulston and others 2012) and the Forest Service Geospatial Technology and Applications Center using the 2011 National Land Cover Database. (Data source: U.S. Department of Agriculture Forest Service, Forest Health Protection)

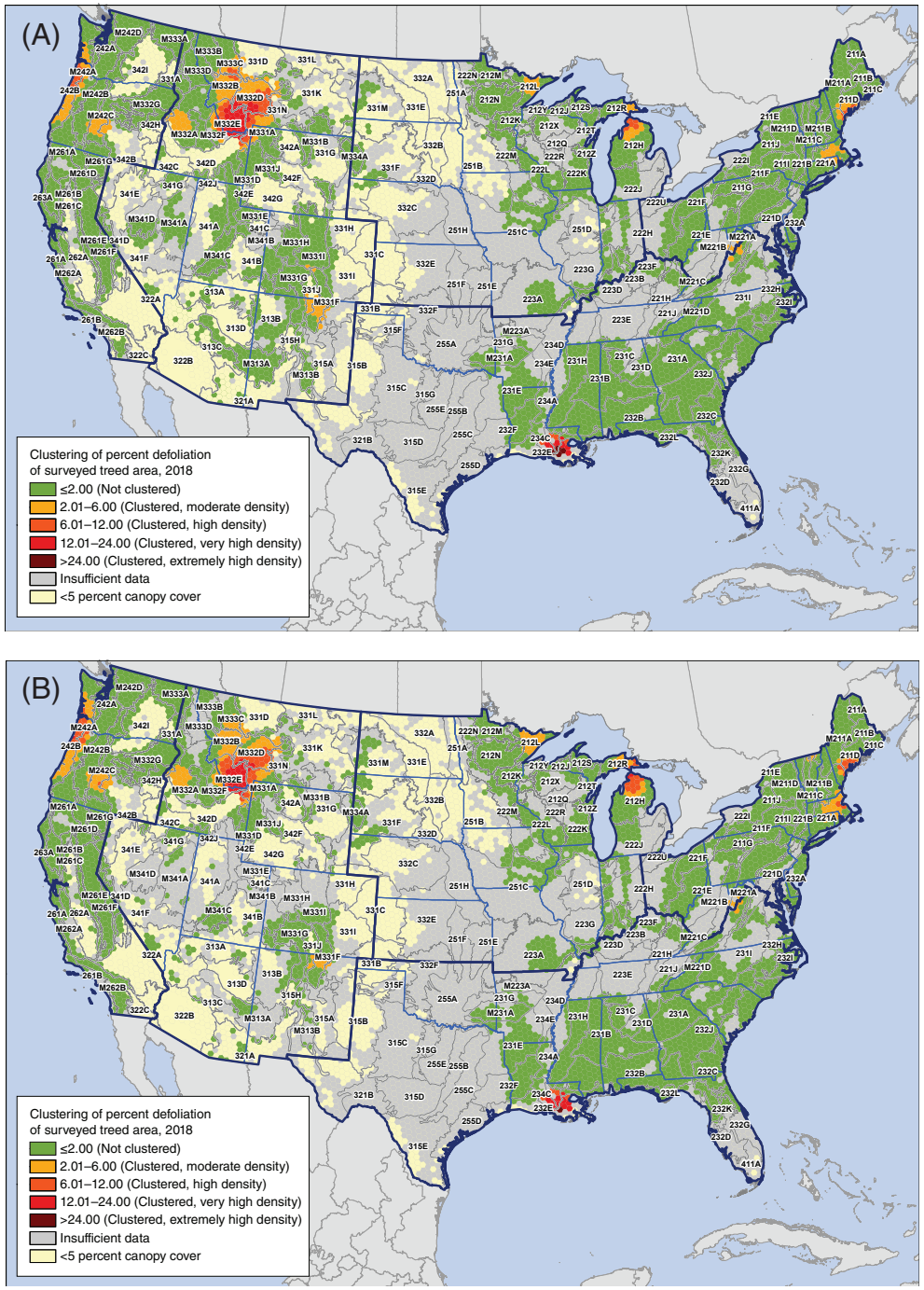

Figure 2.5—Hot spots of percent of surveyed tree canopy cover area with insect and disease defoliation in 2018 for (A) the conterminous 48 States and (B) for separate Forest Health Monitoring regions, by hexagons containing >5 percent tree canopy cover. Values are Getis-Ord Gi* *scores, with values >2 representing significant clustering of high defoliation occurrence densities. (No areas of significant clustering of low densities, <-2, were detected.) The gray lines delineate ecoregion sections (Cleland and others 2007), and blue lines delineate Forest Health Monitoring regions. Tree canopy cover is based on data from a cooperative project between the Multi-Resolution Land Characteristics Consortium (Coulston and others 2012) and the Forest Service Geospatial Technology and Applications Center using the 2011 National Land Cover Database. (Data source: U.S. Department of Agriculture Forest Service, Forest Health Protection)*

was widespread in hardwood stands. These two ecoregion sections were the locations of hot spots of high and moderate defoliation, respectively (fig. 2.5).

White pine needle damage in stands of eastern white pine (*P. strobus*) and forest tent caterpillar in hardwood forests in New England resulted in 0.6 percent defoliation of surveyed canopy area in M211C–Green-Taconic-Berkshire Mountains, 0.4 percent in M211A–White Mountains, and 0.3 percent in M211B–New England Piedmont (fig. 2.4). Additionally, gypsy moth activity resulted in a hot spot of moderate defoliation along the border of West Virginia and Virginia (fig. 2.5).

Thirteen agents and complexes, meanwhile, were associated with approximately 227 000 ha with defoliation in the North Central FHM region (table 2.5). Forest tent caterpillar and spruce budworm (*Choristoneura fumiferana*) were the most commonly detected defoliators, representing 52.5 percent and 39.9 percent of the total defoliation in the region (119 000 ha and 90 000 ha, respectively). Larch casebearer (*Coleophora laricella*) was also somewhat widespread (7000 ha, or 3.1 percent of the total area with defoliation).

A handful of ecoregion sections in the Great Lakes States exhibited the highest levels of defoliation (fig. 2.4):

- In northern Michigan, forest tent caterpillar caused 1.9 percent defoliation of surveyed canopy cover area in 212R–Eastern Upper Peninsula and 1.7 percent in 212H–Northern Lower Peninsula.
- In northeastern Minnesota, spruce budworm resulted in 1.6 percent defoliation in 212L–Northern Superior Uplands.
- In southern Michigan, gypsy moth was associated with defoliation on 0.3 percent of the surveyed tree canopy area in 222J–South Central Great Lakes.

The national (fig. 2.5A) and regional (fig. 2.5B) analyses revealed hot spots of high to very high defoliation in northern Michigan, and of moderate defoliation in northeastern Minnesota.

During 2018, surveyors documented about 171 000 ha with defoliation in the South (table 2.5), with both forest tent caterpillar and baldcypress leafroller (*Archips goyerana*) detected on about 137 000 ha, or 80 percent of the area with defoliation. (Both agents were reported together across large areas of southern Louisiana.) Gypsy moth was recorded on an additional 10 000 ha (5.8 percent).

The ecoregion sections nationally with the highest and third highest percent defoliation were in southern Louisiana: 234C–Atchafalaya and Red River Alluvial Plains (16.1 percent) and 232E–Louisiana Coastal Prairie and Marshes (7.1 percent) (fig. 2.4). Baldcypress leafroller and forest tent caterpillar were the major defoliation agents here and were the causes of the hot spots of extremely high defoliation in the same area, revealed by the analyses of both the entire conterminous United States and the South (fig. 2.5). Relatively high defoliation (3.3 percent)

was also found in M223A–Boston Mountains in northern Arkansas, as a result of an infestation of walkingstick (*Diapheromera femorata*) in hardwood forests there (fig. 2.4).

Alaska and Hawaii

In Alaska, seven mortality agents and complexes were detected on 250 000 ha in 2018 (table 2.3). As in recent years, spruce beetle was the most widely detected mortality agent, encompassing 95.9 percent of the total area with mortality (240 000 ha). A much smaller area of yellow-cedar (*Chamaecyparis nootkatensis*) decline was detected (7000 ha, 2.9 percent of the total). Surveyors attributed a further 2000 ha with mortality to an unknown canker on quaking aspen (*Populus tremuloides*).

An extensive outbreak of spruce beetle caused 133A–Cook Inlet Basin, in the south-central part of the State, to have the highest mortality of surveyed forest and shrubland (1.7 percent) (fig. 2.6). The spruce beetle infestation extended into the neighboring M243B–Alaska Peninsula and M133B–Alaska Range Extension ecoregion sections (0.4 percent mortality in each).

Also in 2018, Alaska surveyors identified 11 defoliators on 201 000 ha (table 2.5). Almost half of the area with defoliation (97 000 ha, 48.2 percent) was attributed to aspen leafminer (*Phyllocnistis populiella*). The next most commonly detected defoliation agent was birch leafminer (*Fenusa pusilla*) on 44 000 ha (21.8 percent). Almost 13 percent of the area with defoliation was associated with an unknown defoliator (26 000 ha), while 9.8 percent was caused by hemlock sawfly (*Neodiprion tsugae*, 20 000 ha) and 7.2 percent with willow leaf blotchminer (*Micrurapteryx salicifoliella*, 14 000 ha).

Defoliation was relatively high across much of Alaska in 2018, particularly the central part of the State. Defoliation was highest in 132C–Tanana-Kuskokwim Lowlands, slightly more than 2.5 percent of surveyed forest and shrubland (fig. 2.7), where aspen leafminer was prevalent. Damage from aspen leafminer was also commonly found in nearby M132C–Yukon-Tanana Uplands (1.2 percent defoliation) and 133B–Copper River Basin (slightly more than 1.0 percent). Willow leaf blotchminer was the most widespread defoliation agent, along with aspen leafminer, in 132A–Yukon-Old Crow Basin (1.9 percent defoliation). In 133A–Cook Inlet Basin (1.8 percent defoliation) of south-central Alaska, birch leafminer was the primary defoliator. In the southwestern part of the State, speckled green fruitworm (*Orthosia hibisci*) was the most commonly detected defoliation agent in M131B–Ahklun Mountains (just more than 1.0 percent defoliation).

In Hawaii, meanwhile, approximately 46 000 ha with mortality were delineated in 2018 (table 2.3). None of this mortality was assigned to an agent, but at least some of this was likely caused by rapid ʻōhiʻa death, a wilt disease that affects ʻōhiʻa lehua (*Metrosideros polymorpha*), a highly ecologically and culturally important tree in Hawaiian native forests (University of Hawai'i 2019). Rapid ʻōhiʻa death is caused by the fungal pathogens *Ceratocystis lukuohia* and

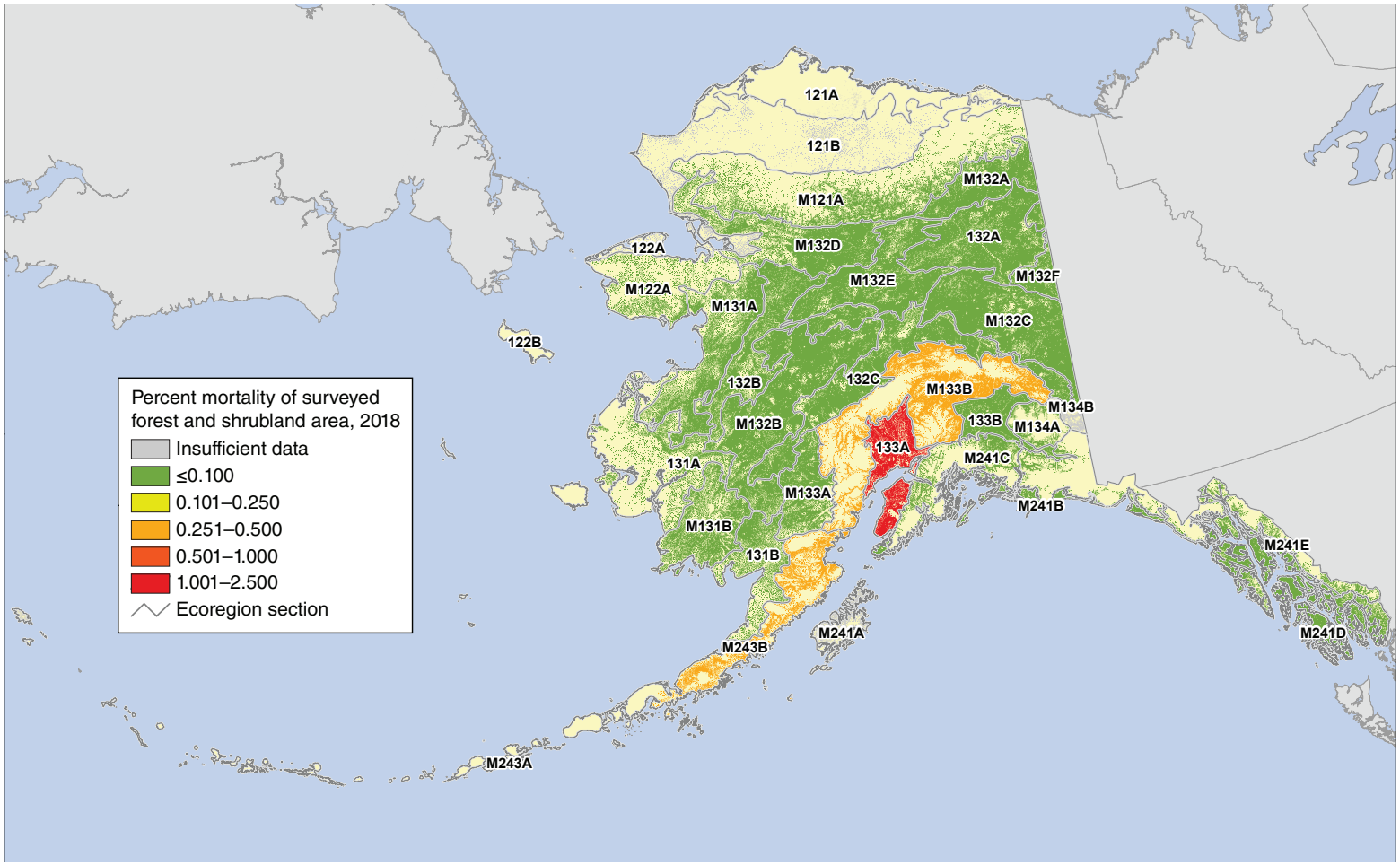

Figure 2.6—Percent of 2018 surveyed Alaska forest and shrubland area within ecoregions with mortality caused by insects and diseases. The gray lines delineate ecoregion sections (Spencer and others 2002). Forest and shrub cover is derived from the 2011 National Land Cover Database. (Data source: U.S. Department of Agriculture Forest Service, Forest Health Protection)

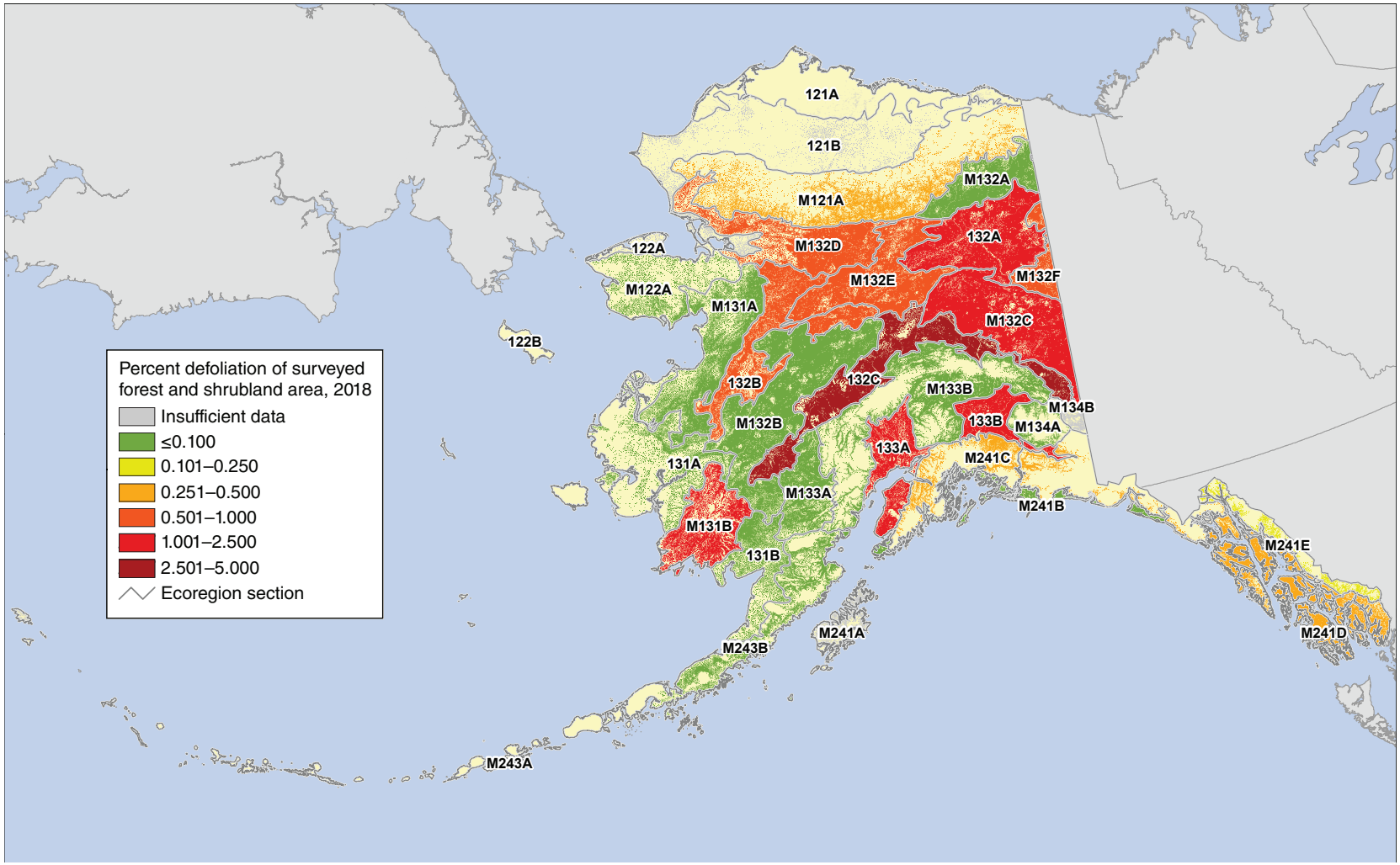

Figure 2.7—Percent of 2018 surveyed Alaska forest and shrubland area within ecoregions with defoliation caused by insects and diseases. The gray lines delineate ecoregion sections (Spencer and others 2002). Forest and shrub cover is derived from the 2011 National Land Cover Database. (Data source: U.S. Department of Agriculture Forest Service, Forest Health Protection)

C. huliohia, but *C. lukuohia* is more aggressive than *C. huliohia* (Barnes and others 2018). Both pathogens have been confirmed on the islands of Hawai‘i (the Big Island) and Kaua‘i, while individual trees infected with *C. huliohia* have been detected on Maui and O‘ahu (University of Hawai‘i 2019). Mortality detected in 2018 was high across many of the wetter areas of the Big Island, particularly in the Montane Wet-Hawai‘i-Kona (MWh-ko) ecoregion on the leeward (west) side of the island, where 2.35 percent of the surveyed tree canopy area had mortality (fig. 2.8). On the south side of the island, Montane Wet-Hawai‘i-Ka‘ū (MWh-ka) had 1.00 percent mortality of surveyed canopy area, while on the windward (east) side, Lowland Wet-Hawai‘i-Hilo-Puna (LWh-hp) had 0.90 percent and Montane Wet-Hawai‘i-Hilo-Puna (MWh-hp) had 0.45 percent. Meanwhile, upland wet areas of Maui also had relatively high mortality. Wet areas on Maui also experienced relatively high mortality, including Lowland Wet-Maui-West (LWm-w), where mortality was 1.13 percent of the surveyed tree canopy area; Montane Wet-Maui-East (MWm-e), 0.66 percent; Mesic-Maui-West (MEm-w), 0.63 percent; and Montane Wet-Maui-West (MWm-w), 0.47 percent. No defoliation was documented in Hawaii during 2018.

CONCLUSION

Continued monitoring of insect and disease outbreaks across the United States will be necessary for determining appropriate follow-up investigation and management activities. Due to the limitations of survey efforts to detect certain important forest insects and diseases, the pests and pathogens discussed in this chapter do not include all the biotic forest health threats that should be considered when making management decisions and budget allocations. However, large-scale assessments of mortality and defoliation severity, including geographical hot spot detection analyses, offer a useful approach for identifying geographic areas where the concentration of monitoring and management activities might be most effective.

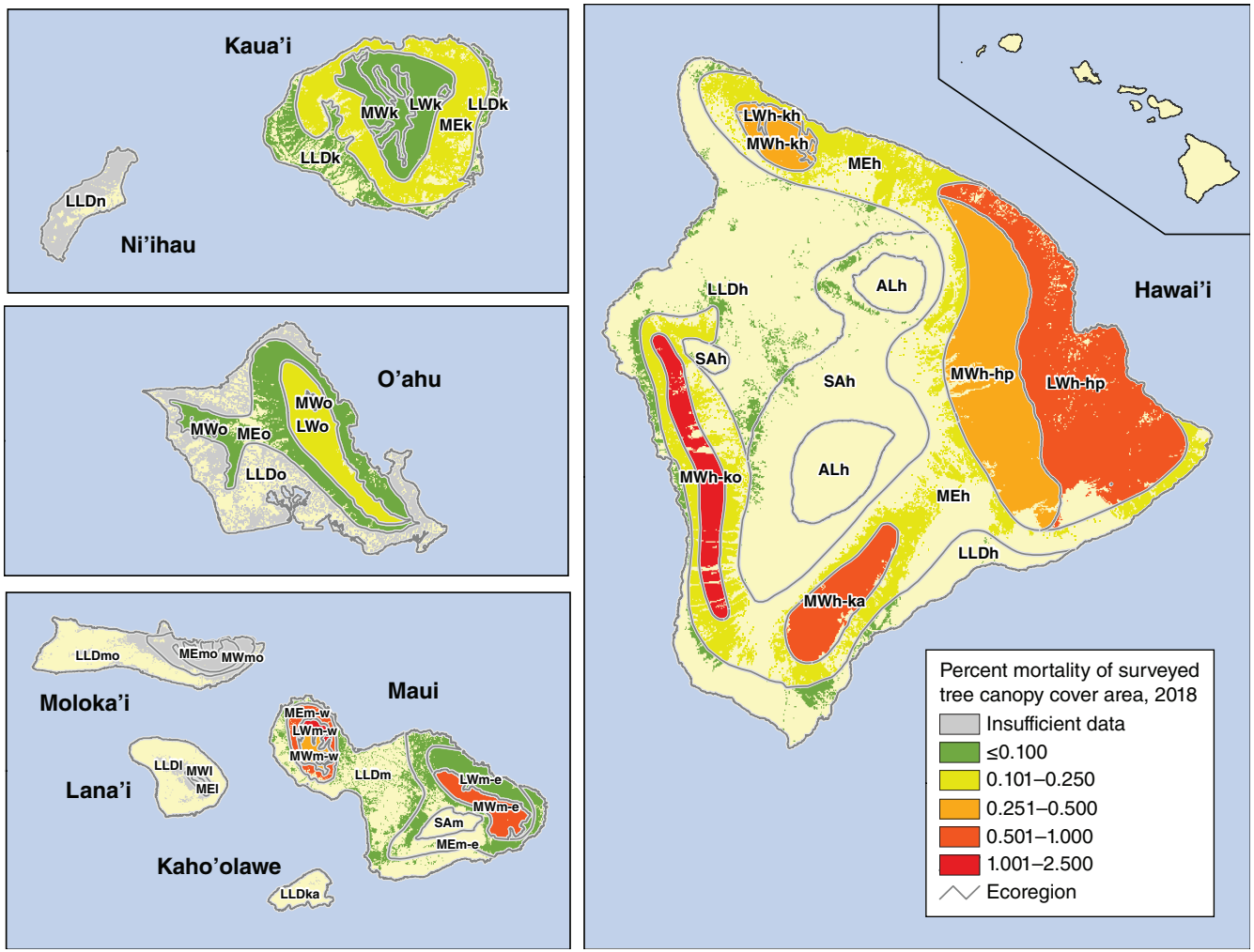

Figure 2.8—Percent of 2018 surveyed Hawaii tree canopy area within island/ecoregion combinations with mortality caused by insects and diseases. Tree canopy cover is based on data from a cooperative project between the Multi-Resolution Land Characteristics Consortium (Coulston and others 2012) and the Forest Service Geospatial Technology and Applications Center using the 2011 National Land Cover Database. See figure 1.2 for ecoregion identification. (Data source: U.S. Department of Agriculture Forest Service, Forest Health Protection)

LITERATURE CITED

Anselin, L. 1992. Spatial data analysis with GIS: an introduction to application in the social sciences. Tech. Rep. 92-10. Santa Barbara, CA: National Center for Geographic Information and Analysis. 53 p.

Barnes, I.; Fourie, A.; Wingfield, M.J. [and others]. 2018. New *Ceratocystis* species associated with rapid death of *Metrosideros polymorpha* in Hawaii. Persoonia-Molecular Phylogeny and Evolution of Fungi. 40(1): 154–181.

Berryman, E.; McMahan, A. 2019. Using tree canopy cover data to help estimate acres of damage. In: Potter, K.M.; Conkling, B.L., eds. Forest Health Monitoring: national status, trends, and analysis 2018. Gen. Tech. Rep. SRS-239. Asheville, NC: U.S. Department of Agriculture Forest Service, Southern Research Station: 125–141.

Brockerhoff, E.G.; Liebhold, A.M.; Jactel, H. 2006. The ecology of forest insect invasions and advances in their management. Canadian Journal of Forest Research. 36(2): 263–268.

Castello, J.D.; Leopold, D.J.; Smallidge, P.J. 1995. Pathogens, patterns, and processes in forest ecosystems. BioScience. 45(1): 16–24.

Cleland, D.T.; Freeouf, J.A.; Keys, J.E. [and others]. 2007. Ecological subregions: sections and subsections for the conterminous United States. Gen. Tech. Rep. WO-76D. Washington, DC: U.S. Department of Agriculture Forest Service. Map; Sloan, A.M., cartographer; presentation scale 1:3,500,000; colored. Also on CD-ROM as a GIS coverage in ArcINFO format or at http://data.fs.usda.gov/geodata/edw/datasets.php. [Date accessed: July 20, 2015].

Coulston, J.W.; Moisen, G.G.; Wilson, B.T. [and others]. 2012. Modeling percent tree canopy cover: a pilot study. Photogrammetric Engineering and Remote Sensing. 78(7): 715–727.

Edmonds, R.L.; Agee, J.K.; Gara, R.I. 2011. Forest health and protection. Long Grove, IL: Waveland Press, Inc. 667 p.

ESRI. 2015. ArcMap® 10.3. Redlands, CA: Environmental Systems Research Institute, Inc.

Forest Health Protection (FHP). 2016. Detection surveys. Fort Collins, CO: U.S. Department of Agriculture Forest Service, Forest Health Technology Enterprise Team. http://www.fs.fed.us/foresthealth/technology/detection_surveys.shtml. [Date accessed: July 23, 2016].

Forest Health Protection (FHP). 2019. Insect and Disease Detection Survey database (IDS). [Online database]. Fort Collins, CO: U.S. Department of Agriculture Forest Service, Forest Health Technology Enterprise Team. https://www.fs.fed.us/foresthealth/applied-sciences/mapping-reporting/gis-spatial-analysis/detection-surveys.shtml#idsdownloads. [Date accessed: July 17, 2019].

Getis, A.; Ord, J.K. 1992. The analysis of spatial association by use of distance statistics. Geographical Analysis. 24(3): 189–206.

Holdenrieder, O.; Pautasso, M.; Weisberg, P.J.; Lonsdale, D. 2004. Tree diseases and landscape processes: the challenge of landscape pathology. Trends in Ecology & Evolution. 19(8): 446–452.

Homer, C.G.; Dewitz, J.A.; Yang, L. [and others]. 2015. Completion of the 2011 National Land Cover Database for the conterminous United States: representing a decade of land cover change information. Photogrammetric Engineering and Remote Sensing. 81(5): 345–354.

Laffan, S.W. 2006. Assessing regional scale weed distributions, with an Australian example using *Nassella trichotoma*. Weed Research. 46(3): 194–206.

Liebhold, A.M.; McCullough, D.G.; Blackburn, L.M. [and others]. 2013. A highly aggregated geographical distribution of forest pest invasions in the USA. Diversity and Distributions. 19: 1208–1216.

Logan, J.A.; Regniere, J.; Powell, J.A. 2003. Assessing the impacts of global warming on forest pest dynamics. Frontiers in Ecology and the Envionment. 1: 130–137.

Lovett, G.M.; Weiss, M.; Liebhold, A.M. [and others]. 2016. Nonnative forest insects and pathogens in the United States: impacts and policy options. Ecological Applications. 26: 1437–1455.

Mack, R.N.; Simberloff, D.; Lonsdale, W.M. [and others]. 2000. Biotic invasions: causes, epidemiology, global consequences, and control. Ecological Applications. 10(3): 689–710.

Manion, P.D. 2003. Evolution of concepts in forest pathology. Phytopathology. 93: 1052–1055.

Parry, D.; Teale, S.A. 2011. Alien invasions: the effects of introduced species on forest structure and function. In: Castello, J.D.; Teale, S.A., eds. Forest health: an integrated perspective. New York: Cambridge University Press: 115–162.

Potter, K.M. 2012. Large-scale patterns of insect and disease activity in the conterminous United States and Alaska from the national Insect and Disease Detection Survey database, 2007 and 2008. In: Potter, K.M.; Conkling, B.L., eds. Forest Health Monitoring 2009 national technical report. Gen. Tech. Rep. SRS-167. Asheville, NC: U.S. Department of Agriculture Forest Service, Southern Research Station: 63–78.

Potter, K.M. 2013. Large-scale patterns of insect and disease activity in the conterminous United States and Alaska from the national Insect and Disease Detection Survey, 2009. In: Potter, K.M.; Conkling, B.L., eds. Forest Health Monitoring: national status, trends, and analysis 2010. Gen. Tech. Rep. SRS-176. Asheville, NC: U.S. Department of Agriculture Forest Service, Southern Research Station: 15–29.

Potter, K.M.; Escanferla, M.E.; Jetton, R.M.; Man, G. 2019a. Important insect and disease threats to United States tree species and geographic patterns of their potential impacts. Forests. 10(4): 304.

Potter, K.M.; Escanferla, M.E.; Jetton, RM. [and others]. 2019b. Prioritizing the conservation needs of United States tree species: evaluating vulnerability to forest insect and disease threats. Global Ecology and Conservation. 18: e00622.

Potter, K.M.; Koch, F.H. 2012. Large-scale patterns of insect and disease activity in the conterminous United States and Alaska, 2006. In: Potter, K.M.; Conkling, B.L., eds. Forest Health Monitoring 2008 national technical report. Gen. Tech. Rep. SRS-158. Asheville, NC: U.S. Department of Agriculture Forest Service, Southern Research Station: 63–72.

Potter, K.M.; Koch, F.H.; Oswalt, C.M.; Iannone, B.V. 2016. Data, data everywhere: detecting spatial patterns in fine-scale ecological information collected across a continent. Landscape Ecology. 31: 67–84.

Potter, K.M.; Paschke, J.L. 2013. Large-scale patterns of insect and disease activity in the conterminous United States and Alaska from the national Insect and Disease Detection Survey database, 2010. In: Potter, K.M.; Conkling, B.L., eds. Forest Health Monitoring: national status, trends, and analysis 2011. Gen. Tech. Rep. SRS-185. Asheville, NC: U.S. Department of Agriculture Forest Service, Southern Research Station: 15–28.

Potter, K.M.; Paschke, J.L. 2014. Large-scale patterns of insect and disease activity in the conterminous United States and Alaska from the national Insect and Disease Survey database, 2011. In: Potter, K.M.; Conkling, B.L., eds. Forest Health Monitoring: national status, trends, and analysis 2012. Gen. Tech. Rep. SRS-198. Asheville, NC: U.S. Department of Agriculture Forest Service, Southern Research Station: 19–34.

Potter, K.M.; Paschke, J.L. 2015a. Large-scale patterns of insect and disease activity in the conterminous United States and Alaska from the national Insect and Disease Survey, 2012. In: Potter, K.M.; Conkling, B.L., eds. Forest Health Monitoring: national status, trends, and analysis 2013. Gen. Tech. Rep. SRS-207. Asheville, NC: U.S. Department of Agriculture Forest Service, Southern Research Station: 19–36.

Potter, K.M.; Paschke, J.L. 2015b. Large-scale patterns of insect and disease activity in the conterminous United States, Alaska, and Hawaii from the national Insect and Disease Survey, 2013. In: Potter, K.M.; Conkling, B.L., eds. Forest Health Monitoring: national status, trends, and analysis 2014. Gen. Tech. Rep. SRS-209. Asheville, NC: U.S. Department of Agriculture Forest Service, Southern Research Station: 19–38.

Potter, K.M.; Paschke, J.L. 2016. Large-scale patterns of insect and disease activity in the conterminous United States and Alaska from the national Insect and Disease Survey, 2014. In: Potter, K.M.; Conkling, B.L., eds. Forest Health Monitoring: national status, trends, and analysis 2015. Gen. Tech. Rep. SRS-213. Asheville, NC: U.S. Department of Agriculture Forest Service, Southern Research Station: 21–40.

Potter, K.M.; Paschke, J.L. 2017. Large-scale patterns of insect and disease activity in the conterminous United States and Alaska from the national Insect and Disease Survey, 2015. In: Potter, K.M.; Conkling, B.L., eds. Forest Health Monitoring: national status, trends, and analysis 2016. Gen. Tech. Rep. SRS-222. Asheville, NC: U.S. Department of Agriculture Forest Service, Southern Research Station: 21–42.

Potter, K.M.; Paschke, J.L.; Zweifler, M. 2018. Large-scale patterns of insect and disease activity in the conterminous United States, Alaska, and Hawaii from the national Insect and Disease Survey, 2016. In: Potter, K.M.; Conkling, B.L., eds. Forest Health Monitoring: national status, trends, and analysis 2017. Gen. Tech. Rep. SRS-233. Asheville, NC: U.S. Department of Agriculture Forest Service, Southern Research Station: 23–44.

Potter, K.M.; Paschke, J.L.; Koch, F.H.; Zweifler, M. 2019. Large-scale patterns of insect and disease activity in the conterminous United States, Alaska, and Hawaii from the national Insect and Disease Survey, 2017. In: Potter, K.M.; Conkling, B.L., eds. Forest Health Monitoring: national status, trends, and analysis 2018. Gen. Tech. Rep. SRS-239. Asheville, NC: U.S. Department of Agriculture Forest Service, Southern Research Station: 21–49.

Reams, G.A.; Smith, W.D.; Hansen, M.H. [and others]. 2005. The Forest Inventory and Analysis sampling frame. In: Bechtold, W.A.; Patterson, P.L., eds. The enhanced Forest Inventory and Analysis program—national sampling design and estimation procedures. Asheville, NC: U.S. Department of Agriculture Forest Service, Southern Research Station: 11–26.

Shima, T.; Sugimoto, S.; Okutomi, M. 2010. Comparison of image alignment on hexagonal and square lattices. In: 2010 IEEE international conference on image processing. [Place of publication unknown]: Institute of Electrical and Electronics Engineers, Inc.: 141–144. DOI: 10.1109/icip.2010.5654351.

Smith, W.B.; Miles, P.D.; Perry, C.H.; Pugh, S.A. 2009. Forest resources of the United States, 2007. Gen. Tech. Rep. WO-78. Washington, DC: U.S. Department of Agriculture Forest Service. 336 p.

Spencer, P.; Nowacki, G.; Fleming, M. [and others]. 2002. Home is where the habitat is: an ecosystem foundation for wildlife distribution and behavior. Arctic Research of the United States. 16: 6–17.

Teale, S.A.; Castello, J.D. 2011. Regulators and terminators: the importance of biotic factors to a healthy forest. In: Castello, J.D.; Teale, S.A., eds. Forest health: an integrated perspective. New York: Cambridge University Press: 81–114.

Tobin, P.C. 2015. Ecological consequences of pathogen and insect invasions. Current Forestry Reports. 1: 25–32.

University of Hawai'i, College of Tropical Agriculture and Human Resources. 2019. Rapid 'ōhi'a death/*Ceratocystis* wilt of 'ōhi'a. http://rapidohiadeath.org. [Date accessed: August 9, 2019].

U.S. Department of Agriculture (USDA) Forest Service. 2008. National forest type data development. http://svinetfc4.fs.fed.us/rastergateway/forest_type/. [Date accessed: May 13, 2008].

White, D.; Kimerling, A.J.; Overton, W.S. 1992. Cartographic and geometric components of a global sampling design for environmental monitoring. Cartography and Geographic Information Systems. 19(1): 5–22.

Zhang, L.; Rubin, B.D.; Manion, P.D. 2011. Mortality: the essence of a healthy forest. In: Castello, J.D.; Teale, S.A., eds. Forest health: an integrated perspective. New York: Cambridge University Press: 17–49.

CHAPTER 3.

Broad-Scale Patterns of Forest Fire Occurrence across the 50 United States and the Caribbean Territories, 2018

Kevin M. Potter

INTRODUCTION

As a pervasive disturbance agent operating at many spatial and temporal scales, wildland fire is a key abiotic factor affecting forest health both positively and negatively. In some ecosystems, for example, wildland fires have been essential for regulating processes that maintain forest health (Lundquist and others 2011). Wildland fire is an important ecological mechanism that shapes the distributions of species, maintains the structure and function of fire-prone communities, and acts as a significant evolutionary force (Bond and Keeley 2005). At the same time, wildland fires have created forest health (i.e., sustainability) problems in some ecosystems (Edmonds and others 2011).

Current fire regimes on more than half of the forested area in the conterminous United States have been moderately or significantly altered from historical regimes (Barbour and others 1999), potentially altering key ecosystem components such as species composition, structural stage, stand age, canopy closure, and fuel loadings (Schmidt and others 2002). Fires in some regions and ecosystems have become larger, more intense, and more damaging because of the accumulation of fuels as a result of prolonged fire suppression (Pyne 2010). In some regions, plant communities have experienced or are undergoing rapid compositional and structural changes as a result of fire suppression (Nowacki and Abrams 2008). Additionally, changes in fire intensity and recurrence could result in decreased forest resilience and persistence (Lundquist and others 2011), and fire regimes altered by global climate change could cause large-scale shifts in vegetation spatial patterns (McKenzie and others 1996).

At the same time, large wildland fires also can have long-lasting social and economic consequences, which include the loss of human life and property, smoke-related human health impacts, and the economic cost and dangers of fighting the fires themselves (Gill and others 2013, Richardson and others 2012).

This chapter presents analyses of daily satellite-based fire occurrence data that map and quantify the locations and intensities of fire occurrences spatially across the conterminous United States, Alaska, Hawaii, and the Caribbean territories in 2018. It also compares 2018 fire occurrences, within a geographic context, to all the recent years for which such data are available. Quantifying and monitoring such large-scale patterns of fire occurrence across the United States can help improve our understanding of the ecological and economic impacts of fire as well as the appropriate management and prescribed use of fire. Specifically, large-scale assessments of fire occurrence can help identify areas where specific management activities may be needed, or where research into the ecological and socioeconomic impacts of fires may be required. Additionally, given the potential for climate change and shifting species distributions to alter historic fire regimes, quantifying the location and frequency

of forest fire occurrences across the United States can help us to better understand emerging spatiotemporal patterns of fire occurrence.

METHODS

Data

Annual monitoring and reporting of active wildland fire events using the Moderate Resolution Imaging Spectroradiometer (MODIS) Active Fire Detections for the United States database (USDA Forest Service 2019) allow analysts to spatially display and summarize fire occurrences across broad geographic regions (Coulston and others 2005; Potter 2012a, 2012b, 2013a, 2013b, 2014, 2015a, 2015b, 2016, 2017, 2018, 2019). A fire occurrence is defined as one daily satellite detection of wildland fire in a 1-km pixel, with multiple fire occurrences possible on a pixel across multiple days resulting from a single wildland fire that lasts more than 1 day. The data are derived using the MODIS Rapid Response System (Justice and others 2002, 2011) to extract fire location and intensity information from the thermal infrared bands of imagery collected daily by two satellites at a resolution of 1 km, with the center of a pixel recorded as a fire occurrence (USDA Forest Service 2019). The Terra and Aqua satellites' MODIS sensors identify the presence of a fire at the time of image collection, with Terra observations collected in the morning and Aqua observations collected in the afternoon. The resulting fire occurrence data represent only whether a fire was active because the MODIS data bands may not differentiate between a hot fire in a relatively small area (0.01 km^2, for example) and a cooler fire over a larger area (1 km^2, for example) if the foreground to background temperature contrast is not sufficiently high. The MODIS Active Fire database does well at capturing large fires during cloud-free conditions but may underrepresent rapidly burning, small, and low-intensity fires, as well as fires in areas with frequent cloud cover (Hawbaker and others 2008). For large-scale assessments, the dataset represents a good alternative to the use of information on ignition points, which may be preferable but can be difficult to obtain or may not exist (Tonini and others 2009). For more information about the performance of this product, see Justice and others (2011). The fire occurrence data additionally do not differentiate fires intentionally set for management purposes (controlled burns), which are common in some parts of the United States, particularly in the South.

It is important to underscore that estimates of burned area and calculations of MODIS-detected fire occurrences are two different metrics for quantifying fire activity within a given year. Most importantly, the MODIS data contain both spatial and temporal components because persistent fire will be detected repeatedly over several days on a given 1-km pixel. In other words, a location can be counted as having a fire occurrence multiple times, once for each day a fire is detected at the location. Analyses of the MODIS-detected fire occurrences, therefore, measure the total number of daily

1-km pixels with fire during a year, as opposed to quantifying only the area on which fire occurred at some point during the course of the year. A fire detected on a single pixel on every day of the year would be equivalent to 365 fire occurrences.

It is worth noting that the Terra and Aqua satellites, which carry the MODIS sensors, were launched in 1999 and 2002, respectively, and will eventually be decommissioned. An alternative fire occurrence data source is the Visible Infrared Imaging Radiometer Suite (VIIRS) sensor on board the Suomi National Polar-orbiting Partnership (Suomi NPP) weather satellite. The transition to this new data source will require a comparison of fire occurrence detections between it and MODIS. This is because VIIRS data are available from 2014 onward, but it will be important for assessments of fire occurrence trends to be able to analyze as long a window of time as possible (i.e., from the beginning of MODIS data availability). Additionally, Landsat 8 fire detection data are available at 30-m resolution from 2015 to present, although some issues may affect the completeness of the data (USDA Forest Service 2019).

Analyses

These MODIS products for 2018, and for the 17 preceding full years of data, were processed in ArcMap® (ESRI 2015) to determine forest fire occurrence density (that is, the number of fire occurrences per 100 km^2 [10 000 ha] of tree canopy coverage area) for each ecoregion section in the conterminous United States (Cleland and others 2007), for ecoregions on each of the major islands of Hawaii (see ch. 1 of this report), and for the islands of the Caribbean territories of Puerto Rico and the U.S. Virgin Islands. For the current analyses, the forest fire occurrence density metrics for the conterminous 48 States, Hawaii, and the Caribbean territories (the number of fire occurrences per 100 km^2 of tree canopy cover area) were calculated after screening out wildland fires that did not intersect with tree canopy data. The tree canopy data had been resampled to 240 m from a 30-m raster dataset that estimates percent tree canopy cover (from 0 to 100 percent) for each grid cell; this dataset was generated from the 2011 National Land Cover Database (NLCD) (Homer and others 2015) through a cooperative project between the Multi-Resolution Land Characteristics Consortium and the U.S. Department of Agriculture Forest Service, Geospatial Technology and Applications Center (GTAC) (Coulston and others 2012). For our purposes, we treated any cell with >0 percent tree canopy cover as forest. Comparable tree canopy cover data were not available for Alaska, so we instead created a 240-m-resolution layer of forest and shrub cover from the 2011 NLCD. The MODIS fire occurrence detection data were then intersected with this layer and with ecoregion sections for the State (Spencer and others 2002) to calculate the number of fire occurrences per 100 km^2 of forest and shrub cover within each ecoregion section in Alaska. In previous Forest Health Monitoring national reports, the number of fire occurrences

per 100 km^2 of forest was determined for the conterminous States, Alaska, and Hawaii using a forest cover mask derived from MODIS imagery by the Forest Service GTAC (USDA Forest Service 2008).

The total numbers of forest fire occurrences were also determined separately for the conterminous States, Alaska, Hawaii, and the Caribbean territories after clipping the MODIS fire occurrences by the canopy cover or tree and shrub cover data.

The fire occurrence density value for each of the ecoregions of the States and for the Caribbean islands in 2018 was then compared with the mean fire density values for the first 17 full years of MODIS Active Fire data collection (2001–2017). Specifically, the difference of the 2018 value and the previous 17-year mean for an ecoregion was divided by the standard deviation across the previous 17-year period, assuming a normal distribution of fire density over time in the ecoregion. The result for each ecoregion was a standardized *z*-score, which is a dimensionless quantity describing the degree to which the fire occurrence density in the ecoregion in 2018 was higher, lower, or the same relative to all the previous years for which data have been collected, accounting for the variability in the previous years. The *z*-score is the number of standard deviations between the observation and the mean of the historic observations in the previous years. Approximately 68 percent of observations would be expected within one standard deviation of the mean, and 95 percent within two standard deviations. Near-normal conditions are classified as those within a single standard deviation of the mean, although such a threshold is somewhat arbitrary. Conditions between about one and two standard deviations of the mean are moderately different from mean conditions but are not significantly different statistically. Those outside about two standard deviations would be considered statistically greater than or less than the long-term mean (at $p < 0.025$ at each tail of the distribution).

Additionally, we used the Spatial Association of Scalable Hexagons (SASH) analytical approach to identify forested areas in the conterminous United States with higher-than-expected fire occurrence density in 2018. This method identifies locations where ecological phenomena occur at greater or lower occurrences than expected by random chance and is based on a sampling frame optimized for spatial neighborhood analysis, adjustable to the appropriate spatial resolution, and applicable to multiple data types (Potter and others 2016). Specifically, it consists of dividing an analysis area into scalable equal-area hexagonal cells within which data are aggregated, followed by identifying statistically significant geographic clusters of hexagonal cells within which mean values are greater or less than those expected by chance. To identify these clusters, we employed a Getis-Ord G_i^* hot spot analysis (Getis and Ord 1992) in ArcMap® 10.3 (ESRI 2015).

The spatial units of analysis were 9,810 hexagonal cells, each approximately 834 km^2 in area, generated in a lattice across the

conterminous United States using intensification of the Environmental Monitoring and Assessment Program (EMAP) North American hexagon coordinates (White and others 1992). These coordinates are the foundation of a sampling frame in which a hexagonal lattice was projected onto the conterminous United States by centering a large base hexagon over the region (Reams and others 2005, White and others 1992). The hexagons are compact and uniform in their distance to the centroids of neighboring hexagons, meaning that a hexagonal lattice has a higher degree of isotropy (uniformity in all directions) than does a square grid (Shima and others 2010). These are convenient and highly useful attributes for spatial neighborhood analyses. These scalable hexagons also are independent of geopolitical and ecological boundaries, avoiding the possibility of different sample units (such as counties, States, or watersheds) encompassing vastly different areas (Potter and others 2016). We selected hexagons 834 km^2 in area because this is a manageable size for making monitoring and management decisions in analyses across the conterminous United States (Potter and others 2016).

Fire occurrence density values for each hexagon were quantified as the number of forest fire occurrences per 100 km^2 of tree canopy cover area within the hexagon. The Getis-Ord G_i^* statistic was used to identify clusters of hexagonal cells with fire occurrence density values higher than expected by chance. This statistic allows for the decomposition of a global measure of spatial association into its contributing factors, by location, and is therefore particularly suitable for detecting outlier assemblages of similar conditions in a dataset, such as when spatial clustering is concentrated in one subregion of the data (Anselin 1992).

Briefly, G_i^* sums the differences between the mean values in a local sample, determined in this case by a moving window of each hexagon and its 18 first- and second-order neighbors (the 6 adjacent hexagons and the 12 additional hexagons contiguous to those 6) and the global mean of the 9,644 hexagonal cells with tree canopy cover (of the total 9,810) in the conterminous United States. As described in Laffan (2006), it is calculated as

$$G_i^*(d) = \frac{\sum_j w_{ij}(d)x_j - W_i^*\bar{x}^*}{s^*\sqrt{\frac{(ns_{1i}^*) - W_i^{*2}}{n-1}}}$$

where

G_i^* = the local clustering statistic (in this case, for the target hexagon)

i = the center of local neighborhood (the target hexagon)

d = the width of local sample window (the target hexagon and its first- and second-order neighbors)

x_j = the value of neighbor j

w_{ij} = the weight of neighbor j from location i (all the neighboring hexagons in the moving window were given an equal weight of 1)

n = number of samples in the dataset (the 9,644 hexagons containing tree cover)

W_i^* = the sum of the weights

$s_1^* i$ = the number of samples within d of the central location (19: the focal hexagon and its 18 first- and second-order neighbors)

$\bar{x}^*$ = the mean of whole dataset (in this case, for all 9,644 hexagons containing tree cover)

s^* = the standard deviation of whole dataset (for all 9,644 hexagons containing tree cover)

G_i^* is standardized as a z-score with a mean of 0 and a standard deviation of 1, with values >1.96 representing significant local clustering of higher fire occurrence densities (p <0.025) and values <-1.96 representing significant clustering of lower fire occurrence densities (p <0.025), because 95 percent of the observations under a normal distribution should be within approximately two standard deviations of the mean (Laffan 2006). Values between -1.96 and 1.96 have no statistically significant concentration of high or low values; a hexagon and its 18 neighbors, in other words, have a normal range of both high and low numbers of fire occurrences per 100 km^2 of tree canopy cover area. It is worth noting that the threshold values are not exact because the correlation of spatial data violates the assumption of independence required for statistical significance (Laffan 2006). In addition, the Getis-Ord approach does not require that the input data be normally distributed, because the local G_i^* values are computed under a randomization assumption, with G_i^* equating to a standardized z-score that asymptotically tends to a normal distribution (Anselin 1992). The z-scores are considered to be reliable, even with skewed data, as long as the local neighborhood encompasses several observations (ESRI 2015), in this case, via the target hexagon and its 18 first- and second-order neighbors.

RESULTS AND DISCUSSION

Trends in Forest Fire Occurrence Detections for 2018

The MODIS Active Fire database recorded 76,692 forest fire occurrences across the conterminous United States in 2018, the ninth most in 18 full years of data collection (fig. 3.1). This was approximately 24 percent less than in 2017 (100,840 total forest fire occurrences), and nearly identical to the annual mean of 76,165 forest fire occurrences across the previous 17 years of data collection. In Alaska, meanwhile, the MODIS database encompassed 690 forest fire occurrences in 2018, about 67 percent fewer than the preceding year (2,064) and about 93 percent fewer than the previous 17-year annual mean of 9,340. Meanwhile, Hawaii had 136 fire occurrences in 2018, an increase of about 216 percent from the previous year (43) but 57 percent below the average of 317 fire occurrences over the previous 17 years. Finally, a single forest fire occurrence was detected in Puerto Rico, 89 percent fewer than the previous average of about 9 per year.

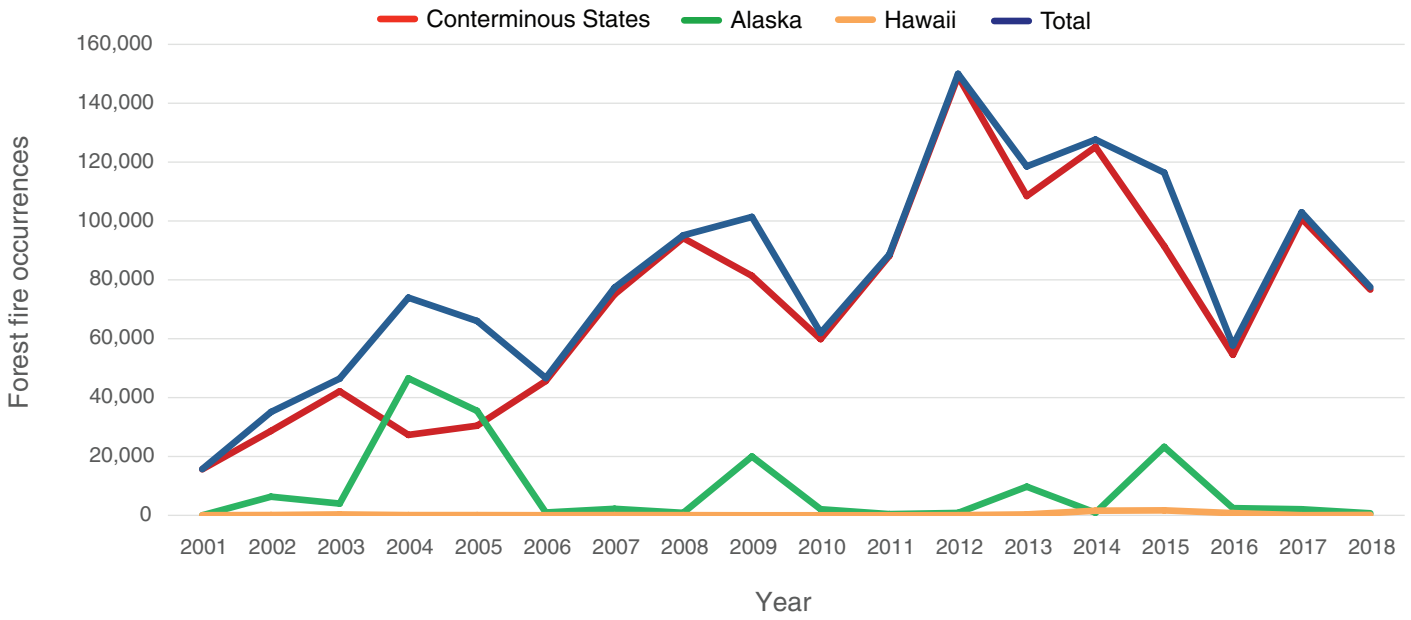

Figure 3.1—Forest fire occurrences detected by MODIS from 2001 to 2018 for the conterminous United States, Alaska, and Hawaii, and for the entire Nation combined. (Data source: U.S. Department of Agriculture Forest Service, Geospatial Technology and Applications Center, in conjunction with the NASA MODIS Rapid Response group)

The decrease in the total number of fire occurrences across the United States derived from MODIS is generally consistent with the official wildland fire statistics, which are based on other data sources and reported a below-normal number of wildfires (National Interagency Coordination Center 2019). In 2018, 58,083 wildland fires were reported across the United States, which was a decrease from 71,499 in 2017. The area burned nationally (3 548 078 ha) was 87 percent of the 2017 burned area total (4 057 413 ha) but 132 percent of the 10-year average (National Interagency Coordination Center 2018, 2019). The number of wildland fires and fire complexes exceeding 16 187 ha (a benchmark threshold for the National Interagency Coordination Center) was 49 in 2018, compared to 44 in 2017 and 19 in 2016 (National Interagency Coordination Center 2017, 2018). As noted in the Methods section, estimates of burned area are different metrics for quantifying fire activity than calculations of MODIS-detected fire occurrences, though the two may be correlated.

Areas with the highest fire occurrence densities in 2018 were in northern California and in north-central Washington (fig. 3.2). Beginning in July, these areas experienced drier-than-normal conditions which expanded

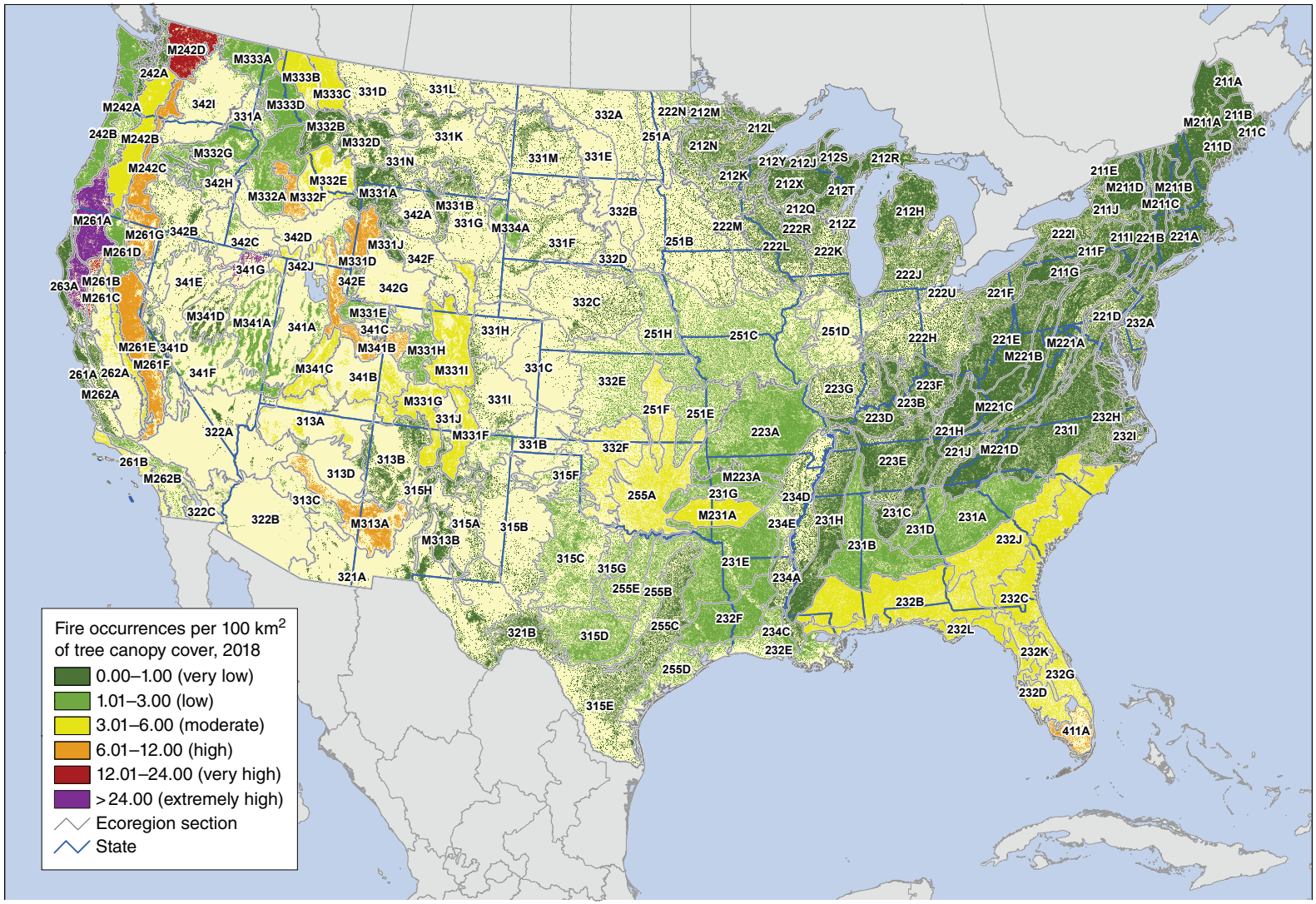

Figure 3.2—The number of forest fire occurrences, per 100 km^2 (10 000 ha) of tree canopy coverage area, by ecoregion section within the conterminous 48 States, for 2018. The gray lines delineate ecoregion sections (Cleland and others 2007). Tree canopy cover is based on data from a cooperative project between the Multi-Resolution Land Characteristics Consortium (Coulston and others 2012) and the Forest Service Geospatial Technology and Applications Center using the 2011 National Land Cover Database. (Source of fire data: U.S. Department of Agriculture Forest Service, Geospatial Technology and Applications Center, in conjunction with the NASA MODIS Rapid Response group)

and intensified through the autumn months, resulting in fuels that were critically dry (National Interagency Coordination Center 2019). The ecoregion section with the highest fire occurrence density was the Northern California Coast Ranges (M261B), which experienced 31.8 fire occurrences/100 km^2 of tree canopy cover (table 3.1) and included the Mendocino Fire Complex, which was the largest recorded fire complex in California history (CAL FIRE 2019), burning 185 800 ha between July 27 and September 18 and costing approximately $220 million for containment (National Interagency Coordination Center 2019). In the neighboring M261A–Klamath Mountains ecoregion section of northern California and southwestern Oregon, fire occurrence densities were also extremely high (29.0 fire occurrences/100 km^2 of tree canopy cover). This ecoregion was the location of the Carr Fire, which burned 92 936 ha in California, killed eight people, and cost approximately $162 million (CAL FIRE 2019, National Interagency Coordination Center 2019), and of

Table 3.1—The 15 ecoregion sections in the conterminous United States with the highest fire occurrence densities in 2018

Section	Name	Tree canopy area	Fire occurrences	Density
		km^2	*number*	*fire occurrences per 100 km^2 of tree canopy coverage area*
M261B	Northern California Coast Ranges	114.1	3,630	31.8
341G	Northeastern Great Basin	24.6	754	30.6
M261A	Klamath Mountains	338.5	9,818	29.0
M261C	Northern California Interior Coast Ranges	18.2	283	15.5
M242D	Northern Cascades	251.1	3,838	15.3
M261E	Sierra Nevada	427.8	4,863	11.4
M261G	Modoc Plateau	128.7	1,427	11.1
411A	Everglades	68.7	630	9.2
M331D	Overthrust Mountains	262.2	2,147	8.2
M313A	White Mountains-San Francisco Peaks-Mogollon Rim	202.5	1,622	8.0
M332F	Challis Volcanics	72.2	547	7.6
M341B	Tavaputs Plateau	92.0	670	7.3
M242C	Eastern Cascades	219.4	1,549	7.1
M333B	Flathead Valley	168.9	1,013	6.0
262A	Great Valley	19.4	114	5.9

the Klondike and Taylor Creek Fires in Oregon, which scorched 70 924 ha and 21 383 ha, respectively.

Three other ecoregion sections in northern California also had high fire occurrence densities: M261C–Northern California Interior Coast Ranges (15.5 fire occurrences/100 km^2 of tree canopy cover), M261E–Sierra Nevada (11.4 fire occurrences/100 km^2 of tree canopy cover), and M261G–Modoc Plateau (11.1 fire occurrences/100 km^2 of tree canopy cover) (fig. 3.2). M261E–Sierra Nevada was the location of the Camp Fire. This fire burned 62 053 ha between November 8 and 25, consumed the town of Paradise, CA, and killed 85 people, making it the deadliest U.S. fire in more than a century (National Interagency Coordination Center 2019).

In northeastern Nevada, 341G–Northeastern Great Basin, an area with relatively sparse tree canopy cover, had an extremely high 30.6 fire occurrences/100 km^2 of canopy cover as a result of the 176 269-ha Martin Fire, which burned in July and was the largest fire in the State's history (National Interagency Coordination Center 2019, Rothberg 2018). Meanwhile, the fire occurrence density in M242D–Northern Cascades (15.3 fire occurrences/100 km^2) in north-central Washington was also high, in part because of the Crescent Mountain Fire, which burned 22 909 ha between July and November, and the Cougar Creek Fire, which burned 17 285 ha during the same period (National Interagency Coordination Center 2019).

High fire occurrence densities (6.01–12.00 fire occurrences/100 km^2 of tree canopy cover) were recorded in a handful of other western ecoregion sections: M331D–Overthrust Mountains, in western Wyoming, southeastern Idaho, and northern Utah; M313A–White Mountains-San Francisco Peaks-Mogollon Rim, in east-central Arizona and west-central New Mexico; M332F–Challis Volcanics in central Idaho; M341B–Tavaputs Plateau, in northeastern Utah and northwestern Colorado; and M242C–Eastern Cascades, in central Washington and Oregon (table 3.1). Only one ecoregion in the Eastern United States had a high fire occurrence density in 2018, 411A–Everglades (9.2) (fig. 3.2).

Higher-than-usual temperatures throughout the year in Alaska, meanwhile, were combined with consistently above-average precipitation throughout the State (National Interagency Coordination Center 2019). As a result, fire occurrence densities across the State were low, which no ecoregions exceeding 1 fire occurrence/100 km^2 of forest and shrub cover (fig. 3.3).

In Hawaii, the dramatic Big Island eruption of lava through 24 new fissures in the lower east rift zone of the Kīlauea volcano burned forests and consumed 700 homes at the very eastern tip of the island (Andrews 2018), resulting in a fire occurrence density of 7.4/100 km^2 of tree canopy cover in the island's Lowland Wet-Hilo-Puna ecoregion (LWh-hp) (fig. 3.4). The eruption also affected the neighboring Mesic ecoregion (MEh), where fire occurrence density was 3.2/100 km^2 of tree canopy cover. All other

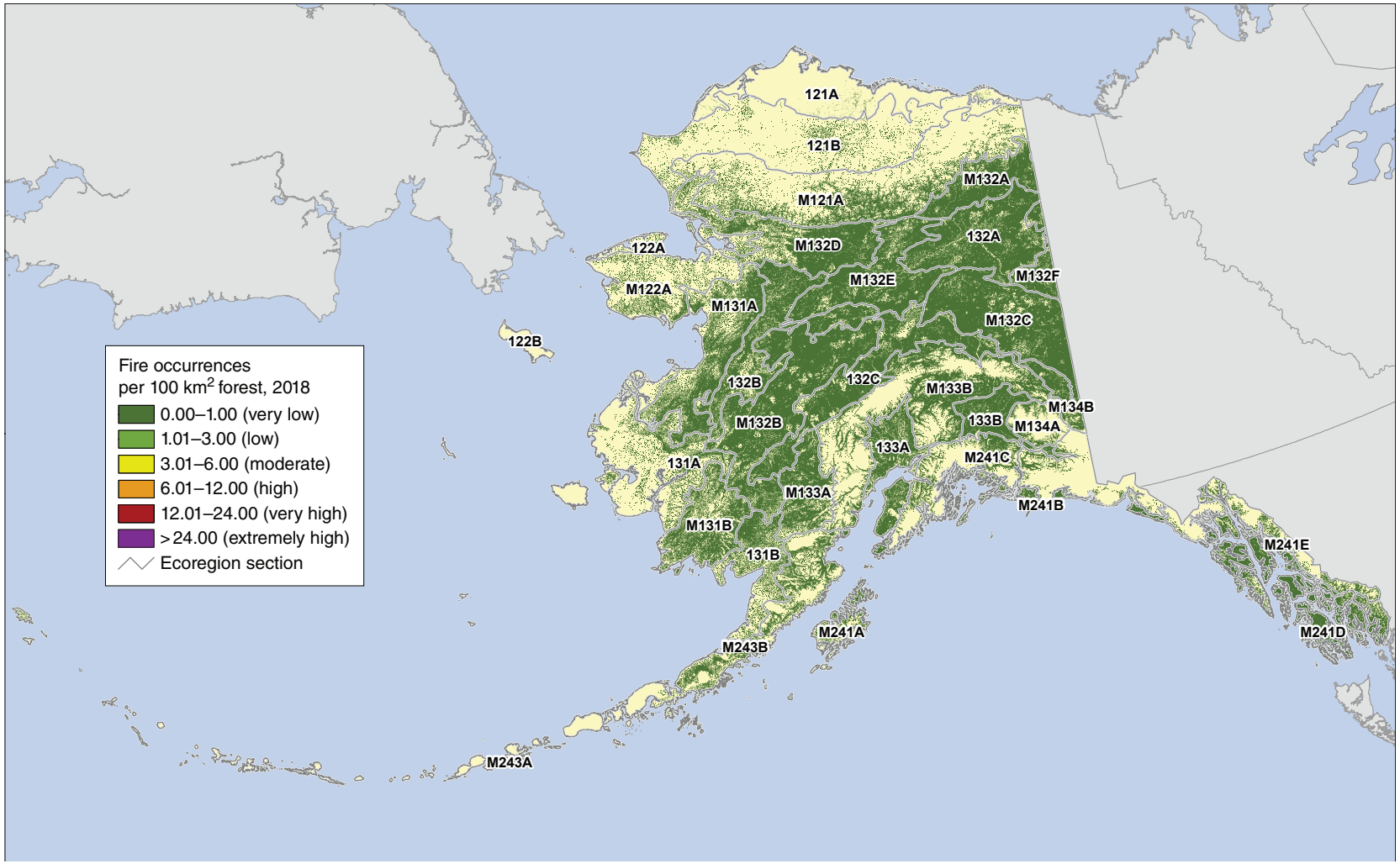

Figure 3.3—The number of forest fire occurrences, per 100 km^2 (10 000 ha) of forest and shrub cover, by ecoregion section within Alaska, for 2018. The gray lines delineate ecoregion sections (Spencer and others 2002). Forest and shrub cover is derived from the 2011 National Land Cover Database. (Source of fire data: U.S. Department of Agriculture Forest Service, Geospatial Technology and Applications Center, in conjunction with the NASA MODIS Rapid Response group)

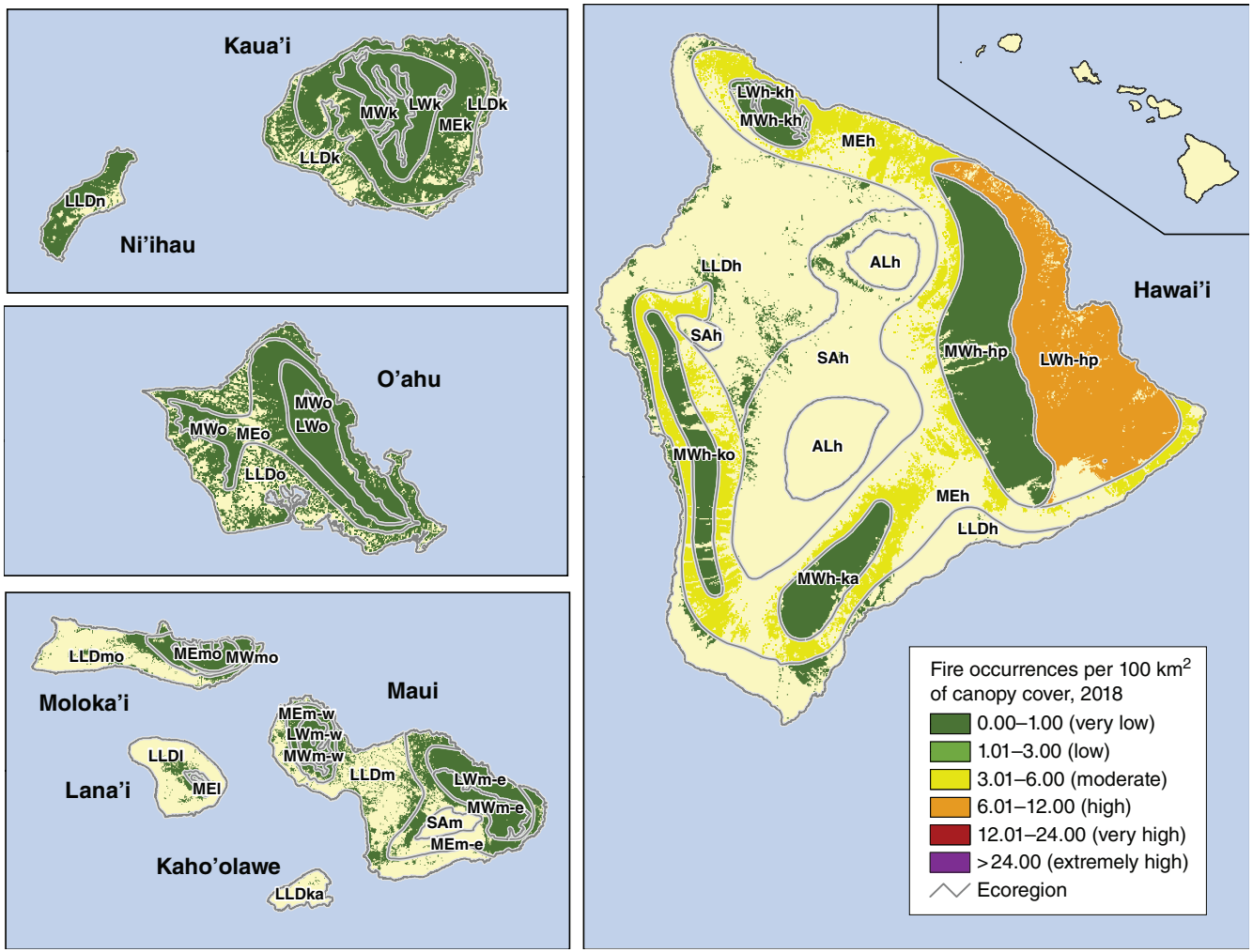

Figure 3.4—The number of forest fire occurrences, per 100 km^2 (10 000 ha) of tree canopy coverage area, by island/ecoregion combination in Hawaii, for 2018. Tree canopy cover is based on data from a cooperative project between the Multi-Resolution Land Characteristics Consortium (Coulston and others 2012) and the Forest Service Geospatial Technology and Applications Center using the 2011 National Land Cover Database. See figure 1.2 for ecoregion identification. (Source of fire data: U.S. Department of Agriculture Forest Service, Geospatial Technology and Applications Center, in conjunction with the NASA MODIS Rapid Response group)

ecoregions in the State had fire occurrence densities of ≤1 fire occurrence/100 km^2 of tree canopy cover.

Finally, fire occurrence densities were all ≤1 fire occurrence/100 km^2 of tree canopy cover for all of the islands constituting the U.S. Caribbean territories (Puerto Rico and the U.S. Virgin Islands) in 2018 (fig. 3.5).

Comparison to Longer Term Trends

The nature of the MODIS Active Fire data makes it possible to contrast, for each ecoregion in the conterminous States, Alaska, and Hawaii, and for each Caribbean island, short-term (2018) forest fire occurrence densities with longer term trends encompassing the first 17 full years of data collection (2001–2017). In general, the ecoregion sections of the conterminous States with the highest annual fire occurrence means are located in the northern Rocky Mountains, California, the Southwest, and the Southeastern Coastal Plain, while most ecoregion sections within the Northeastern, Midwestern, Middle Atlantic, and Appalachian regions experienced ≤3 fire occurrences/100 km^2 of tree canopy cover annually during the multiyear period (fig. 3.6A). The forested ecoregion section that experienced the most annual fire occurrences on average was M332A–Idaho Batholith in central Idaho (mean annual fire occurrence density of 13.4) (table 3.2). Other ecoregion sections with high mean fire occurrence densities (6.01–12.00 fire occurrences/100 km^2 of canopy cover) were located along the Gulf Coast in the Southeast; in coastal, northern, and central areas of California; in north-central Washington; in central Arizona and New Mexico; in the northern Rocky Mountains; and in central Kansas and northeastern Oklahoma (table 3.2). The ecoregion section with the greatest variation in fire occurrence densities from 2001 to 2017 was M332A–Idaho Batholith, with more moderate variation in California, northern Washington, southern and northeastern Oregon, western Montana, and central Arizona and west-central New Mexico (fig. 3.6B). Less variation occurred throughout the central Rocky Mountain States, the Great Basin, the Southeast, and central Oregon and Washington. The lowest levels of variation occurred throughout most of the Midwest and Northeast.

As determined by the calculation of standardized fire occurrence *z*-scores, ecoregion sections in northern California; northeastern Nevada; the central Rocky Mountains of southeastern Idaho, southwestern Wyoming, northeastern Utah, northwestern and south-central Colorado, and northeastern New Mexico; and southern Florida experienced significantly greater fire occurrence densities than normal in 2018, compared to the previous 17-year mean and accounting for variability over time (fig. 3.6C). The ecoregion section with the highest *z*-score in 2018 was 341G–Northeastern Great Basin, location of the Martin Fire. Additionally, some ecoregion sections in the West had moderately or slightly higher fire occurrence density than expected as indicated by their *z*-scores (fig. 3.6C), including M261A–Klamath Mountains in northern California

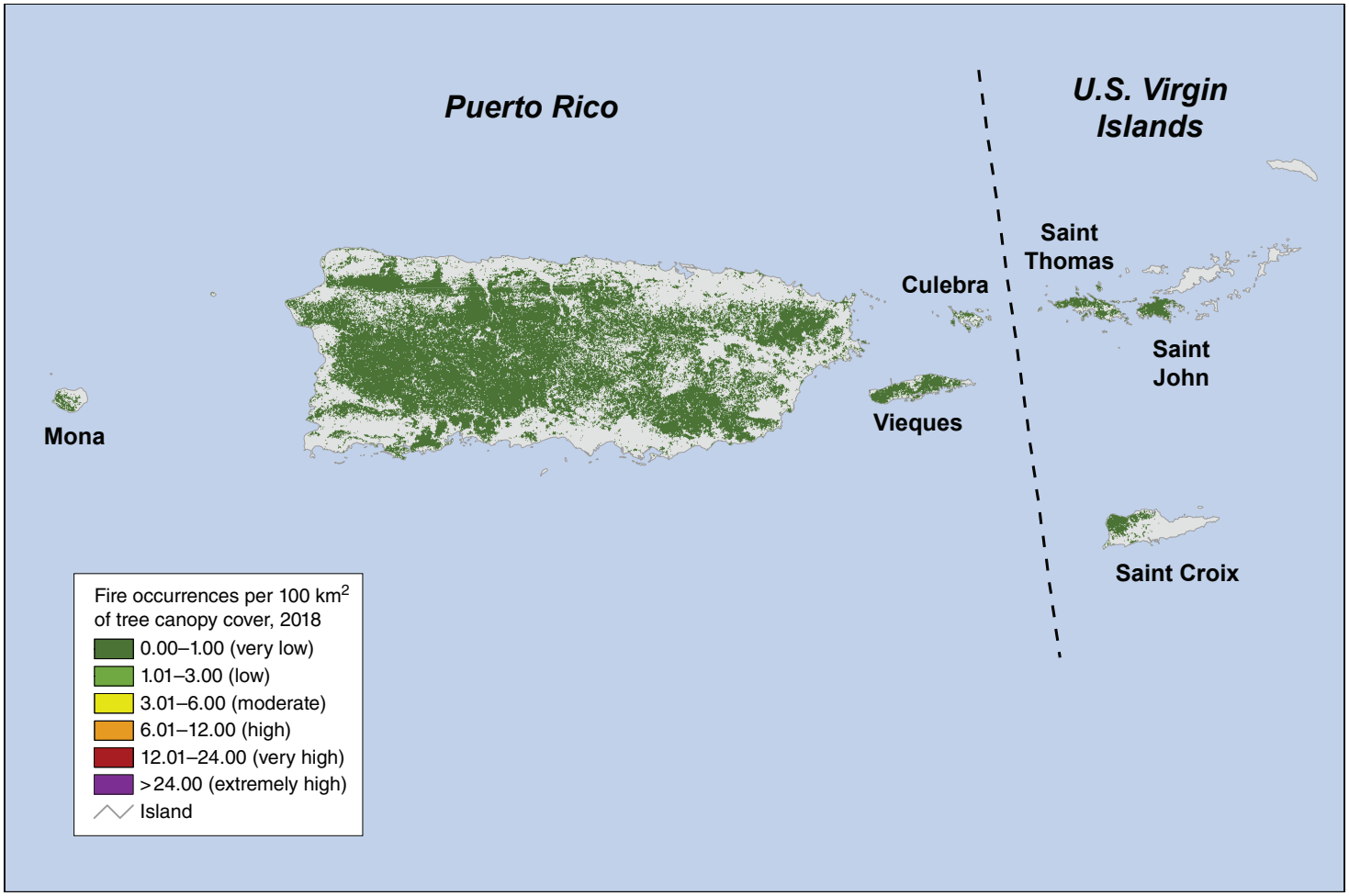

Figure 3.5—The number of forest fire occurrences, per 100 km^2 (10 000 ha) of tree canopy coverage area, by island in Puerto Rico and the U.S. Virgin Islands, for 2018. Tree canopy cover is based on data from a cooperative project between the Multi-Resolution Land Characteristics Consortium (Coulston and others 2012) and the Forest Service Geospatial Technology and Applications Center using the 2011 National Land Cover Database. (Source of fire data: U.S. Department of Agriculture Forest Service, Geospatial Technology and Applications Center, in conjunction with the NASA MODIS Rapid Response group)

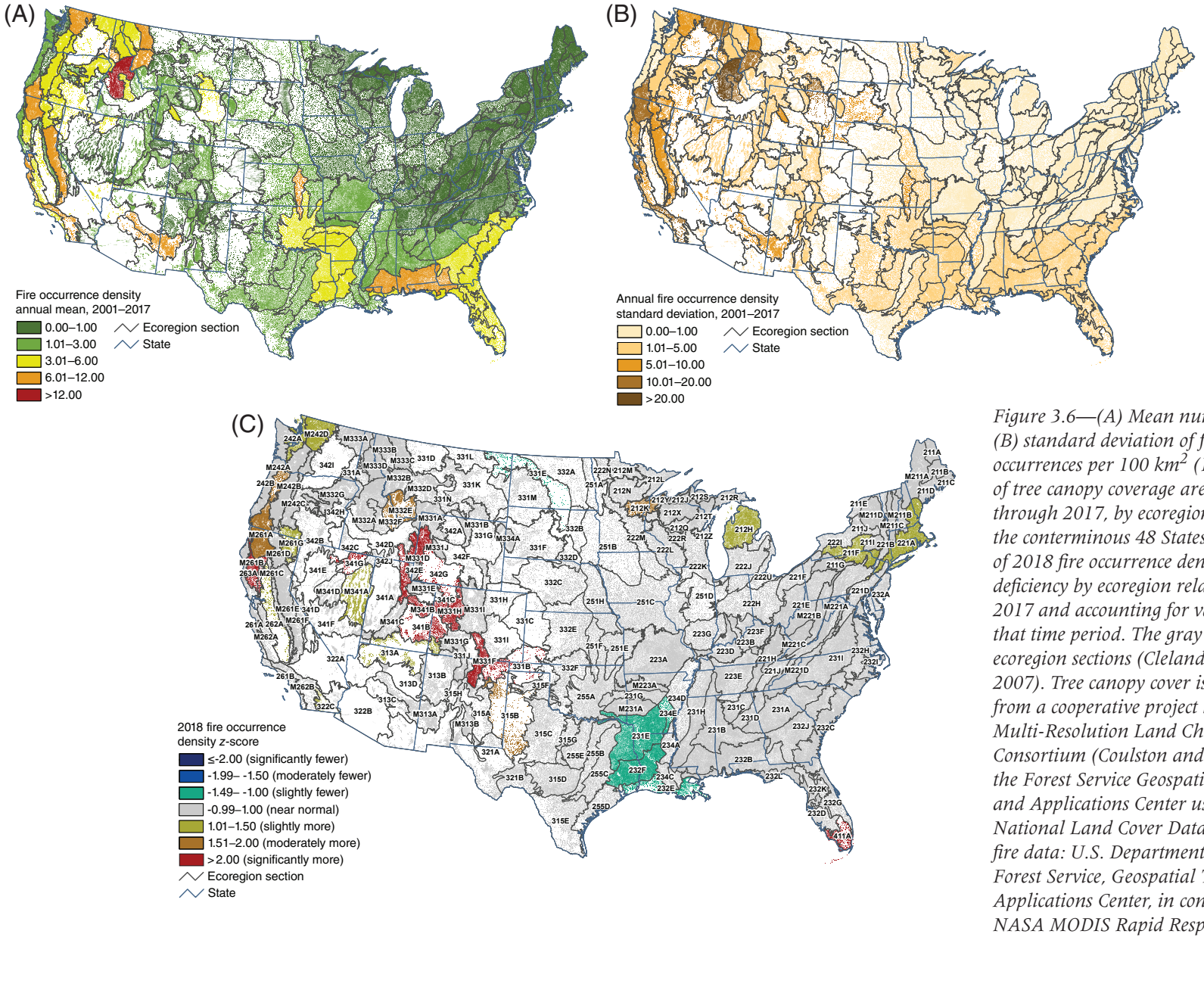

Figure 3.6—(A) Mean number and (B) standard deviation of forest fire occurrences per 100 km^2 (10 000 ha) of tree canopy coverage area from 2001 through 2017, by ecoregion section within the conterminous 48 States. (C) Degree of 2018 fire occurrence density excess or deficiency by ecoregion relative to 2001–2017 and accounting for variation over that time period. The gray lines delineate ecoregion sections (Cleland and others 2007). Tree canopy cover is based on data from a cooperative project between the Multi-Resolution Land Characteristics Consortium (Coulston and others 2012) and the Forest Service Geospatial Technology and Applications Center using the 2011 National Land Cover Database. (Source of fire data: U.S. Department of Agriculture Forest Service, Geospatial Technology and Applications Center, in conjunction with the NASA MODIS Rapid Response group)

Table 3.2—The 15 ecoregion sections in the conterminous United States with the highest annual mean fire occurrence densities from 2001 through 2017

Section	Name	Tree canopy area	Mean annual fire occurrence density
		km^2	*fire occurrences per 100 km^2 of tree canopy coverage area*
M332A	Idaho Batholith	338.9	13.4
M261A	Klamath Mountains	338.5	9.6
M262B	Southern California Mountain and Valley	58.1	9.2
313C	Tonto Transition	17.5	7.8
M261E	Sierra Nevada	427.8	7.7
M313A	White Mountains-San Francisco Peaks-Mogollon Rim	202.5	7.7
251F	Flint Hills	57.8	7.1
261A	Central California Coast	66.8	6.7
M242D	Northern Cascades	251.1	6.1
232B	Gulf Coastal Plains and Flatwoods	888.7	6.1
331A	Palouse Prairie	33.4	6.0
M332B	Northern Rockies and Bitterroot Valley	154.9	6.0
M333C	Northern Rockies	176.3	6.0
M332F	Challis Volcanics	72.2	6.0
232J	Southern Atlantic Coastal Plains and Flatwoods	604.0	5.3

and southwestern Oregon, 242B–Willamette Valley in northwestern Oregon, and M332E–Beaverhead Mountains in east-central Idaho and southwestern Montana. A number of ecoregions in the Midwest and Northeast also experienced slightly or moderately more fire occurrences than normal: 212K–Western Superior Uplands in west-central Minnesota and northwest Wisconsin, 212H–Northern Lower Peninsula in Michigan, 211F–Northern Glaciated Allegheny Plateau in southern New York and northern Pennsylvania, and 221A–Lower New England.

A handful of ecoregion sections in the south-central part of the country, meanwhile, had lower fire occurrence densities in 2018 compared to the longer term as indicated by their *z*-scores: 231E–Mid Coastal Plains-Western in eastern Texas, southwestern Arkansas, and southeastern Oklahoma; 234E–Arkansas Alluvial Plains in southeastern Arkansas; 232F–Coastal Plains and

Flatwoods-Western Gulf in southeastern Texas and central Louisiana; and 232E–Louisiana Coastal Prairie and Marshes in southern Louisiana (fig. 3.6C). Each of these had a very low fire occurrence density score in 2018, with some having somewhat higher annual mean fire occurrence densities for 2001–2017.

In Alaska, meanwhile, moderate mean fire occurrence density existed in the east-central and central parts of the State, encompassing 132A–Yukon-Old Crow Basin and M132E–Ray Mountains (fig. 3.7A). These same areas, along with M132C–Yukon-Tanana Uplands and M132F–North Ogilvie Mountains, experienced the greatest degree of variability over the 17-year period preceding 2018 (fig. 3.7B). In 2018, no ecoregion sections were outside the range of near-normal fire occurrence density (z-score ≤-1 or >1) for the previous 17 years and accounting for variability (fig. 3.7C).

In Hawaii, both mean annual fire occurrence density (fig. 3.8A) and variability (fig. 3.8B) were highest in the Lowland Wet-Hilo-Puna ecoregion (LWh-hp) of the Big Island during the 2001–2017 period. The annual mean was ≤1 fire occurrence/100 km^2 of tree cover for all other ecoregions except the Mesic region on the Big Island (MEh), which was 2.2. In 2018, only one Hawaiian island/ecoregion combination was outside the range of near-normal fire occurrence density, controlling for variability over the previous 17 years (z-score ≤-1 or >1). This was the Lowland/Leeward Dry ecoregion on Maui (LLDm), which had slightly fewer fire occurrences than expected (fig. 3.7C).

All the islands of the Caribbean territories had annual fire occurrence means and standard deviations ≤1 (figs. 3.9A and 3.9B). Among the Caribbean islands, only Puerto Rico was outside the range of near-normal fire occurrence density (z-score ≤-1 or >1) in 2018, having slightly fewer fire occurrences than expected (fig. 3.9C).

Geographical Hot Spots of Fire Occurrence Density

Although summarizing fire occurrence data at the ecoregion section scale allows for the quantification of fire occurrence density across the country, a geographical hot spot analysis can offer insights into where, statistically, fire occurrences are more concentrated than expected by chance. In 2018, the SASH method detected one geographic hot spot of extremely high fire occurrence density (G_i^* >24) and four hot spots of very high fire occurrence density (G_i^* >12 and ≤24) (fig. 3.10). The hot spot of extremely high density was in northern California, in ecoregion sections M261B–Northern California Coast Ranges and M261C–Northern California Interior Coast Ranges. Three of the four hot spots of very high occurrence density were also in northern California and southwestern Oregon, contained within ecoregions shown by earlier analysis to be locations of high fire occurrence density (fig. 3.2). The fourth hot spot was in north-central Washington (M242D–Northern Cascades).

Hot spots of high fire occurrence density (G_i^* >6 and ≤12) were identified in south-central Oregon (M242C–Eastern Cascades and

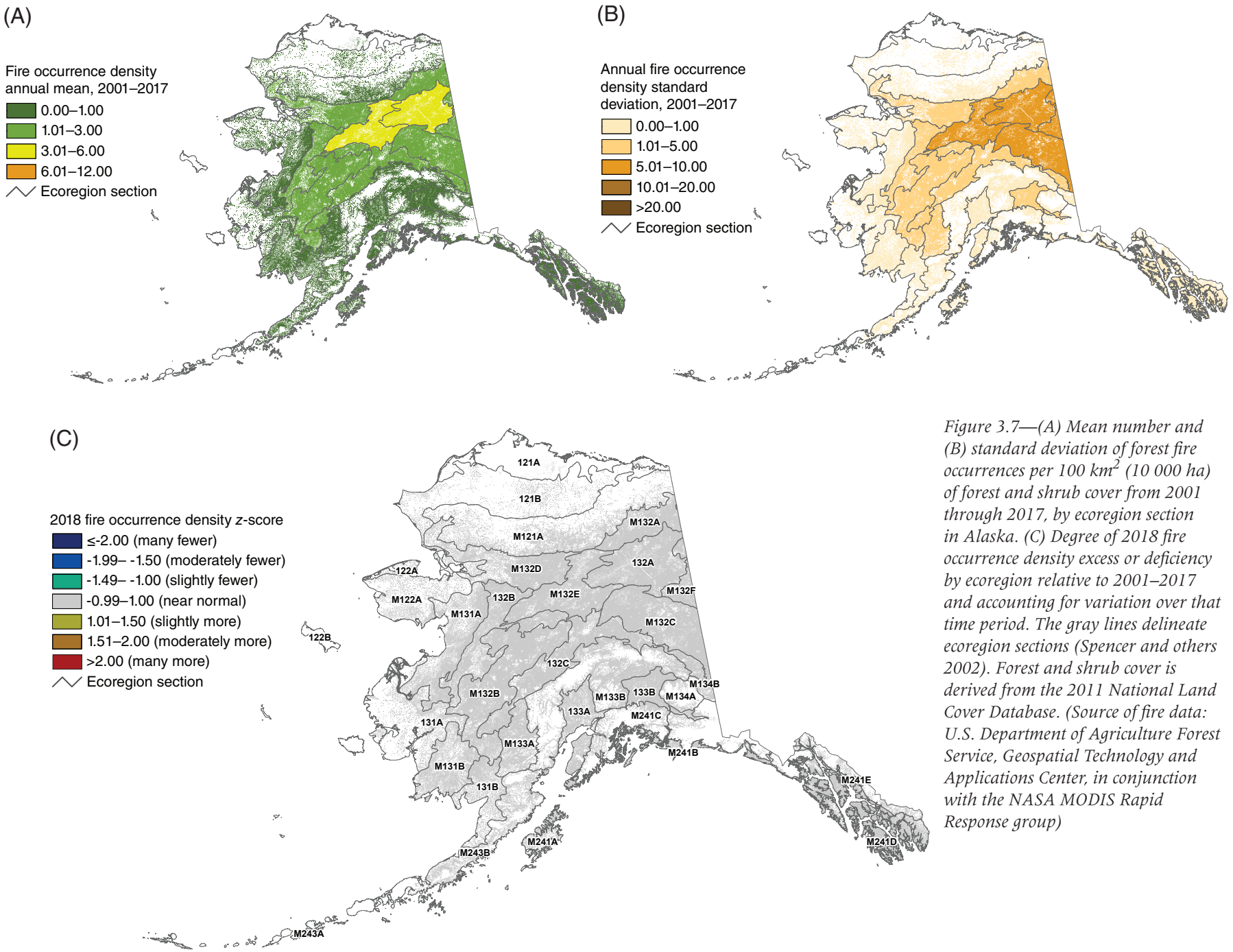

Figure 3.7—(A) Mean number and (B) standard deviation of forest fire occurrences per 100 km^2 (10 000 ha) of forest and shrub cover from 2001 through 2017, by ecoregion section in Alaska. (C) Degree of 2018 fire occurrence density excess or deficiency by ecoregion relative to 2001–2017 and accounting for variation over that time period. The gray lines delineate ecoregion sections (Spencer and others 2002). Forest and shrub cover is derived from the 2011 National Land Cover Database. (Source of fire data: U.S. Department of Agriculture Forest Service, Geospatial Technology and Applications Center, in conjunction with the NASA MODIS Rapid Response group)

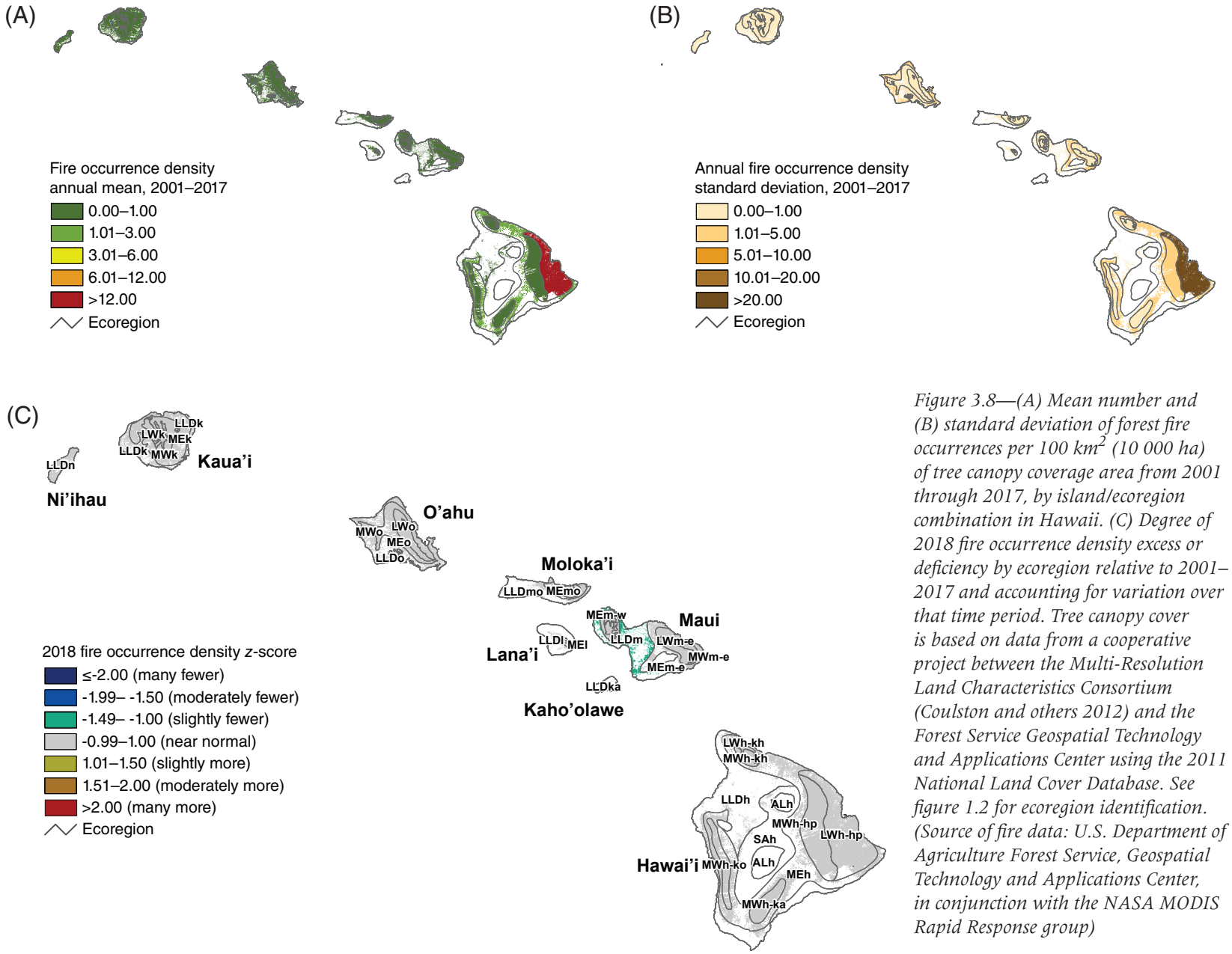

Figure 3.8—(A) Mean number and (B) standard deviation of forest fire occurrences per 100 km^2 (10 000 ha) of tree canopy coverage area from 2001 through 2017, by island/ecoregion combination in Hawaii. (C) Degree of 2018 fire occurrence density excess or deficiency by ecoregion relative to 2001–2017 and accounting for variation over that time period. Tree canopy cover is based on data from a cooperative project between the Multi-Resolution Land Characteristics Consortium (Coulston and others 2012) and the Forest Service Geospatial Technology and Applications Center using the 2011 National Land Cover Database. See figure 1.2 for ecoregion identification. (Source of fire data: U.S. Department of Agriculture Forest Service, Geospatial Technology and Applications Center, in conjunction with the NASA MODIS Rapid Response group)

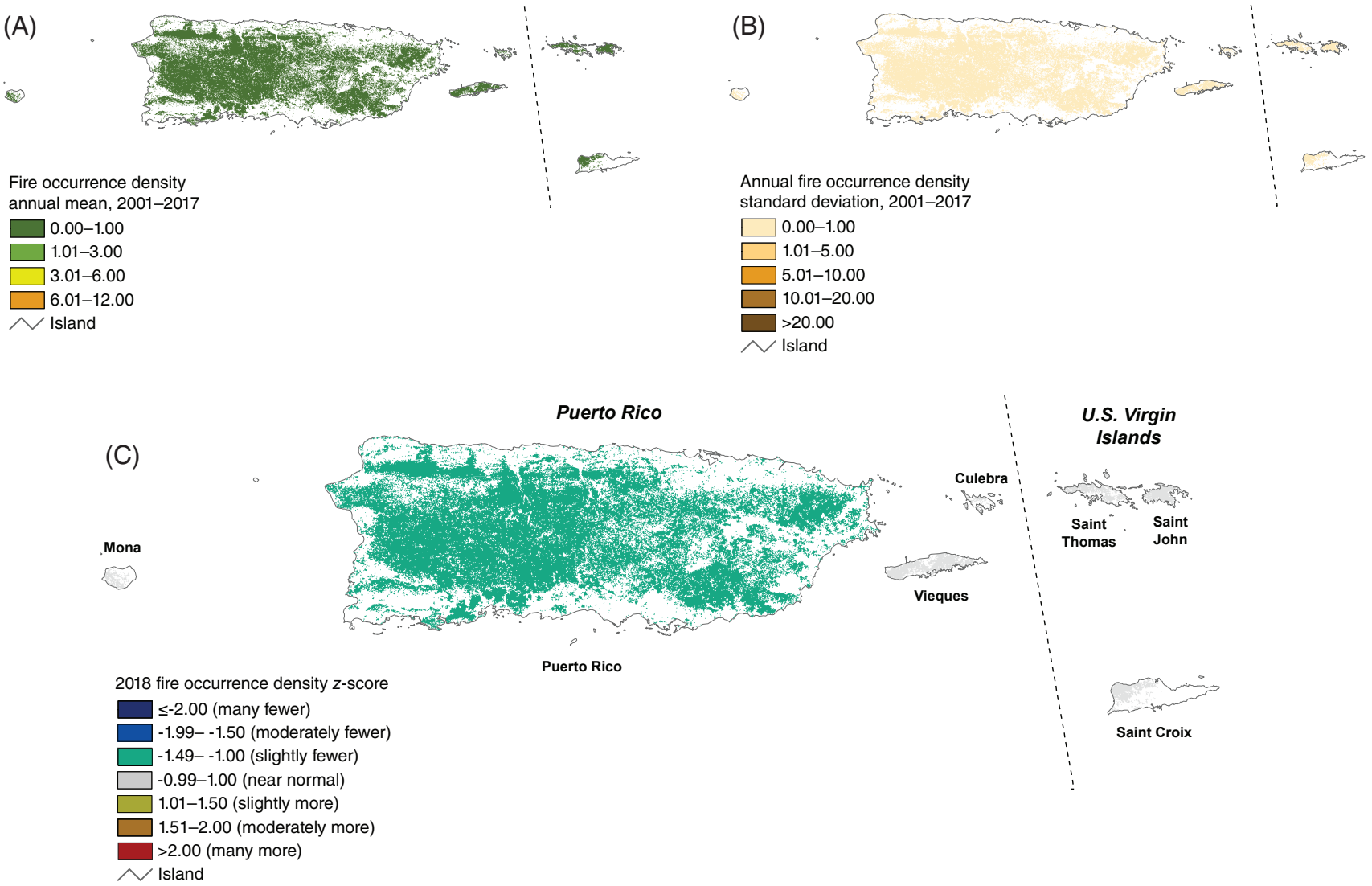

Figure 3.9—(A) Mean number and (B) standard deviation of forest fire occurrences per 100 km^2 (10 000 ha) of forested area from 2001 through 2017, by island in Puerto Rico and the U.S. Virgin Islands. (C) Degree of 2018 fire occurrence density excess or deficiency by ecoregion relative to 2001–2017 and accounting for variation over that time period. Tree canopy cover is based on data from a cooperative project between the Multi-Resolution Land Characteristics Consortium (Coulston and others 2012) and the U.S. Department of Agriculture Forest Service, Geospatial Technology and Applications Center using the 2011 National Land Cover Database.

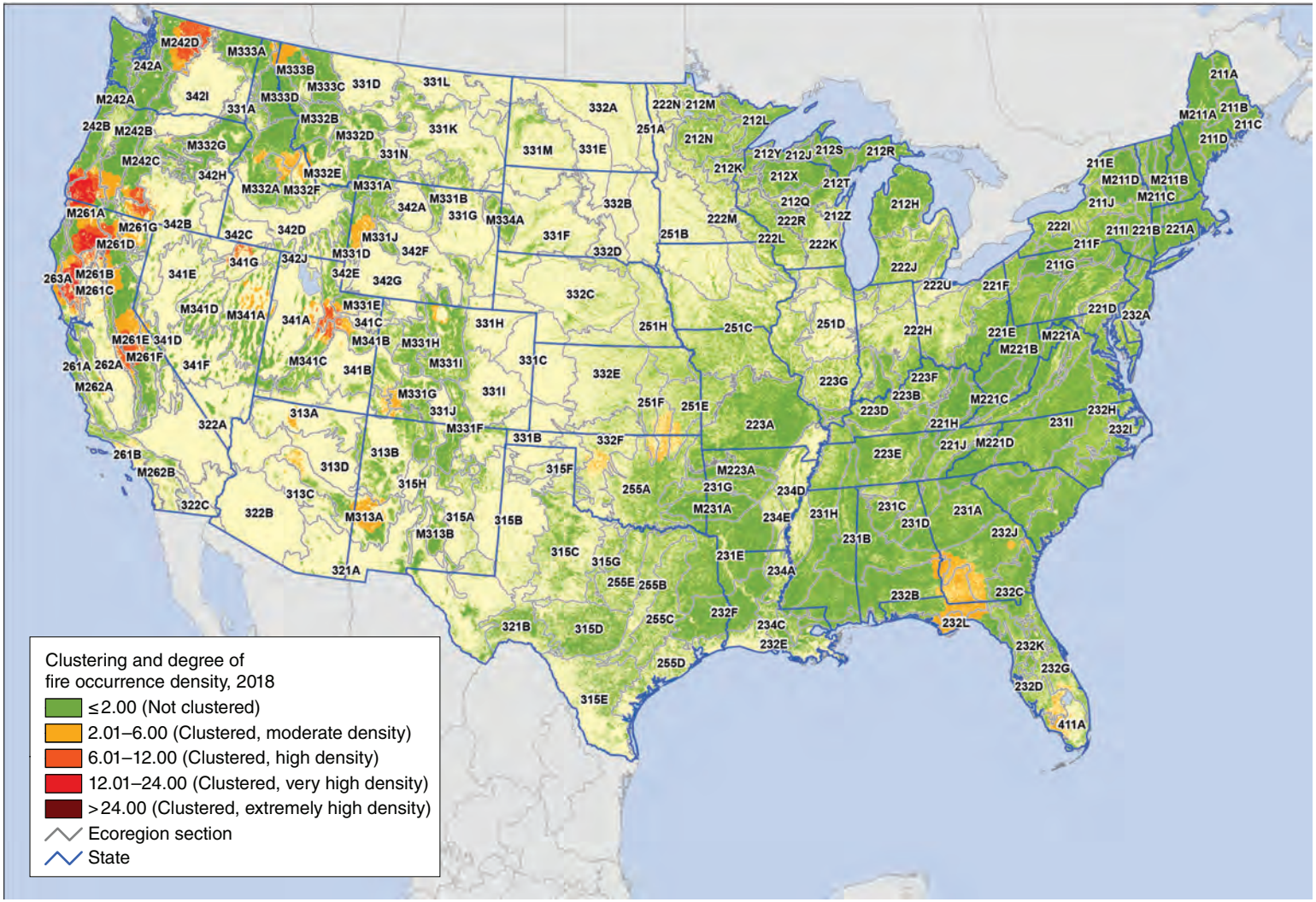

Figure 3.10—Hot spots of fire occurrence across the conterminous United States for 2018. Values are Getis-Ord Gi* *scores, with values >2 representing significant clustering of high fire occurrence densities. (No areas of significant clustering of lower fire occurrence densities, <-2, were detected). The gray lines delineate ecoregion sections (Cleland and others 2007). Background tree canopy cover is based on data from a cooperative project between the Multi-Resolution Land Characteristics Consortium (Coulston and others 2012) and the Forest Service Geospatial Technology and Applications Center using the 2011 National Land Cover Database. (Source of fire data: U.S. Department of Agriculture Forest Service, Geospatial Technology and Applications Center, in conjunction with the NASA MODIS Rapid Response group)*

M261G–Modoc Plateau), the Sierra Nevada of California (M261E), northeastern Nevada (341G–Northeastern Great Basin), and central Utah (M331D–Overthrust Mountains, M331E–Uinta Mountains, M341B–Tavaputs Plateau, and M341C–Utah High Plateau).

Hot spots of moderate fire density in 2018 (G_i^* >2 and ≤6) were identified in scattered locations within the Rocky Mountain States, the southern Plains States, and the Southeast (fig. 3.10). From west to east, these were detected in:

- Northwestern Montana and northern Idaho (M333B–Flathead Valley)
- Central Idaho (M332A–Idaho Batholith, M332E–Beaverhead Mountains, and M332F–Challis Volcanics)
- Eastern Nevada (M341A–East Great Basin and Mountains)
- Northern Arizona (313A–Grand Canyon)
- Central Arizona (M313A–White Mountains-San Francisco Peaks-Mogollon Rim)
- Western Wyoming (M331D–Overthrust Mountains)
- Southwestern New Mexico (M313A–White Mountains-San Francisco Peaks-Mogollon Rim)
- Southwestern Colorado (M331G–South Central Highlands and 313B–Navajo Canyonlands)
- North-central Colorado (M331I–Northern Parks and Ranges)
- West-central Oklahoma (332F–South Central and Red Bed Plains)
- Southeastern Kansas and northeastern Oklahoma (251F–Flint Hills, 255A–Cross Timbers and Prairie, and 251E–Osage Plains)
- Florida Panhandle and southwestern Georgia (232B–Gulf Coastal Plains and Flatwoods, 232J–Southern Atlantic Coastal Plains and Flatwoods, and 232L–Gulf Coastal Lowlands)
- Southern Florida (232D– Florida Coastal Lowlands-Gulf and 411A–Everglades)

CONCLUSIONS AND FUTURE WORK

In 2018, the number of MODIS satellite-detected forest fire occurrences recorded for the conterminous States was the ninth most in 18 full years of data collection and was nearly identical to the annual mean of forest fire occurrences across the previous 17 years of data collection. Ecoregion sections in northern California/southwestern Oregon, north-central Washington, and northeastern Nevada had the highest forest fire occurrence density per 100 km^2 of tree canopy cover area. Geographic hot spots of high fire occurrence density were detected in these same areas, as well as in Utah and the Sierra Nevada of California. Ecoregion sections in northern California; the Cascade Mountains of Oregon and Washington; northern and eastern Nevada; the central Rocky Mountains; central Minnesota; northern Michigan; and the Northeastern States experienced greater fire occurrence density than normal compared to the previous 17-year mean and accounting for variability over time.

Ecoregions in eastern Texas, southern Arkansas, and much of Louisiana, meanwhile, had lower fire occurrence density than expected. Alaska had low fire occurrence densities throughout the State. In Hawaii, the Lowland Wet ecoregion of the Big Island experienced relatively high fire occurrence density because of a volcanic eruption near the eastern tip of the island.

The results of these geographic analyses are intended to offer insights into where fire occurrences have been concentrated spatially in a given year and compared to previous years but are not intended to quantify the severity of a given fire season. Given the limits of MODIS active fire detection using 1-km resolution data, these products also may underrepresent the number of fire occurrences in some ecosystems where small and low-intensity fires are common, and where high cloud frequency can interfere with fire detection. These products can also have commission errors. However, these high-temporal-fidelity products currently offer the best means for daily monitoring of forest fire occurrences.

Future work related to understanding geographic patterns of forest fire occurrences in the United States could include a comparison of the MODIS detections with those of the VIIRS sensor, an analysis of fire occurrence detections by forest cover types, an evaluation of whether the fire occurrences correspond with mapped burned areas, an assessment of the relationships between fire occurrence and drought conditions, and an analysis of the potential ecological consequences of high fire occurrence densities using data such as those available from the Forest Inventory and Analysis program.

Ecological and forest health impacts relating to fire and other abiotic disturbances are scale-dependent properties, which in turn are affected by management objectives (Lundquist and others 2011). Information about the concentration of fire occurrences may help pinpoint areas of concern for aiding management activities and for investigations into the ecological and socioeconomic impacts of forest fire potentially outside the range of historic frequency.

LITERATURE CITED

Andrews, R.G. 2018. America's most hazardous volcano erupted this year. Then it erupted and erupted. The New York Times. December 12. https://www.nytimes.com/2018/12/12/science/kilauea-hawaii-volcano-eruption.html. [Date accessed: July 15, 2019].

Anselin, L. 1992. Spatial data analysis with GIS: an introduction to application in the social sciences. Technical Report 92-10. Santa Barbara, CA: University of California, National Center for Geographic Information and Analysis. 53 p.

Barbour, M.G.; Burk, J.H.; Pitts, W.D. [and others]. 1999. Terrestrial plant ecology. Menlo Park, CA: Addison Wesley Longman, Inc. 649 p.

Bond, W.J.; Keeley, J.E. 2005. Fire as a global "herbivore": the ecology and evolution of flammable ecosystems. Trends in Ecology & Evolution. 20(7): 387–394.

CAL FIRE. 2019. Top 20 largest California wildfires. https://fire.ca.gov/media/5510/top20_acres.pdf. [Date accessed: July 15, 2019].

Cleland, D.T.; Freeouf, J.A.; Keys, J.E. [and others]. 2007. Ecological subregions: sections and subsections for the conterminous United States. Gen. Tech. Rep. WO-76D. Washington, DC: U.S. Department of Agriculture Forest Service. Map; Sloan, A.M., cartographer; presentation scale 1:3,500,000; colored. Also on CD-ROM as a GIS coverage in ArcINFO format or at http://data.fs.usda.gov/geodata/edw/datasets.php. [Date accessed: July 20, 2015].

Coulston, J.W.; Moisen, G.G.; Wilson, B.T. [and others]. 2012. Modeling percent tree canopy cover: a pilot study. Photogrammetric Engineering and Remote Sensing. 78(7): 715–727.

Coulston, J.W.; Ambrose, M.J.; Riitters, K.H.; Conkling, B.L. 2005. Forest Health Monitoring 2004 national technical report. Gen. Tech. Rep. SRS-90. Asheville, NC: U.S. Department of Agriculture Forest Service, Southern Research Station. 81 p.

Edmonds, R.L.; Agee, J.K.; Gara, R.I. 2011. Forest health and protection. Long Grove, IL: Waveland Press, Inc. 667 p.

ESRI. 2015. ArcMap® 10.3. Redlands, CA: Environmental Systems Research Institute.

Getis, A.; Ord, J.K. 1992. The analysis of spatial association by use of distance statistics. Geographical Analysis. 24(3): 189–206.

Gill, A.M.; Stephens, S.L.; Cary, G.J. 2013. The worldwide "wildfire" problem. Ecological Applications. 23(2): 438–454.

Hawbaker, T.J.; Radeloff, V.C.; Syphard, A.D. [and others]. 2008. Detection rates of the MODIS active fire product. Remote Sensing of Environment. 112: 2656–2664.

Homer, C.G.; Dewitz, J.A.; Yang, L. [and others]. 2015. Completion of the 2011 National Land Cover Database for the conterminous United States: representing a decade of land cover change information. Photogrammetric Engineering and Remote Sensing. 81(5): 345–354.

Justice, C.O.; Giglio, L.; Korontzi, S. [and others]. 2002. The MODIS fire products. Remote Sensing of Environment. 83(1–2): 244–262.

Justice, C.O.; Giglio, L.; Roy, D. [and others]. 2011. MODIS-derived global fire products. In: Ramachandran, B.; Justice, C.O.; Abrams, M.J., eds. Land remote sensing and global environmental change: NASA's earth observing system and the science of ASTER and MODIS. New York: Springer: 661–679.

Laffan, S.W. 2006. Assessing regional scale weed distributions, with an Australian example using *Nassella trichotoma*. Weed Research. 46(3): 194–206.

Lundquist, J.E.; Camp, A.E.; Tyrrell, M.L. [and others]. 2011. Earth, wind and fire: abiotic factors and the impacts of global environmental change on forest health. In: Castello, J.D.; Teale, S.A., eds. Forest health: an integrated perspective. New York: Cambridge University Press: 195–243.

McKenzie, D.; Peterson, D.L.; Alvarado, E. 1996. Predicting the effect of fire on large-scale vegetation patterns in North America. Res. Pap. PNW-489. Portland, OR: U.S. Department of Agriculture Forest Service, Pacific Northwest Research Station. 38 p.

National Interagency Coordination Center. 2017. Wildland fire summary and statistics annual report: 2016. http://www.predictiveservices.nifc.gov/intelligence/2016_Statssumm/intro_summary16.pdf. [Date accessed: May 30, 2017].

National Interagency Coordination Center. 2018. Wildland fire summary and statistics annual report: 2017. https://www.predictiveservices.nifc.gov/intelligence/2017_statssumm/intro_summary17.pdf. [Date accessed: April 30, 2018].

National Interagency Coordination Center. 2019. Wildland fire summary and statistics annual report: 2018. https://www.predictiveservices.nifc.gov/intelligence/2018_statssumm/intro_summary18.pdf. [Date accessed: June 27, 2019].

Nowacki, G.J.; Abrams, M.D. 2008. The demise of fire and "mesophication" of forests in the Eastern United States. BioScience. 58(2): 123–138.

Potter, K.M. 2012a. Large-scale patterns of forest fire occurrence in the conterminous United States and Alaska, 2005–07. In: Potter, K.M.; Conkling, B.L., eds. Forest Health Monitoring 2008 national technical report. Gen. Tech. Rep. SRS-158. Asheville, NC: U.S. Department of Agriculture Forest Service, Southern Research Station: 73–83.

Potter, K.M. 2012b. Large-scale patterns of forest fire occurrence in the conterminous United States and Alaska, 2001–08. In: Potter, K.M.; Conkling, B.L., eds. Forest Health Monitoring 2009 national technical report. Gen. Tech. Rep. SRS-167. Asheville, NC: U.S. Department of Agriculture Forest Service, Southern Research Station: 151–161.

Potter, K.M. 2013a. Large-scale patterns of forest fire occurrence in the conterminous United States and Alaska, 2009. In: Potter, K.M.; Conkling, B.L., eds. Forest Health Monitoring: national status, trends, and analysis 2010. Gen. Tech. Rep. SRS-176. Asheville, NC: U.S. Department of Agriculture Forest Service, Southern Research Station: 31–39.

Potter, K.M. 2013b. Large-scale patterns of forest fire occurrence in the conterminous United States and Alaska, 2010. In: Potter, K.M.; Conkling, B.L., eds. Forest Health Monitoring: national status, trends, and analysis 2011. Gen. Tech. Rep. SRS-185. Asheville, NC: U.S. Department of Agriculture Forest Service, Southern Research Station: 29–40.

Potter, K.M. 2014. Large-scale patterns of forest fire occurrence in the conterminous United States and Alaska, 2011. In: Potter, K.M.; Conkling, B.L., eds. Forest Health Monitoring: national status, trends, and analysis 2012. Gen. Tech. Rep. SRS-198. Asheville, NC: U.S. Department of Agriculture Forest Service, Southern Research Station: 35–48.

Potter, K.M. 2015a. Large-scale patterns of forest fire occurrence in the conterminous United States and Alaska, 2012. In: Potter, K.M.; Conkling, B.L., eds. Forest Health Monitoring: national status, trends, and analysis 2013. Gen. Tech. Rep. SRS-207. Asheville, NC: U.S. Department of Agriculture Forest Service, Southern Research Station: 37–53.

Potter, K.M. 2015b. Large-scale patterns of forest fire occurrence in the conterminous United States and Alaska, 2013. In: Potter, K.M.; Conkling, B.L., eds. Forest Health Monitoring: national status, trends, and analysis 2014. Gen. Tech. Rep. SRS-209. Asheville, NC: U.S. Department of Agriculture Forest Service, Southern Research Station: 39–55.

Potter, K.M. 2016. Large-scale patterns of forest fire occurrence in the conterminous United States, Alaska, and Hawaii, 2014. In: Potter, K.M.; Conkling, B.L., eds. Forest Health Monitoring: national status, trends, and analysis 2015. Gen. Tech. Rep. SRS-213. Asheville, NC: U.S. Department of Agriculture Forest Service, Southern Research Station: 41–60.

Potter, K.M. 2017. Large-scale patterns of forest fire occurrence in the conterminous United States, Alaska, and Hawaii, 2015. In: Potter, K.M.; Conkling, B.L., eds. Forest Health Monitoring: national status, trends, and analysis 2016. Gen. Tech. Rep. SRS-222. Asheville, NC: U.S. Department of Agriculture Forest Service, Southern Research Station: 43–62.

Potter, K.M. 2018. Large-scale patterns of forest fire occurrence in the conterminous United States, Alaska, and Hawaii, 2016. In: Potter, K.M.; Conkling, B.L., eds. Forest Health Monitoring: national status, trends, and analysis 2017. Gen. Tech. Rep. SRS-233. Asheville, NC: U.S. Department of Agriculture Forest Service, Southern Research Station: 45–64.

Potter, K.M. 2019. Large-scale patterns of forest fire occurrence across the 50 United States and the Caribbean territories, 2017. In: Potter, K.M.; Conkling, B.L., eds. Forest Health Monitoring: national status, trends, and analysis 2018. Gen. Tech. Rep. SRS-239. Asheville, NC: U.S. Department of Agriculture Forest Service, Southern Research Station: 51–76.

Potter, K.M.; Koch, F.H.; Oswalt, C.M.; Iannone, B.V. 2016. Data, data everywhere: detecting spatial patterns in fine-scale ecological information collected across a continent. Landscape Ecology. 31: 67–84.

Pyne, S.J. 2010. America's fires: a historical context for policy and practice. Durham, NC: Forest History Society. 91 p.

Reams, G.A.; Smith, W.D.; Hansen, M.H. [and others]. 2005. The Forest Inventory and Analysis sampling frame. In: Bechtold, W.A.; Patterson, P.L., eds. The enhanced Forest Inventory and Analysis program—national sampling design and estimation procedures. Asheville, NC: U.S. Department of Agriculture Forest Service, Southern Research Station: 11–26.

Richardson, L.A.; Champ, P.A.; Loomis, J.B. 2012. The hidden cost of wildfires: economic valuation of health effects of wildfire smoke exposure in southern California. Journal of Forest Economics. 18(1): 14–35.

Rothberg, D. 2018. 'It's gone, it's gone': Nation's largest wildfire in Nevada devastates ranches, sage grouse. The Nevada Independent. July 12. https://thenevadaindependent.com/article/its-gone-its-gone-nations-largest-wildfire-in-nevada-devastates-ranches-sage-grouse. [Date accessed: July 15, 2019].

Schmidt, K.M.; Menakis, J.P.; Hardy, C.C. [and others]. 2002. Development of coarse-scale spatial data for wildland fire and fuel management. Gen. Tech. Rep. RMRS-87. Fort Collins, CO: U.S. Department of Agriculture Forest Service, Rocky Mountain Research Station. 41 p.

Shima, T.; Sugimoto, S.; Okutomi, M. 2010. Comparison of image alignment on hexagonal and square lattices. In: 2010 IEEE international conference on image processing. [Place of publication unknown]: Institute of Electrical and Electronics Engineers, Inc.: 141–144. DOI: 10.1109/icip.2010.5654351.

Spencer, P.; Nowacki, G.; Fleming, M. [and others]. 2002. Home is where the habitat is: an ecosystem foundation for wildlife distribution and behavior. Arctic Research of the United States. 16: 6–17.

Tonini, M.; Tuia, D.; Ratle, F. 2009. Detection of clusters using space-time scan statistics. International Journal of Wildland Fire. 18(7): 830–836.

U.S. Department of Agriculture (USDA) Forest Service. 2008. National forest type data development. http://svinetfc4.fs.fed.us/rastergateway/forest_type/. [Date accessed: May 13, 2008].

U.S. Department of Agriculture (USDA) Forest Service. 2019. MODIS active fire mapping program: fire detection GIS data. https://fsapps.nwcg.gov/afm/gisdata.php. [Date accessed: May 7, 2019].

White, D.; Kimerling, A.J.; Overton, W.S. 1992. Cartographic and geometric components of a global sampling design for environmental monitoring. Cartography and Geographic Information Systems. 19(1): 5–22.

CHAPTER 4.

Drought and Moisture Surplus Patterns in the Conterminous United States: 2018, 2016–2018, and 2014–2018

Frank H. Koch
John W. Coulston

INTRODUCTION

Although ecologists do not define the term "drought" consistently (Slette and others 2019), one definition that is applicable to forests is that a drought is a period of precipitation deficit that persists long enough to deplete available soil water, leading to impacts on trees and other plants; in some cases, these impacts include plant injury or death (Anderegg and others 2012, Hanson and Weltzin 2000). Under this definition, droughts affect most forests in the United States, but their frequency and intensity vary considerably between geographic regions (Hanson and Weltzin 2000). These variations define the regions' predominant drought regimes. Most forests in the Western United States are subject to seasonal droughts on a yearly basis. By comparison, forests in the Eastern United States usually exhibit one of the following drought patterns: random (i.e., occurring at any time of year) occasional droughts, as usually observed in the Appalachian Mountains and the Northeast, or frequent late-summer droughts, as usually observed in the Southeastern Coastal Plain and the eastern portion of the Great Plains (Hanson and Weltzin 2000).

In forests, moisture scarcity during droughts can cause considerable tree stress, especially when that scarcity co-occurs with periods of high temperatures (L.D.L. Anderegg and others 2013, Peters and others 2015, Williams and others 2013). Trees and other plants react to this stress by decreasing fundamental growth processes such as cell division and enlargement. Because photosynthesis is less sensitive than these fundamental processes, it decreases slowly at low levels of drought stress but decreases more rapidly as the stress becomes more severe (Kareiva and others 1993, Mattson and Haack 1987). Ultimately, prolonged drought stress can lead to failure of a tree's hydraulic system, resulting in crown death and subsequent tree mortality (Choat and others 2018). In addition to these direct effects, drought stress often makes trees vulnerable to attack by damaging insects and diseases (Clinton and others 1993, Kolb and others 2016, Mattson and Haack 1987, Raffa and others 2008). Droughts also increase wildland fire risk by inhibiting breakdown of organic matter and diminishing the moisture content of downed woody debris and other potential fire fuels (Clark 1989, Keetch and Byram 1968, Schoennagel and others 2004, Trouet and others 2010).

Most forest systems are resistant to short-term droughts, although individual tree species differ in their degree of drought tolerance (Archaux and Wolters 2006, Berdanier and Clark 2016). Because of this resistance, drought duration may be a more critical factor for forests than drought intensity (Archaux and Wolters 2006). For example, forests that experience multiple consecutive years of drought (2–5 years) are much more likely to have high tree mortality than forests that experience a single year of

extreme drought (Guarín and Taylor 2005, Millar and others 2007). Indeed, the latter period is probably short enough that any impacts of the drought on tree growth and function are still reversible (Bigler and others 2006). Stated differently, forests may have to be subjected to a prolonged period of comparatively intense drought conditions before they experience effects similar to those observed with shorter term droughts in other (e.g., rangeland) systems. Therefore, a thorough evaluation of drought impact in forests should include analysis of moisture conditions over multiyear time windows.

In the 2010 Forest Health Monitoring (FHM) annual national report, we described a method for mapping drought conditions across the conterminous United States (Koch and others 2013b). Our objective was to generate fine-scale, drought-related spatial datasets that improve upon similar products available from sources such as the National Oceanic and Atmospheric Administration's National Centers for Environmental Information (e.g., Vose and others 2014) or the U.S. Drought Monitor program (Svoboda and others 2002). The primary inputs are gridded climate data (i.e., monthly raster maps of precipitation and temperature over a 100-year period) created with the Parameter-elevation Regression on Independent Slopes (PRISM) climate mapping system (Daly and others 2002). The method uses a standardized indexing approach that facilitates comparison of a given location's moisture status during different time windows, regardless of their length. The index is more straightforward to calculate than the commonly used Palmer Drought Severity Index, or PDSI (Palmer 1965), and avoids some criticisms of the PDSI (see Alley 1984) regarding its underlying assumptions and limited comparability across space and time. Here, we applied the method outlined in the 2010 FHM report to the most currently available climate data (i.e., the monthly PRISM data through 2018), thereby providing the tenth installment in an ongoing series of annual drought assessments for the conterminous United States from 2009 forward (Koch and Coulston 2015, 2016, 2017, 2018, 2019; Koch and others 2013a, 2013b, 2014, 2015).

This is the fifth year in which we also mapped levels of moisture surplus across the conterminous United States during multiple time windows. While recent refereed literature (e.g., Adams and others 2009, Allen and others 2010, Martínez-Vilalta and others 2012, Peng and others 2011, Williams and others 2013) has usually focused on reports of regional-scale forest decline and mortality due to persistent drought conditions, especially in combination with periods of extremely high temperatures (i.e., heat waves), surplus moisture availability can also be damaging to forests. Abnormally high moisture can be a short-term stressor

(e.g., an extreme rainfall event with subsequent flooding) or a long-term stressor (e.g., persistent wetness caused by a macroscale climatic pattern such as the El Niño-Southern Oscillation), either of which may lead to tree dieback and mortality (Rozas and García-González 2012, Rozas and Sampedro 2013). Such impacts have been observed in both tropical and temperate forests (Hubbart and others 2016, Laurance and others 2009, Rozas and García-González 2012). While surplus-induced impacts in forests may not be as common as drought-induced impacts, a single index that depicts both moisture surplus and deficit conditions provides a more complete indicator of potential forest health issues.

METHODS

We acquired grids for monthly precipitation and monthly mean temperature for the conterminous United States from the PRISM Climate Group website (PRISM Climate Group 2019). At the time of these analyses, gridded datasets were available for all years from 1895 to 2018. The spatial resolution of the grids was approximately 4 km (cell area = 16 km^2). For future applications and to ensure better compatibility with other spatial datasets, all output grids were resampled to a spatial resolution of approximately 2 km (cell area = 4 km^2) using a nearest neighbor approach. The nearest neighbor approach is a computationally simple resampling method that avoids the smoothing of data values observed with methods such as bilinear interpolation or cubic convolution.

Potential Evapotranspiration (PET) Maps

As in our previous drought mapping efforts (Koch and Coulston 2015, 2016, 2017, 2018, 2019; Koch and others 2012a, 2012b, 2013a, 2013b, 2014, 2015), we adopted an approach in which a moisture index value is calculated for each location of interest (i.e., each grid cell in a map of the conterminous United States) during a given time period. Moisture indices are intended to reflect the amount of available water in a location (e.g., to support plant growth). In our case, the index is computed using an approach that considers both the amount of precipitation that falls on a location during the period of interest as well as the level of potential evapotranspiration during this period. Potential evapotranspiration measures the loss of soil moisture through plant uptake and transpiration (Akin 1991). It does not measure actual moisture loss, but rather the loss that would occur if there was no possible shortage of moisture for plants to transpire (Akin 1991, Thornthwaite 1948). Potential evapotranspiration serves as a basic measure of moisture demand. By incorporating potential evapotranspiration along with precipitation, our index thus documents the long-term balance between moisture demand and supply for each location of interest.

To complement the available PRISM monthly precipitation grids, we computed monthly potential evapotranspiration (*PET*) grids using Thornthwaite's formula (Akin 1991, Thornthwaite 1948):

$$PET_m = 1.6 L_{lm} (10 \frac{T_m}{I})^a \qquad (1)$$

where

PET_m = the potential evapotranspiration for a given month m in cm

L_{lm} = a correction factor for the mean possible duration of sunlight during month m for all locations (i.e., grid cells) at a particular latitude l (see Table V in Thornthwaite [1948] for a list of L correction factors by month and latitude)

T_m = the mean temperature for month m in degrees C

I = an annual heat index, calculated as

$$I = \sum_{m=1}^{12} \left(\frac{T_m}{5} \right)^{1.514}$$

where

T_m is the mean temperature for each month m of the year

a = an exponent calculated as $a = 6.75 \times 10^{-7} I^3 - 7.71 \times 10^{-5} I^2 + 1.792 \times 10^{-2} I + 0.49239$ (see Appendix I in Thornthwaite [1948] regarding calculation of I and the empirical derivation of a)

Although only a simple approximation, a key advantage of Thornthwaite's formula is that it has modest input data requirements (i.e., mean temperature values) compared to more sophisticated methods of estimating *PET* such as the Penman-Monteith equation (Monteith 1965), which requires less readily available data on factors such as humidity, radiation, and wind speed. To implement equation (1) spatially, we created a grid of latitude values for determining the L adjustment for any given grid cell (and any given month) in the conterminous United States. We extracted the T_m values for the grid cells from the corresponding PRISM mean monthly temperature grids.

Moisture Index Maps

To estimate baseline conditions, we used the precipitation (*P*) and *PET* grids to generate moisture index grids for the past 100 years (i.e., 1919–2018) for the conterminous United States. We used a moisture index described by Willmott and Feddema (1992), which has been applied in a variety of contexts, including global vegetation modeling (Potter and Klooster 1999) and climate change analysis (Grundstein 2009). Willmott and Feddema (1992) devised the index as a refinement of one described earlier by Thornthwaite (1948) and Thornthwaite and Mather (1955). Their revised index, *MI'*, has the following form:

$$MI' = \begin{cases} P/PET - 1 & , \quad P < PET \\ 1 - PET/P & , \quad P \geq PET \\ 0 & , \quad P = PET = 0 \end{cases} \qquad (2)$$

where

P = precipitation

PET = potential evapotranspiration, as calculated using equation (1)

(P and PET must be in equivalent measurement units, e.g., mm)

This set of equations yields a symmetric, dimensionless index scaled between -1 and 1. A primary advantage of this symmetry is that it enables valid comparisons between any set of locations in terms of their moisture balance (i.e., the balance between moisture demand and supply). MI' can be calculated for any time period but is commonly calculated on an annual basis using P and PET values summed across the entire year (Willmott and Feddema 1992). An alternative to this summation approach is to calculate MI' on a monthly basis (i.e., from total measured precipitation and estimated potential evapotranspiration in each month), and then, for a given time window of interest, calculate its moisture index as the mean of the MI' values for all months in the time window. This "mean-of-months" approach limits the ability of short-term peaks in either precipitation or potential evapotranspiration to negate corresponding short-term deficits, as would happen under a summation approach.

For each year in our study period (i.e., 1919–2018), we used the mean-of-months approach to calculate moisture index grids for three different time windows: 1 year (MI_1'), 3 years (MI_3'), and 5 years (MI_5'). Briefly, the MI_1' grids are the mean (i.e., the mean value for each grid cell) of the 12 monthly MI' grids for each year in the study period, the MI_3' grids are the mean of the 36 monthly grids from January 2 years prior through December of the target year, and the MI_5' grids are the mean of the 60 consecutive monthly MI' grids from January 4 years prior to December of the target year. Thus, the MI_1' grid for the year 2018 is the mean of the monthly MI' grids from January to December 2018, while the MI_3' grid is the mean of the grids from January 2016 to December 2018, and the MI_5' grid is the mean of the grids from January 2014 to December 2018.

Annual and Multiyear Drought Maps

To determine degree of departure from typical moisture conditions, we first created a normal grid, $MI'_{i\ norm}$, for each of our three time windows, representing the mean (i.e., the mean value for each grid cell) of the 100 corresponding moisture index grids (i.e., the MI_1', MI_3', or MI_5' grids, depending on the window; see fig. 4.1). We also created a standard deviation grid, $MI'_{i\ SD}$, for each time window, calculated from the window's 100 individual moisture index grids as well as its $MI'_{i\ norm}$ grid. We subsequently calculated moisture difference z-scores, MDZ_{ij}, for each time window using these derived datasets:

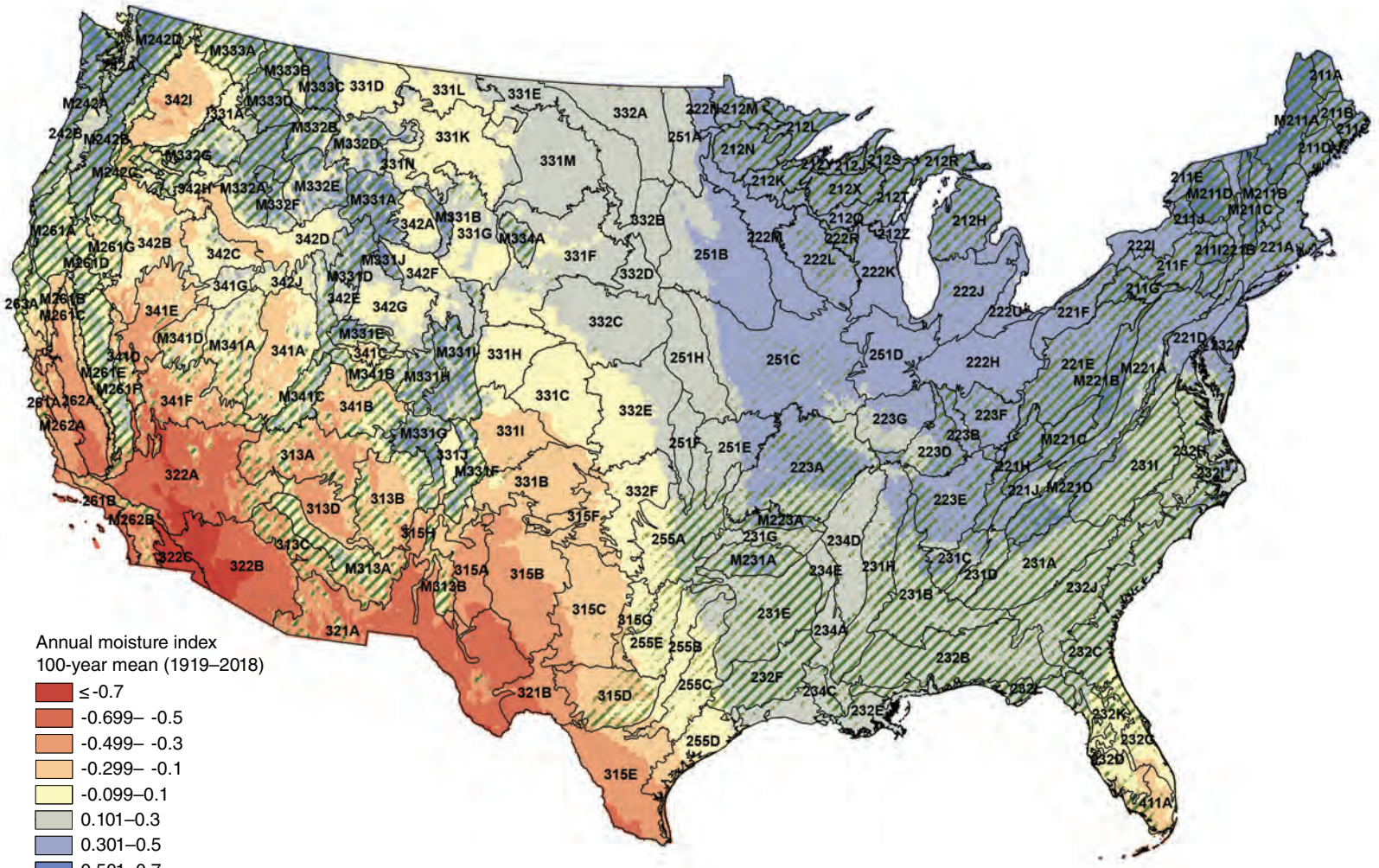

Figure 4.1—The 100-year (1919–2018) mean annual moisture index, or $MI_{1'norm}$*, for the conterminous United States. Ecoregion section (Cleland and others 2007) boundaries and labels are included for reference. Forest cover data (overlaid green hatching) derived from Moderate Resolution Imaging Spectroradiometer (MODIS) imagery by the U.S. Department of Agriculture Forest Service, Remote Sensing Applications Center. (Data source: PRISM Group, Oregon State University)*

$$MDZ_{ij} = \frac{MI_i' - MI_{i\ norm}'}{MI_{i\ SD}'} \quad (3)$$

where

i = the analytical time window (i.e., 1, 3, or 5 years) and j = a particular target year in our 100-year study period (i.e., 1919–2018)

MDZ scores may be classified in terms of degree of moisture deficit or surplus (table 4.1). The classification scheme includes categories (e.g., severe drought, extreme drought) like those associated with the PDSI. The scheme has also been adopted for other drought indices such as the Standardized Precipitation Index, or SPI (McKee and others 1993). Moreover, the breakpoints between *MDZ* categories resemble those used for the SPI, such that we expect the *MDZ* categories to have theoretical frequencies of occurrence that are similar to their SPI counterparts (e.g., approximately 2.3 percent of the time for extreme drought; see McKee and others 1993, Steinemann 2003). More importantly, because of the standardization in equation (3), the breakpoints between categories remain the same regardless of the size of the time window of interest. For comparative analysis, we generated and classified *MDZ* maps of the conterminous United States, based on all three time windows, for the target year 2018.

Table 4.1—Moisture difference *z*-score (*MDZ*) value ranges for nine wetness and drought categories, along with each category's approximate theoretical frequency of occurrence

MDZ	Category	Frequency
≤-2	Extreme drought	2.3%
-1.999 to -1.5	Severe drought	4.4%
-1.499 to -1	Moderate drought	9.2%
-0.999 to -0.5	Mild drought	15.0%
-0.499 to 0.5	Near normal conditions	38.2%
0.501 to 1	Mild moisture surplus	15.0%
1.001 to 1.5	Moderate moisture surplus	9.2%
1.501 to 2	Severe moisture surplus	4.4%
>2	Extreme moisture surplus	2.3%

RESULTS AND DISCUSSION

The 100-year (1919–2018) mean annual moisture index, or $MI_1'_{norm}$, grid (fig. 4.1) serves as a synopsis of moisture regimes in the conterminous United States. (The 100-year $MI_3'_{norm}$ and $MI_5'_{norm}$ grids were very similar to the mean $MI_1'_{norm}$ grid, and so are not shown here.) Wet climates ($MI' > 0$) are typical in the Eastern United States, especially the Northeast. An anomaly worth noting is southern Florida, primarily ecoregion sections (Cleland and others 2007) 232D–Florida Coastal Lowlands-Gulf, 232G–Florida Coastal Lowlands-Atlantic, and 411A–Everglades. This region appears to be dry relative to other parts of the East, which is an effect of its tropical climate, which has distinct wet (primarily summer months) and dry (late fall to early spring) seasons. Although southern Florida usually receives a high level of precipitation during the wet season, it can

be insufficient to offset the region's lengthy dry season (Duever and others 1994) or its high level of temperature-driven evapotranspiration, especially during the late spring and summer months, resulting in negative *MI′* values. This differs markedly from the pattern observed in the driest parts of the Western United States, especially the Southwest (e.g., sections 322A–Mojave Desert, 322B–Sonoran Desert, and 322C–Colorado Desert), where potential evapotranspiration is very high, as in southern Florida, but precipitation levels are typically very low. In fact, because of generally lower precipitation than the East, dry climates (*MI′* <0) are typical across much of the Western United States. Nevertheless, mountainous areas in the central and northern Rocky Mountains as well as the Pacific Northwest are relatively wet, such as ecoregion sections M242A–Oregon and Washington Coast Ranges, M242B–Western Cascades, M331G–South Central Highlands, and M333C–Northern Rockies. This is driven in part by large amounts of winter snowfall in these regions (Hanson and Weltzin 2000).

Figure 4.2 shows the annual (i.e., 1-year) *MDZ* map for 2018 for the conterminous United States. The map shows substantial contrast between the eastern and western portions of the country. From the Rocky Mountains westward, a majority of forested areas experienced at least mild drought (*MDZ* ≤-0.5) conditions in 2018, meaning that conditions were noticeably drier than normal in regions that already have dry moisture regimes (see fig. 4.1). Yet, contiguous areas of severe to extreme drought (*MDZ* ≤-1.5) were limited in number and geographic extent. Ecoregion sections in the West with the most noticeable concentrations of severe to extreme drought during 2018 included M242B–Western Cascades, portions of M242A–Oregon and Washington Coast Ranges and M261A–Klamath Mountains, and the northwestern corner of M333C–Northern Rockies, immediately adjacent to the United States-Canada border. There were other areas of severe to extreme drought in the central Rockies: ecoregion sections M331G–South Central Highlands, M331H–North Central Highlands and Rocky Mountains, and M331I–Northern Parks and Ranges. Similarly sized clusters of severe to extreme drought appeared in nearby sections 313B–Navajo Canyonlands and 313D–Painted Desert, but they occurred in areas with little forest cover.

In the Eastern United States, drought conditions during 2018 were largely confined to two geographic areas: northern New England and southern Florida. In the former region, small pockets of moderate drought (-1.5 < *MDZ* ≤ -1) were interspersed with a mix of mild surplus to mild drought conditions (-1 < *MDZ* ≤ 1). Ecoregion sections exhibiting this pattern included M211A–White Mountains, M211B–New England Piedmont, M211C–Green-Taconic-Berkshire Mountains, and M211D–Adirondack Highlands. In southern Florida, a significant cluster of severe to extreme drought appeared in section 411A–Everglades, while moderate to severe drought conditions occurred in 232G–Florida Coastal Lowlands-Atlantic, particularly along portions of the Atlantic

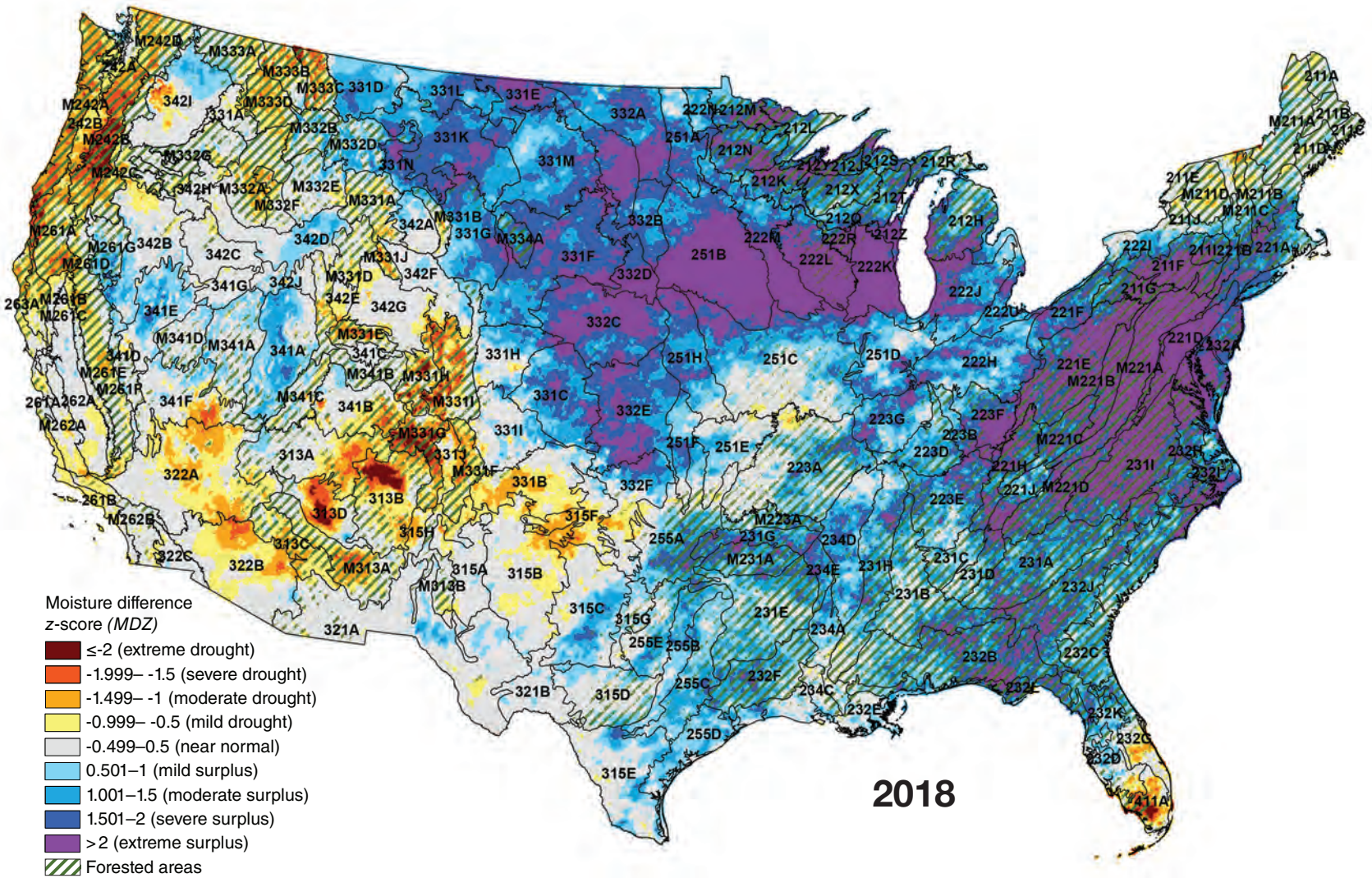

Figure 4.2—The 2018 annual (i.e., 1-year) moisture difference z*-score, or* MDZ*, for the conterminous United States. Ecoregion section (Cleland and others 2007) boundaries and labels are included for reference. Forest cover data (overlaid green hatching) derived from MODIS imagery by the U.S. Department of Agriculture Forest Service, Remote Sensing Applications Center. (Data source: PRISM Group, Oregon State University)*

coastline. Superficially, these two drought hot spots may appear to be similar, but it is worth recalling that, as depicted by the $MI_1'_{norm}$ grid (fig. 4.1), southern Florida has a drier moisture regime than virtually all other regions of the Eastern United States, including northern New England. Elsewhere in the East, moisture surplus conditions were widespread during 2018, including large contiguous areas of extreme surplus (*MDZ* >2) in the Mid-Atlantic and northern Great Plains regions.

Overall, the 2018 *MDZ* map (fig. 4.2) is consistent with summary metrics reported for the year (NOAA NCEI 2019). For example, the percentage of the country that was very dry was close to zero from October through December, while at the same time the percentage that was very wet ranged from approximately 13 percent to approximately 30 percent. Drought conditions were most extreme during spring (April–June) and most extensive geographically from July through September, but these were offset by unusually wet conditions in the latter portion of the year.

At a regional scale, moisture conditions in the Southwestern United States appeared to improve substantially in 2018 compared to 2017 (fig. 4.3), when a large contiguous zone of extreme drought (*MDZ* ≤-2) encompassed almost all of the "Four Corners" region (southeastern Utah, southwestern Colorado, northwestern New Mexico, and northeastern Arizona). This apparent improvement belies the fact that 2018 was the warmest year on record for the Southwest and represents the continuation of a 40-year warming trend that is likely to allow moderate or worse drought conditions to persist in parts of the region for the foreseeable future (NOAA NCEI 2019). This warming trend—which is widely acknowledged as a global phenomenon (Cook and others 2016, Rahmstorf and others 2017)—has also contributed to the emergence of drought in the Pacific Northwest region, as decreased summer and fall precipitation as well as increased potential evapotranspiration have resulted in larger moisture deficits than the region experienced historically (Abatzoglou and others 2014).

Decreases in drought extent and severity in the southern portion of California in 2018 (fig. 4.2) relative to 2017 (fig. 4.3), particularly in sections M262B–Southern California Mountain and Valley and M261E–Sierra Nevada, may seem noteworthy for a region that recently has experienced dramatic forest health impacts due to drought. Between 2010 and 2017, more than 129 million trees in California were killed by direct or indirect drought effects (Buluç and others 2017). In the central and southern Sierra Nevada Mountains, tree mortality approached 50 percent overall and 90 percent for ponderosa pine (*Pinus ponderosa*) (Fettig and others 2019). Nevertheless, the apparent improvement in moisture conditions in California during 2018

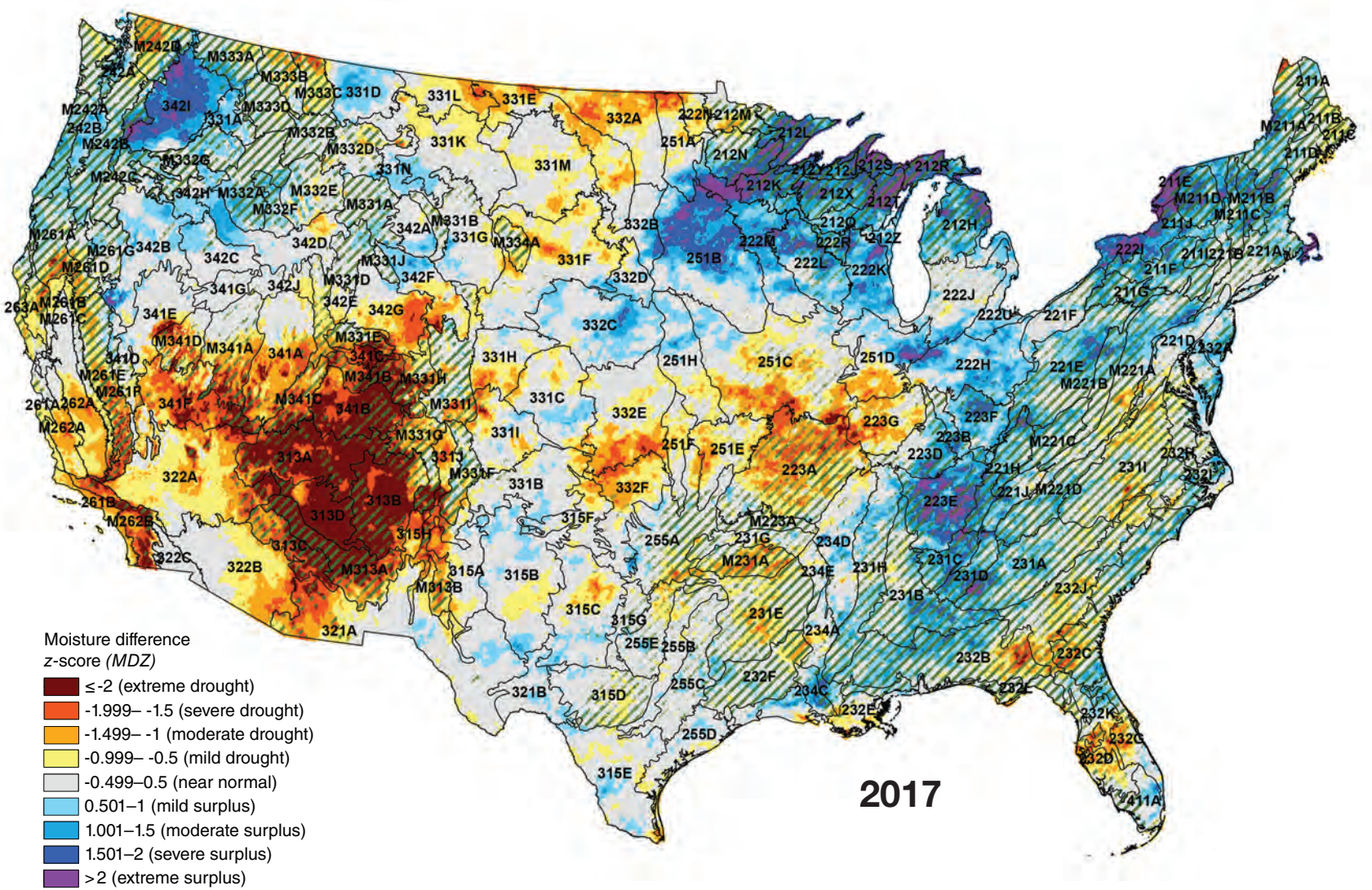

Figure 4.3—The 2017 annual (i.e., 1-year) moisture difference z*-score, or* MDZ*, for the conterminous United States. Ecoregion section (Cleland and others 2007) boundaries and labels are included for reference. Forest cover data (overlaid green hatching) derived from MODIS imagery by the U.S. Department of Agriculture Forest Service, Remote Sensing Applications Center. (Data source: PRISM Group, Oregon State University)*

must be viewed in the context of predictions that the State's moisture regime will be increasingly volatile in the future, with both extreme droughts and extreme wet events expected to become more frequent (Swain and others 2018). As is the case elsewhere, this volatility is likely to develop as a consequence of warming temperatures (Ullrich and others 2018). However, California's Mediterranean climate (i.e., dry summers and wet winters) makes it especially susceptible to abrupt swings between moisture extremes (Swain and others 2018).

Even in the face of warming temperatures, areas of persistent and intense drought have remained uncommon in the Eastern United States. For example, nearly all areas in the East that experienced moderate or worse drought conditions during 2017 (fig. 4.3) saw a return to near normal or even moisture surplus conditions in 2018 (fig. 4.2), although the aforementioned area of drought in northern New England became more extensive. The 3-year (2016–2018; fig. 4.4) and 5-year (2014–2018; fig. 4.5) *MDZ* maps serve as further illustration of the relative infrequency of prolonged droughts (i.e., spanning multiple years) in the East. The only notable areas of the Eastern United States where moderate or worse drought conditions (*MDZ* ≤-1) occurred in both the 3- and 5-year *MDZ* maps were in section 411A–Everglades, in very small portions of 232C–Atlantic Coastal Flatwoods and 232G–Florida Coastal Lowlands-Atlantic, and along the coastline of Maine (sections 211C–Fundy Coastal and Interior and 211D–Central Maine Coastal and Embayment). In the 3-year *MDZ* map (fig. 4.4), clusters of moderate or worse drought conditions also occurred in sections 223A–Ozark Highlands, 251C–Central Dissected Till Plains, 315F–Northern Texas High Plains, and 322F–South Central and Red Bed Plains. These clusters were much less prominent in the 5-year map (fig. 4.5), indicating that the drought conditions developed primarily within the last few years and probably were preceded by near-normal conditions in 2014–2015. Furthermore, only one of these sections (i.e., 223A) contains much forest.

In contrast, nearly all forested areas in the Western United States have experienced moderate or worse drought conditions that have persisted over multiple consecutive years. Outside of the Four Corners region, most of these areas exhibited lower *MDZ* values in the 5-year map than in the 3-year map, suggesting that moisture conditions improved in the 2016–2018 period relative to 2014–2015. Still, the near-ubiquity of drought conditions in Western U.S. forests—circumstances that extend back several decades in some parts of the West (Groisman and Knight 2008, Mueller and others 2005, Woodhouse and others 2010)—has undeniable implications for long-term forest health.

Areas of moisture surplus depicted in the 3-year (fig. 4.4) and 5-year (fig. 4.5) *MDZ* maps further underscore some dramatic differences between the Eastern and Western United States. Strikingly, the maps show almost no areas of severe to extreme moisture surplus

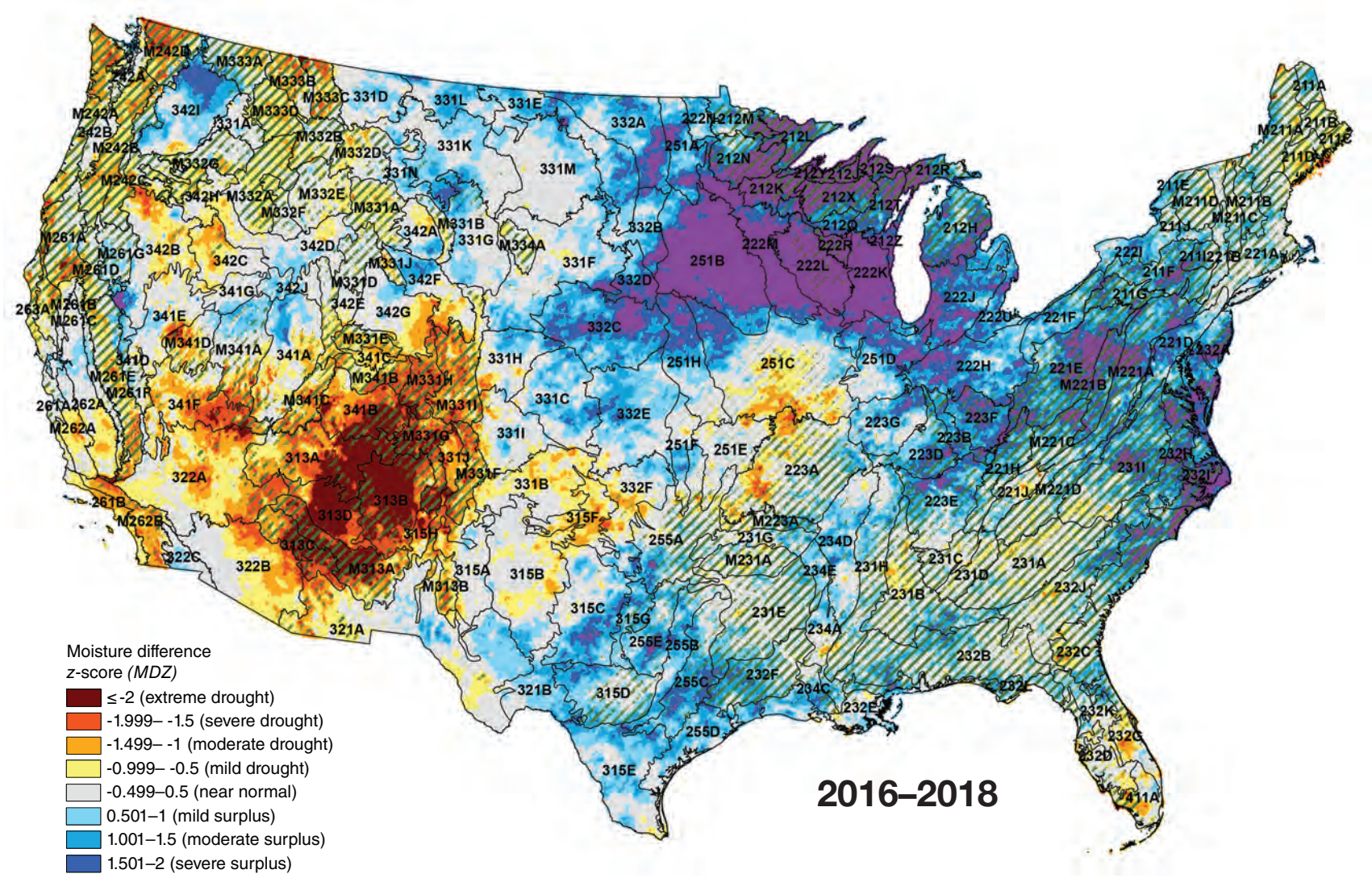

*Figure 4.4—The 2016–2018 (i.e., 3-year) moisture difference z-score (*MDZ*) for the conterminous United States. Ecoregion section (Cleland and others 2007) boundaries are included for reference. Forest cover data (overlaid green hatching) derived from MODIS imagery by the U.S. Department of Agriculture Forest Service, Remote Sensing Applications Center. (Data source: PRISM Group, Oregon State University)*

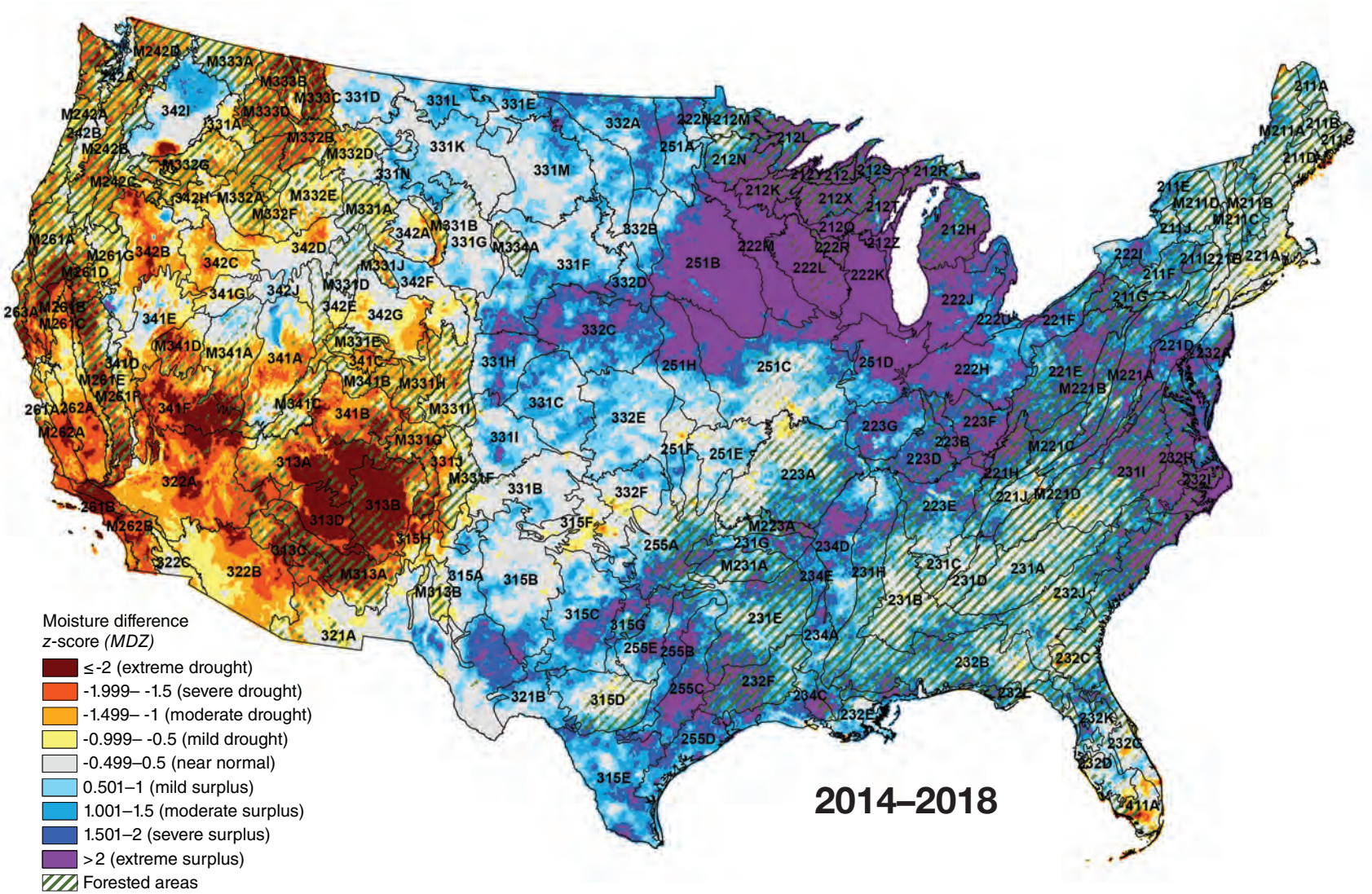

Figure 4.5—The 2014–2018 (i.e., 5-year) moisture difference z*-score (*MDZ*) for the conterminous United States. Ecoregion section (Cleland and others 2007) boundaries are included for reference. Forest cover data (overlaid green hatching) derived from MODIS imagery by the U.S. Department of Agriculture Forest Service, Remote Sensing Applications Center. (Data source: PRISM Group, Oregon State University)*

west of the Rocky Mountains. The solitary exception is in the southwestern corner of section 342B–Northwestern Basin and Range, an area that has little forest. In addition, the northern portion of 342I–Columbia Basin showed a severe moisture surplus in the 3-year *MDZ* map (fig. 4.4) but only moderate surplus in the 5-year map (fig. 4.5). By comparison, a nearly continuous swath of severe to extreme moisture surplus stretched across much of the Eastern United States in both the 3- and 5-year maps, from the western Great Lakes region (e.g., forested sections 212J–Southern Superior Uplands, 212K–Western Superior Uplands, 212Q–North Central Wisconsin Uplands, 212R–Eastern Upper Peninsula, 212X–Northern Highlands, 212Y–Southwest Lake Superior Clay Plain, 222L–North Central U.S. Driftless and Escarpment, and 222R–Wisconsin Central Sands) to eastern North Carolina and South Carolina (e.g., sections 231I–Central Appalachian Piedmont, 232C–Atlantic Coastal Flatwoods, 232H–Middle Atlantic Coastal Plains and Flatwoods, and 232I–Northern Atlantic Coastal Flatwoods). The geographic footprint of the swath was close to identical in the two maps. Another contiguous area of moisture surplus covered parts of Louisiana and Texas (e.g., sections 231E–Mid Coastal Plains-Western, 232F–Coastal Plains and Flatwoods-Western Gulf, 234C–Atchafalaya and Red River Alluvial Plains, 255A–Cross Timbers and Prairie, 255B–Blackland Prairies, 255C–Oak Woods and Prairies, 255E–Texas Cross Timbers and Prairie, and 315G–Eastern Rolling Plains). In general, the 3-year *MDZ* map showed a lower degree of moisture surplus in this area than the 5-year map, which may signal an ongoing shift from surplus to drought conditions.

The forest health impacts of these prolonged surpluses are unclear. Localized damage due to flooding is reasonably common in U.S. forests, but impacts related to surplus conditions more broadly are not well documented. Recent research has suggested that persistent excess moisture can increase vulnerability of forests to pathogens and other disease-causing agents (Hubbart and others 2016). These agents may be further enabled during times of high climate variability, such as when a period of drought occurs immediately before or after a period of moisture surplus, or when wet and warm conditions co-occur (Hubbart and others 2016). Despite the uncertainty, continued monitoring is advisable for the areas of persistent moisture surplus identified in the 3- and 5-year *MDZ* maps.

Future Efforts

We intend to provide 1-year, 3-year, and 5-year *MDZ* maps of the conterminous United States as an annually recurring component of national forest health reporting. To interpret the maps appropriately, it is critical to recognize their limitations. Foremost, the *MDZ* approach omits some factors that can affect a location's moisture supply at a finer spatial scale, such as winter snowpack, surface runoff, or groundwater storage. Moreover, while the maps use a standardized index scale that applies to time windows of any size, it is still important

to choose a window size that is analytically appropriate. For example, an extreme drought that lasts for 5 years will have substantially different forest health ramifications than an extreme drought that ends after only 1 year. We believe the 1-year, 3-year, and 5-year *MDZ* maps provide a fairly comprehensive short-term picture, but a region's longer term moisture history may also be meaningful with respect to the health of its forests. For instance, in regions where droughts have been frequent historically (e.g., occurring on an annual or nearly annual basis), some tree species may be better drought-adapted than others (McDowell and others 2008); because of this variability, long periods of persistent and intense drought conditions could lead to eventual changes in regional forest composition (Mueller and others 2005). Compositional changes may also emerge from long periods of persistent moisture surplus (McEwan and others 2011). Such changes are likely to affect regional responses to future drought or surplus conditions, fire regimes, and the status of ecosystem services such as nutrient cycling and wildlife habitat (W.R.L. Anderegg and others 2013, DeSantis and others 2011). In future work, we hope to deliver better quantitative evidence to forest managers and other decisionmakers regarding relationships between moisture extremes and significant forest health impacts such as regional-scale tree mortality (e.g., Mitchell and others 2014). We also intend to investigate the capacity of moisture extremes to serve as inciting factors for other forest threats such as wildfire or pest outbreaks.

LITERATURE CITED

Abatzoglou, J.T.; Rupp, D.E.; Mote, P.W. 2014. Seasonal climate variability and change in the Pacific Northwest of the United States. Journal of Climate. 27(5): 2125–2142.

Adams, H.D.; Guardiola-Claramonte, M.; Barron-Gafford, G.A. [and others]. 2009. Temperature sensitivity of drought-induced tree mortality portends increased regional die-off under global-change-type drought. Proceedings of the National Academy of Sciences. 106(17): 7063–7066.

Akin, W.E. 1991. Global patterns: climate, vegetation, and soils. Norman, OK: University of Oklahoma Press. 370 p.

Allen, C.D.; Macalady, A.K.; Chenchouni, H. [and others]. 2010. A global overview of drought and heat-induced tree mortality reveals emerging climate change risks for forests. Forest Ecology and Management. 259(4): 660–684.

Alley, W.M. 1984. The Palmer Drought Severity Index: limitations and assumptions. Journal of Climate and Applied Meteorology. 23: 1100–1109.

Anderegg, L.D.L.; Anderegg, W.R.L.; Berry, J.A. 2013. Not all droughts are created equal: translating meteorological drought into woody plant mortality. Tree Physiology. 33(7): 672–683.

Anderegg, W.R.L.; Berry, J.A.; Field, C.B. 2012. Linking definitions, mechanisms, and modeling of drought-induced tree death. Trends in Plant Science. 17(12): 693–700.

Anderegg, W.R.L.; Kane, J.M.; Anderegg, L.D.L. 2013. Consequences of widespread tree mortality triggered by drought and temperature stress. Nature Climate Change. 3(1): 30–36.

Archaux, F.; Wolters, V. 2006. Impact of summer drought on forest biodiversity: what do we know? Annals of Forest Science. 63: 645–652.

Berdanier, A.B.; Clark, J.S. 2016. Multiyear drought-induced morbidity preceding tree death in southeastern U.S. forests. Ecological Applications. 26(1): 17–23.

Bigler, C.; Bräker, O.U.; Bugmann, H. [and others]. 2006. Drought as an inciting mortality factor in Scots pine stands of the Valais, Switzerland. Ecosystems. 9(3): 330–343.

Buluç, L.; Fischer, C.; Ko, J. [and others]. 2017. Drought and tree mortality in the Pacific Southwest region. [Fact sheet]. Washington, D.C.: U.S. Department of Agriculture Forest Service, Office of Sustainability and Climate. 14 p.

Choat, B.; Brodribb, T.J.; Brodersen, C.R. [and others]. 2018. Triggers of tree mortality under drought. Nature. 558(7711): 531–539.

Clark, J.S. 1989. Effects of long-term water balances on fire regime, north-western Minnesota. Journal of Ecology. 77: 989–1004.

Cleland, D.T.; Freeouf, J.A.; Keys, J.E. [and others]. 2007. Ecological subregions: sections and subsections for the conterminous United States. Gen. Tech. Rep. WO-76D. Washington, DC: U.S. Department of Agriculture Forest Service. Map; Sloan, A.M., cartographer; presentation scale 1:3,500,000; colored. Also on CD-ROM as a GIS coverage in ArcINFO format.

Clinton, B.D.; Boring, L.R.; Swank, W.T. 1993. Canopy gap characteristics and drought influences in oak forests of the Coweeta Basin. Ecology. 74(5): 1551–1558.

Cook, J.; Oreskes, N.; Doran, P.T. [and others]. 2016. Consensus on consensus: a synthesis of consensus estimates on human-caused global warming. Environmental Research Letters. 11(4): 048002.

Daly, C.; Gibson, W.P.; Taylor, G.H. [and others]. 2002. A knowledge-based approach to the statistical mapping of climate. Climate Research. 22: 99–113.

DeSantis, R.D.; Hallgren, S.W.; Stahle, D.W. 2011. Drought and fire suppression lead to rapid forest composition change in a forest-prairie ecotone. Forest Ecology and Management. 261(11): 1833–1840.

Duever, M.J.; Meeder, J.F.; Meeder, L.C.; McCollum, J.M. 1994. The climate of south Florida and its role in shaping the Everglades ecosystem. In: Davis, S.M.; Ogden, J.C., eds. Everglades: the ecosystem and its restoration. Delray Beach, FL: St. Lucie Press: 225–248.

Fettig, C.J.; Mortenson, L.A.; Bulaon, B.M.; Foulk, P.B. 2019. Tree mortality following drought in the central and southern Sierra Nevada, California, U.S. Forest Ecology and Management. 432: 164–178.

Groisman, P.Y.; Knight, R.W. 2008. Prolonged dry episodes over the conterminous United States: new tendencies emerging during the last 40 years. Journal of Climate. 21: 1850–1862.

Grundstein, A. 2009. Evaluation of climate change over the continental United States using a moisture index. Climatic Change. 93: 103–115.

Guarín, A.; Taylor, A.H. 2005. Drought triggered tree mortality in mixed conifer forests in Yosemite National Park, California, USA. Forest Ecology and Management. 218: 229–244.

Hanson, P.J.; Weltzin, J.F. 2000. Drought disturbance from climate change: response of United States forests. The Science of the Total Environment. 262: 205–220.

Hubbart, J.A.; Guyette, R.; Muzika, R.M. 2016. More than drought: precipitation variance, excessive wetness, pathogens and the future of the western edge of the Eastern Deciduous Forest. Science of The Total Environment. 566–567: 463–467.

Kareiva, P.M.; Kingsolver, J.G.; Huey, B.B., eds. 1993. Biotic interactions and global change. Sunderland, MA: Sinauer Associates, Inc. 559 p.

Keetch, J.J.; Byram, G.M. 1968. A drought index for forest fire control. Res. Pap. SE-38. Asheville, NC: U.S. Department of Agriculture Forest Service, Southeastern Forest Experiment Station. 33 p.

Koch, F.H.; Coulston, J.W. 2015. 1-year (2013), 3-year (2011–2013), and 5-year (2009–2013) drought maps for the conterminous United States. In: Potter, K.M.; Conkling, B.L., eds. Forest Health Monitoring: national status, trends, and analysis 2014. Gen. Tech. Rep. SRS-209. Asheville, NC: U.S. Department of Agriculture Forest Service, Southern Research Station: 57–71. Chapter 4.

Koch, F.H.; Coulston, J.W. 2016. 1-year (2014), 3-year (2012–2014), and 5-year (2010–2014) maps of drought and moisture surplus for the conterminous United States. In: Potter, K.M.; Conkling, B.L., eds. Forest Health Monitoring: national status, trends, and analysis 2015. Gen. Tech. Rep. SRS-213. Asheville, NC: U.S. Department of Agriculture Forest Service, Southern Research Station: 61–78. Chapter 4.

Koch, F.H.; Coulston, J.W. 2017. Moisture deficit and surplus in the conterminous United States for three time windows: 2015, 2013–2015, and 2011–2015. In: Potter, K.M.; Conkling, B.L., eds. Forest Health Monitoring: national status, trends, and analysis 2016. Gen. Tech. Rep. SRS-222. Asheville, NC: U.S. Department of Agriculture Forest Service, Southern Research Station: 63–80. Chapter 4.

Koch, F.H.; Coulston, J.W. 2018. Moisture deficit and surplus in the conterminous United States for three time windows: 2016, 2014–2016, and 2012–2016. In: Potter, K.M.; Conkling, B.L., eds. Forest Health Monitoring: national status, trends, and analysis 2017. Gen. Tech Rep. SRS-233. Asheville, NC: U.S. Department of Agriculture Forest Service, Southern Research Station: 65–84. Chapter 4.

Koch, F.H.; Coulston, J.W. 2019. Drought and moisture surplus patterns in the conterminous United States: 2017, 2015–2017, and 2013–2017. In: Potter, K.M.; Conkling, B.L., eds. Forest Health Monitoring: national status, trends, and analysis 2018. Gen. Tech Rep. SRS-239. Asheville, NC: U.S. Department of Agriculture Forest Service, Southern Research Station: 77–96. Chapter 4.

Koch, F.H.; Coulston, J.W.; Smith, W.D. 2012a. High-resolution mapping of drought conditions. In: Potter, K.M.; Conkling, B.L., eds. Forest Health Monitoring 2008 national technical report. Gen. Tech. Rep. SRS-158. Asheville, NC: U.S. Department of Agriculture Forest Service, Southern Research Station: 45–62. Chapter 4.

Koch, F.H.; Coulston, J.W.; Smith, W.D. 2012b. Mapping drought conditions using multi-year windows. In: Potter, K.M.; Conkling, B.L., eds. Forest Health Monitoring 2009 national technical report. Gen. Tech. Rep. SRS-167. Asheville, NC: U.S. Department of Agriculture Forest Service, Southern Research Station: 163–179. Chapter 10.

Koch, F.H.; Smith, W.D.; Coulston, J.W. 2013a. Recent drought conditions in the conterminous United States. In: Potter, K.M.; Conkling, B.L., eds. Forest Health Monitoring: national status, trends, and analysis 2011. Gen. Tech. Rep. SRS-185. Asheville, NC: U.S. Department of Agriculture Forest Service, Southern Research Station: 41–58. Chapter 4.

Koch, F.H.; Smith, W.D.; Coulston, J.W. 2013b. An improved method for standardized mapping of drought conditions. In: Potter, K.M.; Conkling, B.L., eds. Forest Health Monitoring: national status, trends, and analysis 2010. Gen. Tech. Rep. SRS-176. Asheville, NC: U.S. Department of Agriculture Forest Service, Southern Research Station: 67–83. Chapter 6.

Koch, F.H.; Smith, W.D.; Coulston, J.W. 2014. Drought patterns in the conterminous United States and Hawaii. In: Potter, K.M.; Conkling, B.L., eds. Forest Health Monitoring: national status, trends, and analysis 2012. Gen. Tech. Rep. SRS-198. Asheville, NC: U.S. Department of Agriculture Forest Service, Southern Research Station: 49–72. Chapter 4.

Koch, F.H.; Smith, W.D.; Coulston, J.W. 2015. Drought patterns in the conterminous United States, 2012. In: Potter, K.M.; Conkling, B.L., eds. Forest Health Monitoring: national status, trends, and analysis 2013. Gen. Tech. Rep. SRS-207. Asheville, NC: U.S. Department of Agriculture Forest Service, Southern Research Station: 55–69. Chapter 4.

Kolb, T.E.; Fettig, C.J.; Ayres, M.P. [and others]. 2016. Observed and anticipated impacts of drought on forest insects and diseases in the United States. Forest Ecology and Management. 380: 321–334.

Laurance, S.G.W.; Laurance, W.F.; Nascimento, H.E.M. [and others]. 2009. Long-term variation in Amazon forest dynamics. Journal of Vegetation Science. 20(2): 323–333.

Martínez-Vilalta, J.; Lloret, F.; Breshears, D.D. 2012. Drought-induced forest decline: causes, scope and implications. Biology Letters. 8(5): 689–691.

Mattson, W.J.; Haack, R.A. 1987. The role of drought in outbreaks of plant-eating insects. BioScience. 37(2): 110–118.

McDowell, N.; Pockman, W.T.; Allen, C.D. [and others]. 2008. Mechanisms of plant survival and mortality during drought: why do some plants survive while others succumb to drought? New Phytologist. 178: 719–739.

McEwan, R.W.; Dyer, J.M.; Pederson, N. 2011. Multiple interacting ecosystem drivers: toward an encompassing hypothesis of oak forest dynamics across eastern North America. Ecography. 34: 244–256.

McKee, T.B.; Doesken, N.J.; Kleist, J. 1993. The relationship of drought frequency and duration to time scales. In: Eighth conference on applied climatology. [Place of publication unknown]: American Meteorological Society: 179–184.

Millar, C.I.; Westfall, R.D.; Delany, D.L. 2007. Response of high-elevation limber pine (*Pinus flexilis*) to multiyear droughts and 20th-century warming, Sierra Nevada, California, USA. Canadian Journal of Forest Research. 37: 2508–2520.

Mitchell, P.J.; O'Grady, A.P.; Hayes, K.R.; Pinkard, E.A. 2014. Exposure of trees to drought-induced die-off is defined by a common climatic threshold across different vegetation types. Ecology and Evolution. 4(7): 1088–1101.

Monteith, J.L. 1965. Evaporation and environment. Symposia of the Society for Experimental Biology. 19: 205–234.

Mueller, R.C.; Scudder, C.M.; Porter, M.E. [and others]. 2005. Differential tree mortality in response to severe drought: evidence for long-term vegetation shifts. Journal of Ecology. 93: 1085–1093.

National Oceanic and Atmospheric Administration (NOAA) National Centers for Environmental Information (NCEI). 2019. State of the climate: drought for annual 2018. https://www.ncdc.noaa.gov/sotc/drought/201813. [Date accessed: August 22, 2019].

Palmer, W.C. 1965. Metereological drought. Washington, DC: U.S. Department of Commerce Weather Bureau. 58 p.

Peng, C.; Ma, Z.; Lei, X. [and others]. 2011. A drought-induced pervasive increase in tree mortality across Canada's boreal forests. Nature Climate Change. 1(9): 467–471.

Peters, M.P.; Iverson, L.R.; Matthews, S.N. 2015. Long-term droughtiness and drought tolerance of eastern US forests over five decades. Forest Ecology and Management. 345: 56–64.

Potter, C.S.; Klooster, S.A. 1999. Dynamic global vegetation modelling for prediction of plant functional types and biogenic trace gas fluxes. Global Ecology and Biogeography. 8(6): 473–488.

PRISM Climate Group. 2019. 2.5-arcmin (4 km) gridded monthly climate data. http://www.prism.oregonstate.edu. [Date accessed: August 1, 2019].

Raffa, K.F.; Aukema, B.H.; Bentz, B.J. [and others]. 2008. Cross-scale drivers of natural disturbances prone to anthropogenic amplification: the dynamics of bark beetle eruptions. BioScience. 58(6): 501–517.

Rahmstorf, S.; Foster, G.; Cahill, N. 2017. Global temperature evolution: recent trends and some pitfalls. Environmental Research Letters. 12(5): 054001.

Rozas, V.; García-González, I. 2012. Too wet for oaks? Inter-tree competition and recent persistent wetness predispose oaks to rainfall-induced dieback in Atlantic rainy forest. Global and Planetary Change. 94–95: 62–71.

Rozas, V.; Sampedro, L. 2013. Soil chemical properties and dieback of *Quercus robur* in Atlantic wet forests after a weather extreme. Plant and Soil. 373(1–2): 673–685.

Schoennagel, T.; Veblen, T.T.; Romme, W.H. 2004. The interaction of fire, fuels, and climate across Rocky Mountain forests. BioScience. 54(7): 661–676.

Slette, I.J.; Post, A.K.; Awad, M. [and others]. 2019. How ecologists define drought, and why we should do better. Global Change Biology. 25(10): 3193–3200.

Steinemann, A. 2003. Drought indicators and triggers: a stochastic approach to evaluation. Journal of the American Water Resources Association. 39(5): 1217–1233.

Svoboda, M.; LeComte, D.; Hayes, M. [and others]. 2002. The drought monitor. Bulletin of the American Meteorological Society. 83(8): 1181–1190.

Swain, D.L.; Langenbrunner, B.; Neelin, J.D.; Hall, A. 2018. Increasing precipitation volatility in twenty-first-century California. Nature Climate Change. 8(5): 427–433.

Thornthwaite, C.W. 1948. An approach towards a rational classification of climate. Geographical Review. 38(1): 55–94.

Thornthwaite, C.W.; Mather, J.R. 1955. The water balance. Publications in Climatology. 8(1): 1–104.

Trouet, V.; Taylor, A.H.; Wahl, E.R. [and others]. 2010. Fire-climate interactions in the American West since 1400 CE. Geophysical Research Letters. 37(4): L04702.

Ullrich, P.A.; Xu, Z.; Rhoades, A.M. [and others]. 2018. California's drought of the future: a midcentury recreation of the exceptional conditions of 2012–2017. Earth's Future. 6(11): 1568–1587.

Vose, R.S.; Applequist, S.; Squires, M. [and others]. 2014. Improved historical temperature and precipitation time series for U.S. climate divisions. Journal of Applied Meteorology and Climatology. 53(5): 1232–1251.

Williams, A.P.; Allen, C.D.; Macalady, A.K. [and others]. 2013. Temperature as a potent driver of regional forest drought stress and tree mortality. Nature Climate Change. 3(3): 292–297.

Willmott, C.J.; Feddema, J.J. 1992. A more rational climatic moisture index. Professional Geographer. 44(1): 84–87.

Woodhouse, C.A.; Meko, D.M.; MacDonald, G.M. [and others]. 2010. A 1,200-year perspective of 21st century drought in southwestern North America. Proceedings of the National Academy of Sciences. 107(50): 21283–21288.

CHAPTER 5.

Tree Mortality

Mark J. Ambrose

INTRODUCTION

Tree mortality is a natural process in all forest ecosystems. High mortality can be an indicator of forest health problems. On a regional scale, high mortality levels may indicate widespread insect or disease impacts. High mortality may also occur if a large proportion of the forest in a particular region is made up of older, senescent stands. The approach presented here seeks to detect mortality patterns that might reflect changes to ecosystem processes at large scales. In many cases, the proximate cause of mortality may be discernable. Understanding proximate causes of mortality ***may*** provide insight into whether the mortality is within the range of natural variation or reflects more fundamental changes to ecological processes.

DATA

Forest Inventory and Analysis (FIA) Phase 2 (P2) data were the basis of the mortality analysis. Forest Inventory and Analysis P2 data are collected across forested land throughout the United States, with approximately one plot per 6,000 acres of forest, using a rotating panel sample design (Bechtold and Patterson 2005). Field plots are divided into spatially balanced panels, with one panel being measured each year. A single cycle of measurements consists of measuring all panels. This "annualized" method of inventory was adopted, State by State, beginning in 1999. The cycle length (i.e., number of years required to measure all plot panels) ranges from 5 to 10 years.

An analysis of mortality requires data collected at a minimum of two points in time. Therefore, mortality analysis was possible for areas where data from repeated plot measurements using consistent sampling protocols were available (i.e., where one cycle of measurements had been completed and at least one panel of the next cycle had been measured, and where there had been no changes to the protocols affecting measurements of trees or saplings). In this report, as in recent years, the repeated P2 data were available for all of the Central and Eastern States. The most recent cycle of remeasurements for each State was used in this analysis.

In addition, mortality data have become available from parts of the Western United States. In the West, plots are remeasured on a 10-year cycle. Thus, estimates of growth and mortality from the Western States are based on less than a complete cycle of remeasurement. Working from an incomplete cycle of remeasurement, the effective sampling intensity for growth and mortality estimates is significantly lower than FIA's standard of one plot per 6,000 acres (table 5.1). Therefore, the percent sampling error on growth and mortality estimates tends to be large. Results are not presented for ecoregions where fewer than 25 plots had been remeasured or where the percent error was unacceptably high. Nevertheless, results presented for the West should be viewed as preliminary. Because of this, results from the West are discussed separately from those from the Eastern and Central United States. The

division of Eastern/Central vs. Western States, as well as the forest cover within those States, is shown in figure 5.1.

METHODS

The Forest Inventory and Analysis program calculates the growth, mortality, and removal volume on each plot over the interval between repeated measurements. These values are stored in the FIA database (FIADB, version 8.0) (Burrill and others 2018). The FIA's EVALIDator (ver. 1.8.0) is an online tool for querying the FIADB and generating area-based reports on forest characteristics (USDA Forest Service, FIA Program 2019). EVALIDator was used to obtain net growth rates and mortality rates over the most recent measurement cycle for each of 113 ecoregion sections (Cleland and others 2007, McNab and others 2007) covering the Eastern and Central United States and 23 ecoregion sections in the Western[1] United States. For most States, the most recent cycle of available data ran through 2017[2] (e.g., data collected from 2011 through 2017).

Table 5.1—Western States from which repeated Forest Inventory and Analysis Phase 2 measurements were available, the time period spanned by the data, and the effective sample intensity (based on the proportion of plots that had been remeasured) in the available datasets

State	Time period	Effective sample intensity
Arizona	2001–2017	one plot: 8,571 acres
California	2001–2017	one plot: 8,571 acres
Colorado	2002–2017	one plot: 10,000 acres
Idaho	2004–2017	one plot: 15,000 acres
Montana	2003–2017	one plot: 12,000 acres
Nevada	2004–2017	one plot: 15,000 acres
New Mexico	2005–2017	one plot: 20,000 acres
Oregon	2001–2016	one plot: 8,571 acres
Utah	2000–2017	one plot: 7,500 acres
Washington	2002–2016	one plot: 12,000 acres
Wyoming[a]	2000–2017	one plot: 8,571 acres

[a] Mortality estimates for Wyoming are based on a comparison of annualized inventory data with data from the final periodic inventory.

To compare mortality across forest types and climate zones, the ratio of annual mortality to gross growth (MRATIO) was used as a standardized mortality indicator (Coulston and others 2005).

The MRATIO has proven to be a useful indicator of forest health, but it can be a problematic indicator, especially when growth rates are very low. The MRATIO can also be difficult to interpret when there is high uncertainty to growth estimates. Both of these are the case with the data currently

[1] At the time that this analysis was being completed, updates being made to EVALIDator and FIADB made it impossible to generate growth estimates for the Interior West, so MRATIOs were only calculated for the West Coast States.

[2] Overall, the most recent data available for any State ranged from 2015 to 2018.

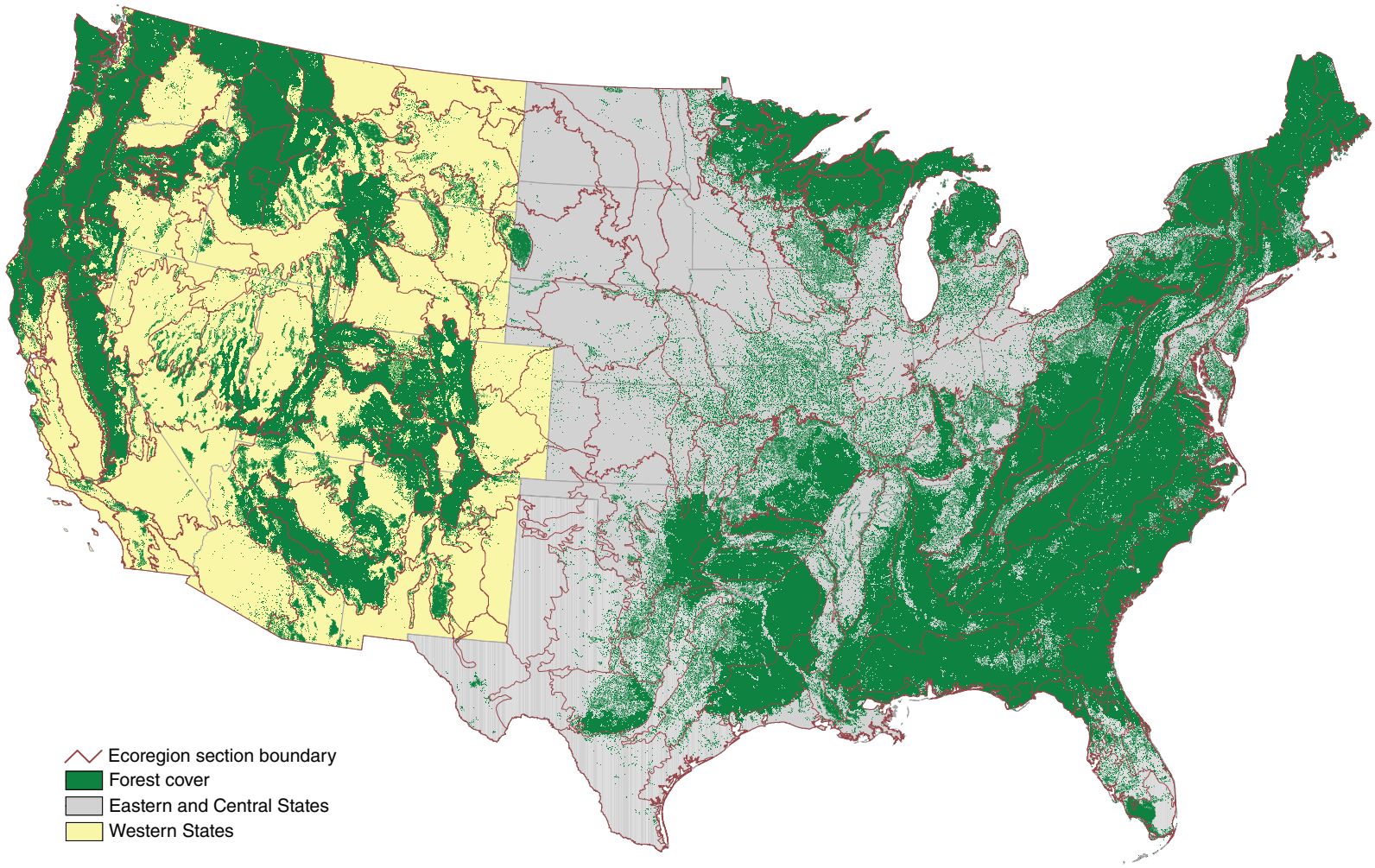

Figure 5.1—Forest cover in the States where mortality was analyzed by ecoregion section (Cleland and others 2007). Mortality in Eastern and Central States was analyzed using a complete remeasurement cycle; in most Western States, mortality was analyzed using a partial cycle of remeasurements, and results there should be considered preliminary. Forest cover was derived from MODIS satellite imagery (USDA Forest Service 2008).

available from the West. Therefore, mortality as a percentage of live growing stock also was calculated:

$$\text{Mortality percent} = m / v_l * 100$$

where

m = annual mortality (cubic feet per year)

v_l = total live tree volume (cubic feet)

When both this mortality percentage and the MRATIO are high, it suggests a possibly serious forest health concern.

To identify causal agents for the observed mortality, EVALIDator was also used to summarize by the reported "cause of death" associated with the observed mortality. Causes of death are reported as general categories (e.g., insects, fire, weather). For each ecoregion with a high MRATIO, EVALIDator was used to generate a table of annual mortality volume by FIA species group (Burrill and others 2018) and cause of death. From these tables, it is possible to make reasonable assumptions about the particular insects or diseases that may be affecting particular regions. Care must be used in interpreting these causes because tree mortality may actually be caused by a combination of factors such as drought and insects. Further information about the causes of mortality is provided by the aerial survey of insects and disease (see ch. 2 in this report). It is difficult to directly match aerial survey data to mortality observed on FIA plots due to both the difference in timing when mortality is recorded and difficulty matching plot locations with aerial survey mortality polygons. However, aerial survey information has been incorporated into the discussion by referencing State Forest Health Highlights, which reflect in large part the results of aerial surveys.

In addition, mortality rates were derived for each forest type group (Burrill and others 2018, USDA Forest Service 2008) for each ecoregion section across the United States. At times, identifying the forest type experiencing high mortality can be more useful than identifying the species group, especially when the cause of death is abiotic. Results by forest type group are only reported when they help reveal a pattern that is not evident from analysis of species group alone.

RESULTS AND DISCUSSION

The MRATIO values are shown in figure 5.2. The MRATIO can be large if an over-mature forest is senescing and losing a cohort of older trees. If forests are not naturally senescing, a high MRATIO (>0.6) may indicate high mortality due to some acute cause (insects or pathogens) or due to generally deteriorating forest health conditions. The ecoregion sections with the highest MRATIOs are labeled on the map. In the discussion that follows, the focus is placed on the ecoregion sections having MRATIOs >0.6.

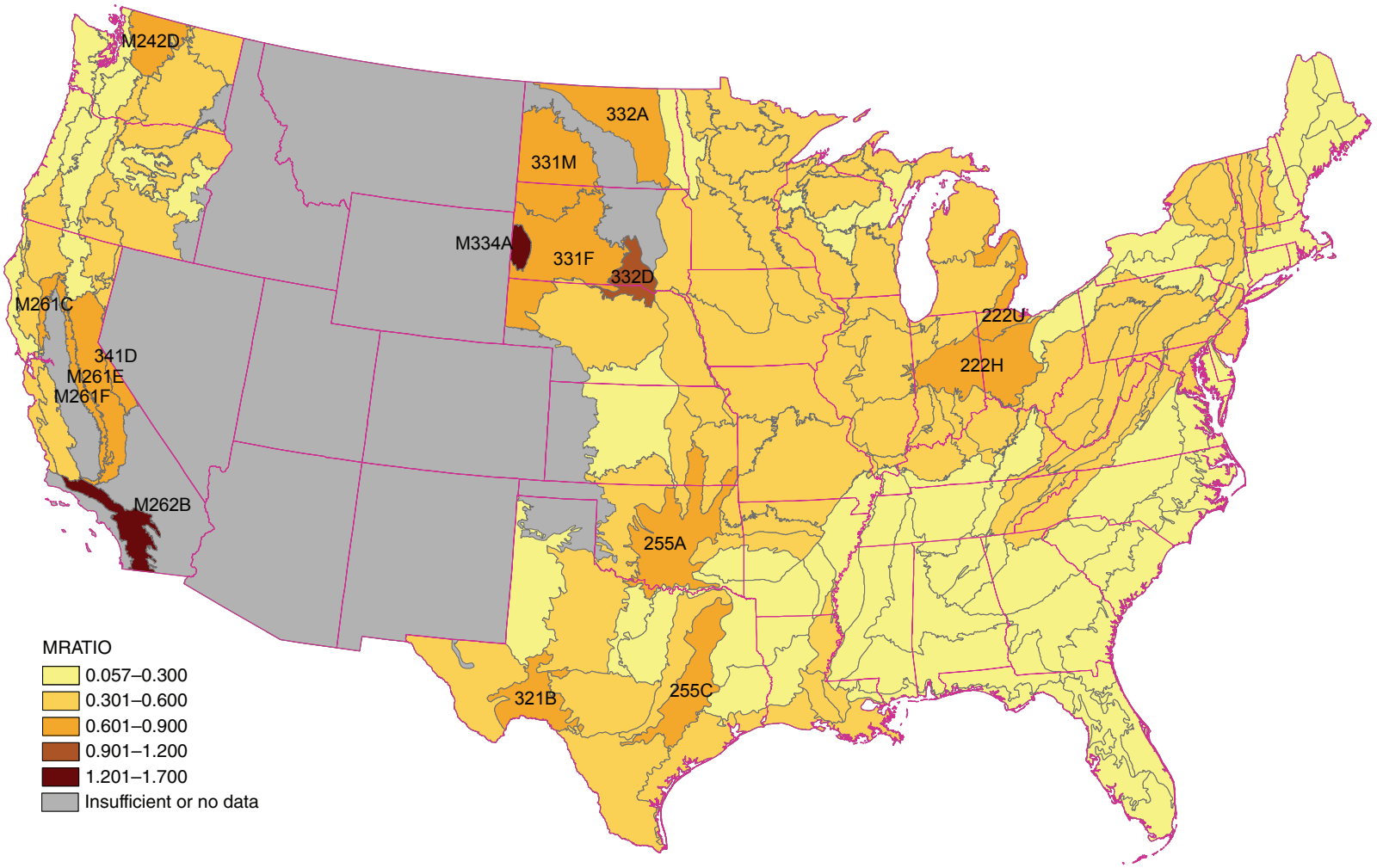

Figure 5.2—Tree mortality expressed as the ratio of annual mortality volume to gross annual growth volume (MRATIO) by ecoregion section (Cleland and others 2007). (Data source: U.S. Department of Agriculture Forest Service, Forest Inventory and Analysis Program)

Eastern and Central States

The highest MRATIOs occurred in ecoregion sections 332D–North-Central Great Plains (MRATIO = 1.08) in South Dakota and Nebraska and M334A–Black Hills (MRATIO = 1.21). Other areas of high mortality relative to growth on the Great Plains were ecoregions 331F–Western Great Plains (MRATIO = 0.81) in South Dakota and Nebraska, 331M–Missouri Plateau (MRATIO = 0.68) in North and South Dakota, and 332A-Northeastern Glaciated Plains (MRATIO = 0.80) in North Dakota. In these Great Plains ecoregions where mortality is high relative to growth, the predominant vegetation is grassland. Although the ecoregion sections are quite large, there was relatively little forest land to measure (e.g., 135 forested plots in section 331F and 108 plots in section 331M). In the Plains, tree growth is generally slow because of naturally dry conditions. Where the number of sample plots is small and tree growth is naturally slow, care must be taken in interpreting mortality relative to growth.

In ecoregion section M334A–Black Hills (MRATIO = 1.21), the vast majority (93 percent) of mortality occurred in the ponderosa and Jeffrey pine species group. For the entire ecoregion section, 72 percent of mortality was caused by insects, while 16 percent was caused by fire (table 5.2); for ponderosa/Jeffrey pine, insects and fire were responsible for 75 percent and 17 percent of mortality,

Table 5.2—Ecoregion sections in the Eastern and Central United States having the highest mortality relative to growth (MRATIO), annual growth and mortality rates, and associated causes of mortality

Ecoregion section	Average annual mortality	Average annual gross growth	MRATIO	Major causes of mortality[a]
	------- *cubic feet per year* -------			
M334A–Black Hills	49,157,466	40,643,847	1.21	Insects (72%), fire (16%)
332D–North-Central Great Plains	12,841,746	11,919,536	1.08	Weather-related (46%), fire (24%)
255C–Oak Woods and Prairies	116,902,469	141,752,979	0.82	Weather-related (69%), disease (14%)
321B–Stockton Plateau	7,685,163	9,381,332	0.82	Weather-related (67%), fire (32%)
331F–Western Great Plains	11,966,303	14,721,800	0.81	Fire (48%), weather-related (21%)
332A–Northeastern Glaciated Plains	8,029,281	10,033,026	0.80	Weather-related (45%), animals (12%), disease (10%)
222U–Lake Whittlesey Glaciolacustrine Plain	47,912,169	64,702,192	0.74	Insects (73%)
255A–Cross Timbers and Prairie	18,731,996	27,304,630	0.69	Disease (44%), weather-related (29%), fire (14%)
331M–Missouri Plateau	6,131,103	8,955,926	0.68	Weather-related (70%), disease (11%)
222H–Central Till Plains-Beech-Maple	112,895,664	173,456,876	0.65	Insects (44%), weather-related (12%)

[a] Agents identified as causing at least 10 percent of the mortality.

respectively. Mortality in this ecoregion is most likely related to mountain pine beetle (*Dendroctonus ponderosae*). There had been an ongoing pine beetle outbreak in the Black Hills region (Ball and others 2015, 2016; South Dakota Department of Agriculture 2011, 2012, 2013, 2014). Pine beetle activity has declined dramatically in the region since 2015 (Ball and others 2017, Wyoming State Forestry Division 2017). The pine beetle outbreak has ended, but reported mortality remains high because results, based on the most recent cycles of FIA data, reflect mortality over the period that includes the peak of the outbreak in 2015.

In 332D–North-Central Great Plains (MRATIO = 1.08), 46 percent of mortality was weather-related, while another 24 percent of mortality was due to fire (table 5.2). Almost half of the mortality occurred in the cottonwood and aspen species group. Mortality was also high in the white oak, ponderosa and Jeffrey pine, and other eastern soft hardwoods species groups. Adverse weather was responsible for almost all of the cottonwood/aspen mortality. However, the majority of oak and pine mortality was due to fire. Adverse weather conditions, including both droughts and excessively wet conditions, occurred multiple times during the remeasurement cycle. These included a drought that affected almost all of Nebraska in 2012 and 2013 and a major drought in South Dakota in 2017 (Ball and others 2017; Nebraska Forest Service 2012, 2013; South Dakota Department of Agriculture 2012). A number of other agents may have contributed to the mortality, including oak decline, which has been reported in northern and eastern Nebraska (Nebraska Forest Service 2017, 2018), bur oak blight (*Tubakia iowensis*), and Dutch elm disease (*Ophiostoma novo-ulmi*) (Ball and others 2017, 2018).

In ecoregion section 331F–Western Great Plains (MRATIO = 0.81), fire caused 48 percent of mortality; another 21 percent of mortality was weather-related (table 5.2). In this ecoregion, most of the mortality (about 75 percent) occurred in the ponderosa and Jeffrey pine species group. In this species group, 52 percent of mortality was due to fire, and 27 percent was due to adverse weather. Only 9 percent of pine mortality was related to insects. Adverse weather events included a drought in 2012 and 2013, affecting much of South Dakota and Nebraska (South Dakota Department of Agriculture 2012; Nebraska Forest Service 2012, 2013). In western Nebraska, ips beetles have caused pine mortality, especially in trees stressed by drought or fire (Nebraska Forest Service 2015, 2016, 2017).

In ecoregion section 331M–Missouri Plateau (MRATIO = 0.68), about 71 percent of the mortality (by volume) occurred in the cottonwood and aspen species group. About 70 percent of total mortality (table 5.2) and 89 percent of cottonwood/aspen mortality was identified as weather-related. Adverse weather conditions, including both drought and excessively wet conditions, occurred during the remeasurement cycle (Ball and others 2017; Johnson 2017; North Dakota Forest Service 2012, 2013; South Dakota Department

of Agriculture 2012). Multiple tree-damaging storm events, including both hail storms and tornadoes, also occurred over that period (Johnson 2017; North Dakota Forest Service 2016). About 11 percent of total mortality (table 5.2) and 5 percent of cottonwood/aspen mortality was caused by disease. Cottonwood canker fungi have been identified as a problem throughout North Dakota (North Dakota Forest Service 2014, 2015); these fungi may be contributing to the observed cottonwood mortality.

The majority of the mortality in ecoregion 332A–Northeastern Glaciated Plains (MRATIO = 0.80) of North Dakota was split among the cottonwood and aspen (48 percent), ash (13 percent), white oak (20 percent), and other eastern soft hardwoods (19 percent) species groups. About 45 percent of the mortality overall (table 5.2) and 38 percent of cottonwood/aspen mortality was related to adverse weather. North Dakota experienced numerous storm events over the past several years, including 435 hail events and 66 tornadoes during the 2015 and 2016 growing seasons. Damage due to hail storms can make trees susceptible to a number of fungal diseases (North Dakota Forest Service 2015, 2016). About 12 percent of mortality was attributed to animals; almost all of this occurred in the cottonwood/aspen species group.

Mortality relative to growth was also rather high (MRATIO = 0.74) in ecoregion section 222U–Lake Whittlesey Glaciolacustrine Plain. There the majority of the mortality (73 percent) was ash. About 73 percent of mortality in that ecoregion was caused by insects (table 5.2), and insects were responsible for 97 percent of ash mortality. Most of this mortality was due to emerald ash borer (*Agrilus planipennis*), which has produced extremely high ash mortality throughout Ohio and Michigan (Michigan Department of Natural Resources 2014, 2015, 2016, 2017; Ohio Department of Natural Resources, Division of Forestry 2014, 2015). In fact, emerald ash borer has caused the death of the "vast majority" of native ash in northwestern Ohio (Ohio Department of Natural Resources, Division of Forestry 2016, 2017).

Similarly, in the adjacent ecoregion 222H–Central Till Plains-Beech-Maple (MRATIO = 0.65) in Ohio and Indiana, much of the mortality (48 percent) was ash and 91 percent of ash mortality was due to insects, most likely emerald ash borer. Indeed, emerald ash borer has been confirmed throughout the ecoregion as well as throughout Indiana (Marshall, 2017, 2018; Ohio Department of Natural Resources, Division of Forestry 2016, 2017). For species other than ash, adverse weather was the single most important mortality-causing agent, accounting for 12 percent of mortality overall (table 5.2).

Ecoregion 255C–Oak Woods and Prairies in Texas also had relatively high mortality (MRATIO = 0.82). About 53 percent of the mortality occurred in the red and white oak species groups, and another 16 percent occurred in the loblolly and shortleaf pine species group. The majority (69 percent) of mortality in this ecoregion section was identified

as weather-related (table 5.2). Weather was responsible for 75 percent of oak mortality and 52 percent of pine mortality. A record-setting drought in 2011 affected Oklahoma and Texas (Oklahoma Forestry Services 2014, 2015, 2016). It was reported as weakening both pines and hardwoods in Texas, making them susceptible to a variety of pests and pathogens (Smith 2013, 2014). Disease was the reported cause of another 14 percent of mortality (table 5.2). Oak wilt has been a major problem in oak woodlands in central Texas (Smith 2014; Texas A & M Forest Service 2015, 2016) and probably contributed to the red and white oak mortality. Pine engraver beetle (*Ips* spp.) has been a problem in Texas' pine forests and may have contributed to mortality in the loblolly and shortleaf pine (Smith 2014; Texas A & M Forest Service 2015, 2016, 2017).

Ecoregion 255A–Cross Timbers and Prairie experienced relatively high mortality (MRATIO = 0.69). About 52 percent of the mortality occurred in the red and white oak species groups. Disease was the reported cause of 44 percent of mortality; 29 percent of mortality was weather-related; 14 percent of mortality was due to fire (table 5.2). Among the oaks, disease was responsible for about 67 percent of the mortality, while weather was responsible for 19 percent. As mentioned above, a record drought in 2011 and 2012 affected Oklahoma and Texas, stressing trees. Oklahoma has been working with Texas to monitor the impacts of drought on forest health in both States (Oklahoma Forestry Services 2014, 2015, 2016). Oaks have been especially strongly affected by the drought (Oklahoma Forestry Services 2017). Following the drought, Hypoxylon canker, caused by the fungus *Biscogniauxia atropunctata*[3] (McBride and Appel 2016), has become a problem on the drought-stressed trees (Oklahoma Forestry Services 2017).

In ecoregion section 321B–Stockton Plateau (MRATIO = 0.82), 67 percent of mortality was related to adverse weather and another 32 percent was due to fire (table 5.2). About 89 percent of mortality occurred in the western woodland softwoods species group. Most of this mortality probably was related to the previously discussed drought that affected Texas beginning in 2011.

Western States

As mentioned above, in all Western States, less than the full panel of plots have been remeasured. Thus, the mortality results presented here should be considered preliminary. Also, one must be aware that, because of the longer 10-year measurement cycle in the West, results shown represent mortality that may have occurred any time during the period spanned by the data (see table 5.1), which may have been as long as 17 years.

For a large portion of the West, no MRATIO could be calculated. At the time this chapter was being written, due to changes being made to the

[3] The fungal pathogen *Hypoxylon atropunctatum* has recently been moved to the genus *Biscogniauxia*, but the term "Hypoxylon canker" remains in common usage.

FIADB, growth estimates were not available for the Interior West FIA region. Thus, no MRATIOs were calculated for ecoregions in those States. MRATIOs were also not calculated for some ecoregions in West Coast States. This was because either (1) fewer than 25 plots had been remeasured in an ecoregion, or (2) the percent sampling error for the growth estimate was too high (>100 percent). One expects that as the first cycle of plot remeasurements is completed in future years, it will be possible to estimate MRATIOs for most of the West.

West Coast ecoregion sections having the highest MRATIOs are shown in table 5.3 with the major causes of mortality identified. Seeing that fire and weather as well as insects and disease were responsible for significant mortality, for these West Coast ecoregions we examined mortality numbers both by forest type group and species group. We would expect that patterns of mortality caused by biotic factors (insects, disease) would be most apparent when looking at species groups affected, while patterns of mortality caused by abiotic factors (weather, fire) would be most apparent when looking at forest types affected.

Of the ecoregions of the West Coast States where the MRATIO could be calculated, ecoregion section M262B–Southern California Mountain and Valley (MRATIO = 1.67)

Table 5.3—Ecoregion sections in West Coast States having the highest mortality relative to growth (MRATIO), annual growth and mortality rates, and associated causes of mortality

Ecoregion section	Average annual mortality	Average annual gross growth	MRATIO	Major causes of mortality[a]
	--------- *cubic feet per year* ---------			
M262B–Southern California Mountain and Valley	19,950,233	11,961,582	1.67	Fire (57%), insects (14%)
341D–Mono	6,203,870	7,534,619	0.82	Insects (47%), fire (39%)
M242D–Northern Cascades	289,680,840	369,562,663	0.78	Insects (36%), fire (25%), weather-related (16%), disease (13%)
M261E–Sierra Nevada	390,937,815	548,833,831	0.71	Fire (32%), disease (30%), weather-related (13%), insects (13%)
M261C–Northern California Interior Coast Ranges	5,057,305	7,112,102	0.71	Fire (48%), disease (23%), weather-related (13%)
M261F–Sierra Nevada Foothills	18,375,520	29,763,584	0.62	Disease (23%), weather-related (18%), fire (13%)

[a] Agents identified as causing at least 10 percent of the mortality.

stands out. This is the highest MRATIO found anywhere in the United States. Fire was responsible for 57 percent of this mortality (table 5.3). Insects were responsible for another 14 percent of mortality. About half of the mortality in this ecoregion section occurred in the western oak forest type group, and most of that mortality was due to fire. Fire was also responsible for most of the morality in the pinyon/juniper forest type group, where 9 percent of the ecoregion's mortality occurred. Insects were responsible for almost all the mortality in the ponderosa pine forest type group and about 44 percent of the mortality in the California mixed conifer forest type group (about 33 percent of the mortality occurred in the ponderosa and Jeffrey pine species group and about 22 percent in the other western softwoods species group).

In ecoregion section 341D–Mono (MRATIO = 0.82), about 60 percent of mortality occurred in the western woodland softwoods species group, and about 23 percent was in the lodgepole pine species group. All of the lodgepole pine mortality was attributed to insects, while for western woodland softwoods about 57 percent of mortality was due to fire, and about 30 percent was due to insects.

In M261E–Sierra Nevada (MRATIO = 0.71), mortality occurred in a large number of species groups, with the highest mortality suffered by true firs (43 percent), ponderosa and Jeffrey pine (17 percent), and sugar pine (12 percent). A variety of agents (insects, disease, fire, and weather) contributed to the observed mortality. Disease was the single most important cause of mortality in the true fir and sugar pine species groups.

In M261C–Northern California Interior Coast Ranges (MRATIO = 0.71), almost all of the mortality occurred in the western oak forest type group. About 40 percent of the mortality was oaks, and about 60 percent was other western softwoods. Just over half of the oak mortality and about 40 percent of the softwood mortality was due to fire.

Similarly, in M261F–Sierra Nevada Foothills (MRATIO = 0.62), almost all of the mortality occurred in the western oak forest type group. About 63 percent of the mortality was oaks, about 18 percent was other western softwoods, and 9 was ponderosa/Jeffrey pine. However, in this ecoregion section, a variety of agents (disease, weather, fire, and insects) all contributed to the observed mortality (table 5.3) and about 41 percent of mortality could not be definitely attributed to a known causal agent.

At a broad scale, we see that, in much of California, tree mortality is often related to a combination of prolonged drought (2011–2015 statewide; 2011–2017 in parts of the State), bark beetles, and fire (California Forest Pest Council 2015, 2016, 2017). These factors have interacted, leading to high mortality, especially in southern California. Overstocked stands in many parts of the State have contributed to the drought stress and susceptibility of forests to insects and wildfires (California Forest Pest Council 2015, 2016, 2017). It should also be

noted that the same drought which led to high mortality (directly or indirectly) would also have reduced growth over the measurement period; reduced growth also contributes to a high MRATIO (see Methods section).

Aside from California, the highest MRATIO (0.78) occurred in ecoregion section M242D—Northern Cascades. There, mortality occurred in a large number of species groups, including Engelmann and other spruces (27 percent), true firs (23 percent), lodgepole pine (15 percent), and Douglas-fir (15 percent). While insects and fire were the most significant mortality-causing agents, other factors, including disease and adverse weather, also contributed to the observed mortality (table 5.3).

Figure 5.3 shows the ratio of annual mortality to standing live tree volume for the United States. In most of the country, the ecoregion sections having high mortality relative to standing volume are the same regions that had high MRATIOs (fig. 5.2).

Focusing on the Interior West, we see clusters of ecoregion sections where mortality is high relative to standing live tree volume: a cluster of mountain ecoregion sections in western Montana, central Idaho, and northwestern Wyoming (M331A, M331J, M332A, M332B, M332D, M332E, M332F, and M333C); in the Front Range of Colorado and southern Wyoming (M331I) and the South-Central Highlands of Colorado and northern New Mexico (M331G) together with the Uinta Mountains of Utah (M331E); and in northeastern Nevada (341G). In all of these ecoregion sections, annual mortality exceeded 2.5 percent of live volume (table 5.4).

In northeastern Nevada's ecoregion section 341G–Northeastern Great Basin, fire was the major cause of mortality (table 5.4). About 56 percent of the mortality occurred in the true fir species group, and about 70 percent of the fir mortality was due to fire.

In Colorado and Wyoming's ecoregion section M331I–Northern Parks and Ranges, 64 percent of the mortality was lodgepole pine, and another 19 percent was the Englemann and other spruces species group; almost all of this mortality was attributed to insects. The ecoregion includes areas that have experienced major outbreaks of mountain pine beetle as well as spruce beetle (*D. rufipennis*) (Colorado State Forest Service 2016; Wyoming State Forestry Division 2016, 2017). These same pests, as well as fir engraver beetle (*Scolytus ventralis*), have been affecting ecoregion M331E–Uinta Mountains (USDA Forest Service, Uinta-Wasatch-Cache National Forest, no date; Utah Department of Natural Resources, Forestry, Fire, & State Lands 2016), where 66 percent of mortality was lodgepole pine and 13 percent was Englemann and other spruces. Here, also, most of the mortality was caused by insects. In ecoregion section M331G–South-Central Highlands, about two-thirds of mortality overall was caused by insects. In this ecoregion, about 61 percent of mortality was Englemann and other spruces; 96 percent of spruce mortality was due to insects. In this area, spruce beetle has caused significant mortality

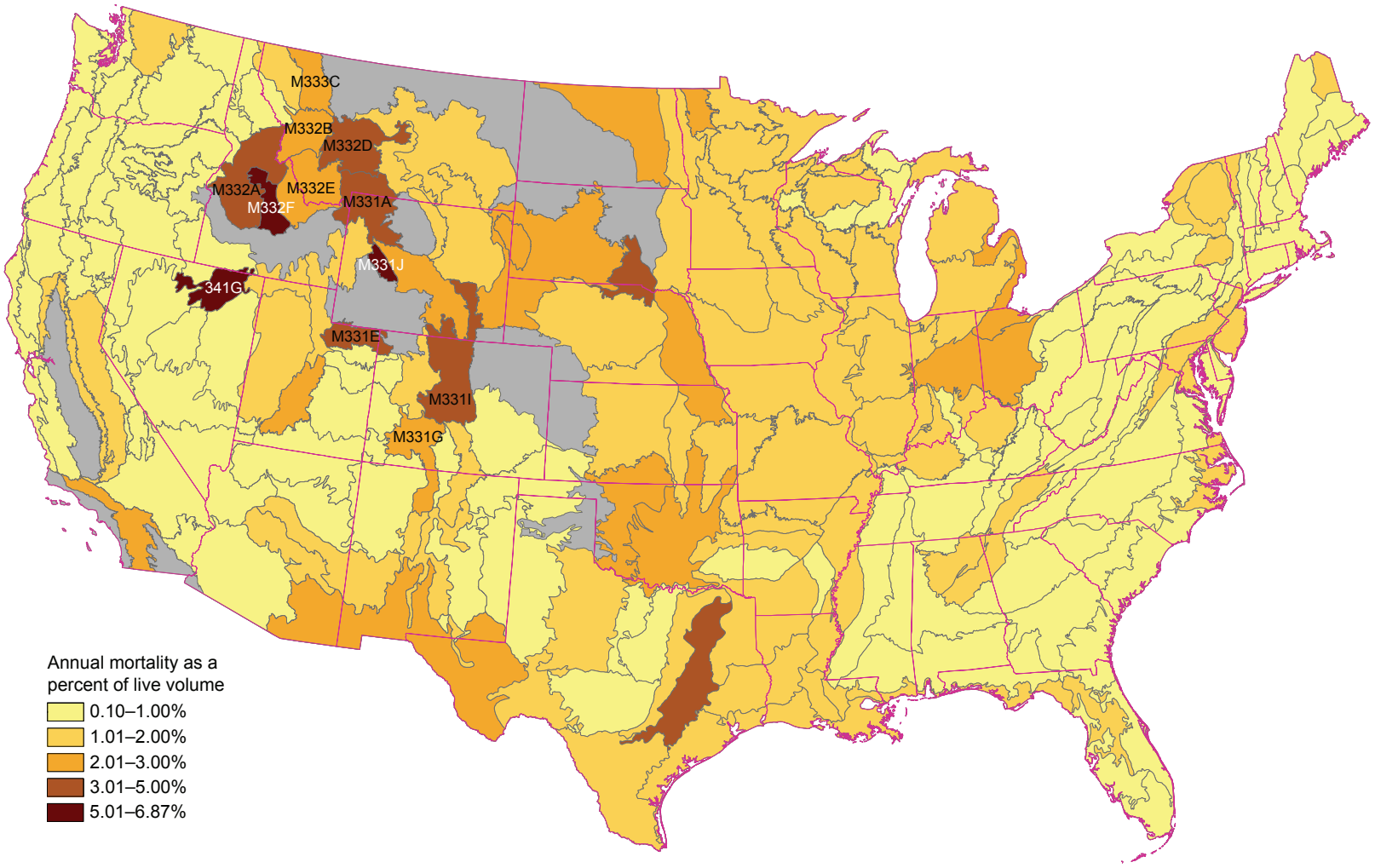

Figure 5.3—Annual tree mortality expressed as a percentage of standing live tree volume by ecoregion section (Cleland and others 2007). (Data source: U.S. Department of Agriculture Forest Service, Forest Inventory and Analysis Program)

Table 5.4—Ecoregion sections in Interior West States having the highest mortality relative to standing live tree volume and associated causes of mortality

Ecoregion section	Average annual mortality	Standing live tree volume	Mortality relative to standing volume	Major causes of mortality[a]
	cubic feet per year	*cubic feet*		
341G–Northeastern Great Basin	6,774,796	98,564,467	6.87%	Fire (57%), insects (29%)
M332F–Challis Volcanics	137,664,825	2,176,648,229	6.32%	Fire (50%), insects (42%)
M331J–Wind River Mountains	51,789,732	938,456,464	5.52%	Insects (72%), fire (18%)
M331I–Northern Parks and Ranges	531,523,774	12,437,622,452	4.27%	Insects (85%)
M332D–Belt Mountains	202,524,949	4,892,340,858	4.14%	Insects (86%)
M331A–Yellowstone Highlands	340,716,778	8,247,943,183	4.13%	Insects (57%), fire (28%)
M331E–Uinta Mountains	102,559,418	2,845,948,640	3.60%	Insects (66%), disease (22%)
M332A–Idaho Batholith	539,075,204	17,585,337,151	3.07%	Fire (55%), insects (26%)
M331G–South-Central Highlands	295,137,741	9,861,651,126	2.99%	Insects (66%), disease (12%), fire (12%)
M332B–Northern Rockies and Bitterroot Valley	180,135,382	6,083,853,253	2.96%	Insects (51%), fire (38%)
M332E–Beaverhead Mountains	141,598,785	5,386,335,877	2.63%	Insects (76%), fire (16%)
M333C–Northern Rockies	202,302,538	7,766,591,480	2.60%	Fire (53%), disease (25%), insects (15%)

[a] Agents identified as causing at least 10 percent of the mortality.

(Colorado State Forest Service 2016, 2017; Norlander 2013; Zegler 2015, 2016; Zegler and Formby 2017).

In the areas of high mortality in Montana, Idaho, and northwestern Wyoming (ecoregion sections M331A, M331J, M332A, M332B, M332D, M332E, M332F, and M333C), insects and fire were the most significant causes of mortality (table 5.4). This region includes areas suffering outbreaks of mountain pine beetle (Montana Department of Natural Resources and Conservation 2014, 2016) as well as major fires (Idaho Department of Lands 2014). However, several other insect and disease issues have been identified in this region and may have contributed to the mortality. In most of these ecoregion sections (M331A, M331J, M332A, M332B, M332D, and M332E), the lodgepole pine species group suffered the highest mortality, most of which was due to insects. However, many other species groups, including Douglas-fir, true firs, and Englemann and other spruces also suffered non-trivial mortality.

SUMMARY

This analysis shows that, in most of the Eastern and Central United States, mortality is low relative to tree growth. The areas of highest mortality occur in the mostly riparian forests of Great Plains ecoregions. A common characteristic of most of the ecoregions having high mortality is that they are on the margins of land suitable for forest growth, being very dry. Thus, they tend to be extremely vulnerable to changes in weather patterns that might produce prolonged and/or extreme drought. Drought, combined with a variety of other biotic and/or abiotic stressors, is likely responsible for much of the mortality observed.

However, one insect pest issue does stand out in the East. In ecoregion sections 222H–Central Till Plains-Beech-Maple and 222U–Lake Whittlesey Glaciolacustrine Plain, ash mortality due to emerald ash borer is extremely high.

The preliminary analysis of the Western United States shows that, in many parts of the Interior West, mortality is very high as a percent of standing live tree volume and that several West Coast ecoregion sections have high MRATIOs. All of these areas correspond to regions where insect outbreaks (ch. 2) as well as fire (ch. 3) and/or severe drought (ch. 4) have occurred. These three mortality-causing agents are related in that drought stresses trees, making them more susceptible to insect attack, while both drought and insect-killed trees create conditions favorable for wildfires.

It is also important to realize that the analyses presented in this chapter alone cannot tell the complete story regarding tree mortality. Mortality that is concentrated in highly fragmented forest or nonforest areas adjacent to human development may not be detected because the available FIA data do not cover most urban areas or other places not defined as forest by FIA. Also, these analyses are unlikely to detect a pest or pathogen attacking a particular tree species in a mixed-species forest where other species are growing vigorously. This is especially true of species (e.g., ash) that make up a relatively small proportion of many eastern forests. For example, it is known that emerald ash borer has been causing very high ash mortality in many Eastern and Central States in recent years (USDA APHIS 2018; Ohio Department of Natural Resources, Division of Forestry 2016). Yet, this mortality stands out only in ecoregion sections 222H—Central Till Plains-Beech-Maple and 222U—Lake Whittlesey Glaciolacustrine Plain. Elsewhere in the East, though ash mortality is known to be extremely high, the mortality is masked because ash is a relatively minor component of the forest.

To gain a more complete understanding of mortality, one should consider the results of this analysis together with other indicators of forest health. Forest Inventory and Analysis tree damage data (Burrill and others 2018), as well as Evaluation Monitoring projects that focus on particular mortality-causing agents (ch. 8–9), can provide insight into smaller scale or species-specific mortality issues. Large-scale analyses

of forest-damaging events, including insect and disease activity (ch. 2) and fire (ch. 3), are also important for understanding mortality patterns. This can be especially important in the West, where mortality data are limited.

LITERATURE CITED

Ball, J.; Warnke, M.; Garbisch, B. 2015. Forest health highlights in South Dakota 2015. Pierre: South Dakota Department of Agriculture, Division of Resource Conservation and Forestry. 9 p. https://www.fs.fed.us/foresthealth/protecting-forest/forest-health-monitoring/monitoring-forest-highlights.shtml. [Date accessed: May 9, 2018].

Ball, J.; Pyser, N.; Warnke, M. 2016. State of South Dakota forest health highlights 2016. Pierre: South Dakota Department of Agriculture, Division of Resource Conservation and Forestry. 6 p. https://www.fs.fed.us/foresthealth/protecting-forest/forest-health-monitoring/monitoring-forest-highlights.shtml. [Date accessed: May 9, 2018].

Ball, J.; Seidl, A.; Warnke, M. 2017. State of South Dakota forest health highlights 2017. Pierre: South Dakota Department of Agriculture, Division of Resource Conservation and Forestry. 8 p. https://sdda.sd.gov/conservation-forestry/forest-health/SDHighlights_2017-2.pdf. [Date accessed: July 23, 2019].

Ball, J.; Seidl, A.; Warnke, M. 2018. State of South Dakota forest health highlights 2018. Pierre: South Dakota Department of Agriculture, Division of Resource Conservation and Forestry. 12 p. https://sdda.sd.gov/conservation-forestry/forest-health/SDHighlights_2018.pdf. [Date accessed: July 1, 2019].

Bechtold, W.A.; Patterson, P.L., eds. 2005. The enhanced Forest Inventory and Analysis program—national sampling design and estimation procedures. Gen. Tech. Rep. SRS-80. Asheville, NC: U.S. Department of Agriculture Forest Service, Southern Research Station. 85 p.

Burrill, E.A.; Wilson, A.M.; Turner, J.A. [and others]. 2018. The Forest Inventory and Analysis Database: database description and users manual for Phase 2 (version 8.0). Washington, DC: U.S. Department of Agriculture Forest Service. 946 p. http://fia.fs.fed.us/library/database-documentation/. [Date accessed: July 16, 2019].

California Forest Pest Council. 2015. 2015 California forest health highlights. 21 p. https://www.fs.fed.us/foresthealth/protecting-forest/forest-health-monitoring/monitoring-forest-highlights.shtml. [Date accessed: May 9, 2018].

California Forest Pest Council. 2016. 2016 California forest health highlights. 31 p. https://www.fs.fed.us/foresthealth/protecting-forest/forest-health-monitoring/monitoring-forest-highlights.shtml. [Date accessed: May 9 2018].

California Forest Pest Council. 2017. 2017 California forest health highlights. 38 p. https://www.fs.usda.gov/Internet/FSE_DOCUMENTS/fseprd578578.pdf. [Date accessed: May 9, 2018].

Cleland, D.T.; Freeouf, J.A.; Keys, J.E. [and others]. 2007. Ecological subregions: sections and subsections for the conterminous United States. Gen. Tech. Rep. WO-76D. Washington, DC: U.S. Department of Agriculture Forest Service. Map; Sloan, A.M., cartographer; presentation scale 1:3,500,000; colored. Also on CD-ROM as a GIS coverage in ArcINFO format.

Colorado State Forest Service. 2016. 2015 report on the health of Colorado's forests – 15 years of change. Fort Collins, CO: Colorado State Forest Service. 32 p. https://csfs.colostate.edu/media/sites/22/2016/02/ForestHealthReport-2015.pdf. [Date accessed: July 30, 2019].

Colorado State Forest Service. 2017. 2016 report on the health of Colorado's forests – fire and water. Fort Collins, CO: Colorado State Forest Service. 36 p. https://csfs.colostate.edu/media/sites/22/2017/02/CSU_304464_ForestReport-2016-www.pdf. [Date accessed: July 30, 2019].

Coulston, J.W.; Ambrose, M.J.; Stolte. K.S. [and others]. 2005. Criterion 3 – health and vitality. In: Conkling, B.L.; Coulston, J.W.; Ambrose, M.J., eds. Forest Health Monitoring 2001 national technical report. Gen. Tech. Rep. SRS-81. Asheville, NC: U.S. Department of Agriculture Forest Service, Southern Research Station: 39–82.

Idaho Department of Lands. 2014. 2014 forest health highlights. 7 p. https://www.fs.fed.us/foresthealth/docs/fhh/ID_FHH_2014.pdf. [Date accessed: July 30, 2019].

Johnson, L. 2017. Forest health highlights: North Dakota 2017. 12 p. https://www.ag.ndsu.edu/ndfs/documents/north-dakota-forest-health-highlights-2017.pdf. [Date accessed: July 23, 2019].

Marshall, P.T. 2017. 2017 Indiana forest health highlights. Vallonia, IN: Indiana Department of Natural Resources. 17 p. https://www.in.gov/dnr/forestry/files/fo-Forest_Health_Highlights_2017.pdf. [Date accessed: June 20, 2019].

Marshall, P.T. 2018. 2018 Indiana forest health highlights. Vallonia, IN: Indiana Department of Natural Resources. 17 p. https://www.in.gov/dnr/forestry/files/fo-Forest_Health_Highlights_2018.pdf. [Date accessed: June 20, 2019].

McBride, S.; Appel, D. 2016. Hypoxylon canker of oaks. College Station, TX: Texas A & M AgriLife Extension Service. 4 p. https://agrilifecdn.tamu.edu/coastalbend/files/2015/02/Hypoxylon-Canker-of-Oaks-Disease.pdf. [Date accessed: August 20, 2019].

McNab, W.H.; Cleland, D.T.; Freeouf, J.A. [and others], comps. 2007. Description of ecological subregions: sections of the conterminous United States [CD-ROM]. Gen. Tech. Report WO-76B. Washington, DC: U.S. Department of Agriculture Forest Service. 80 p.

Michigan Department of Natural Resources. 2014. 2014 forest health highlights. 51 p. https://www.fs.fed.us/foresthealth/protecting-forest/forest-health-monitoring/monitoring-forest-highlights.shtml. [Date accessed: April 27, 2018].

Michigan Department of Natural Resources. 2015. 2015 forest health highlights. 50 p. https://www.fs.fed.us/foresthealth/protecting-forest/forest-health-monitoring/monitoring-forest-highlights.shtml. [Date accessed: April 8, 2018].

Michigan Department of Natural Resources. 2016. 2016 forest health highlights. 51 p. https://www.fs.fed.us/foresthealth/protecting-forest/forest-health-monitoring/monitoring-forest-highlights.shtml. Date accessed: April 8, 2018].

Michigan Department of Natural Resources. 2017. 2017 forest health highlights. 31 p. https://www.michigan.gov/documents/dnr/frsthlthhghlghts_513144_7.pdf. [Date accessed: May 8, 2018].

Montana Department of Natural Resources and Conservation, Forest Pest Management Program. 2014. Montana forest health highlights 2014. 4 p. https://www.fs.fed.us/foresthealth/docs/fhh/MT_FHH_2014.pdf. [Date accessed: July 30, 2019].

Montana Department of Natural Resources and Conservation, Forest Pest Management Program. 2016. Montana forest health highlights 2016. 4 p. http://dnrc.mt.gov/divisions/forestry/docs/assistance/pests/conditions-highlights/fhh_2016.pdf. [Date accessed: July 30, 2019].

Nebraska Forest Service. 2012. Nebraska forest health highlights 2012. 5 p. https://www.fs.fed.us/foresthealth/protecting-forest/forest-health-monitoring/monitoring-forest-highlights.shtml. [Date accessed: May 1, 2018].

Nebraska Forest Service. 2013. Nebraska forest health highlights 2013. 4 p. https://www.fs.fed.us/foresthealth/protecting-forest/forest-health-monitoring/monitoring-forest-highlights.shtml. [Date accessed: June 2, 2018].

Nebraska Forest Service. 2015. Nebraska forest health highlights 2015. 6 p. https://www.fs.fed.us/foresthealth/protecting-forest/forest-health-monitoring/monitoring-forest-highlights.shtml. [Date accessed: May 10, 2018].

Nebraska Forest Service. 2016. Nebraska forest health highlights 2016. 6 p. https://www.fs.fed.us/foresthealth/protecting-forest/forest-health-monitoring/monitoring-forest-highlights.shtml. [Date accessed: May 10, 2018].

Nebraska Forest Service. 2017. Nebraska forest health highlights 2017. 6 p. https://www.fs.fed.us/foresthealth/docs/fhh/NE_FHH_2017.pdf. [Date accessed: August 25, 2018].

Nebraska Forest Service. 2018. Nebraska forest health highlights 2018. 3 p. https://nfs.unl.edu/publications/downloads/NE2018Forest%20Health%20Highlights-3.pdf. [Date accessed: July 12, 2019].

Norlander, D. 2013. 2013 New Mexico forest health condition report. 17 p. http://www.emnrd.state.nm.us/SFD/FWHPlan/documents/2013NMSFconditionsreport.pdf. [Date accessed: July 30, 2019].

North Dakota Forest Service. 2012. North Dakota forest health highlights 2012. 12 p. https://www.fs.fed.us/foresthealth/protecting-forest/forest-health-monitoring/monitoring-forest-highlights.shtml. [Date accessed: May 15, 2018].

North Dakota Forest Service. 2013. North Dakota forest health highlights 2013. 12 p. https://www.fs.fed.us/foresthealth/protecting-forest/forest-health-monitoring/monitoring-forest-highlights.shtml. [Date accessed: April 26, 2018].

North Dakota Forest Service. 2014. North Dakota forest health highlights 2014. 24 p. https://www.fs.fed.us/foresthealth/protecting-forest/forest-health-monitoring/monitoring-forest-highlights.shtml. [Date accessed: April 12, 2018].

North Dakota Forest Service. 2015. North Dakota forest health highlights 2015. 24 p. https://www.fs.fed.us/foresthealth/protecting-forest/forest-health-monitoring/monitoring-forest-highlights.shtml. [Date accessed: April 12, 2018].

North Dakota Forest Service. 2016. North Dakota forest health highlights 2016. 4 p. https://www.ag.ndsu.edu/ndfs/documents/north-dakota-forest-health-highlights-2016.pdf. [Date accessed: August 25, 2018].

Ohio Department of Natural Resources, Division of Forestry. 2014. 2014 Ohio forest health highlights. 7 p. Columbus, OH: Ohio Department of Natural Resources, Division of Forestry. https://www.fs.fed.us/foresthealth/protecting-forest/forest-health-monitoring/monitoring-forest-highlights.shtml. [Date accessed: April 27, 2018].

Ohio Department of Natural Resources, Division of Forestry. 2015. 2015 Ohio forest health highlights. 8 p. Columbus, OH: Ohio Department of Natural Resources, Division of Forestry. https://www.fs.fed.us/foresthealth/protecting-forest/forest-health-monitoring/monitoring-forest-highlights.shtml. [Date accessed: April 17, 2018].

Ohio Department of Natural Resources, Division of Forestry. 2016. 2016 Ohio forest health highlights. 8 p. Columbus, OH: Ohio Department of Natural Resources, Division of Forestry. https://www.fs.fed.us/foresthealth/protecting-forest/forest-health-monitoring/monitoring-forest-highlights.shtml. [Date accessed: April 17, 2018].

Ohio Department of Natural Resources, Division of Forestry. 2017. 2017 Ohio forest health highlights. 7 p. Columbus, OH: Ohio Department of Natural Resources, Division of Forestry. https://www.fs.fed.us/foresthealth/docs/fhh/OH_FHH_2017.pdf. [Date accessed: July 7, 2019].

Oklahoma Forestry Services. 2014. Oklahoma forest health highlights 2014. 5 p. https://www.fs.fed.us/foresthealth/protecting-forest/forest-health-monitoring/monitoring-forest-highlights.shtml. [Date accessed: April 2, 2018].

Oklahoma Forestry Services. 2015. Oklahoma forest health highlights 2015. 6 p. https://www.fs.fed.us/foresthealth/protecting-forest/forest-health-monitoring/monitoring-forest-highlights.shtml. [Date accessed: April 3, 2018].

Oklahoma Forestry Services. 2016. Oklahoma forest health highlights 2016. 6 p. https://www.fs.fed.us/foresthealth/protecting-forest/forest-health-monitoring/monitoring-forest-highlights.shtml. [Date accessed: April 2, 2018].

Oklahoma Forestry Services. 2017. Oklahoma forest health highlights 2017. 7 p. https://www.fs.fed.us/foresthealth/docs/fhh/OK_FHH_2017.pdf. [Date accessed: August 25, 2018].

Smith, L.A. 2013. Forest health insects and diseases conditions Texas 2013. Longview, TX: Texas A & M Forest Service. 5 p. https://www.fs.fed.us/foresthealth/protecting-forest/forest-health-monitoring/monitoring-forest-highlights.shtml. [Date accessed: April 27, 2018].

Smith, L.A. 2014. Forest health highlights in Texas 2014. Longview, TX: Texas A & M Forest Service. 1 p. https://www.fs.fed.us/foresthealth/protecting-forest/forest-health-monitoring/monitoring-forest-highlights.shtml. [Date accessed: April 27, 2018].

South Dakota Department of Agriculture. 2011. South Dakota forest health highlights 2011. Pierre: South Dakota Department of Agriculture, Division of Resource Conservation and Forestry. 4 p. https://www.fs.fed.us/foresthealth/protecting-forest/forest-health-monitoring/monitoring-forest-highlights.shtml. [Date accessed: May 1 2018].

South Dakota Department of Agriculture. 2012. South Dakota 2012 forest health highlights. Pierre: South Dakota Department of Agriculture, Division of Resource Conservation and Forestry. 5 p. https://www.fs.fed.us/foresthealth/protecting-forest/forest-health-monitoring/monitoring-forest-highlights.shtml. [Date accessed: March 15, 2018].

South Dakota Department of Agriculture. 2013. South Dakota 2013 forest health highlights. Pierre: South Dakota Department of Agriculture, Division of Resource Conservation and Forestry. 5 p. https://www.fs.fed.us/foresthealth/protecting-forest/forest-health-monitoring/monitoring-forest-highlights.shtml. [Date accessed: March 15, 2018].

South Dakota Department of Agriculture. 2014. South Dakota 2014 forest health highlights. Pierre: South Dakota Department of Agriculture, Division of Resource Conservation and Forestry. 7 p. https://www.fs.fed.us/foresthealth/protecting-forest/forest-health-monitoring/monitoring-forest-highlights.shtml. [Date accessed: March 15, 2018].

Texas A & M Forest Service. 2015. Forest health highlights in Texas 2015. Longview, TX: Texas A & M Forest Service. 1 p. https://www.fs.fed.us/foresthealth/protecting-forest/forest-health-monitoring/monitoring-forest-highlights.shtml. [Date accessed: April 20, 2018].

Texas A & M Forest Service. 2016. Forest health highlights in Texas 2016. Longview, TX: Texas A & M Forest Service. 1 p. https://www.fs.fed.us/foresthealth/protecting-forest/forest-health-monitoring/monitoring-forest-highlights.shtml. [Date accessed: April 20, 2018].

Texas A & M Forest Service. 2017. Forest health highlights 2017. Longview, TX: Texas A & M Forest Service. 2 p. https://www.fs.fed.us/foresthealth/protecting-forest/forest-health-monitoring/monitoring-forest-highlights.shtml. [Date accessed: May 21, 2018].

U.S. Department of Agriculture (USDA) Animal and Plant Health Inspection Service (APHIS). 2018. Emerald ash borer. https://www.aphis.usda.gov/aphis/resources/pests-diseases/hungry-pests/the-threat/emerald-ash-borer/emerald-ash-borer-beetle. [Date accessed: August 31, 2018].

U. S. Department of Agriculture (USDA) Forest Service. 2008. National forest type dataset. http://data.fs.usda.gov/geodata//rastergateway/forest_type/index.php. [Date accessed: September 13, 2016].

U. S. Department of Agriculture (USDA) Forest Service, Forest Inventory and Analysis (FIA) Program. 2019. Forest Inventory EVALIDator web-application Version 1.8.0. St. Paul, MN: U.S. Department of Agriculture Forest Service, Northern Research Station. http://apps.fs.fed.us/Evalidator/evalidator.jsp. [Date accessed: May 13, 2019].

U.S. Department of Agriculture (USDA) Forest Service, Uinta-Wasatch-Cache National Forest. [N.d.]. Beetle activity on the Uinta-Wasatch-Cache National Forest. http://www.fs.usda.gov/detail/uwcnf/home/?cid=STELPRDB5145143. [Date accessed: July 25, 2017].

Utah Department of Natural Resources, Forestry, Fire, & State Lands. 2016. Utah forest health highlights 2016. 3 p. https://www.fs.fed.us/foresthealth/protecting-forest/forest-health-monitoring/monitoring-forest-highlights.shtml. [Date accessed: April 24, 2018].

Wyoming State Forestry Division. 2016. 2016 Wyoming forest health highlights. 16 p. https://www.fs.fed.us/foresthealth/docs/fhh/WY_FHH_2016.pdf. [Date accessed: August 25, 2018].

Wyoming State Forestry Division. 2017. 2017 Wyoming forest health highlights. 17 p. https://www.fs.fed.us/foresthealth/docs/fhh/WY_FHH_2017.pdf. [Date accessed: August 25, 2018].

Zegler, T. 2015. New Mexico forest health conditions, 2015. 17 p. http://www.emnrd.state.nm.us/SFD/FWHPlan/documents/2015_NMconditionsreport_low_shortIIpdf.pdf. [Date accessed: July 30, 2019].

Zegler, T. 2016. New Mexico forest health conditions, 2016. 18 p. http://www.emnrd.state.nm.us/SFD/FWHPlan/documents/2016_NMconditionsreport_short.pdf. [Date accessed: July 30, 2019].

Zegler, T.; Formby, J.P. 2017. New Mexico forest health conditions 2017. 35 p. http://www.emnrd.state.nm.us/SFD/FWHPlan/documents/NMForestHealthConditionsReportComplete.pdf. [Date accessed: July 30, 2019].

SECTION 2.

Analyses of Long-Term Forest Health Trends and Presentations of New Techniques

CHAPTER 6.

A Forest Health Retrospective: National and Regional Results from 20 Years of Insect and Disease Survey Data

Kevin M. Potter
Julie C. Canavin
Frank H. Koch

INTRODUCTION

The Forest Health Monitoring (FHM) national program of the U.S. Department of Agriculture Forest Service determines status, changes, and trends in indicators of forest condition across all forested lands (ch. 1). One of the central objectives of the FHM annual national reports is to present forest health indicator information from a national perspective, or from a multi-State regional perspective when appropriate, using data collected by the Forest Health Protection (FHP) and Forest Inventory and Analysis (FIA) programs of the Forest Service, as well as from other sources. A standing chapter in each edition of the annual "Forest Health Monitoring: National Status, Trends, and Analysis" report, for example, quantifies forest area affected by insects and disease on a yearly basis using data from the FHP national Insect and Disease Survey (IDS) (FHP 2016, 2019) (ch. 2). This is particularly important because forest insects and diseases, particularly nonnative invasive agents, are among the most serious threats to the forests of the United States and are causing widespread ecological and economic impacts on the forests of the Nation (Logan and others 2003, Lovett and others 2016, Tobin 2015). Repeated analyses of regularly collected indicator data, such as from the national IDS, enable the detection of trends over time and can help establish a baseline for future comparisons (Riitters and Tkacz 2004).

Although the FHM reports address annual spatial extent and patterns of insect and disease detections (Coulston 2007, 2009; Potter 2012, 2013; Potter and Koch 2012; Potter and Paschke 2013, 2014, 2015a, 2015b, 2016, 2017; Potter and others 2018, 2019c; ch. 2 of this report), there has been no comprehensive medium-term analysis of insect and disease damage to forests in the FHM reports. Understanding these patterns will allow for better broad-scale decision making associated with the management of forests, and for detailed analyses of the ecological impacts of important insect and disease agents. Additionally, medium-term analyses of IDS data represent a highly useful component for the forest disturbance section of the Resources Planning Act (RPA) Assessment, which reports on status and trends of renewable resources on forest and rangelands every 10 years. Previous RPA Assessment reports (USDA Forest Service 2012, 2016) broadly summarized IDS mortality and defoliation data available in annual FHM reports. This chapter presents a more detailed and comprehensive retrospective analysis examining trends in different aspects of forest health in recent decades that will lay the foundation for developing future forest health projections in forthcoming RPA Assessment reports, as well as providing context to annual FHM reports and informing land management planning. Resources Planning Act Assessments summarize some indicators within four broad U.S. regions. These encompass areas that are similar but not identical to those of the five FHM regions (fig. 6.1).

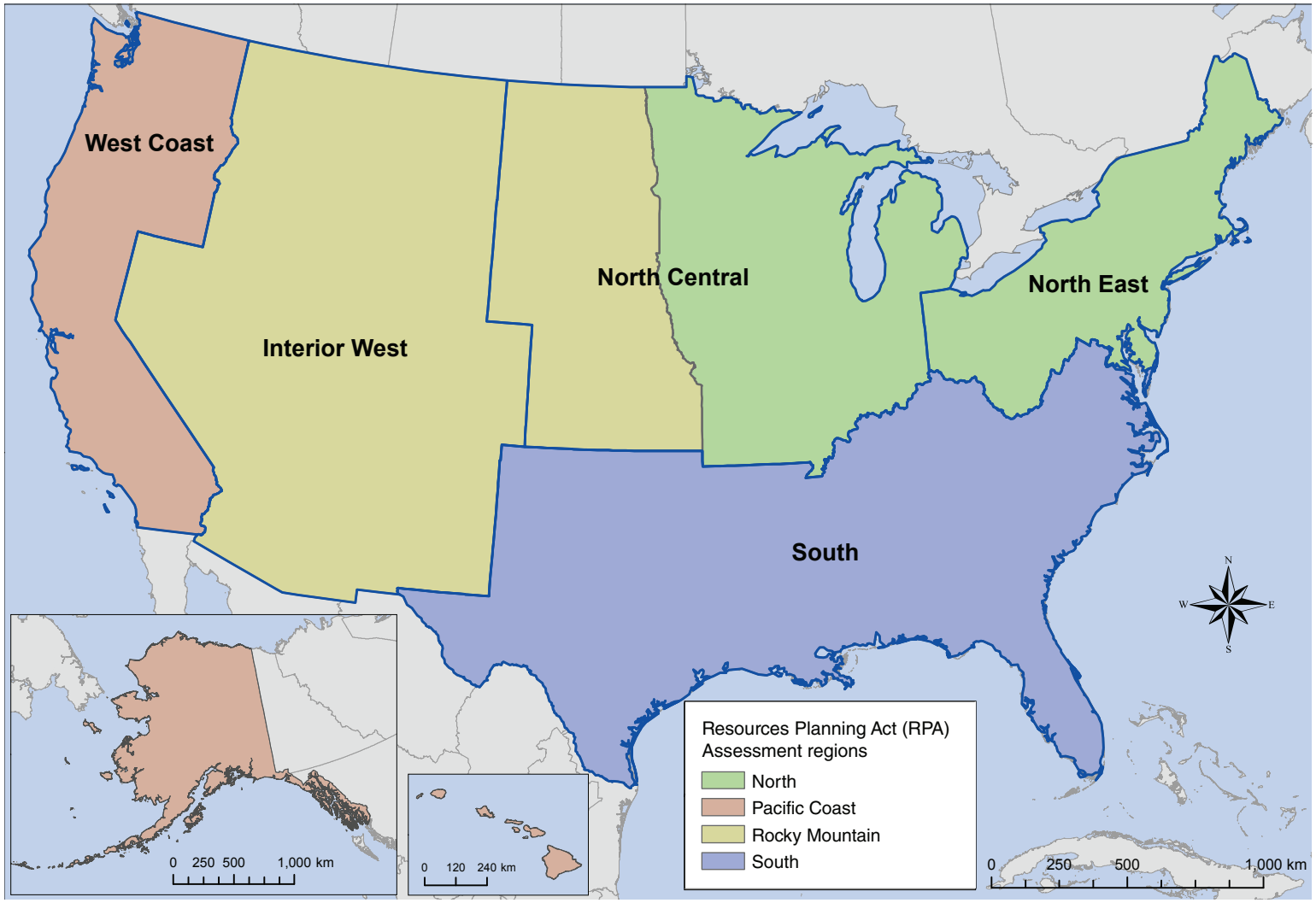

Figure 6.1—Comparison of the Forest Health Monitoring (FHM) and Resources Planning Act (RPA) Assessment regions. The blue lines delineate FHM regions, which are labeled on the map. The RPA Assessment regions are delineated by color, with labels in the legend. Alaska and Hawaii, which are part of the Pacific Coast RPA region, are not shown to scale with map of the conterminous United States.

METHODS

Data

Monitoring the occurrence of forest pest and pathogen activity at regional scales is important because understanding where it occurs, as well as the severity of associated damage, is important for decisions by land managers, including allocation of attention and response to the significant impact insects and diseases can have on forest health across landscapes, including on forest structure, composition, biodiversity, and species distributions (Castello and others 1995). Forest Health Protection national IDS data (FHP 2016, 2019) consist of information on forest disturbances and their causal agents recorded by trained aerial surveyors in low-altitude light aircraft as well as by ground observers. Geospatial IDS data are stored in the national IDS database. On average, the annual surveyed footprint area was 266 655 000 ha nationally for the period from 1999 (the first year that surveyed area was recorded nationally) to 2016, with a maximum of 320 712 000 ha in 2007 and a minimum of 225 928 000 ha in 2012 (fig. 6.2). Within regions, 93 475 000 ha were surveyed on average annually in the North RPA Assessment region, 59 470 000 in the South RPA region, 56 849 000 ha in the Rocky Mountain RPA region, and 55 425 000 ha in the Pacific Coast RPA region. Alaska and Hawaii are a part of the Pacific Coast region, with 14 259 000 ha

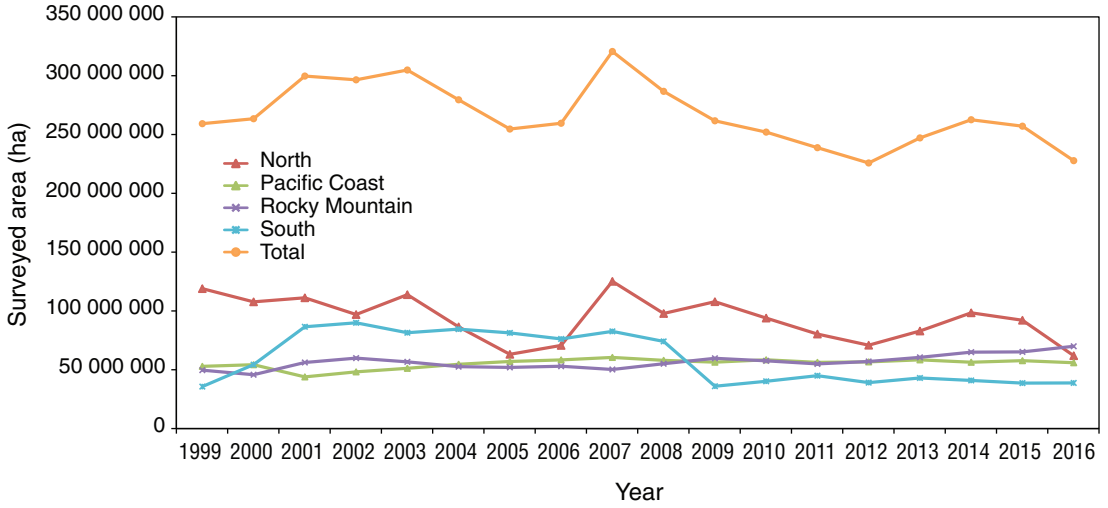

Figure 6.2—National Insect and Disease Survey (IDS) area surveyed by year, nationally and within four Resources Planning Act (RPA) Assessment regions.

surveyed on average each year in Alaska. In Hawaii, approximately 126 000 ha were surveyed in 2013 and 366 000 ha in 2015.

The IDS data identify areas of mortality and defoliation caused by insect and disease activity. Because of the general insect and disease aerial sketch-mapping process (i.e., recording of digital polygons by a human interpreter aboard an aircraft), all quantities are approximate "footprint" areas for each agent, delineating areas of visible damage within which the agent or complex is present. Unaffected trees may exist within the footprint, and the amount of damage within the footprint is not consistently reflected in the estimates of forest area affected. Depending on the level of damage to the forest in a given area and the convergence of other stress factors such as drought, a disease or insect might be considered a mortality-causing agent in one location and a defoliation-causing agent in another. Differences in data collection, attribute recognition, and coding procedures may exist among States and regions.

It is additionally important to note that some important forest insects are not easily detected nor thoroughly quantified through aerial detection surveys because they affect hosts that are widely dispersed throughout highly diverse forests or cause damage that is otherwise hard to detect. These pests include such insects as emerald ash borer (*Agrilus planipennis*) and hemlock woolly adelgid (*Adelges tsugae*), and such diseases as laurel wilt (*Raffaelea lauricola*), Dutch elm disease (*Ophiostoma novo-ulmi*), white pine blister rust (*Cronartium ribicola*), and thousand cankers disease (*Geosmithia morbida*), as well as mortality complexes (such as oak decline). At times, surveyors have drawn large polygons to encompass large or relatively large areas affected by dispersed insect or disease agents across diverse forested landscapes.

Recent years have seen a transition in how the IDS data are collected. Beginning in 2015, surveyors began to switch from the Digital Aerial Sketch Mapping (DASM) approach to the Digital Mobile Sketch Mapping (DMSM) approach (Berryman and McMahan 2019). This transition was complete for the 2018 survey season. The new DMSM approach allows surveyors to both define the extent of an area experiencing damage and to estimate percent range of the area within the polygon that is affected (1–3 percent, 4–10 percent, 11–29 percent, 30–50 percent, and >50 percent). With DMSM, it is therefore possible to generate an adjusted estimate of the area affected by each mortality or defoliation agent detection by multiplying the area of damage within each polygon (after masking by tree canopy cover) by the midpoint of the estimated range of percent affected (Berryman and McMahan 2019). To be consistent with the damage data collected throughout the 1997–2016 analysis window using the older DASM approach, however, DMSM data from 2015 and 2016 were treated as footprints of areas exposed to mortality or defoliation damage. Additionally, the DMSM data collection framework includes both polygon geometry, used for damage areas where boundaries are discrete and obvious from the air,

and point geometry, used for small clusters of damage where the size and shape of the damage are less important than recording the location of damage. For our analyses, points were assigned an area of 0.8 ha (about 2 acres). Finally, DMSM allows for the use of grid cells (of 240-, 480-, 960-, or 1920-m resolution) to estimate the percent of trees affected by damages that may be widespread and diffuse. When calculating the total areas affected by each damage agent, we used the entire areas of these grid cells (e.g., 240-m cell = 5.76 ha).

Analyses

To examine medium-term trends in insect and disease damage to the forests of the United States, we organized and analyzed 20 years of IDS data, then produced an assessment of trends in forest area exposed to insects and disease in multiple timeframes and within the four RPA Assessment regions (fig. 6.1). This was done annually, in four 5-year time windows (1997–2001, 2002–2006, 2007–2011, and 2012–2016), and in two 10-year windows (1997–2006, 2007–2016). We chose 1997–2016 as the analysis period because it offered a 20-year window of time that was convenient for analysis and generally avoided complications associated with the switch from the DASM to the DMSM damage data collection framework.

Using ArcMap® (ESRI 2015), we assembled spatial data from the IDS database separately for mortality and for defoliation damage annually for each of the years from 1997 to 2016. For mortality, we further sorted the damage data into those attributed to insects versus those caused by diseases, those within each of three insect guilds, and those that were the result of infestation by nonnative invasive species and those that were not. Nonnative invasive species are defined as those with origins outside the United States. The insect agent guild assignments (foliage feeders, phloem- or wood-borers [hereafter referred to as "bark beetles"], and sap feeders) were based on Liebhold and others (2013). For defoliation, we sorted the damage data into those attributed to insects and those associated with diseases, and into those caused by nonnative invasive species and those that were not. The IDS database includes reports of general tree species declines (e.g., "oak decline" or "yellow-cedar decline"), but we did not include those in this set of analyses because the causes of declines are generally uncertain or complex and can be at least in part the result of abiotic factors. The IDS data additionally include some agents called "multi-agent complexes" because they include both a disease agent and one or more insect vectors (such as "beech bark disease complex" and "root disease and beetle complex" [formerly "subalpine fir mortality complex"]). For our purposes, we classified these as diseases. Finally, the IDS damage codes were revised in 2015 (and first used in the field the following year) to include new agents, reclassify agents into appropriate categories, and correct agent names. We adjusted our classifications of the data from before 2016 to reflect these changes.

We derived spatial footprints for each combination of damage type and group of agents for each year by dissolving the relevant damage polygons in ArcMap® (ESRI 2015). We next merged the dissolved data within temporal windows (5-year: 1997–2001, 2002–2006, 2007–2011, and 2012–2016, and 10-year: 1997–2006, 2007–2016) and dissolved the datasets again. Finally, we intersected these datasets with tree canopy data for the conterminous States and Hawaii and with forest and shrubland cover for Alaska. The tree canopy data were resampled to 240 m from a 30-m raster dataset that estimates percent tree canopy cover (from 0 to 100 percent) for each grid cell; this dataset was generated from the 2011 National Land Cover Database (NLCD) (Homer and others 2015) through a cooperative project between the Multi-Resolution Land Characteristics Consortium and the Forest Service Geospatial Technology and Applications Center (Coulston and others 2012). We treated any cell with >0 percent tree canopy cover as forest. Comparable tree canopy cover data were not available for Alaska, so we instead created a 240-m-resolution layer of forest and shrub cover from the 2011 NLCD. The data also were intersected with the RPA Assessment regions (fig. 6.1) to allow for broad regional comparisons.

RESULTS AND DISCUSSION

Mortality

Our analyses focused on determining the footprint of treed area affected by insect and disease agents within four 5-year and two 10-year increments based on IDS detections of agents of tree mortality and defoliation. We elected to report only the 5-year results here because of their higher temporal resolution. Across all insect and disease agents nationally, the treed area exposed to mortality-causing agents was relatively low, about 3.1 million ha, for the first 5-year period (1997–2001), followed by a dramatic increase to 14.2 million ha for the next period (2002–2006) and a subsequent decline over the last two intervals (9.9 million ha for 2007–2011 and 6.9 million ha for 2012–2016) (fig. 6.3A, table 6.1).

The peak for 2002–2006 is explained in part by the large polygons used to delineate diffuse emerald ash borer mortality in Michigan in 2004, 2005, and 2006 and balsam woolly adelgid (*Adelges piceae*) mortality in the balsam fir (*Abies balsamea*) forests of Maine in 2006 (Potter and Koch 2012). This is additionally reflected in the regional mortality footprint for the North region (fig. 6.4, table 6.1). Other than the 2002–2006 period, mortality was relatively low in the North, as it was in the South. The mortality footprints in both the Rocky Mountain and Pacific Coast regions were comparatively large, with the peak for the Rocky Mountain region occurring in the 2007–2011 interval, reflecting the particularly high impacts of bark beetles, especially mountain pine beetle (*Dendroctonus ponderosae*) during 2008, 2009, and 2010 (Potter 2012, 2013; Potter and Paschke 2013). Meanwhile, the Pacific Coast region had dual peaks during the 2002–2006 and 2012–2016 periods. Fir engraver (*Scolytus ventralis*) and western pine beetle (*Dendroctonus brevicomis*)

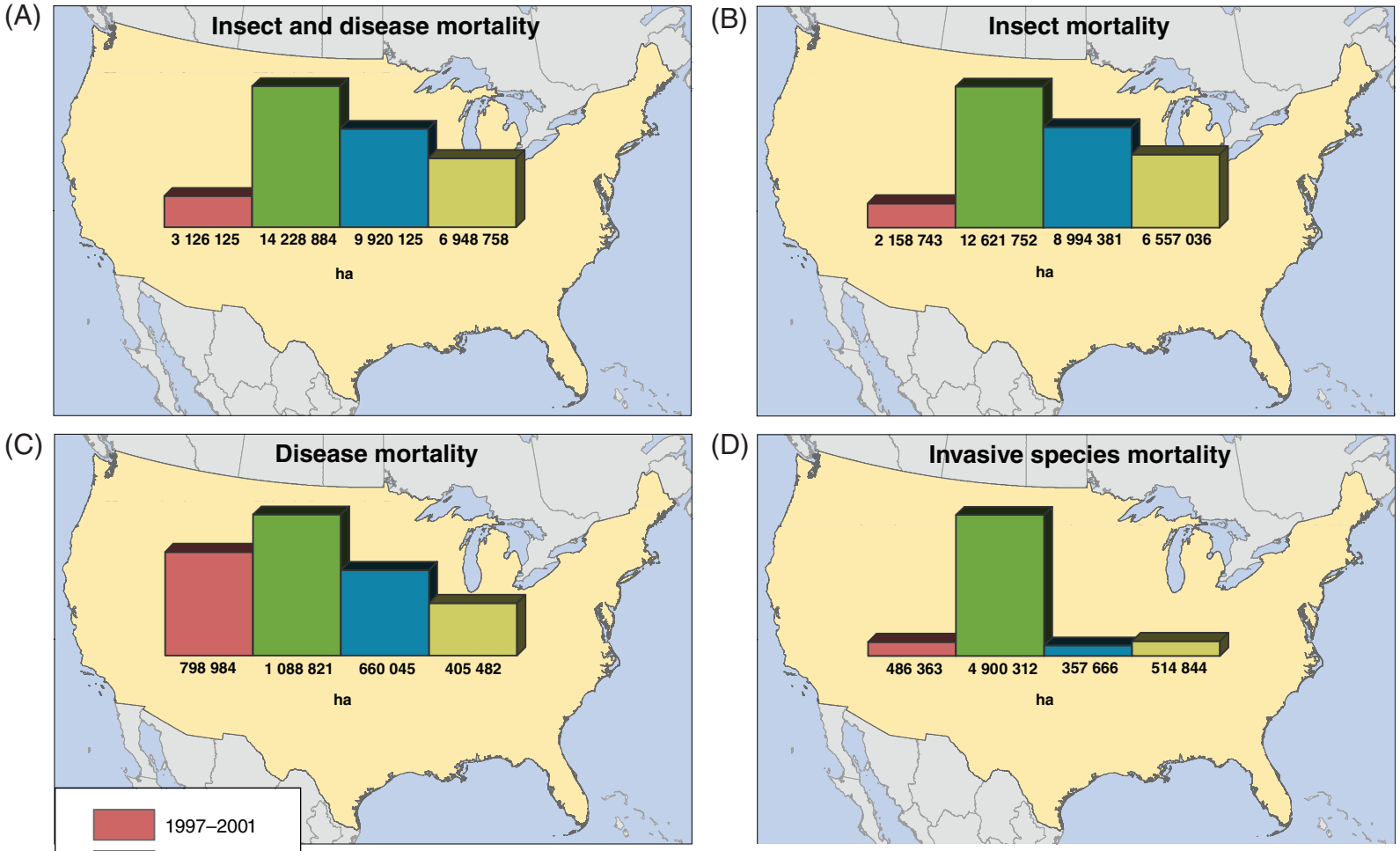

Figure 6.3—U.S. area of mortality, in hectares, from national Insect and Disease Survey (IDS) data in 5-year intervals for (A) all insect and disease agents, (B) insect agents, (C) disease agents, and (D) nonnative invasive agents. The IDS data were dissolved within the 5-year intervals to create footprints of affected areas, which were then masked by tree canopy data for the conterminous States and Hawaii and with forest and shrubland cover for Alaska. (Alaska and Hawaii are included in the Pacific Coast region.) Note differences in the scales of the results among the different groups of agents.

Table 6.1—Mortality attributed to three different insect guilds and to diseases from national Insect and Disease Survey (IDS) data, within four Resources Planning Act (RPA) assessment regions and in 5-year intervals

		Area of mortality				
		RPA Region				
Agent	Years	North	Pacific Coast	Rocky Mountain	South	Total area of mortality
		ha				*ha*
Bark beetles	1997–2001	279	883 943	1 098 548	63 829	2 046 598
	2002–2006	1 824 430	2 263 292	4 522 989	69 796	8 680 507
	2007–2011	330 115	2 056 066	6 192 061	8635	8 586 878
	2012–2016	359 719	3 479 449	2 569 319	14 167	6 422 653
Foliage feeders	1997–2001	2914	14 582	22	0	17 517
	2002–2006	65 491	9200	32	75 876	150 599
	2007–2011	220 752	2120	0	10 251	233 122
	2012–2016	28 129	0	63	0	28 192
Sap feeders	1997–2001	485	3718	38 611	0	42 814
	2002–2006	2 627 102	3883	18 446	6395	2 655 826
	2007–2011	11 574	32 114	4711	11 908	60 307
	2012–2016	28 676	14 106	31 139	1795	75 717
Diseases	1997–2001	348 374	9520	440 394	697	798 984
	2002–2006	256 689	18 406	811 649	2077	1 088 821
	2007–2011	111 175	31 947	516 922	2	660 045
	2012–2016	74 212	96 171	234 723	376	405 482
Total	1997–2001	416 860	976 172	1 667 836	65 257	3 126 125
	2002–2006	4 807 773	3 579 073	5 687 672	154 366	14 228 884
	2007–2011	705 573	2 241 977	6 941 753	30 822	9 920 125
	2012–2016	510 420	3 608 089	2 806 249	24 001	6 948 758

Note: All values are "footprint" areas masked by treed canopy area. The sum of different types of agents may not equal the total within regions for a reporting period because of overlapping polygons of different types of damage.

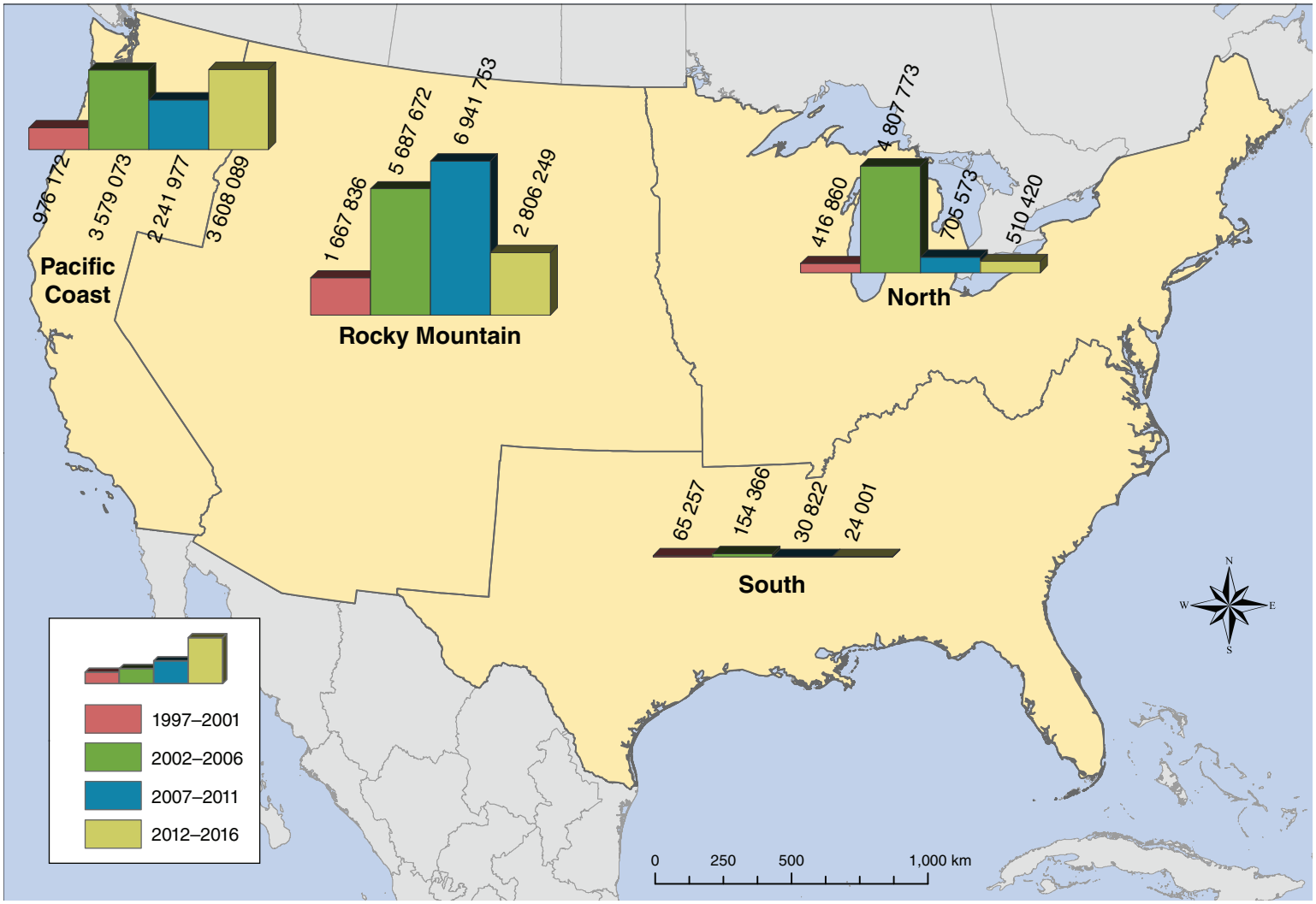

Figure 6.4—Area of mortality, in hectares, attributed to both insect and disease agents from national Insect and Disease Survey (IDS) data, within four Resources Planning Act (RPA) Assessment regions and in 5-year intervals. The IDS data were dissolved within the 5-year intervals to create footprints of affected areas, which were then masked by tree canopy data for the conterminous States and Hawaii and with forest and shrubland cover for Alaska. (Alaska and Hawaii are included in the Pacific Coast region.)

were particularly damaging in 2015 and 2016, leading to the latter peak (Potter and Paschke 2017, Potter and others 2018). Bark beetles also were the main contributors to the earlier peak (Coulston 2007, 2009). Because the large majority of all mortality was caused by insects (between 69 and 94 percent across the four 5-year periods nationally, with similar regional percentages), the 5-year footprints of insect mortality were similar to the footprints across all agents, both nationally (fig. 6.3B) and regionally (fig. 6.5). The 2002–2006 timeframe represented the peak of insect-caused mortality nationally, with mortality recorded on approximately 12.6 million ha of treed area.

As with insect-related mortality, the tree canopy area exposed to disease-caused mortality also was highest during the 2002–2006 period with approximately 1.1 million ha (fig. 6.3C), though this was <8 percent of the total area of recorded mortality during this timeframe. Much of the disease mortality was associated with subalpine fir (*Abies lasiocarpa*) mortality complex, which was used to document mortality caused by the interaction of root diseases (primarily those caused by *Armillaria* spp.) and infestation by western balsam bark beetle (*Dryocoetes confusus*) in spruce/fir forest types.[1] This resulted in the Rocky Mountain region having the greatest area of mortality attributed to disease agents in each of the 5-year periods, with the maximum in 2002–2006 (fig. 6.6). During that timeframe, oak wilt (*Ceratocystis fagacearum*) was a widespread issue repeatedly in the North and during 2005 in the South, while large areas of beech bark disease infestations were identified in 2002 and 2003 in the North. Nationally, disease mortality increased from about 800 000 ha in 1997–2001 to the 1.1 million-ha peak in 2002–2006, which was then followed by declines over the next two reporting periods, to about 660 000 ha in 2007–2011 to 400 000 ha in 2012–2016. This was also the pattern in the Rocky Mountain region, but the Pacific Coast region saw a modest increasing trend over time while the North had a steady decline (fig. 6.6). For the Pacific Coast region, this is attributable to the combination of an increase in sudden oak death mortality of tanoak (*Notholithocarpus densiflorus*) in northern California and southwestern Oregon caused by the pathogen *Phytophthora ramorum*, and the 2015 and 2016 detection in Hawaii of rapid ʻōhiʻa death (Potter and Paschke 2015a, 2015b, 2016, 2017; Potter and others 2018). Rapid ʻōhiʻa death, a wilt disease caused by the fungal pathogens *Ceratocystis lukuohia* and *C. huliohia* (Barnes and others 2018), affects ʻōhiʻa lehua (*Metrosideros polymorpha*), a highly ecologically and culturally important tree in Hawaiian native forests (University of Hawaiʻi 2019). For the North, meanwhile, detections of beech bark disease, which is the primary disease mortality agent in the region, has declined in recent years. Meanwhile, very little disease mortality was reported in the South during any of the reporting intervals.

[1] In 2015, the "subalpine fir mortality complex" aerial survey damage agent code was retired and replaced with "root disease and beetle complex." It was primarily used in Forest Service Region 2.

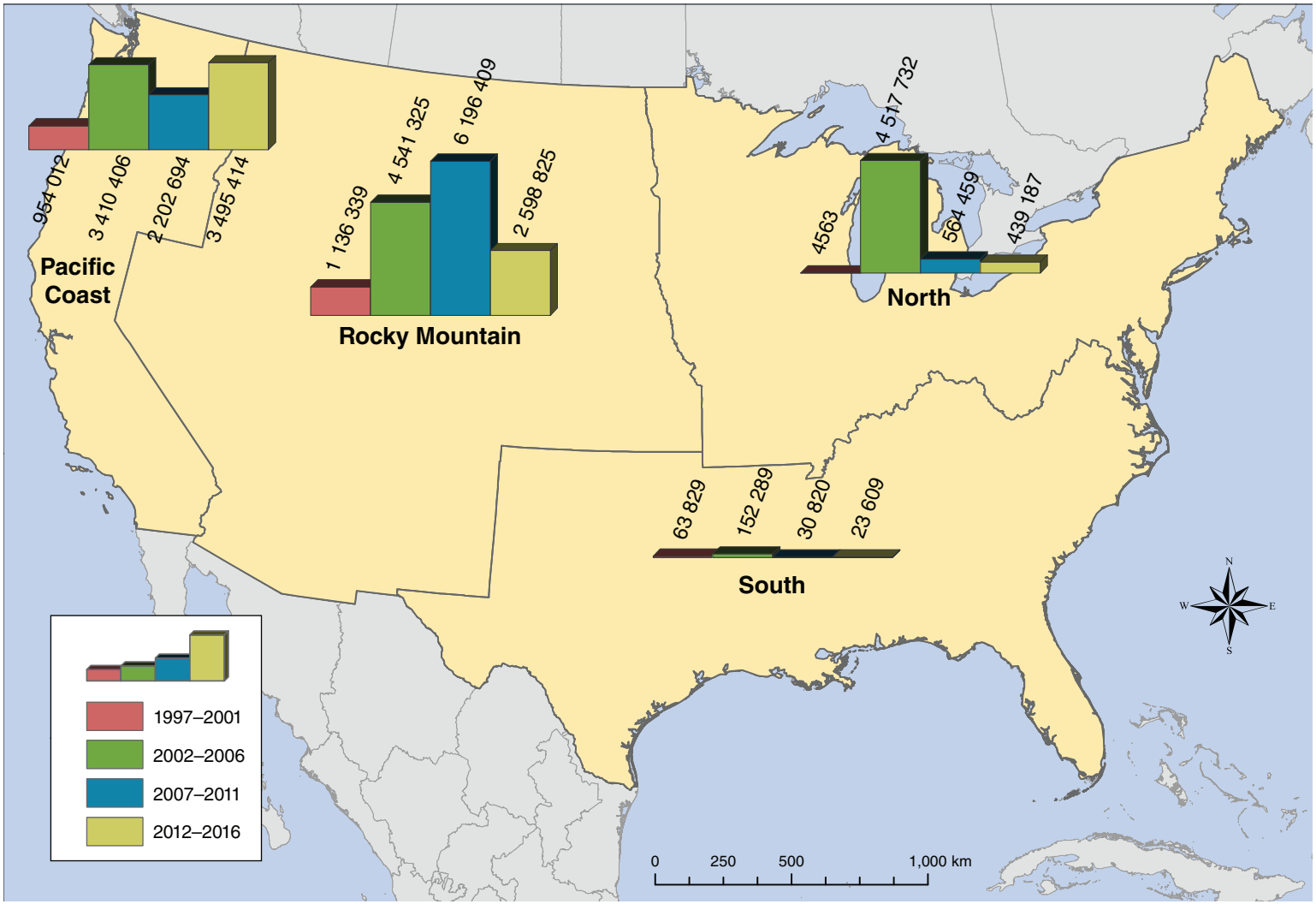

Figure 6.5—Area of mortality, in hectares, attributed to insect agents from national Insect and Disease Survey (IDS) data, within four Resources Planning Act (RPA) Assessment regions and in 5-year intervals. The IDS data were dissolved within the 5-year intervals to create footprints of affected areas, which were then masked by tree canopy data for the conterminous States and Hawaii and with forest and shrubland cover for Alaska. (Alaska and Hawaii are included in the Pacific Coast region.)

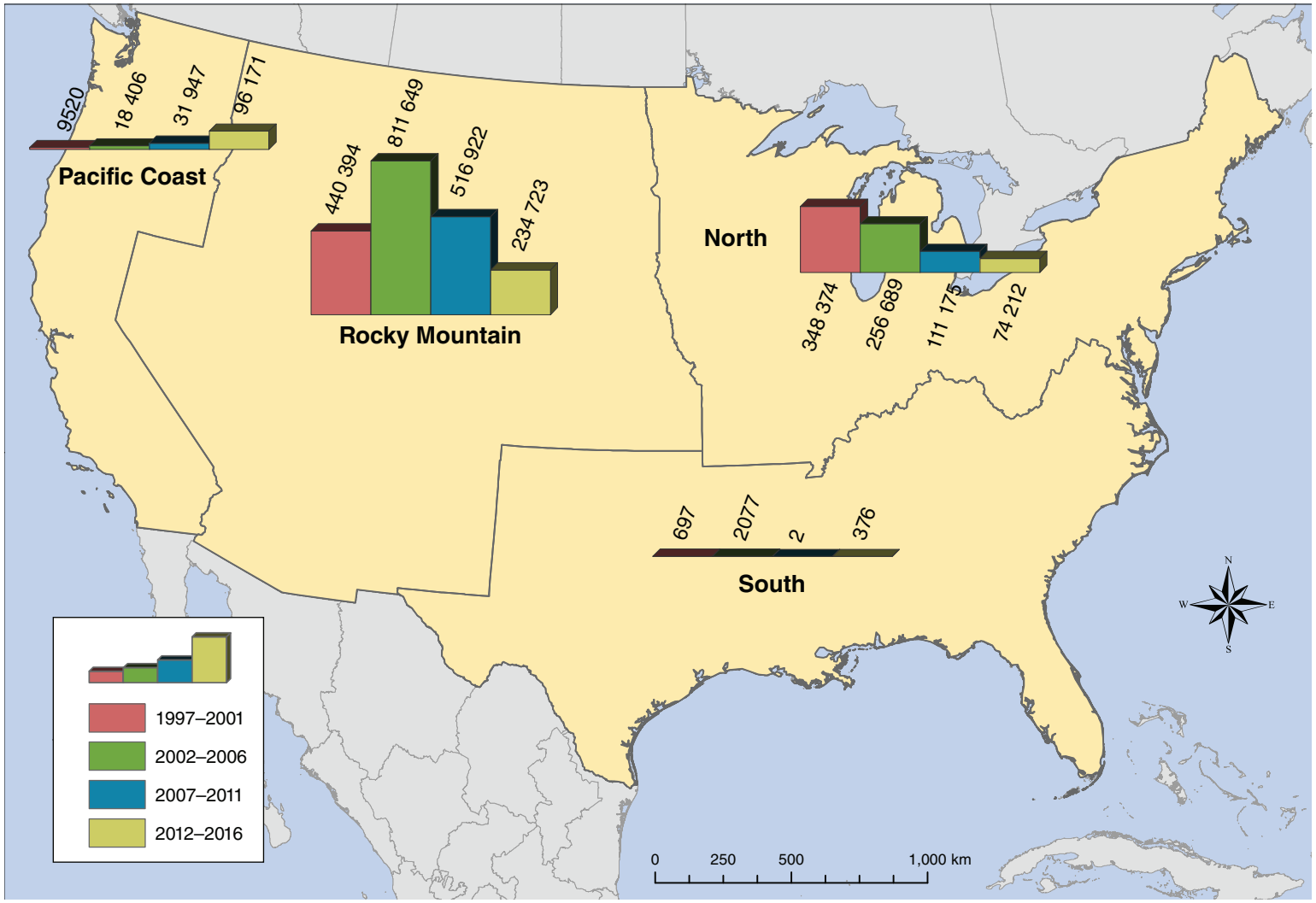

Figure 6.6—Area of mortality, in hectares, attributed to disease agents from national Insect and Disease Survey (IDS) data, within four Resources Planning Act (RPA) Assessment regions and in 5-year intervals. The IDS data were dissolved within the 5-year intervals to create footprints of affected areas, which were then masked by tree canopy data for the conterminous States and Hawaii and with forest and shrubland cover for Alaska. (Alaska and Hawaii are included in the Pacific Coast region.)

The amount of treed area exposed to nonnative invasive mortality agents nationally was generally about half a million ha during the 5-year reporting periods, with the exception of 2002–2006 (fig. 6.3D). As noted above, surveyors delineated large polygons of diffuse mortality associated with balsam woolly adelgid in Maine in 2006 and with emerald ash borer in Michigan in 2004, 2005, and 2006. Both of these are nonnative invasive insects, so this resulted in a tenfold increase in the amount of detected forest mortality attributed to invasive species. Nationally, the proportion of the total mortality footprint associated with invasive insects and diseases decreased from 14.8 percent in 1997–2001 and 34.4 percent in 2002–2006 to 3.6 percent in 2007–2011 and 7.4 percent in 2012–2016. Among the RPA Assessment regions, only in the North was a large proportion of the 5-year mortality footprints consistently attributed to nonnative invasive agents (fig. 6.7). This ranged from 35.1 percent in 2007–2011 (when outbreaks of several native insects occurred) to 98.5 percent in 2002–2006. The suite of agents associated with this mortality has evolved over time in the North. In the first assessment period (1997–2001), the most commonly detected invasive agents were beech bark disease, European gypsy moth (*Lymantria dispar dispar*), oak wilt, and hemlock woolly adelgid. In the second and third assessment periods (2002–2006 and 2007–2011), these agents were joined by balsam woolly adelgid, emerald ash borer, and Dutch elm disease, with emerald ash borer detected in an increasingly large number of States. This emerald ash borer trend continued for the final period (2012–2016), and a single new invasive agent, red pine scale (*Matsucoccus resinosae*), was detected. In the South, relatively small areas and percentages of invasive agents (specifically, hemlock woolly adelgid and oak wilt) were detected during the first two assessment periods (1.1 percent and 5.5 percent). These increased in the final two periods (71.8 percent and 21.9 percent) as hemlock woolly adelgid was more widely identified and as emerald ash borer was included in the aerial survey data for the first time in 2016. Invasive agents were the cause of only a very small proportion of the mortality footprint area in the two western regions (between 0.3 percent and 7.2 percent in the Rocky Mountain region and between 0.7 percent and 3.0 percent in the Pacific Coast region). In the Rocky Mountains, either balsam woolly adelgid or white pine blister rust was detected every year, with both found in some years. In the Pacific Coast region, meanwhile, Port-Orford-cedar root disease (*Phytophthora lateralis*) was detected every year, and sudden oak death was found annually beginning in 2008. Mortality attributed to balsam woolly adelgid was also found in most years, and rapid ʻōhiʻa death was detected in Hawaii in 2015 and 2016.

When comparing the relative importance of agents categorized in one of three insect feeding guilds (foliage feeders, bark beetles, and sap feeders) or as diseases, bark beetles nationally encompassed the largest area (table 6.1) and proportion of treed mortality area during each of the four assessment periods: 65.5 percent

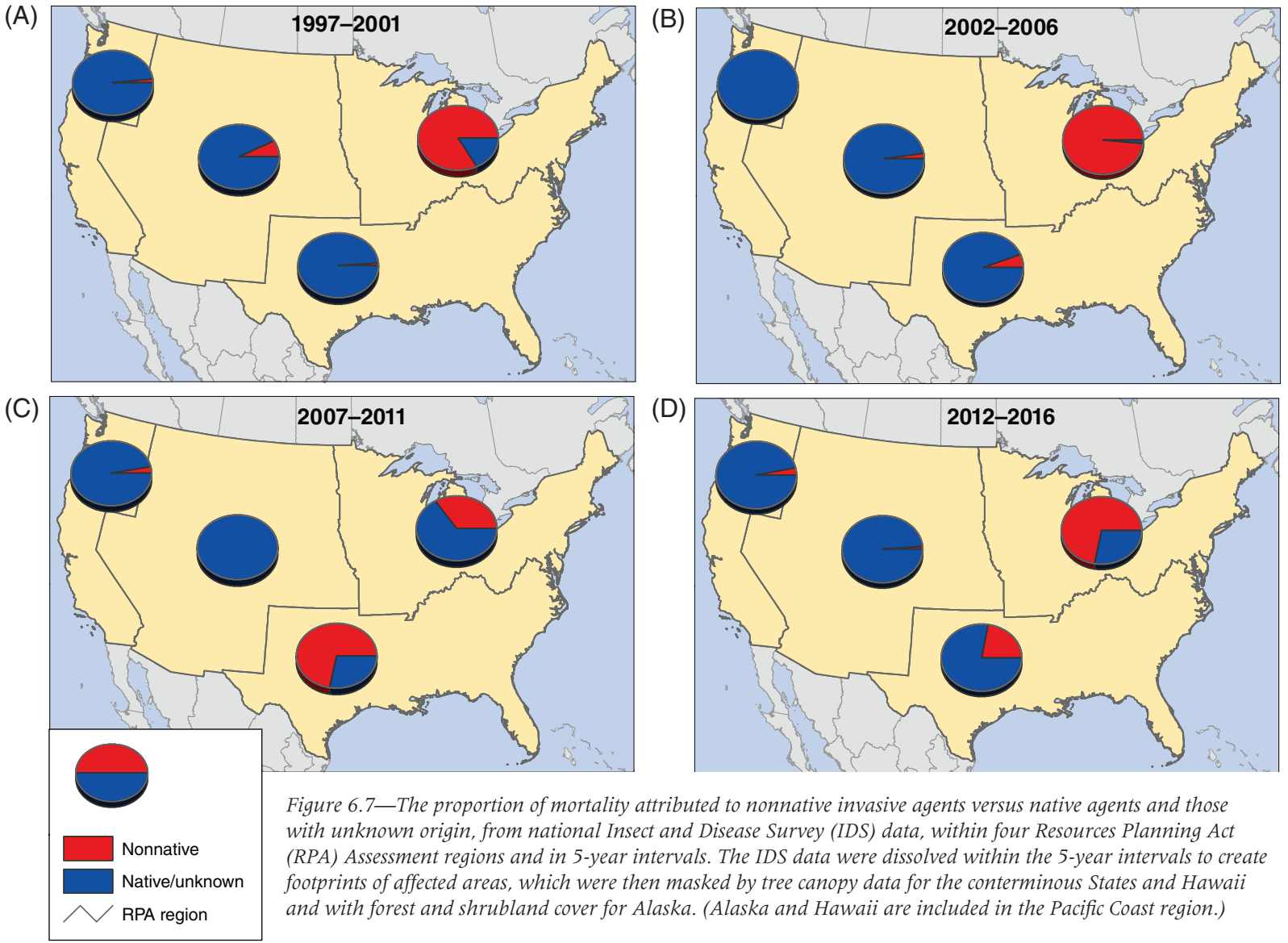

Figure 6.7—The proportion of mortality attributed to nonnative invasive agents versus native agents and those with unknown origin, from national Insect and Disease Survey (IDS) data, within four Resources Planning Act (RPA) Assessment regions and in 5-year intervals. The IDS data were dissolved within the 5-year intervals to create footprints of affected areas, which were then masked by tree canopy data for the conterminous States and Hawaii and with forest and shrubland cover for Alaska. (Alaska and Hawaii are included in the Pacific Coast region.)

for 1997–2001, 61.0 percent for 2002–2006, 86.6 percent for 2007–2011, and 92.4 percent for 2012–2016. The only period during which another guild accounted for >10 percent of the treed mortality area was 2002–2006, which included the large polygons of diffuse mortality associated with balsam woolly adelgid, a sap feeder. Sap feeders represented 18.7 percent of detected mortality area that period. Otherwise, sap feeders and foliage feeders accounted for a very small amount of mortality. During most intervals, diseases were the second most widely detected nationally (5.8 to 25.6 percent).

In the two western regions (Pacific Coast and Rocky Mountain), bark beetles make up the large majority of mortality detected in all the 5-year intervals (fig. 6.8, table 6.1). The proportion of mortality associated with diseases in the Rocky Mountain region was relatively high (7.4 percent to 26.4 percent), attributed to subalpine fir mortality complex and, to a lesser degree, white pine blister rust. Bark beetles also encompassed an increasingly large proportion of the mortality in the North over time, reflecting the increasing extent and impact of emerald ash borer and, to much lesser degree, of eastern larch beetle (*Dendroctonus simplex*). (Almost all of the mortality in the North during the first 5-year period was associated with disease, specifically beech bark disease, while the majority of the 2002–2006 mortality was associated with balsam woolly adelgid, a sap feeder.) Bark beetles were important in the South in the first and last assessment periods, and to a lesser degree in the second period, because of southern pine beetle (*Dendroctonus frontalis*) infestations. During 2007–2011, foliage feeders had a relatively large mortality footprint in the South because of a severe gypsy moth infestation in Virginia. Infestation of hemlock woolly adelgid in the Southern Appalachians resulted in a relatively large sap feeder footprint during that same timeframe as well as the following one (2012–2016).

It is worth noting that forest mortality (as well as defoliation) may be underrepresented in the South in these datasets. This is partly due to the heterogeneity of the landscape, more intense management cycles (particularly pine plantations), and higher growth and decay rates leading to more rapid forest recovery after disturbance and, ultimately, signatures that are less persistent and more difficult to detect during aerial surveys. For example, mortality from southern pine beetle is notably underrepresented during the 1997–2001 and 2002–2006 time periods, which coincided with the second largest outbreak of this insect since 1960 that culminated in almost 400 000 ha of damaged timber and over $1 billion in economic losses (Nowak and others 2008). The FHM program traditionally records southern pine beetle infestations as “spots” of activity, often before these spots expand and envelop larger areas. Furthermore, the availability of markets often leads to rapid response in the form of salvage clearcutting, thinning, and clearcutting ahead of an active spot to disrupt it from further expansion. Thus, ubiquitous management regimes across the South routinely limit

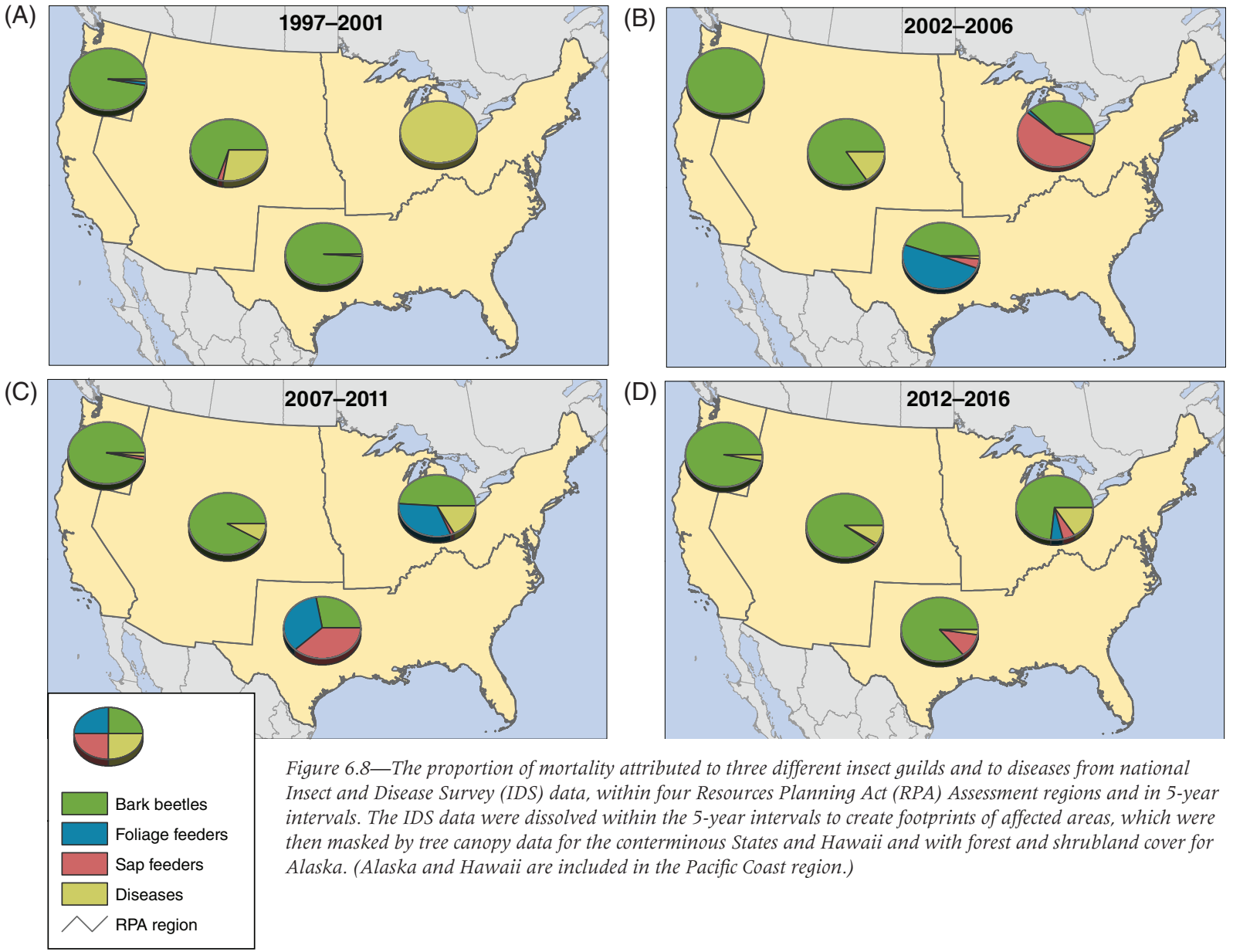

Figure 6.8—The proportion of mortality attributed to three different insect guilds and to diseases from national Insect and Disease Survey (IDS) data, within four Resources Planning Act (RPA) Assessment regions and in 5-year intervals. The IDS data were dissolved within the 5-year intervals to create footprints of affected areas, which were then masked by tree canopy data for the conterminous States and Hawaii and with forest and shrubland cover for Alaska. (Alaska and Hawaii are included in the Pacific Coast region.)

bark beetle mortality to small areas with short-lived disturbance signatures. Typically, the impact of bark beetles in the region is much larger than what is reflected in outright beetle-induced mortality because many more healthy trees end up being cut to disrupt the expansion of a spot infestation or as part of salvage sales.

Defoliation

In addition to mortality, the IDS data include the spatial extent and putative causal agents of forest defoliation. The area affected by defoliation in most 5-year windows exceeded that affected by mortality and was relatively consistent over time: 13.2 million ha in 1997–2001, 11.0 million ha in 2002–2006, 9.7 million ha in 2007–2011, and 11.4 million ha in 2012–2016 (fig. 6.9A).

Regionally, the North experienced the most defoliation for the first two timeframes, but the defoliation footprint there declined across assessment periods while the area of defoliation grew in the Rocky Mountains in the final two assessment windows (fig. 6.10). The earlier defoliation in the North was attributed to a variety of agents, the most commonly detected of which included forest tent caterpillar (*Malacosoma disstria*), mostly in quaking aspen (*Populus tremuloides*) stands in the Great Lakes States and later in New England hardwood stands; gypsy moth in oak (*Quercus* spp.) and other hardwood stands in the Northeast; spruce budworm (*Choristoneura fumiferana*) in white spruce (*Picea glauca*) and balsam fir forests in Great Lakes States; large aspen tortrix (*Choristoneura conflictana*) in Great Lakes States; and jack pine budworm (*Choristoneura pinus*) in jack pine (*Pinus banksiana*) and fir stands in Michigan. Defoliation area during the first assessment periods was inflated somewhat by large polygons of diffuse defoliation, including forest tent caterpillar in northern Wisconsin, northern Minnesota, and the Upper Peninsula of Michigan, and locust leafminer (*Odontota dorsalis*) in southern Indiana in 2001. In the later assessment periods, gypsy moth was often a widely detected agent in the Northeast, along with a suite of other defoliators that included forest tent caterpillar, winter moth (*Operophtera brumata*), fall cankerworm (*Alsophila pometaria*), and oak leafroller (*Archips semiferana*), while spruce budworm and forest tent caterpillar were often widely detected in the Great Lakes States, along with jack pine budworm, large aspen tortrix, and several other agents.

In the Rocky Mountains, meanwhile, the large majority of defoliation has been caused by western spruce budworm, with particularly large outbreaks in recent years (Potter and Paschke 2015a, 2015b, 2016, 2017; Potter and others 2018). During the earlier assessment periods, these outbreaks were only identified in the southern Rockies, but they began also to be detected in the northern Rockies beginning in 2002 and 2003, becoming more widespread there in later assessment periods while continuing in the southern Rockies. In the South, the area on which defoliation was recorded was relatively small for the first three 5-year periods but increased by >400 percent in the final period relative to the average for the previous windows (fig. 6.10). This was the result of large polygons of diffuse fall cankerworm defoliation in eastern Virginia in 2012 and 2013 and of yellow poplar

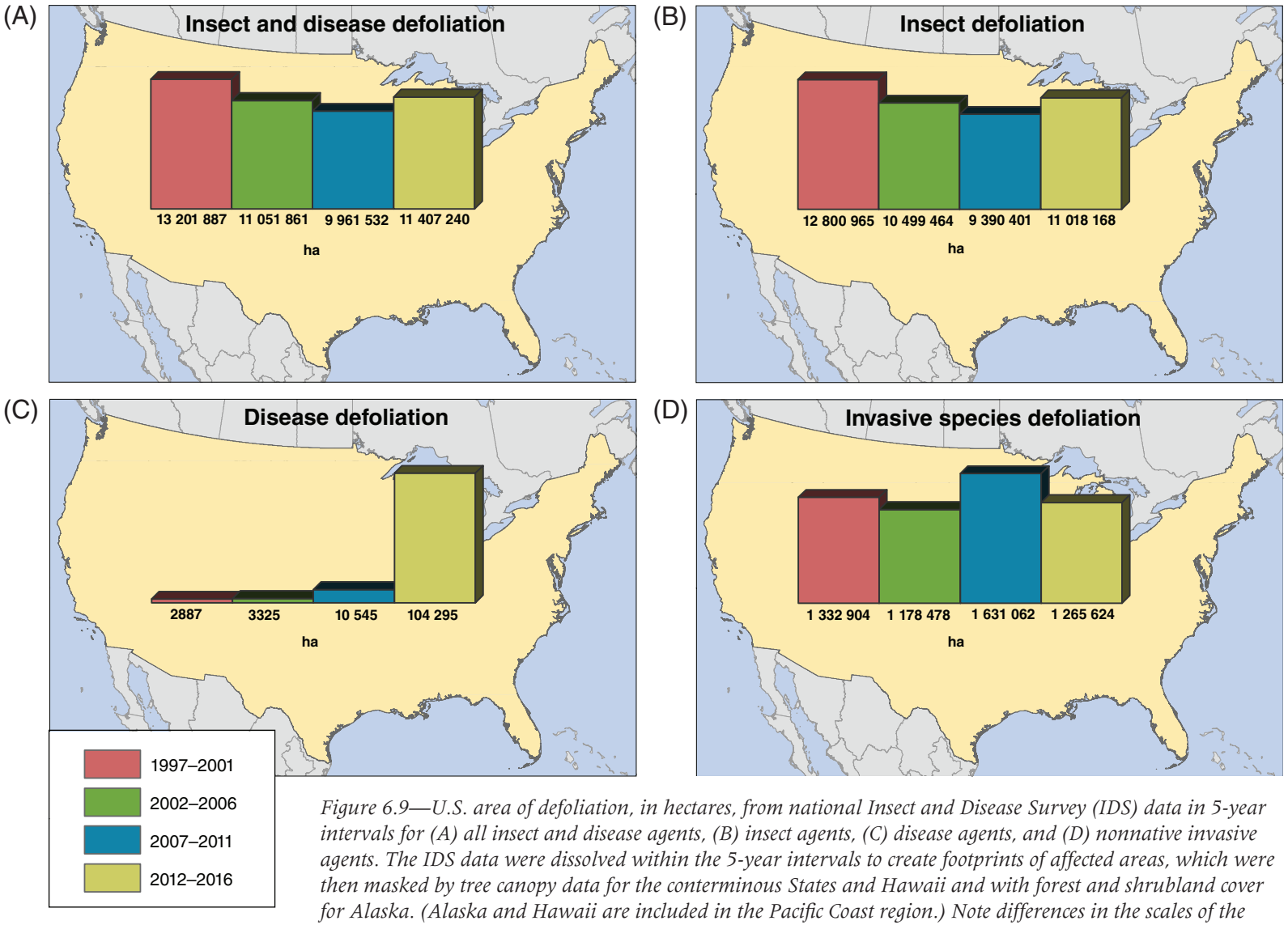

Figure 6.9—U.S. area of defoliation, in hectares, from national Insect and Disease Survey (IDS) data in 5-year intervals for (A) all insect and disease agents, (B) insect agents, (C) disease agents, and (D) nonnative invasive agents. The IDS data were dissolved within the 5-year intervals to create footprints of affected areas, which were then masked by tree canopy data for the conterminous States and Hawaii and with forest and shrubland cover for Alaska. (Alaska and Hawaii are included in the Pacific Coast region.) Note differences in the scales of the results among the different groups of agents.

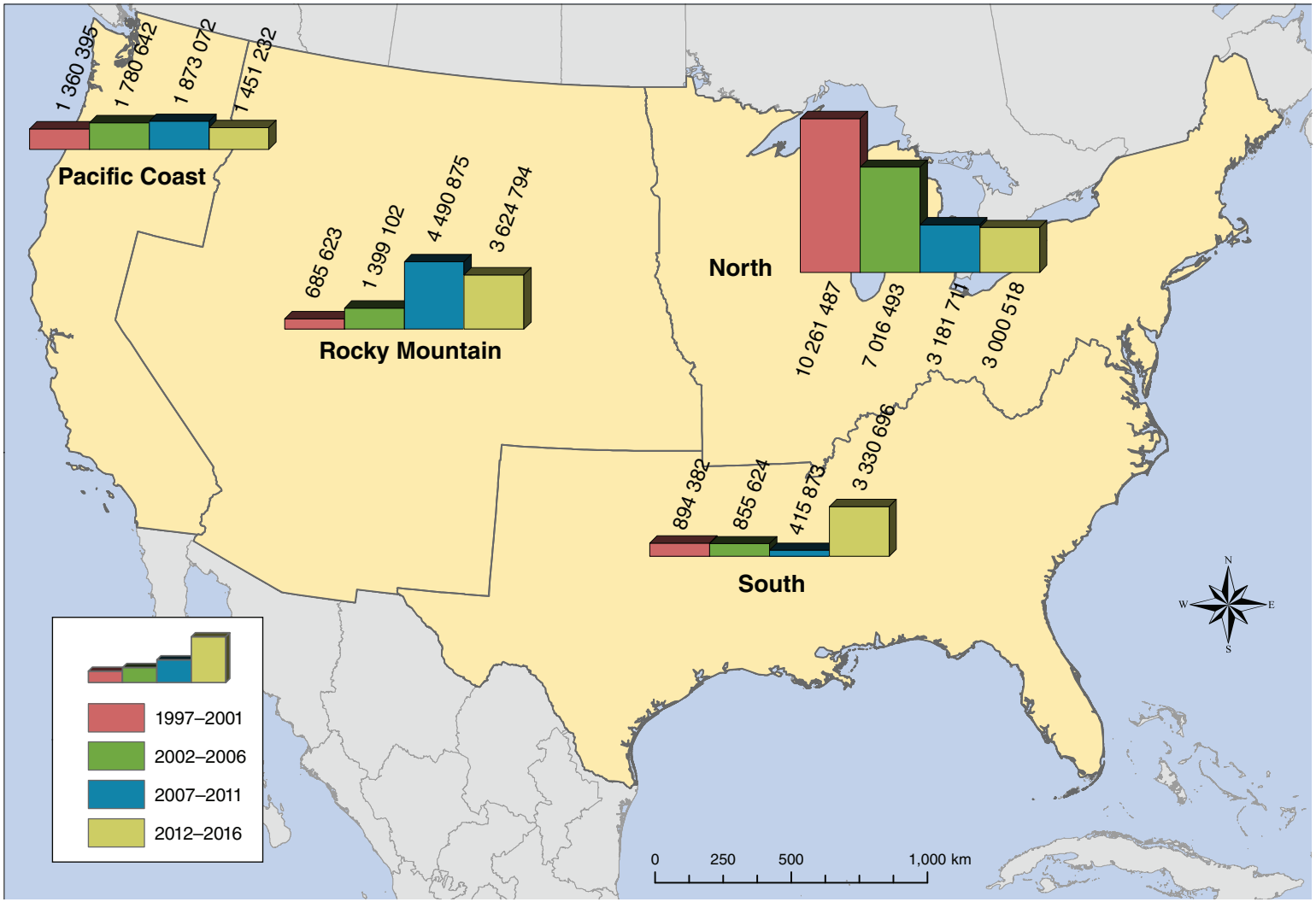

Figure 6.10—Area of defoliation, in hectares, attributed to both insect and disease causes from national Insect and Disease Survey (IDS) data, within four Resources Planning Act (RPA) Assessment regions and in 5-year intervals. The IDS data were dissolved within the 5-year intervals to create footprints of affected areas, which were then masked by tree canopy data for the conterminous States and Hawaii and with forest and shrubland cover for Alaska. (Alaska and Hawaii are included in the Pacific Coast region.)

weevil (*Odontopus calceatus*) in western North Carolina in 2015. Across the 20 years of IDS data, forest tent caterpillar was consistently widely recorded across large areas of the South, particularly in Louisiana and South Carolina. Leafrollers (baldcypress leafrollers [*Archips goyerana*] after 2004 and fruittree leafrollers [*Archips argyrospila*] before that) were consistently detected in Louisiana baldcypress (*Taxodium distichum*) stands. Gypsy moth was regularly recorded in hardwood forests of Virginia from 2001 to 2009.

Finally, a moderate level of defoliation was recorded consistently in the Pacific Coast region across the four 5-year timeframes. In most years, the majority of the defoliation in the region was detected in Alaska. This defoliation was attributed to a variety of causal agents, with aspen leafminer (*Phyllocnistis populiella*) the agent most widely detected in many years. Other common defoliators included willow leaf blotchminer (*Micrurapteryx salicifoliella*) in willows, larch sawfly (*Pristiphora erichsonii*) in western larch (*Larix occidentalis*), and spruce aphid (*Elatobium abietinum*) in Sitka spruce (*Picea sitchensis*). Meanwhile, in the three conterminous States included in the Pacific Coast region, defoliation by western spruce budworm was commonly delineated in Washington State, with especially large infestations in 2011 and 2012. Swiss needlecast (caused by the pathogen *Phaeocryptopus gaeumannii*) was an issue for Douglas-fir (*Pseudotsuga menziesii*) in both Oregon and Washington during early years of IDS data collection, while larch casebearer (*Coleophora laricella*) was often detected in Oregon. A very extensive outbreak of pine butterfly (*Neophasia menapia*) occurred in ponderosa pine (*Pinus ponderosa*) stands in eastern Oregon in 2011 and, to a lesser degree, in 2012.

The large majority of defoliation nationally across the assessment periods was attributed to insects (fig. 6.9B) rather than diseases (fig. 6.9C). The amount of insect defoliation was consistent across time, while disease defoliation was mostly negligible until the 2012–2016 timeframe, when it increased tenfold from 2007–2011. The increase in the detection of disease defoliation occurred in three of the four RPA Assessment regions, with the exception of the South. In the North, this was the result of an infestation of white pine needle damage in 2016 along with an outbreak of anthracnose in 2013. Surveyors in recent years also detected Lophodermium needle cast (*Lophodermium* spp.) in Oregon and Washington ponderosa pine stands in the Pacific Coast region and Marssonina blight (*Drepanopeziza* spp.) in quaking aspen stands of the northern Rocky Mountain region. Meanwhile, regional patterns of insect defoliation (not shown) largely matched those of total defoliation (fig. 6.10).

The amount of defoliation attributable to nonnative invasive species was largely consistent across reporting periods, ranging between 1.2 million ha and 1.6 million ha (fig. 6.9D). Nationally, invasive agents accounted for 10.4 percent of defoliated area in 1997–2001, 11.2 percent in 2002–2006, 17.4 percent in 2007–2011, and 11.5 percent in 2012–2016. Invasive defoliating agents were more important in the

East than in the West, particularly in the North region, where invasive agents accounted for a greater share of defoliation in recent periods (48.1 percent and 42.9 percent) compared to the first two timeframes (11.2 percent and 15.7 percent) (fig. 6.11). Gypsy moth was a major invasive defoliating agent throughout much of the North in all four periods. Other important agents were winter moth in the Northeast, larch casebearer in tamarack (*Larix laricina*) stands of the Great Lakes States, birch leafminer (*Fenusa pusilla*) in New England, and balsam woolly adelgid in Maine (especially in 2002–2006). The South exhibited relatively high proportions of invasive defoliators for the first three timeframes (8.4 percent to 20.0 percent), mostly the result of gypsy moth detections in Virginia. A small percentage of defoliation in the Pacific Coast region (0.3 percent to 3.8 percent) was the result of invasive agents, specifically larch casebearer affecting western larch in Oregon and Washington, and birch leafminer in Alaska. Less than 1 percent of defoliation in the Rocky Mountain region was ever attributed to invasive agents.

CONCLUSIONS

Insects and diseases affect a variety of aspects of forest structure and function and can be considered either negative or positive depending on management objectives (Edmonds and others 2011). Generally, mortality by insects and diseases that exceeds baseline conditions is considered undesirable and unhealthy. Nearly all native tree species of the conterminous United States are affected by at least one harmful insect or disease agent, with invasive insects and diseases on average considerably more severe than native ones (with some important exceptions such as native bark beetles) (Potter and others 2019a) and most likely to negatively affect the genetic integrity of the host species they infest (Potter and others 2019b).

This chapter presents results from a national retrospective analysis of pest and pathogen detections using annual data from the FHP national IDS. Specifically, the project aims to evaluate trends in the extent, severity, and periodicity of major insect and disease threats, providing context for the annual FHM reports. Understanding these trends will allow for future analyses that focus on developing better attribution of tree mortality and volume loss to the corresponding threats, as well as generating future forest health impact projections. Incorporating these products into the national RPA Assessment will allow for analyses within a framework of social and economic trends and projections.

Key findings of this overview of 20 years of IDS data include:

- The tree canopy area affected by mortality agents has been consistently large across the three most recent 5-year assessment periods, with the most mortality reported in 2002–2006.

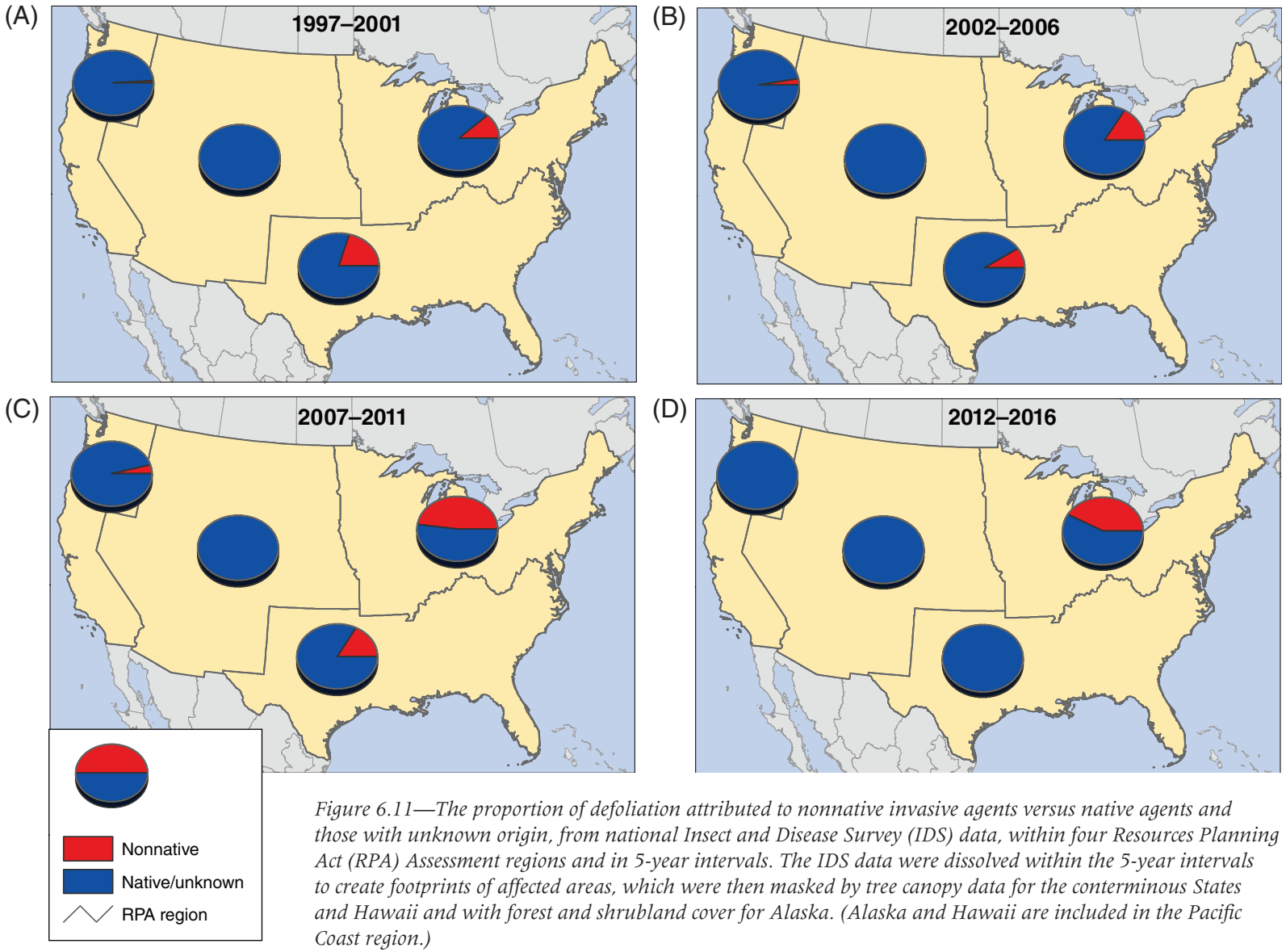

Figure 6.11—The proportion of defoliation attributed to nonnative invasive agents versus native agents and those with unknown origin, from national Insect and Disease Survey (IDS) data, within four Resources Planning Act (RPA) Assessment regions and in 5-year intervals. The IDS data were dissolved within the 5-year intervals to create footprints of affected areas, which were then masked by tree canopy data for the conterminous States and Hawaii and with forest and shrubland cover for Alaska. (Alaska and Hawaii are included in the Pacific Coast region.)

- The four RPA Assessment regions exhibit different temporal patterns of area exposed to mortality: the North had the most in 2002–2006, the Pacific Coast had mortality peaks in 2002–2006 and 2012–2016, the Rocky Mountains had the most mortality in 2007–2011 followed by 2002–2006, and the South had comparatively limited areas exposed to mortality.
- Insects have been much more widespread agents of mortality than diseases, with bark beetles consistently the most important mortality agents across regions and over time, especially in the West.
- The tree canopy area affected by defoliation agents has remained relatively consistent over time and has usually exceeded or equaled the area affected by mortality agents.
- Insects are much more important agents of defoliation, but disease defoliation increased markedly during the final 5-year assessment period.
- Nonnative invasive insects and diseases had a larger relative impact on forests in the North, through both mortality and defoliation, than elsewhere in the United States. At the same time, nonnative invasive agents are having significant impacts elsewhere as well, including Hawaii, where rapid ʻōhiʻa death is causing considerable mortality to one of the State's most ecologically and culturally important tree species.
- Nationally, the tree canopy area affected by invasive agents of mortality and defoliation has remained relatively consistent over time.
- The use of large polygons to encompass broad areas of diffuse damage complicates the interpretation of mortality and defoliation spatial data. Newer aerial survey protocols are likely to avoid these problems (Berryman and McMahan 2019), but appropriately incorporating these large polygons from earlier survey efforts may present a challenge.

By looking across different threats to forest health over time, this retrospective analysis addresses forest mortality and defoliation, as well as the impacts of invasive species. Evaluating trends in these threats at a national scale provides context to managers attempting to understand the implications and scope of current forest health threats. Future projections will provide managers with information to assist in land management planning and decision making.

LITERATURE CITED

Barnes, I.; Fourie, A.; Wingfield, M.J. [and others]. 2018. New *Ceratocystis* species associated with rapid death of *Metrosideros polymorpha* in Hawaii. Persoonia-Molecular Phylogeny and Evolution of Fungi. 40(1): 154–181.

Berryman, E.; McMahan, A. 2019. Using tree canopy cover data to help estimate acres of damage. In: Potter, K.M.; Conkling, B.L., eds. Forest Health Monitoring: national status, trends, and analysis 2018. Gen. Tech. Rep. SRS-239. Asheville, NC: U.S. Department of Agriculture Forest Service, Southern Research Station: 125–141.

Castello, J.D.; Leopold, D.J.; Smallidge, P.J. 1995. Pathogens, patterns, and processes in forest ecosystems. BioScience. 45(1): 16–24.

Coulston, J.W. 2007. Insect and disease activity (2003). In: Ambrose, M.J.; Conkling, B.L., eds. Forest Health Monitoring: 2005 national technical report. Gen. Tech. Rep SRS-104. Asheville, NC: U.S. Department of Agriculture Forest Service, Southern Research Station: 33–40.

Couston, J.W. 2009. Insects and diseases. In: Ambrose, M.J.; Conkling, B.L., eds. Forest Health Monitoring: 2006 national technical report. Gen. Tech. Rep. SRS-117. Asheville, NC: U.S. Department of Agriculture Forest Service, Southern Research Station: 47–51.

Coulston, J.W.; Moisen, G.G.; Wilson, B.T. [and others]. 2012. Modeling percent tree canopy cover: a pilot study. Photogrammetric Engineering and Remote Sensing. 78(7): 715–727.

Edmonds, R.L.; Agee, J.K.; Gara, R.I. 2011. Forest health and protection. Long Grove, IL: Waveland Press, Inc. 667 p.

ESRI. 2015. ArcMap® 10.3. Redlands, CA: Environmental Systems Research Institute, Inc.

Forest Health Protection (FHP). 2016. Detection surveys. Fort Collins, CO: U.S. Department of Agriculture Forest Service, Forest Health Technology Enterprise Team. http://www.fs.fed.us/foresthealth/technology/detection_surveys.shtml. [Date accessed: July 23, 2016].

Forest Health Protection (FHP). 2019. Insect and Disease Detection Survey database (IDS). [Online database]. Fort Collins, CO: U.S. Department of Agriculture Forest Service, Forest Health Technology Enterprise Team. https://www.fs.fed.us/foresthealth/applied-sciences/mapping-reporting/gis-spatial-analysis/detection-surveys.shtml#idsdownloads. [Date accessed: July 17, 2019].

Homer, C.G.; Dewitz, J.A.; Yang, L. [and others]. 2015. Completion of the 2011 National Land Cover Database for the conterminous United States: representing a decade of land cover change information. Photogrammetric Engineering and Remote Sensing. 81(5): 345–354.

Liebhold, A.M.; McCullough, D.G.; Blackburn, L.M. [and others]. 2013. A highly aggregated geographical distribution of forest pest invasions in the USA. Diversity and Distributions. 19: 1208–1216.

Logan, J.A.; Regniere, J.; Powell, J.A. 2003. Assessing the impacts of global warming on forest pest dynamics. Frontiers in Ecology and the Envionment. 1: 130–137.

Lovett, G.M.; Weiss, M.; Liebhold, A.M. [and others]. 2016. Nonnative forest insects and pathogens in the United States: impacts and policy options. Ecological Applications. 26: 1437–1455.

Nowak, J.; Asaro, C.; Klepzig, K.; Billings, R. 2008. The southern pine beetle initiative: working for healthier forests. Journal of Forestry. 106: 261–267.

Potter, K.M. 2012. Large-scale patterns of insect and disease activity in the conterminous United States and Alaska from the national Insect and Disease Detection Survey database, 2007 and 2008. In: Potter, K.M.; Conkling, B.L., eds. Forest Health Monitoring 2009 national technical report. Gen. Tech. Rep. SRS-167. Asheville, NC: U.S. Department of Agriculture Forest Service, Southern Research Station: 63–78.

Potter, K.M. 2013. Large-scale patterns of insect and disease activity in the conterminous United States and Alaska from the national Insect and Disease Detection Survey, 2009. In: Potter, K.M.; Conkling, B.L., eds. Forest Health Monitoring: national status, trends, and analysis 2010. Gen. Tech. Rep. SRS-176. Asheville, NC: U.S. Department of Agriculture Forest Service, Southern Research Station: 15–29.

Potter, K.M.; Escanferla, M.E.; Jetton, R.M.; Man, G. 2019a. Important insect and disease threats to United States tree species and geographic patterns of their potential impacts. Forests. 10(4): 304.

Potter, K.M.; Escanferla, M.E.; Jetton, RM. [and others]. 2019b. Prioritizing the conservation needs of United States tree species: evaluating vulnerability to forest insect and disease threats. Global Ecology and Conservation. 18: e00622.

Potter, K.M.; Koch, F.H. 2012. Large-scale patterns of insect and disease activity in the conterminous United States and Alaska, 2006. In: Potter, K.M.; Conkling, B.L., eds. Forest Health Monitoring 2008 national technical report. Gen. Tech. Rep. SRS-158. Asheville, NC: U.S. Department of Agriculture Forest Service, Southern Research Station: 63–72.

Potter, K.M.; Paschke, J.L. 2013. Large-scale patterns of insect and disease activity in the conterminous United States and Alaska from the national Insect and Disease Detection Survey database, 2010. In: Potter, K.M.; Conkling, B.L., eds. Forest Health Monitoring: national status, trends, and analysis 2011. Gen. Tech. Rep. SRS-185. Asheville, NC: U.S. Department of Agriculture Forest Service, Southern Research Station: 15–28.

Potter, K.M.; Paschke, J.L. 2014. Large-scale patterns of insect and disease activity in the conterminous United States and Alaska from the national Insect and Disease Survey database, 2011. In: Potter, K.M.; Conkling, B.L., eds. Forest Health Monitoring: national status, trends, and analysis 2012. Gen. Tech. Rep. SRS-198. Asheville, NC: U.S. Department of Agriculture Forest Service, Southern Research Station: 19–34.

Potter, K.M.; Paschke, J.L. 2015a. Large-scale patterns of insect and disease activity in the conterminous United States and Alaska from the national Insect and Disease Survey, 2012. In: Potter, K.M.; Conkling, B.L., eds. Forest Health Monitoring: national status, trends, and analysis 2013. Gen. Tech. Rep. SRS-207. Asheville, NC: U.S. Department of Agriculture Forest Service, Southern Research Station: 19–36.

Potter, K.M.; Paschke, J.L. 2015b. Large-scale patterns of insect and disease activity in the conterminous United States, Alaska, and Hawaii from the national Insect and Disease Survey, 2013. In: Potter, K.M.; Conkling, B.L., eds. Forest Health Monitoring: national status, trends, and analysis 2014. Gen. Tech. Rep. SRS-209. Asheville, NC: U.S. Department of Agriculture Forest Service, Southern Research Station: 19–38.

Potter, K.M.; Paschke, J.L. 2016. Large-scale patterns of insect and disease activity in the conterminous United States and Alaska from the national Insect and Disease Survey, 2014. In: Potter, K.M.; Conkling, B.L., eds. Forest Health Monitoring: national status, trends, and analysis 2015. Gen. Tech. Rep. SRS-213. Asheville, NC: U.S. Department of Agriculture Forest Service, Southern Research Station: 21–40.

Potter, K.M.; Paschke, J.L. 2017. Large-scale patterns of insect and disease activity in the conterminous United States and Alaska from the national Insect and Disease Survey, 2015. In: Potter, K.M.; Conkling, B.L., eds. Forest Health Monitoring: national status, trends, and analysis 2016. Gen. Tech. Rep. SRS-222. Asheville, NC: U.S. Department of Agriculture Forest Service, Southern Research Station: 21–42.

Potter, K.M.; Paschke, J.L.; Koch, F.H.; Zweifler, M. 2019c. Large-scale patterns of insect and disease activity in the conterminous United States, Alaska, and Hawaii from the national Insect and Disease Survey, 2017. In: Potter, K.M.; Conkling, B.L., eds. Forest Health Monitoring: national status, trends, and analysis 2018. Gen. Tech. Rep. SRS-239. Asheville, NC: U.S. Department of Agriculture Forest Service, Southern Research Station: 21–49.

Potter, K.M.; Paschke, J.L.; Zweifler, M. 2018. Large-scale patterns of insect and disease activity in the conterminous United States, Alaska, and Hawaii from the national Insect and Disease Survey, 2016. In: Potter, K.M.; Conkling, B.L., eds. Forest Health Monitoring: national status, trends, and analysis 2017. Gen. Tech. Rep. SRS-233. Asheville, NC: U.S. Department of Agriculture Forest Service, Southern Research Station: 23–44.

Riitters, K.H.; Tkacz, B. 2004. The U.S. Forest Health Monitoring program. In: Wiersma, G.B., ed. Environmental monitoring. Boca Raton, FL: CRC Press: 669–683.

Tobin, P.C. 2015. Ecological consequences of pathogen and insect invasions. Current Forestry Reports. 1: 25–32.

University of Hawai'i, College of Tropical Agriculture and Human Resources. 2019. Rapid 'ōhi'a death/*Ceratocystis* wilt of 'ōhi'a. http://rapidohiadeath.org. [Date accessed: August 9, 2019].

U.S. Department of Agriculture (USDA) Forest Service. 2012. Future of America's forest and rangelands: Forest Service 2010 Resources Planning Act Assessment. Gen. Tech. Rep. WO-87. Washington, DC. 198 p.

U.S. Department of Agriculture (USDA) Forest Service. 2016. Future of America's forests and rangelands: update to the 2010 Resources Planning Act Assessment. Gen. Tech. Report WO-GTR-94. Washington, DC. 250 p.

CHAPTER 7.

Satellite-based Evidence of Forest Stress and Decline across the Conterminous United States for 2016, 2017, and 2018

Steven P. Norman
William M. Christie

INTRODUCTION

Remote sensing's role in forest monitoring is evolving. Satellite imagery is now systematically used to recognize and track forest disturbances in near-real time (Brown and others 2008, Chastain and others 2015, Hargrove and others 2009, Spruce and others 2011) and for retrospective insights (Meddens and others 2012, Norman and others 2016, Vogelmann and others 2012). Apart from mapping disturbance, high-frequency satellite data provide a reliable way to track vegetation phenology (Hargrove and others 2009, Norman and others 2017), and as vegetation phenology is an important indicator of variation in seasonal climate and the carbon cycle, it warrants being monitored over the long term (Hufkens and others 2012, Wu and others 2014). High-frequency monitoring is slowly shifting the way we monitor forests from periodic or "as needed" efforts toward the systematic tracking of forests and disturbances with remote sensing at weekly to seasonal frequency.

High-frequency monitoring is important as much observed forest change is ephemeral, lasting less than a season. Meanwhile, more consequential impacts to forest structure can be hard to recognize or track except immediately after a disturbance event occurs or during select seasons of the year (Norman and others 2014). Some disturbances have minor or neutral effects, such as leaf stripping in spring or an understory prescribed fire. Others can damage or kill trees, suppress growth for the entire season, or set back succession for decades. As viewed from above using remote sensing, these nuances can blur, yet persistence is a key disturbance indicator that has previously seen little use.

When remote sensing imagery was costly and computational speeds were limiting, research emphasized the refinement of indices that could better identify and map disturbances (e.g., Miller and Thode 2007). As technology has advanced, we now leverage long-underutilized stacks of data for the temporal information they contain (Schroeder and others 2017, Wulder and others 2012). With systematic monitoring across all lands and at broad scales, analysts no longer need to "chase" disturbance events as special projects individually as much as they once did, and this introduces a hierarchical efficiency to monitoring (Chastain and others 2015). High-frequency monitoring allows us to isolate ephemeral from what are more likely to be substantial or impactful changes and to track disturbance events as they unfold during a single growing season or over multiple years. By taking such a systematic, all-lands approach, analysts can detect near-real-time and progressive forest decline, the cumulative effects of multiple disturbances, and successional recovery—all seamlessly across jurisdictions.

Few satellite systems provide enough frequency to produce seamless, long-term maps at continental scale with unobstructed views multiple times per growing season. The twice-daily Moderate Resolution Imaging Spectroradiometer (MODIS) system has that capability. In this chapter, we use a new measure of disturbance, which is based on the magnitude

and duration of change, rather than just magnitude at one snapshot in time. Combining both aspects of disturbance allows us to isolate locations with substantive and sustained disturbance impacts indicating forest stress and decline across the conterminous United States.

METHODS

Data Used

For this effort, we required a satellite data stream that had consistently high frequency to provide multiple clear observations each month, or more often, for the conterminous United States and that could be reliably and efficiently processed. We chose the twice-daily MODIS Normalized Difference Vegetation Index (NDVI) data stream from the Terra and Aqua satellites provided by NASA's Global Inventory Monitoring and Modeling Studies (GIMMS) Global Agricultural Monitoring (GLAM) system (see https://glam1.gsfc.nasa.gov). These GIMMS/GLAM products provide separate cloud-filtered, 8-day maximum-NDVI products for both the Terra and Aqua satellites that pass overhead a few hours apart every day. As daytime clouds persist in some locations for weeks, we further processed these paired 8-day products into 24-day compositing periods at 8-day time steps. This provided us with a continuous NDVI time series stack for each of the approximately 145,000,000 MODIS cells in the conterminous United States. The dataset used forms the basis of the U.S. Department of Agriculture Forest Service's *ForWarn II* vegetation change recognition and tracking system (see https://forwarn.forestthreats.org/, Hargrove and others 2009).

Baseline Selection

Any calculation of change requires some formally designated baseline from which comparisons are calculated, and many are possible. As MODIS time series are built from daily data, their history provides a fairly robust record of normal seasonal vegetation phenology, and year-to-year variation in this seasonal dynamic can interfere with the signal from disturbance and vice versa (Norman and others 2017). In this analysis, we use the maximum NDVI value observed during the same 8 weeks over 3 years prior to each of the 3 years analyzed. Had we used the prior year's value, expectations for areas with multiyear drought would be artificially low, as would the NDVI of areas with partial decline within a cell as occurs with progressive beetle kill or logging. However, with a 3-year baseline, severe disturbances that occurred up to 3 years before may linger as they have not yet recovered. This baseline choice may confound estimates of annual disturbance rates because disturbances that are year-exclusive such as non-lethal defoliations or annual drought will not be captured the same way as those disturbances with effects that accumulate such as logging or beetle kill.

Vegetation Index Selection

Efforts to estimate forest biomass or cover using foliage-sensitive indices have a long history, but the information that any given

index holds can vary greatly across vegetation types and seasons. Therefore, use of a single index is a challenge when interpreting complex landscapes at continental scales, as change may not uniformly equate to the severity of effects (Miller and Thode 2007). With respect to this project, a practical problem with 240-m-resolution MODIS imagery is quantifying changes in fractional forest, grass, or shrub cover, as an NDVI decline in drought-sensitive low-NDVI open forests can imply more consequence than the same percent decline in a high-NDVI dense forest (Norman and others 2016). A simple adjustment to the denominator in the standard NDVI formula reduces this problem, resulting in the relative difference NDVI, or RdNDVI (equation [1]):

$$RdNDVI = (NDVI_{baseline} - NDVI_{current}) / \sqrt{(NDVI_{baseline} + NDVI_{current})} \quad (1)$$

In addition to the mixed or fractional pixel issue, this adjustment also helps partially overcome problems that arise from NDVI's nonlinear responsiveness, that is, the so-called NDVI "saturation" effect. When forest cover is low, adding (or losing) a few trees has a greater effect on NDVI than losing just a few trees in a densely forested cell. By taking the square root of the denominator, cells with high and low NDVI values will decrease more similarly when both areas experience the same absolute change in NDVI.

Thresholding Magnitude and Duration

Only "summer" periods, defined as the 14 periods with end dates between June 9 and September 21, are used for this project. This seasonal choice avoids most interannual variation in the timing of eastern spring and fall in addition to winter irregularities caused by variable snowpack. Across much of the West, however, variability in the timing of the mid-summer NDVI decline may increase the importance of drought as dry, open western forests are substantially more responsive to drought at that time of year than are dense eastern deciduous forests. Use of summer periods also implies that most disturbances that occur after late summer of the calendar year (such as fall fires or hurricanes) will be omitted, although severe disturbances will typically be reflected in the subsequent year's change map.

Somewhat arbitrary thresholds were imposed to isolate forest disturbances of high magnitude and long duration. We reclassed period maps using NDVI values below -9.4-percent change to 1, then summed the number of periods departed at that threshold in excess of 6 to isolate sustained summer impacts whether consecutive or not. We produced annual maps showing cells where seven or more summer periods were

departed at that threshold of magnitude. These steps isolated those places that were both more severely and persistently disturbed for three successive summers.

To restrict this analysis to forested cells at 240-m MODIS resolution, we developed a mask based on the 30-m Landsat-based National Land Cover Database (NLCD) for 2010 (see https://www.mrlc.gov/). A MODIS cell was classified as forest when it had a majority NLCD composition of evergreen, deciduous, or mixed forest. For visualization purposes, we used block statistics to sum the number of forested cells that passed the tests for departure described above in a 4-km grid for each year. We then calculated recent trends by comparing the count for 2018 to the mean of 2016 and 2017 to show where 2018's 4-km^2 departure was improving or worsening. We used zonal statistics to identify the 20 counties with the most forest departure in the East and West and assessed the primary causes of NDVI decline for those locations. For this list, we first ranked counties according to the percent of their total forest area disturbed, created a separate ranking using the absolute number of disturbed cells, and then took the mean of these two 2018 ranks. That approach provided an evenly weighted ranking system based on the relative and absolute amount of detected disturbance.

Datasets for Assessment

We leveraged ancillary datasets to determine the primary cause of observed NDVI declines. These include relevant chapters of recent Forest Health Monitoring reports (Koch and Coulston 2017, 2018, 2019; Potter 2019; Potter and others 2018, 2019, 2020), the monthly record of the Palmer Drought Severity Index (https://www.ncdc.noaa.gov/temp-and-precip/drought/historical-palmers), and annual summary reports of insects and diseases from State and Federal monitoring efforts (see https://www.fs.fed.us/foresthealth/publications/fhp/index.shtm). Locations that experienced large wildfires are identified through use of calendar-dated suppression perimeters (https://www.geomac.gov/). Areas of timber production are generally identified using aerial evidence of industrial logging and Forest Service Forest Inventory and Analysis (FIA) reports (see https://www.fia.fs.fed.us/slides/current-data.pdf). Regional insights are available from the various State timber industry product output and use reports published periodically by the FIA program (Bentley and Steppleton 2013, Johnson 2001, Smith and others 2004).

We expect that our summer NDVI decline maps will only partially correspond with full-year drought maps (Koch and Coulston 2017, 2018, 2019) as we ignore autumn and winter drought. Moreover, forests vary in their ability to convey summer drought stress according to their spatial structure and composition (Norman and others 2016). Similarly, we do not expect perfect correspondence with insect and disease surveys due to inconsistencies of aerial monitoring efforts (Potter and others 2018, 2019, 2020) and MODIS' known limitations of detecting scattered or small-patch tree decline (Eklundh and others

2009, Meddens and others 2012, Spruce and others 2011). Correspondence with annual wildfire detections (Potter 2019) is also nuanced by seasonal differences in the timing of fire and our summer analysis period.

RESULTS AND ASSESSMENTS

Using our MODIS-based approach, we generated three seamless maps of the conterminous United States that show where substantive and sustained summer disturbance occurred during 2016, 2017, and 2018. Through concerted use of magnitude and duration—two quasi-independent measures of severity—we capture growing season impacts better than simply estimating severity from change observed during just part of the growing season. In the sections below, we assess the emergent patterns and their likely primary causes.

2016 Assessment

South—Late summer annual drought helps explain NDVI declines in Georgia, north Florida, and the southern edge of the Appalachians (fig. 7.1A). The extensive Appalachian wildfires of 2016 occurred after summer, so they are not indicated on this year's map. The South-Central United States (eastern Texas, eastern Oklahoma, Arkansas, and Louisiana) were experiencing wetter-than-normal conditions, yet they exhibit significant departure, much like the broader band of southeastern U.S. Coastal Plain States. As our approach detects all forms of canopy disturbance, most of this change in the Southeast likely resulted from timber harvesting as the regional pattern is recurrent across years (Hansen and others 2013). Forest Inventory and Analysis data show that private lands of the South have consistently produced the most pulpwood and timber products in the United States. Comparisons of MODIS cells having strong NDVI decline with recent aerial photos confirm industrial logging's importance, even within areas of drought in the Coastal Plain. Drought in areas of recent clearcuts may amplify this pattern due to nonforest's high sensitivity to drought stress.

Northeast—Moderate to extreme drought emerged across southern New England during late 2015, and by the summer of 2016 its effects on NDVI commingled with an extensive gypsy moth (*Lymantria dispar dispar*) defoliation, particularly across Rhode Island and eastern Connecticut. By June of 2016, western New York was in moderate drought, and then by July, drought extended into central Pennsylvania where gypsy moths also contributed to localized NDVI decline. Declines in the upper Midwest are scattered and include spruce budworm (*Choristoneura fumiferana*) defoliation in Michigan's Upper Peninsula and extreme wind/hail damage in Montmorency County, MI, and Lake of the Woods County, MN.

West—South Dakota's Black Hills show extensive NDVI decline, which likely reflects the moderate drought and the cumulative effects of mountain pine beetles (*Dendroctonus ponderosae*) over the prior 3 years. From Wyoming, Montana, and Idaho, widespread but patchy declines result from drought combined with western spruce budworm (*Choristoneura freemani*)

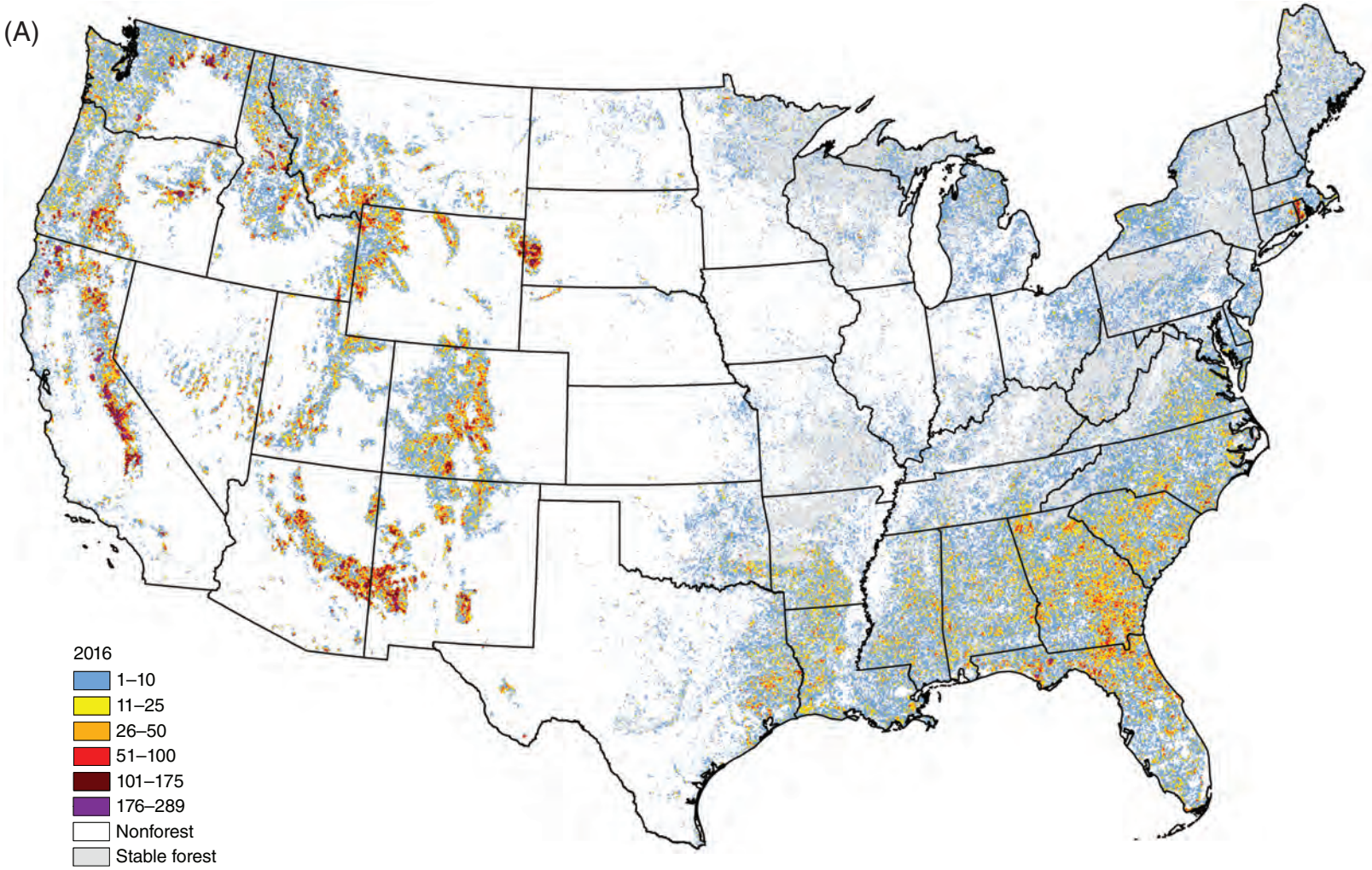

Figure 7.1—Number of forested MODIS cells per 4 km^2 having NDVI decline of at least 9.5 percent over 3 years for (A) 2016, (B) 2017, and (C) 2018.
(continued to next pages)

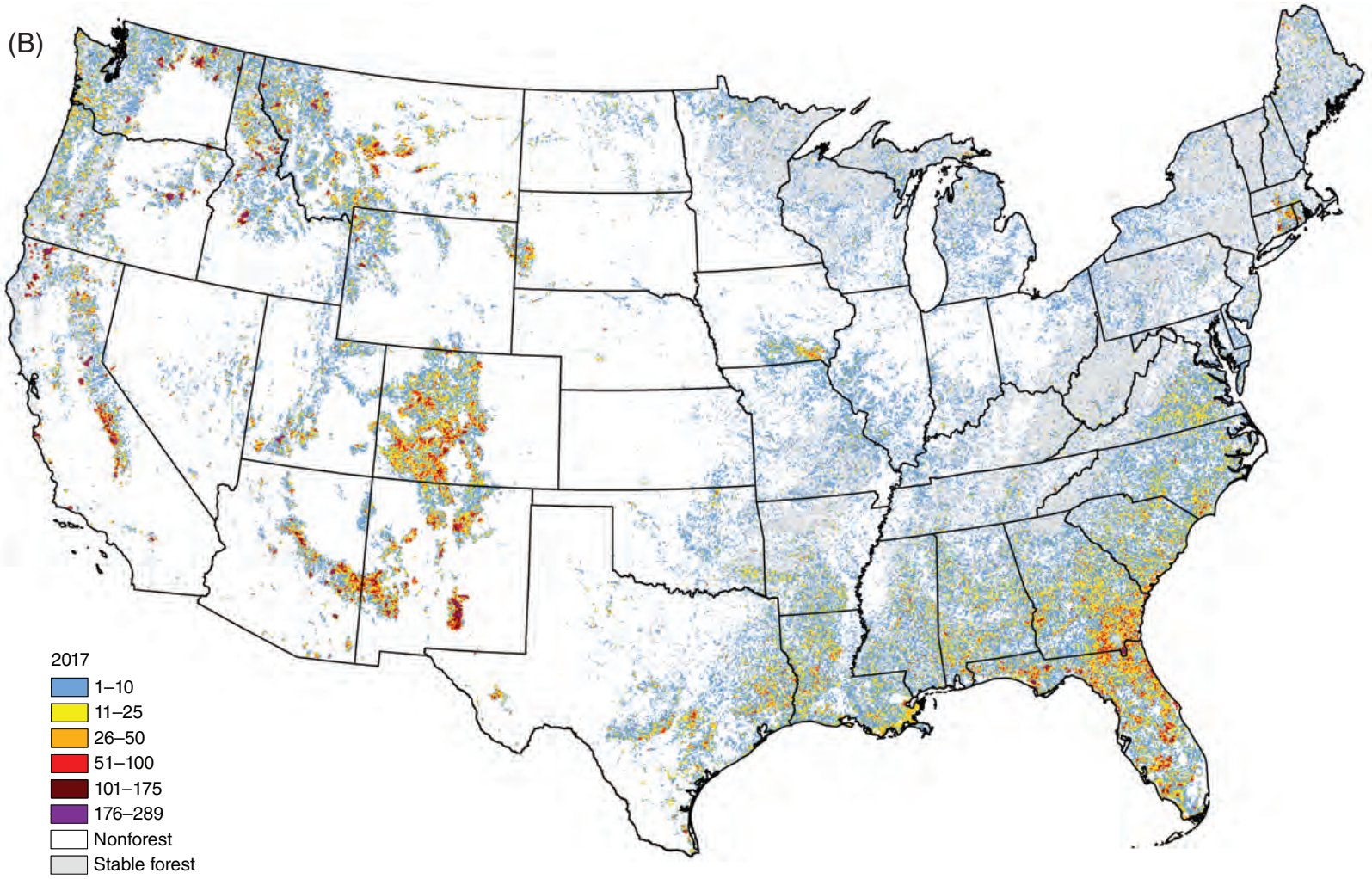

Figure 7.1 (continued)—Number of forested MODIS cells per 4 km^2 having NDVI decline of at least 9.5 percent over 3 years for (A) 2016, (B) 2017, and (C) 2018. (continued to next page)

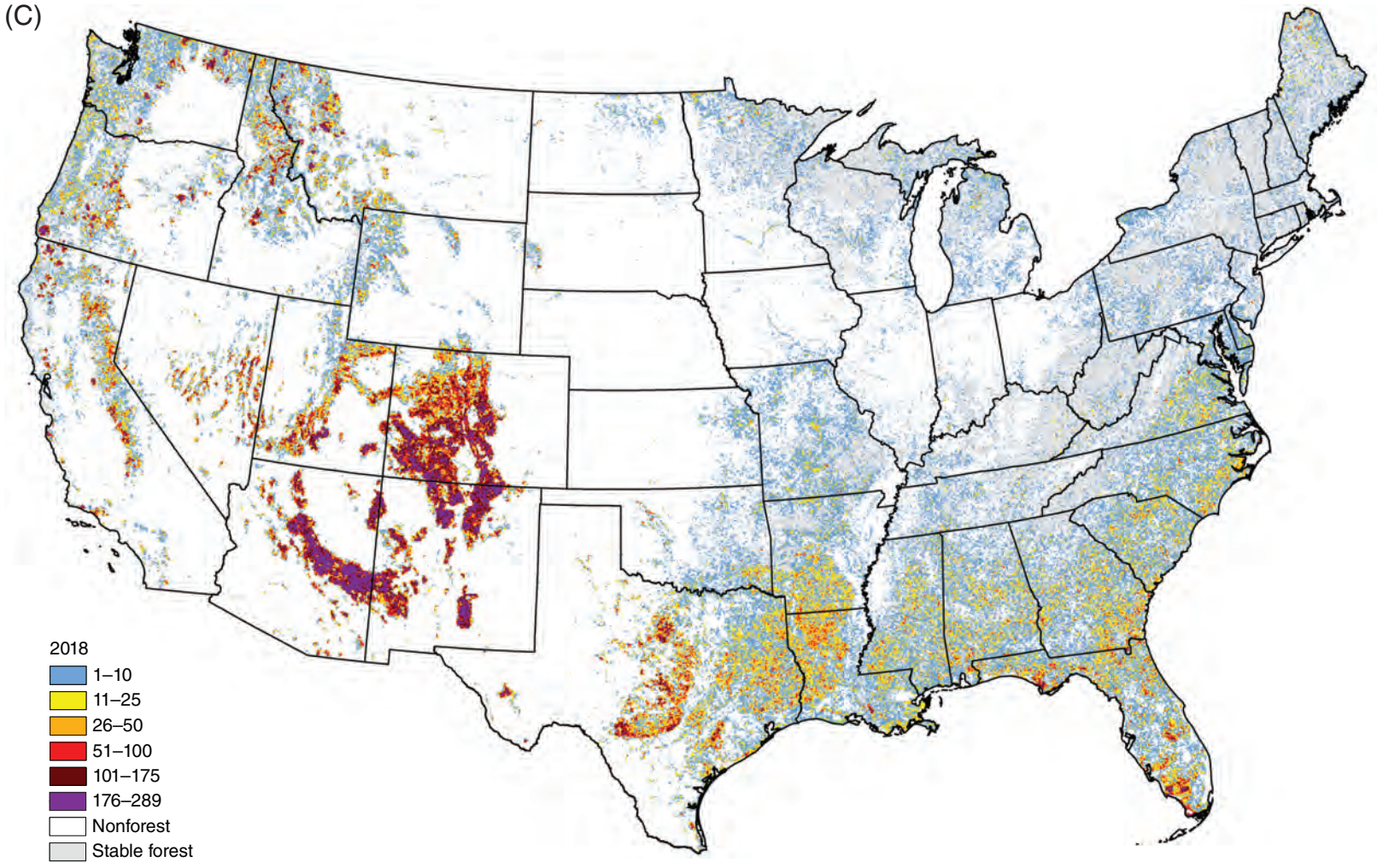

Figure 7.1 (continued)—Number of forested MODIS cells per 4 km^2 having NDVI decline of at least 9.5 percent over 3 years for (A) 2016, (B) 2017, and (C) 2018.

and localized wildfires. In eastern Oregon's Blue Mountains, western (*D. brevicomis*) and mountain pine beetles, moderate to severe drought, and wildfire contributed to NDVI declines. Across the Coast and Cascade Ranges, insects and wildfire were likely more important causes of decline than the mild drought. In California's Sierras, an exceptional multiyear drought caused mass tree mortality from bark beetles and woodborers. Wildfire led to additional localized NDVI decline. In central Arizona and New Mexico, moderate drought combined with wildfire, beetles, and spruce aphids (*Elatobium abietinum*) to produce declines. In southern Utah, western spruce budworm and other insects during an abnormally dry summer led to spotty declines, and in Colorado, patchy dry weather was likely less important than spruce beetles, western spruce budworms, bark beetles, and localized wildfire. Commercial logging is common in some landscapes including portions of the coastal range of the Pacific Northwest and low to middle elevations of the interior. With cumulative stressors across the West, few forested landscapes escaped NDVI declines for 2016.

2017 Assessment

South—The drought that prevailed across the Piedmont and Appalachians during late 2016 persisted locally into early summer of 2017, but it had largely abated by mid- to late summer with evidence of a few fall 2016 wildfires remaining (fig. 7.1.B). From eastern Texas to Alabama, much wetter than average conditions prevailed. Late-season moisture came from Hurricane Harvey that made landfall in late August, causing widespread flooding in eastern Texas, yet it occurred too late in the summer to be reflected in these maps. Wind damage from Hurricane Irma is absent, as it made landfall in early September—also too late for this 2017 map. Mortality from pine bark beetles spread across Mississippi, Alabama, Georgia, north Florida, and western North Carolina, and much of the NDVI decline shows results from logging activity over the prior 3 years.

Northeast—Most of the Northeast experienced normal or above-normal precipitation during the summer of 2017. The anomaly north of Iowa's southern border is from local drought. Dryer-than-average conditions had occurred from the Chesapeake Bay through southern New England during the early summer, but drought only persisted through the growing season in Long Island, Connecticut, and coastal Maine. Rhode Island experienced gypsy moth defoliation again in 2017, but more activity was observed in eastern Connecticut and nearby Massachusetts. Insect and disease reports describe emerald ash borer (*Agrilus planipennis*) mortality for many Northeastern States, yet MODIS's coarse spatial resolution is ill-suited for detecting scattered canopy damage in mixed vegetation or in species-rich forests, and this limitation is reflected by this map.

West—During the summer of 2017, severe drought prevailed in Montana and the western Dakotas with localized moderate drought elsewhere. This pattern of stress contrasts with that of 2016 when drought prevailed across most of the West. Even though affected by drought in

both 2016 and 2017, the condition of the Black Hills shows more impact in 2016. Elsewhere, the patchiness of decline is clearly evident in 2017, and this likely results from reduced drought stress combined with localized fire and insect-related decline caused by fir engraver (*Scolytus ventralis*), spruce beetles, and mountain pine beetles. As a 3-year baseline is used in these change maps, severity for 2017 reflects cumulative mortality since the fall of 2014.

2018 Assessment

At the time of this analysis, complete insect and disease aerial survey data for 2018 were not yet available, so a complete assessment of defoliators and borers is not yet possible. However, the extensive insect defoliation that plagued southern New England in 2016 and 2017 was greatly abated, as shown on figure 7.1C. Bark beetles continued to kill trees across much of the West, and as a 3-year baseline is used, local areas of mortality since 2015 can persist on the 2018 map.

For much of the summer, severe to extreme drought impacted a vast area from southern California to Texas. Hardest hit was the Four Corners area of Utah, Colorado, Arizona, and New Mexico, and this region shows extreme departure unlike anything seen for 2016 or 2017. In late 2017, Hurricane Irma severely impacted southwestern Florida, and some impacts have become evident on the 2018 map, such as in the coastal mangrove forest. Absent, however, are impacts from 2018's Hurricanes Florence and Michael that occurred too late to show up on this map. Damage from October's Hurricane Michael was particularly extensive across Florida's panhandle into southwestern Georgia and southeastern Alabama, so it will show up strongly on the 2019 map with the same approach.

Figures 7.1A, 7.1B, and 7.1C reveal where substantive and sustained disturbances were observed annually for 2016, 2017, and 2018, respectively. Figure 7.2 provides a contextual interpretation of the 2018 season that reveals the directional change in disturbance compared to the mean NDVI decline of the prior 2 years. Areas in blue show less disturbance relative to the recent past (i.e., "gain" or "improvement"), while reds show where declines worsened during 2018's summer. Accordingly, blue areas relate to where 2016 or 2017 experienced severe disturbance and 2018 saw a reprieve from further loss. Note in particular southern New England's gypsy moth activity and the areas of drought and beetle damage in California's Southern Sierra and North Dakota's Black Hills region. Consistent with figure 7.1C, the most extensive area of red includes Texas and the Four Corners area; in 2018, drought stress was far worse there than it was during the 2 prior years. The mosaic of light blue and light red in north Georgia and surrounding States generally reflects the patchiness of industrial logging, with the landscape experiencing a continuous cycle of clearcutting and regeneration as a shifting mosaic. In the West, large burn scars show up as both coarse patches of red or blue depending on when they occurred, with red having burnt recently and blue representing a recovering state.

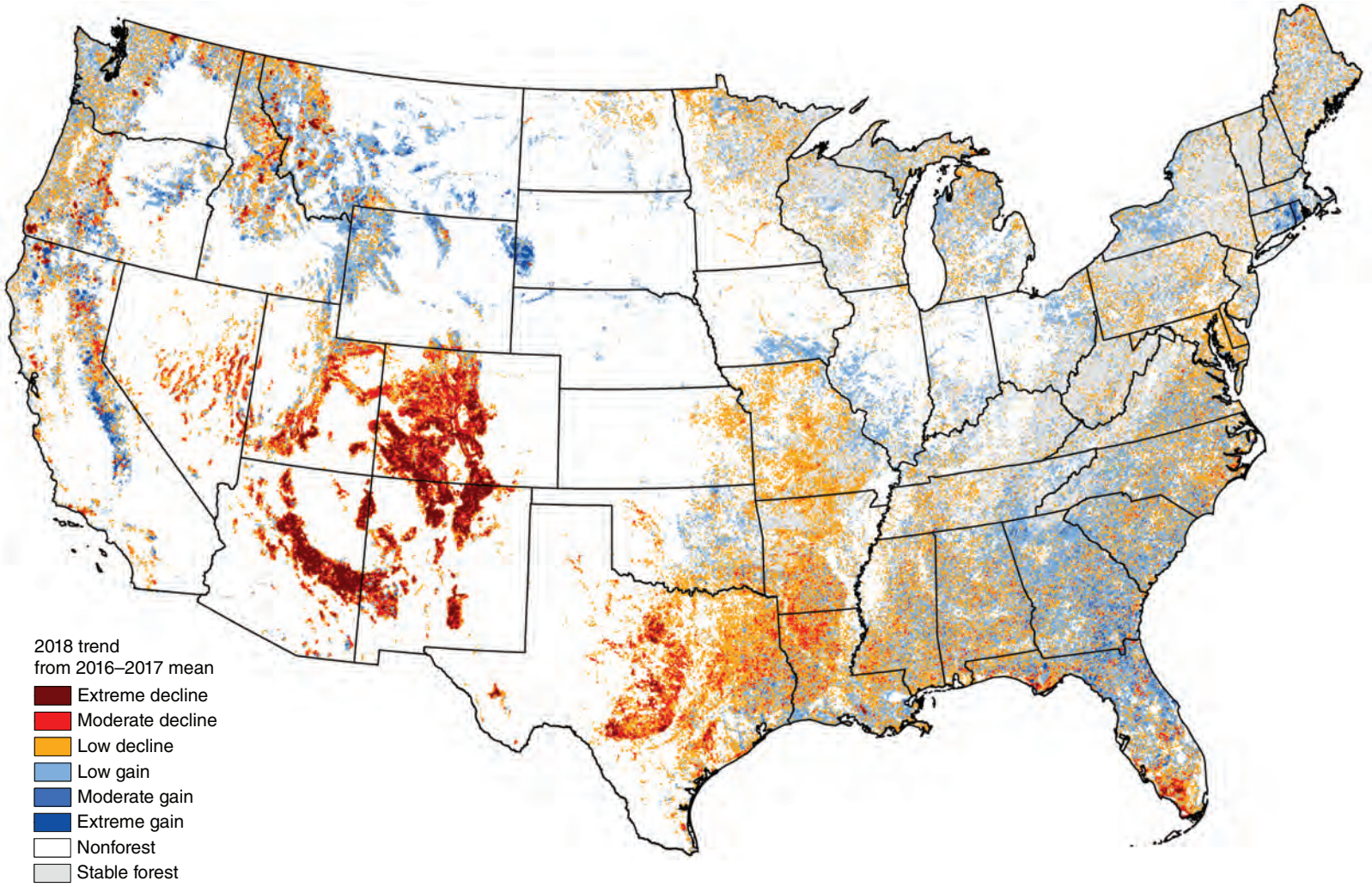

Figure 7.2—The 3-year trend in substantive and sustained forest disturbances from the summers of 2016–2017 (figs. 7.1A and 7.1B) compared to summer 2018 (fig. 7.1C).

Blue may also represent relief from just one of several compounding causes. Note that while the Southern Sierra Nevada was in drought during 2018, the hard-hit centers of mortality in red during all 3 years (figs. 7.1A, 7.1B, 7.1C) show up in blue on figure 7.2. Blue does not necessarily denote successional recovery, although it can be that, as noted with the response from wildfires, given the shifting 3-year window being used.

Drought is the leading disturbance cause for the 20 counties in the East and West that show the strongest relative NDVI declines for 2018 (table 7.1). Two southern Florida counties that were impacted by Hurricane Irma made the eastern list. All western counties ranking high in terms of substantive and sustained disturbance did so because of the influence of the extreme drought in the Four Corners area. Many of these counties had compounded disturbances from drought, beetles, and wildfire, and while the 2018 drought appears to be the primary stressor, mortality from other causes since late 2015 may also explain why these counties ranked high.

DISCUSSION AND CONCLUSIONS

Routine broad-scale use of remote sensing is practical for assessing many forest health concerns. Every remote sensing data stream has its strengths, and the high-temporal-frequency MODIS imagery used in this chapter is exceptional because it allows disturbance tracking in near-real time, and with that it provides a more nuanced consideration of growing season impacts as measured by

Table 7.1—Eastern (top) and Western (bottom) U.S. counties exhibiting the most substantive and sustained disturbance during the summer of 2018

2018 Rank[a]	County and State	Percentage of county forested	Percentage of forest disturbed in 2018[b]	Leading disturbance causes[c]
East				
1	Jeff Davis Co., TX	8.8	87.2	Drought
2	San Saba Co., TX	12.2	87.3	Drought
3	Palo Pinto Co., TX	28.0	70.8	Drought
4	Eastland Co., TX	11.3	86.0	Drought
5	Stephens Co., TX	11.1	79.1	Drought
6	Lampasas Co., TX	9.3	94.9	Drought
7	Comal Co., TX	37.3	61.6	Drought
8	Coryell Co., TX	17.4	63.8	Drought
9	Gillespie Co., TX	6.5	90.8	Drought
10	Erath Co., TX	7.5	82.2	Drought
11	Bosque Co., TX	17.2	61.8	Drought
12	Burnet Co., TX	23.5	57.5	Drought
13	Llano Co., TX	9.0	77.0	Drought
14	Uvalde Co., TX	17.1	54.1	Drought
15	Collier Co., FL	53.0	37.1	Fire, Hurricane Irma
16	Hays Co., TX	26.5	54.8	Drought
17	Monroe Co., FL	31.7	40.1	Hurricane Irma
18	Real Co., TX	47.3	44.5	Drought
19	Young Co., TX	6.9	81.4	Drought
20	Kimble Co., TX	5.6	77.0	Drought
West				
1	Gila Co., AZ	35.4	91.6	Drought, fire
2	Navajo Co., AZ	10.8	84.5	Drought, fire, insects
3	Colfax Co., NM	34.2	80.2	Drought, fire, insects
4	Rio Arriba Co., NM	40.0	78.8	Drought, fire, insects
5	Montrose Co., CO	28.6	81.0	Drought, fire, insects
6	Apache Co., AZ	22.3	76.3	Drought, fire, insects
7	Fremont Co., CO	47.6	78.8	Drought, fire, insects
8	Lincoln Co., NM	10.6	82.6	Drought, insects

continued

Table 7.1 (continued)—Eastern (top) and Western (bottom) U.S. counties exhibiting the most substantive and sustained disturbance during the summer of 2018

2018 Rank[a]	County and State	Percentage of county forested	Percentage of forest disturbed in 2018[b]	Leading disturbance causes[c]
9	Otero Co., NM	15.8	76.6	Drought, insects
10	San Miguel Co., CO	36.0	79.4	Drought, insects
11	Taos Co., NM	50.3	73.0	Drought, insects
12	La Plata Co., CO	47.5	74.3	Drought, fire, insects
13	Graham Co., AZ	14.7	74.3	Drought, fire, insects
14	Costilla Co., CO	32.5	78.4	Drought, fire, insects
15	Sandoval Co., NM	19.2	73.3	Drought, fire, insects
16	Greenlee Co., AZ	42.8	72.4	Drought, fire, insects
17	Las Animas Co., CO	14.2	73.0	Drought, insects
18	Park Co., CO	38.1	69.5	Drought, fire, insects
19	Garfield Co., UT	18.7	66.9	Drought, fire, insects
20	San Juan Co., UT	5.8	74.3	Drought, insects

[a] Counties rank highest for having more absolute disturbed area and for a higher percentage of their total forest disturbed.

[b] The percentage of county disturbed in 2018 is derived from the number of majority-forested MODIS cells having at least 9.5-percent 3-year NDVI decline for seven or more 8-day periods during the summer months.

[c] The primary disturbance cause is inferred from ancillary datasets described in the methodology section. When multiple causes of disturbance are present, only one needs to increase for 2018 for this rank.

magnitude and duration. Like every forest monitoring approach, this too brings its share of caveats, with the most important outlined below.

MODIS' 240-m resolution can be too coarse to recognize some forest damage of concern such as loss of individual species in mixed stands, particularly in the East. Only when species are sufficiently dominant within a MODIS grid cell can decline or mortality be clearly resolved. Surviving trees or other vegetation can compensate for minor losses, particularly in the productive East when using NDVI. This is illustrated by the inability of MODIS to capture mortality from the emerald ash borer or the southern pine beetle (*Dendroctonus frontalis*), but it applies more generally to mixed stands. For such fine-textured monitoring needs, tailored applications of 30-m Landsat, 10-m Sentinel 2, or sub-meter-resolution imagery are warranted.

Forests that experience gradual decline over multiple years are hard to capture with short-term baselines. The 3-year baseline used in this chapter helps with that, but some NDVI declines occur over many years or a decade. These declines are not captured by this particular technique, but longer baselines are possible. However, in mixed forests, slow mortality often allows compensatory growth from adjacent vegetation that can mask damage entirely. This also relates to the limitation of the vegetation indices that can only separate species when they occur as dominants in simple vegetation types.

Even with the corrective use of RdNDVI and forest masking, MODIS' coarse resolution means that edge or open forests often have high proportions of grass and shrub cover. Since grass and shrubs are highly sensitive to summer drought, observed changes may not be a direct measure of forest change akin to canopy damage or tree mortality.

Four thresholds in this analysis are somewhat subjective. First, use of a moving 3-year baseline adds complexity to the interpretation of maps, as some disturbances persist longer

than others sometimes apart from ecological impacts. Second, the choice of an RdNDVI departure magnitude threshold of -9.5 percent means that results may be less sensitive to the loss of individual species in mixed stands than severe annual drought in open forests that may just include reduced tree growth. Third, the choice of calendar dates to define the summer analytical period is phenologically imperfect for some regions. Finally, our choice of duration thresholds is similarly limiting because of how it relates to differing phenological growing seasons. We have attempted to convey more clarity and transparency in these maps by simplifying these assumptions with judicious thresholds.

With this, like any coarse-resolution remote sensing product, there is a critical need for assessment and interpretation, which may need to occur at landscape to local scales. In many cases, though not all, field observations or detailed ancillary data are critical for accurately assigning causation. This is most important where there are multiple agents of change present at the same place and time.

These maps show only areas of relative NDVI decline, not recovery, and understanding that balance would help address the higher-level question of sustainability that we are not pursuing here. For example, forest recovery can contextualize disturbance in areas that experience clearcut logging or patch-mosaic wildfires. Within productive mixed forests with finer resolution gap phase processes at work, however, NDVI recovery and disturbance can occur concomitantly within a single MODIS cell.

The maps in this chapter reveal summer patterns of stress and decline across the conterminous United States from all causes that had a substantive and sustained impact on forest canopies. This change includes mid- to large-sized patchy tree mortality and NDVI declines caused by logging, development, mining, insects and disease, fire, wind, hail, and drought somewhat indiscriminately, though not inclusively as MODIS's resolution is ill-suited for resolving low-density canopy damage in mixed stands. In areas such as the Southeastern U.S. Coastal Plain and Piedmont that experience continuous and patchy logging, it is difficult to reliably isolate forest disturbance impacts from insects and disease, wind, or wildfire at MODIS resolution. While this problem is not eliminated by higher resolution imagery (e.g., Hanson and others 2013), more intense analysis that leverages frequent, high-resolution imagery may be needed to separate the various interactive causes of forest change with confidence.

The power of MODIS is that it is rooted in twice-daily observations that permit a product quality and efficient seamlessness that is unmatched by any existing finer resolution datasets. With a reliable history that goes back to 2003 (and less reliably to 2000), monitoring questions can be addressed at sub-seasonal frequency looking back over a decade and a half. With high-frequency observations, MODIS also provides enough monitoring consistency to systematically address seasonal disturbance duration, not just magnitude. Seasonal duration introduces a new dimensionality to the concept

of severity that in many cases can likely result in more accurate estimates of disturbance impacts while providing nuanced insights into the disturbances that may be present.

As remote sensing technologies and processing capabilities evolve, we are poised to advance forest health monitoring in novel ways. National maps such as these convey where large-scale stressors are problematic and how regions and landscapes differ in terms of the structure and variability of their disturbance dynamic. More focused monitoring questions are necessarily pursued at finer resolution to understand landscape and local change. Together, such scaled efforts can provide a hierarchical sense of forest stress and decline with unparalleled context and precision.

LITERATURE CITED

Bentley, J.W.; Steppleton, C.D. 2013. Southern pulpwood production, 2011. Resour. Bull. SRS-194. Asheville, NC: U.S. Department of Agriculture Forest Service, Southern Research Station. 38 p.

Brown, J.F.; Wardlow, B.D.; Tadesse, T. [and others]. 2008. The vegetation drought response index (VegDRI): a new integrated approach for monitoring drought stress in vegetation. GIScience & Remote Sensing. 45: 16–46.

Chastain, R.A.; Fisk, H.; Ellenwood, J.R. [and others]. 2015. Near-real time delivery of MODIS-based information on forest disturbances. In: Lippitt, C.D.; Stow, D.A.; Coulter, L.L., eds. Time sensitive remote sensing. New York: Springer: 147–164.

Eklundh, L.; Johansson, T.; Solberg, S. 2009. Mapping insect defoliation in Scots pine with MODIS time-series data. Remote Sensing of Environment. 113(7): 1566–1573.

Hansen, M.C.; Potapov, P.V.; Moore, R. [and others]. 2013. High-resolution global maps of 21st-century forest cover change. Science. 342: 850–853.

Hargrove, W.W.; Spruce, J.P.; Gasser, G.E.; Hoffman, F.M. 2009. Toward a national early warning system for forest disturbances using remotely sensed canopy phenology. Photogrammetric Engineering & Remote Sensing. 75: 1150–1156.

Hufkens, K.; Friedl, M.; Sonnentag, O. [and others]. 2012. Linking near-surface and satellite remote sensing measurements of deciduous broadleaf forest phenology. Remote Sensing of Environment. 117: 307–321.

Johnson, T.G., ed. 2001. United States timber industry—an assessment of timber product output and use, 1996. Gen. Tech. Rep. SRS-45. Asheville, NC: U.S. Department of Agriculture Forest Service, Southern Research Station. 145 p.

Koch, F.H.; Coulston, J.W. 2017. Moisture deficit and surplus in the conterminous United States for three time windows: 2016, 2014–2016, and 2012–2016. In: Potter, K.M.; Conkling, B.L., eds. Forest Health Monitoring: national status, trends, and analysis 2016. Gen. Tech. Rep. SRS-222. Asheville, NC: U.S. Department of Agriculture Forest Service, Southern Research Station: 63–80.

Koch, F.H.; Coulston, J.W. 2018. Moisture deficit and surplus in the conterminous United States for three time windows: 2016, 2014–2016, and 2012–2016. In: Potter, K.M.; Conkling, B.L., eds. Forest Health Monitoring: national status, trends, and analysis 2017. Gen. Tech. Rep. SRS-233. Asheville, NC: U.S. Department of Agriculture Forest Service, Southern Research Station: 65–84.

Koch, F.H.; Coulston, J.W. 2019. Drought and moisture surplus patterns in the conterminous United States: 2017, 2015–2017, and 2013–2017. In: Potter, K.M.; Conkling, B.L., eds. Forest Health Monitoring: national status, trends, and analysis 2018. Gen. Tech. Rep. SRS-239. Asheville, NC: U.S. Department of Agriculture Forest Service, Southern Research Station: 77–96.

Meddens, A.J.H.; Hicke, J.A.; Ferguson C.A. 2012. Spatiotemporal patterns of observed bark beetle-caused tree mortality in British Columbia and the Western United States. Ecological Applications. 22(7): 1876–1891.

Miller, J.D.; Thode, A.E. 2007. Quantifying burn severity in a heterogeneous landscape with a relative version of the delta Normalized Burn Ratio (dNBR). Remote Sensing of Environment. 109: 66–80.

Norman, S.P.; Hargrove, W.W.; Christie, W.M. 2017. Spring and autumn phenological variability across environmental gradients of Great Smoky Mountains National Park. Remote Sensing. 9(5): 407.

Norman, S.P.; Hargrove, W.W.; Spruce, J.P.; Christie, W.M. 2014. Monitoring forest disturbances across seasons using the *ForWarn* recognition and tracking system. In: Potter, K.M.; Conkling, B.L., eds. Forest Health Monitoring: national status, trends, and analysis 2013. Gen. Tech. Rep. SRS-207. Asheville, NC: U.S. Department of Agriculture Forest Service, Southern Research Station: 85–99.

Norman, S.P.; Koch, F.; Hargrove, W.W. 2016. Review of broad-scale drought monitoring of forests: toward an integrated data mining approach. Forest Ecology and Management. 380: 346–358.

Potter, K.M. 2019. Large-scale patterns of forest fire occurrence across the 50 United States and Caribbean Territories, 2017. In: Potter, K.M.; Conkling, B.L., eds. Forest Health Monitoring: national status, trends, and analysis 2018. Gen. Tech. Rep. SRS-239. Asheville, NC: U.S. Department of Agriculture Forest Service, Southern Research Station: 51–76.

Potter, K.M.; Paschke, J.L.; Zweifler, M.O. 2018. Large-scale patterns of insect and disease activity in the conterminous United States, Alaska, and Hawaii from the national Insect and Disease Survey, 2016. In: Potter, K.M.; Conkling, B.L., eds. Forest Health Monitoring: national status, trends, and analysis 2017. Gen. Tech. Rep. SRS-233. Asheville, NC: U.S. Department of Agriculture Forest Service, Southern Research Station: 23–44.

Potter, K.M.; Paschke, J.L.; Zweifler, M.O. 2019. Large-scale patterns of insect and disease activity in the conterminous United States, Alaska, and Hawaii from the national Insect and Disease Survey, 2017. In: Potter, K.M.; Conkling, B.L., eds. Forest Health Monitoring: national status, trends, and analysis 2018. Gen. Tech. Rep. SRS-239. Asheville, NC: U.S. Department of Agriculture Forest Service, Southern Research Station: 21–48.

Potter, K.M.; Paschke, J.L.; Koch, F.H.; Berryman, E.M. 2020. Large-scale patterns of insect and disease activity in the conterminous United States, Alaska, and Hawaii from the national Insect and Disease Survey, 2018. In: Potter, K.M.; Conkling, B.L., eds. Forest Health Monitoring: national status, trends, and analysis 2019. Gen. Tech. Rep. SRS-250. Asheville, NC: U.S. Department of Agriculture Forest Service, Southern Research Station: 27–55.

Schroeder, T.A.; Schleeweis, K.G.; Moisen, G.G. [and others]. 2017. Testing a Landsat-based approach for mapping disturbance causality in U.S. forests. Remote Sensing of Environment. 195: 230–243.

Smith, W.B.; Miles, P.D.; Vissage, J.S.; Pugh, S.A. 2004. Forest resources of the United States, 2002. Gen. Tech. Rep. NC-241. St. Paul, MN: U.S. Department of Agriculture Forest Service, North Central Research Station. 137 p.

Spruce, J.P.; Sader, S.; Ryan, R.E. [and others]. 2011. Assessment of MODIS NDVI time series data products for detecting forest defoliation by gypsy moth outbreaks. Remote Sensing of Environment. 1152: 427–437.

Vogelmann, J.E.; Xian, G.; Homer, C.; Tolk, B. 2012. Monitoring gradual ecosystem change using Landsat time series analysis: case studies in selected forest and rangeland ecosystems. Remote Sensing of Environment. 122: 92–105.

Wu, C.; Gonsamo, A.; Gough, C.M. [and others]. 2014. Modeling growing season phenology in North American forests using seasonal mean vegetation indices from MODIS. Remote Sensing of Environment. 147: 79–88.

Wulder, M.A.; Masek, J.G.; Cohen, W.B. [and others]. 2012. Opening the archive: how free data has enabled the science and monitoring promise of Landsat. Remote Sensing of Environment. 122: 2–10.

Each year the Forest Health Monitoring (FHM) program funds a variety of Evaluation Monitoring (EM) projects, which are "designed to determine the extent, severity, and causes of undesirable changes in forest health identified through Detection Monitoring (DM) and other means" (FHM 2015). In addition, EM projects can produce information about forest health improvements. Evaluation Monitoring projects are submitted, reviewed, and selected through an established process. More detailed information about how EM projects are selected, the most recent call letter, lists of EM projects awarded by year, and EM project poster presentations can all be found on the FHM website: https://www.fs.fed.us/foresthealth/protecting-forest/forest-health-monitoring/index.shtml.

Beginning in 2008, each FHM annual national report contains summaries of recently completed EM projects. Each summary provides an overview of the project and results, citations for products and other relevant information, and a contact for questions or further information. The summaries provide an introduction to the kinds of monitoring projects supported by FHM and include enough information for readers to pursue specific interests. Two project summaries are included in this report.

LITERATURE CITED

Forest Health Monitoring (FHM). 2015. Evaluation monitoring. https://www.fs.fed.us/foresthealth/fhm/em/index.shtml. [Date accessed: August 5, 2019].

SECTION 3.

Evaluation Monitoring Project Summaries

CHAPTER 8.

Assessment and Etiology of Thousand Cankers Disease within the Native Range of Black Walnut (*Juglans nigra*)

Jennifer Juzwik
Melanie Moore
Geoffrey Williams
Matthew Ginzel

INTRODUCTION

Thousand cankers disease (TCD) is caused by a fungus (*Geosmithia morbida*) vectored by the walnut twig beetle (WTB), *Pityophthorus juglandis* (Coleoptera: Curculionidae: Scolytinae). This pest complex was first described in Colorado where it has caused the widespread death of eastern black walnut (*Juglans nigra*) along the Front Range and throughout the Western United States (Tisserat and others 2009). In August 2010, TCD was found in Knoxville, TN—the first discovery of the disease within the native range of black walnut (Grant and others 2011). Since that time, six other States in the Midwest and East have detected the beetle or pathogen on black walnut trees: Virginia, Pennsylvania, North Carolina, Maryland, Ohio, and Indiana (Juzwik and others 2015, Seybold and others 2012).

In 2012, the Ohio Department of Natural Resources captured eight adult beetles near a veneer mill in Butler County. Hundreds and/or thousands of WTB adults were captured during more intensive surveys conducted in the subsequent year. The outbreak was centered on several dead and dying black walnut trees in adjoining residential neighborhoods (Ashwood Knolls and Avalon Station) approximately 5 km from the mill. These trees exhibited advanced symptoms of TCD, including yellowing and thinning canopies and branch dieback. In Indiana, a trap tree survey conducted in 2011 detected no WTB but rather recovered *G. morbida* associated with a weevil, *Stenomimus pallidus*, at one site in the Yellowwood State Forest in Brown County, IN (Juzwik and others 2015). This was the first report of *G. morbida* from Indiana and the first report of the fungus from an insect other than WTB. Although the pathogen responsible for TCD is present at the site, the trees remain non-symptomatic at this time. From a similar survey conducted on TCD-symptomatic trees in Butler County, OH, in 2014, *G. morbida* was recovered from *Xyleborinus saxeseni*, *Xylosandrus crassiusculus*, and *S. pallidus* (Juzwik and others 2016). This association of *G. morbida* with beetles other than WTB suggests that they may be capable of transmitting the fungus in areas affected by TCD. In the Western States, eastern black walnuts are typically killed within 2 years after initial symptoms appear; however, smaller trees and those growing on poor sites decline more rapidly (Tisserat and others 2009). Recent observations in Knoxville, TN, and Richmond, VA, suggest, however, that TCD progresses more slowly within the native range of eastern black walnut, and some trees may even appear to survive the disease (Griffin 2015).

The goal of this study was to monitor the health of TCD-symptomatic trees and surrounding trees and assess the roles of *G. morbida* and other fungal pathogens in affecting tree health. This information is essential for understanding the etiology and potential threat of this disease complex within the native range of eastern black walnut. In the first objective, we monitored changes in forest health at Yellowwood State Forest, Brown County, IN, and Butler County, OH, where *G. morbida* alone and TCD, respectively, have been found.

Specifically, we assessed the change in canopy condition of trees at varying spatial scales from the epicenter of the TCD outbreak in Butler County, OH. We also compared the change in canopy condition of trees from the epicenter to other parts of Butler County and an area with *G. morbida* and no WTB (i.e., Indiana).

For the etiology objective, we evaluated the potential for *G. morbida* and other fungal pathogens of walnut to cause branch dieback. Specifically, field experiments were established in 2015 to determine (1) whether multiple inoculations with *G. morbida* in the absence of the WTB can lead to branch death over two growing seasons, and (2) the relative virulence of *G. morbida* compared to other known or putative canker pathogens of eastern black walnut within its native range. It is important to understand the role of *G. morbida* in causing branch dieback and tree death in TCD-affected trees so that effective and cost-efficient control methods can be devised. Other native, canker-causing fungi of eastern black walnut have been found to colonize TCD-symptomatic trees (McDermott-Kubeczko 2015, Montecchio and others 2015). Known canker pathogens of eastern black walnut that occur in the native range of the species include several *Fusarium* species and *Botryosphaeria dothidea* (Carlson and others 1993, Pijut 2005). Other fungi (e.g., *Diplodia seriata*, *Biscogniauxia atropunctata*) are known to cause bark diseases on other hardwood species and have been found on eastern black walnut, but their pathogenicity on walnut has not been proven.

METHODS AND RESULTS

Assessment (Objective 1)

Data Collection—During late spring 2015, we marked and collected standard tree measurements for 61 eastern black walnuts growing at five sites in Butler County, OH. At Yellowwood State Forest (Brown County, IN), we marked 40 black walnuts growing along four transects in an unmanaged plantation where *G. morbida* has been recovered. Over the next 3 years, we evaluated these trees for (1) symptoms of TCD and (2) the percentage of live crown (to the nearest 10 percent) during the growing season (June–September). Although three trees were symptomatic for TCD at Ashwood Knolls (Butler County, OH), percent live crown at each site generally ranged from 70 to 90 percent at the beginning of the study. From 2015–2017, we visually assessed the percent live crown of each tree every other week from June–September. In 2018, visual assessments of percent live crown were conducted on a monthly basis throughout the growing season. Only the crown condition assessment nearest to July 1 each year was used in our analysis, because that time corresponded to when crowns were fullest during the growing season. To detect any WTB at each site, two pheromone-baited four-unit funnel traps were deployed and serviced at the same interval as crown ratings.

Analysis of Percent Live Crown—To determine whether there was a significant difference in the rate of crown deterioration of TCD-symptomatic trees ($n = 3$) compared to nearby non-symptomatic trees in the TCD

epicenter (i.e., Avalon Station and Ashwood Knolls, $n = 9$) and the rest of Butler County, OH ($n = 49$), data were subsetted and compared at three levels of spatial scale (table 8.1). A fourth level of analysis was included to compare rate of change in crown condition between Butler County, OH, where TCD was present ($n = 12$), other sites in Butler County ($n = 49$), and Yellowwood State Forest (Brown County, IN), where only *G. morbida* is present ($n = 40$).

All data analysis was performed in R (R Foundation for Statistical Computing, Vienna). At each spatial scale, cumulative probit-link mixed model regressions were fitted with the Laplace approximation to test for significance of interaction between year and group. Individual trees were treated as a random effect, and year and group as fixed effects. A significant improvement in model fit upon inclusion of interaction between year and group in a likelihood ratio test indicated a difference in rate of change in crown condition between sites. Interannual changes in crown condition between years within groups were analyzed with a Kruskal-Wallis rank-sum test.

Results—At all four levels of analysis, the inclusion of random terms improved model fit (table 8.1). In Ashwood Knolls and adjacent Avalon Station, TCD-symptomatic trees had a marginally lower percent live crown across years in the interactive model ($z = -1.82$, $p = 0.07$) and higher rate of annual deterioration in crown condition ($LR = 7.29$, $p < 0.01$). Overall rate of percent live crown loss in Ashwood Knolls and Avalon Station was not significantly different from the rest of Butler County, OH ($LR = 2.44$, $p = 0.12$). However, there was a significant decrease in crown condition overall in Butler County, OH ($z = -2.67$, $p < 0.01$). When TCD-symptomatic trees in Ashwood Knolls and

Table 8.1—Spatial levels of analysis used in modelling percent of live crown in *Juglans nigra* at varying spatial scales in areas with thousand cankers disease (TCD)[a]

				Psuedo-R^{2} [b]	
Spatial level of analysis	Groups compared in the analysis			Fixed	Fixed + random
Neighborhood: by tree	TCD-symptomatic	Other trees in epicenter		0.63	0.68
County: by tree	TCD-symptomatic	Other trees in Butler County, OH		0.23	0.55
County: by neighborhood	TCD epicenter	Other trees in Butler County, OH		0.01	0.51
TCD epicenter; Butler County, OH; Brown County, IN	TCD epicenter	Other trees in Butler County, OH	Yellowwood State Forest (Brown County, IN)	0.02	0.47

[a] In Butler County, OH, both the vector and pathogen were present, whereas only the TCD pathogen was present in Brown County, IN.
[b] Calculated using Nagelkerke method (1991).

Avalon Station were compared to neighboring trees and the rest of Butler County, OH, crown loss was significantly faster in TCD-symptomatic trees (LR = 4.3, p <0.01), and TCD-symptomatic trees had lower average crown condition across years (z = -2.30, p = 0.02). Across sites in Butler County, OH, and Brown County, IN, no parameters for main or interactive effects were significant (p >0.1).

The only significant interannual changes in crown condition detected between two subsequent years within a group were a significant improvement in percent of live crown in non-symptomatic trees in Avalon Station and Ashwood Knolls from 86.7 ± 2.9 to 95.6 ± 2.4 between 2015 and 2016 (fig. 8.1A) and a decrease in overall percent live crown outside of the TCD epicenter in Ohio from 85.1 ± 1.7 to 74.9 ± 3.0 between 2017 and 2018 (fig. 8.1B).

Etiology: Branch Health and Canker Development (Objective 2)

Methods—Nineteen eastern black walnut trees (18- to 60-cm diameter at breast height [d.b.h.]) either open-grown or on forest edge in three Butler County, OH, metro parks and 20 eastern black walnut trees (25- to 47-cm d.b.h.) in a plantation (established 1977) in Brown County, IN, were identified for two experiments in each location. Four branches on nine trees in Ohio and five branches on 10 trees in Indiana were selected and randomized to receive one of four/five treatments in mid-June 2015. Treatments consisted of inoculations with three or four fungal species and a water control. Inocula of locally obtained isolates of *F. solani*, *D. seriata*, and *G. morbida* were used in both States. In addition, *B. dothidea* was included in the Indiana trials. The experiments were repeated with the same treatments in mid-September 2015 but on 10 trees in each location. Aliquots (0.2 ml) of aqueous suspensions of fungal spores or of sterile distilled water were placed in 24 to 42 drilled holes (10-mm diameter and depth to outermost sapwood) of healthy (>95 percent leaves green) branches (5 to 8 cm in diameter) with number of holes dependent on branch diameter. Inoculations were designed to result in a density of one canker per 12-cm^2 bark surface area. Thus, all holes were made in a 30- to 40-cm length on each branch to achieve this density. Following inoculation, holes were covered with epoxy resin and the branches marked with brightly colored plastic flagging. The condition of each branch was rated in mid-June and early to mid-September of the two growing seasons following treatment. Branches were harvested on the final monitoring date: mid-September 2016 for mid-June 2015 inoculation trials and mid-September 2017 for mid-September 2015 inoculations. The ~40-cm-long segment of each inoculated branch area was cut, placed in two poly-bags, and stored in sealed plastic containers at 2 °C until processed. In the laboratory (Minnesota Agricultural Experiment Station Biosafety Level 2 Facility, University of Minnesota, St. Paul), bark was carefully removed to expose any cankers or dead tissue around each inoculation point and data on canker sizes recorded. Tissue from margins of each canker was plated on 1/4-strength potato

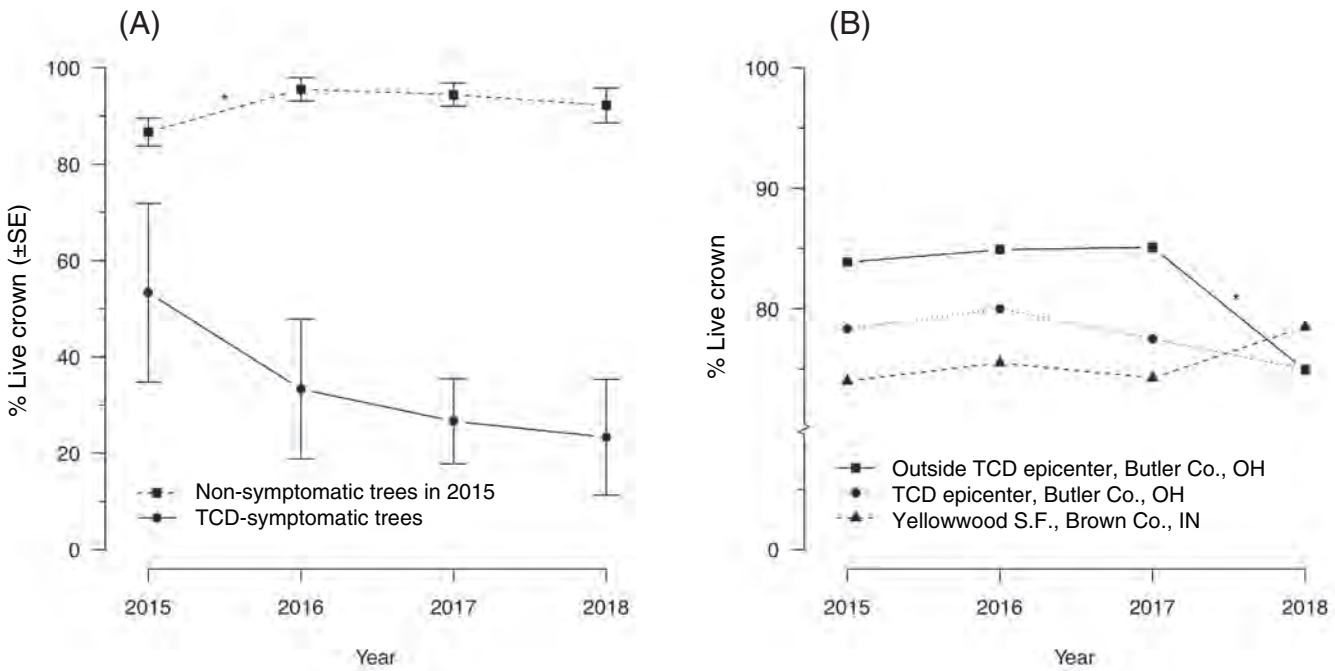

Figure 8.1—Average percent live crown of Juglans nigra. *Asterisk indicates significant change between years (Kruskal-Wallis rank sum test, p <0.05). (A) Thousand cankers disease (TCD)-symptomatic and non-symptomatic trees in the TCD epicenter (Ashwood Knolls and Avalon Station) in Butler County, OH. (B) TCD epicenter compared to other sites in Butler County, OH, and sites in Brown County, IN.*

dextrose agar amended with chloramphenicol (100 mg/L) and streptomycin sulfate (100 mg/L) in attempts to recover the fungi originally applied. Fungi isolated were identified using cultural morphology, microscopic characteristics, and polymerase chain reaction (PCR) and DNA sequencing. Branch condition data and bark canker frequencies were subjected to log-linear modeling analyses using R (R Foundation for Statistical Computing, Vienna). Canker area data were also analyzed in R using mixed-effects models.

Results of June 2015 inoculation trials— Several branches died in each location over the two growing seasons; however, none had been inoculated with *G. morbida*. No differences ($p = 0.797$) were found for branch condition ratings over 15 months among treatments for both locations combined (data not shown). No differences were found in proportions of inoculation points with cankers or general necrosis (>0.25-cm^2 diameter) on branches across all treatments within each location (data not shown). Mean canker sizes in Indiana were

similar across treatments (fig. 8.2). In Ohio, the smallest mean canker sizes were found for control and *D. seriata* branches compared to those associated with *F. solani* isolates (*F. solani* species complex [FSSC] phylogenetic species 6 and 25) and *G. morbida* (p <0.001). No evidence of canker coalescence was observed for the latter treatment. The various fungi were recovered from associated, resultant cankers over a wide range of frequencies (data not shown).

Results of September 2015 inoculation trials—No branches died in response to inoculation in Ohio; however, one or two branches died in response to inoculation with three of four fungal treatments and the control, respectively, in Indiana. In general, the condition ratings for inoculated branches were similar to each other as they varied over 24 months within each location (data not shown), although the preponderance of ratings shifted from ≤5 percent to 10 to 20 percent for September compared to June inoculations. Although no differences were found in proportions of inoculation points with cankers or general necrosis across all treatments within each location, the proportions for September inoculation points were higher than those for June (p <0.0001). Mean canker sizes were lowest for water-inoculated branches (p = 0.0019) and similar (p = 0.992) for *D. seriata* and *B. dothidea* in Indiana (fig. 8.2). Furthermore, mean canker sizes were largest (average = 3.09 cm^2) on *G. morbida*-inoculated branches compared to *F. solani* branches and the other three treatments (p <0.001). In Ohio, mean canker sizes were lowest for water-inoculated branches (p <0.001) and similar for *D. seriata* and *F. solani* (p = 0.98). *G. morbida* inoculation also resulted in the largest mean canker sizes compared to those associated with all other treatments (p <0.001). Coalescing of *G. morbida* cankers was observed along the longitudinal axis of inoculated branch segments on 44 percent of branches from Indiana and Ohio. Bark splitting extending for most of the branch segment length was observed for 39 percent of the *G. morbida* branches in both States and appeared to be caused by strong callus formation response of the host. However, *G. morbida* was infrequently recovered from the margin of cankers found on inoculated branches: 8.5 percent of assayed cankers per branch in Indiana and 1 percent of assayed cankers per branch in Ohio. In contrast, *F. solani* was commonly recovered, i.e., 84 percent of assayed cankers per branch in both States.

DISCUSSION

Walnut twig beetle and/or *G. morbida* have been detected in isolated locations across the native range of eastern black walnut, but establishment of WTB and accompanying mortality have been less pronounced than in the Western United States. Our investigation of tree decline at varying spatial scales from a TCD epicenter revealed that the disease did not spread to neighboring trees and there was no new TCD development. Thousand cankers disease-symptomatic trees had a lower percent live crown rating and higher rate of deterioration in crown condition compared to neighboring trees

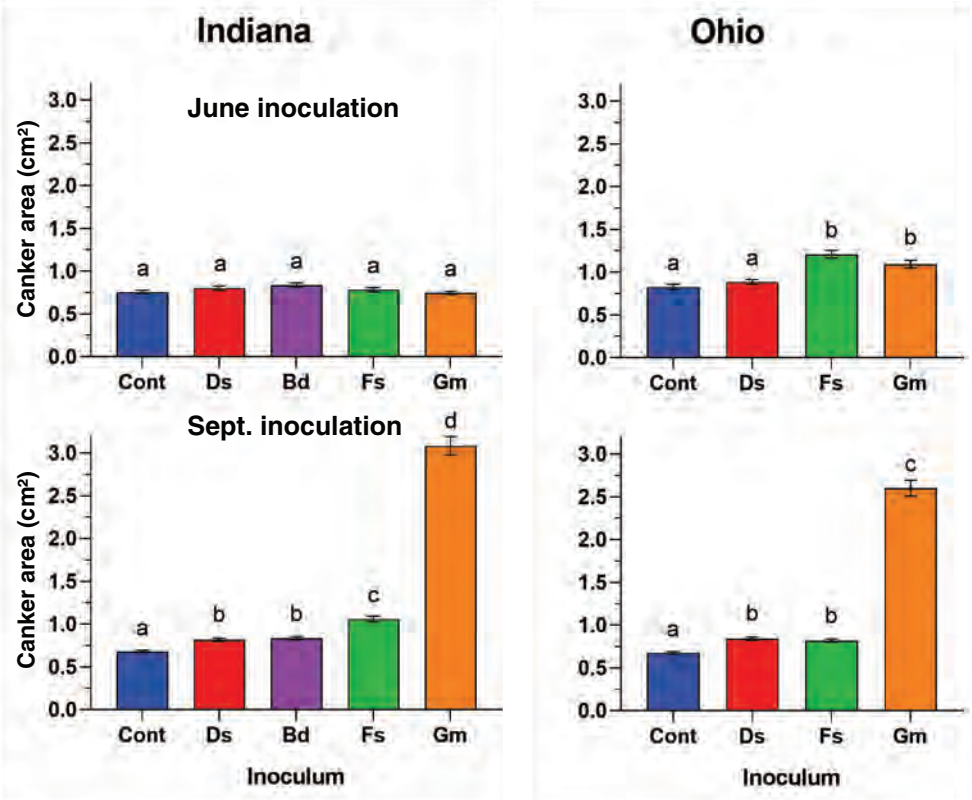

Figure 8.2—Mean size (cm^2) of cankers of field-grown Juglans nigra *in two Eastern States 15 (June) and 24 (September) months after multiple inoculations with known or putative canker-causing fungi. Inoculum used: CON = water control; DS =* Diplodia seriata*; BD =* Botryosphaeria dothidea*; FS =* Fusarium solani*; GM =* Geosmithia morbida*. Error bars are standard error. Bars with the same letter are not significantly different according to the Tukey least significant difference test, p <0.05.*

in the epicenter and the rest of Butler County, OH, suggesting that the disease was localized to those individual trees. In fact, disease symptoms appeared on no new trees throughout our study, and the rate of crown decline in trees at the epicenter as a whole did not differ from that of other study sites in Butler County, OH. Focal trees at our site in Brown County, IN, were in a generally poorer condition than those in Ohio, which can likely be attributed to the suppressed or codominant position of these trees and the presence of woody invasive plants within the 30-year-old unmanaged plantation.

Ecological factors, including environmental conditions or biotic interactions, likely play a role in the etiology of TCD. Based on a case study of two locations in the Eastern United States, Griffin (2015) attributed the rapid progression of TCD in the Western United States and resilience of eastern black walnut in the Eastern United States to abiotic factors, namely rainfall. Such climatic and ecological factors may have contributed to the improvement in crown condition in Avalon Station and Ashwood Knolls in 2015 and 2016 and the overall decline of crown condition in Ohio. Climate regimes in the Western and Eastern United States differ significantly with respect to total amount and the degree of seasonality in temperature, precipitation, and humidity. Climatic differences between the expanded and native ranges of eastern black walnut could affect growth and dispersal of *G. morbida* by modifying suitability for infection and canker development under the bark and influencing its competitive interactions with other fungi.

Multiple inoculations of eastern black walnut branches (5- to 8-cm diameter) in Indiana and Ohio with *G. morbida* in the absence of WTB pressure (survey data from P. Marshall, Indiana Department of Natural Resources, and D. Kenny, Ohio Department of Agriculture) did not result in any branch death in Ohio and one dead branch in Indiana. The inoculation density used was based on numbers of WTB galleries and/or *G. morbida* cankers counted on peeled branches of TCD-symptomatic eastern black walnut in a Butler County, OH, site in late summer 2014 and 2015. Walnut twig beetle populations had dropped to zero detectable levels in 2014 and 2015, and a single beetle was captured in Ohio each year from 2016–2018.[1] The canker densities documented ranged from a mean of 4 to 20 (with or without WTB galleries) per 100 cm^2 of bark surface area. Thus, the target density of this study (8.5 cankers/100 cm^2) was reasonable and a valid test for the first objective. To our knowledge, no other field tree inoculations with *G. morbida* have used more than three points per branch or stem.

A clear difference in the size of cankers resulting from *G. morbida* inoculations was found for late summer versus late spring or early summer inoculation dates. The range of canker areas (for measurable cankers) for the latter inoculation time ranged from 0.26 to 2.22 cm^2 in Indiana and 0.09 to 3.73 cm^2

[1] Personal communication. 2019. Daniel Kenny, Plant Health Administrator, Ohio Department of Agriculture, 8995 E. Main Street, Reynoldsburg, OH 43068.

in Ohio compared to that of canker areas for mid-September inoculations (0.17 to 12.18 cm^2 for Indiana and 0.34 to 8.07 cm^2 for Ohio). Previous studies of canker development by other pathogens have demonstrated effects of season on tree susceptibility to infection and/or canker development (e.g., *Ophiognomonia clavigignenti-juglanacearum*) (Ostry and Moore 2008). The mean canker areas for our June 2015 trials fall within the range of those reported by Sitz and others (2017) for *G. morbida* field inoculations of eastern black walnut saplings in Colorado. In the latter case, eight genetically distinct isolates of *G. morbida* were used to inoculate three wounds made along a 20-cm length of a branch above a stem crotch on each tree and resulting cankers measured 9 weeks later. The maximum sizes of *G. morbida* cankers found in our September 2015 inoculation trials were difficult to measure because coalescence with adjacent cankers occurred (along longitudinal axis of branches).

Of the two or three other pathogens compared to *G. morbida*, only the *F. solani* isolates (FSSC phylogenetic species 6 and 25) used in Ohio for the June 2015 inoculation trial caused cankers of significantly larger size than controls and *D. seriata*. The relative size of *F. solani* cankers found 15 months later were 10 percent larger than cankers caused by *G. morbida*, but differences were not significant. In a Colorado trial comparing relative *F. solani* canker sizes to those of *G. morbida* 9 weeks after June inoculation, the *F. solani* cankers were 47 and 37 percent smaller than *G. morbida* cankers in August 2014 and August 2015, respectively (Sitz and others 2017). The phylogenetic species used in the Colorado and in our trials are known to co-occur with *G. morbida*, and their natural occurrence may contribute to size of canker development on eastern black walnut (Montecchio and others 2015). Results of coinoculation of eastern black walnut with *F. solani* FSSC 6 in Colorado did not yield a synergistic response in terms of canker size (Sitz and others 2017).

CONCLUSIONS

Our assessment study revealed no new symptomatic trees, and no adult WTB were captured throughout the course of study, suggesting that TCD does not progress in the absence of the primary vector. In fact, very few WTB have been captured in Ohio since the mass emergence in 2013. It appears that if mass attack is not followed by similar attacks in subsequent years that host responses may indeed prevent further development of cankers in absence of the WTB. Although *G. morbida* was isolated from ambrosia beetles and weevils at the TCD epicenter in Ohio and from weevils at the site in Indiana (Juzwik and others 2015, 2016), our findings support the hypothesis that this assemblage of alternate vectors has little impact on disease severity and spread.

Based on the results of our etiology experiments, we speculate that branch dieback could occur following multiple years of mass attack of eastern black walnut branches by WTB, particularly in late summer and early fall. However, if 1 year of mass attack is not followed by similar attacks in subsequent years,

we speculate that host responses may indeed prevent further development of cankers in absence of the WTB as previously mentioned. This speculation is supported in part by the published field observations of arrested TCD symptom development in Tennessee and Virginia attributed to changes in precipitation patterns (Griffin 2015).

For more information, contact: Matthew Ginzel, mginzel@purdue.edu.

ACKNOWLEDGMENTS

We thank the following cooperators: Metroparks of Butler County, Ohio State Extension Butler County, Ross and Jaime Gille, Bill Barnett, Phil Marshall, and Vince Burkle. We also thank Paul Castillo, Emily Franzen, Gabriel Hughes, and Bridget Blood for their assistance in the field. Funding for this project was provided from USDA Forest Service Forest Health Monitoring–Evaluation and Monitoring (grant IN-15-071).

LITERATURE CITED

Carlson, J.E.; Mielke, M.E.; Appleby, J.E. [and others]. 1993. Survey of black walnut canker in plantations in five Central States. Northern Journal of Applied Forestry. 10: 10–13.

Grant, J.F.; Windham, M.T.; Haun, W.G. [and others]. 2011. Initial assessment of thousand cankers disease on black walnut, *Juglans nigra*, in eastern Tennessee. Forests. 2: 741–748.

Griffin, G.J. 2015. Status of thousand cankers disease on eastern black walnut in the Eastern United States at two locations over 3 years. Forest Pathology. 45: 203–214.

Juzwik, J.; Banik, M.T.; Reed, S.E. [and others]. 2015. *Geosmithia morbida* found on weevil species *Stenomimus pallidus* in Indiana. Plant Health Progress. 16: 6–10.

Juzwik, J.; McDermott-Kubeczko, M.; Stewart, T.J.; Ginzel, M.D. 2016. First report of *Geosmithia morbida* on ambrosia beetles emerged from thousand cankers-diseased *Juglans nigra* in Ohio. Plant Disease. 100(6): 1238–1238. https://doi.org/10.1094/PDIS-10-15-1155-PDN.

McDermott-Kubeczko, M. 2015. Fungi isolated from black walnut branches in Indiana and Tennessee urban areas. St. Paul, MN: University of Minnesota. 117 p. M.S. thesis.

Montecchio, L.; Faccoli, M.; Short, D.P.G. [and others]. 2015. First report of *Fusarium solani* phylogenetic species 25 associated with early stages of thousand cankers disease on *Juglans nigra* and *Juglans regia* in Italy. Plant Disease. 99: 1183.

Nagelkerke, N.J. 1991. A note on a general definition of the coefficient of determination. Biometrika. 78: 691–692.

Ostry, M.E.; Moore, M. 2008. Response of butternut selections to inoculation with *Sirococcus clavigignenti-juglandacearum*. Plant Disease. 92: 1336–1338.

Pijut, P.M. 2005. Diseases in hardwood tree plantings. FNR-221. West Lafayette, IN: Hardwood Tree Improvement and Regeneration Center. 14 p. https://www.extension.purdue.edu/extmedia/FNR/FNR-221.pdf. [Date accessed: May 9, 2019].

Seybold, S.J.; Coleman, T.W.; Dallara, P.L. [and others]. 2012. Recent collecting reveals new state records and geographic extremes in the distribution of the walnut twig beetle, *Pityophthorus juglandis* Blackman (Coleoptera: Scolytidae), in the United States. Pan-Pacific Entomologist. 88: 277–280.

Sitz, R.A.; Luna, E.K.; Caballero, J.I. [and others]. 2017. Virulence of genetically distinct *Geosmithia morbida* isolates to black walnut and their response to coinoculation with *Fusarium solani*. Plant Disease. 101: 116–120.

Tisserat, N.; Cranshaw, W.; Leatherman, D. [and others]. 2009. Black walnut mortality in Colorado caused by the walnut twig beetle and thousand cankers disease. Plant Health Progress. 10(1): 1-10. DOI:10.1094/PHP-2009-0811-01-RS.

CHAPTER 9.

Woodboring Beetle Colonization of Conifers Killed by Fire and Bark Beetles: Implications for Forest Restoration and Black-backed Woodpecker Conservation

Chris Ray
Daniel R. Cluck
Robert L. Wilkerson
Rodney B. Siegel
Angela M. White
Gina L. Tarbill
Sarah C. Sawyer
Christine A. Howell

INTRODUCTION

Woodboring beetles (Cerambycidae and Buprestidae) are common in coniferous forests of the Western United States, where they are considered secondary forest pests because they generally colonize trees killed or weakened by disturbance (Furniss and Carolin 1977), including wildfire and outbreaks of primary forest pests such as bark beetles (Scolytinae). Disturbances caused by wildfire and bark beetle outbreak (BBO) are expected to be increasingly common in the coming decades (Bentz and others 2010, Kitzberger and others 2017), providing more potential habitat for woodboring beetles. Although woodboring beetle activities can reduce timber values (Lowell and Cahill 1996), woodborers also contribute to ecological services such as snag decomposition and nutrient recycling (Kahl and others 2017), and serve as prey for early-seral habitat specialists like the black-backed woodpecker (*Picoides arcticus*), a species of management interest (Siegel and others 2018) that feeds primarily on the larvae of woodboring beetles (Murphy and Lehnhausen 1998). Understanding how woodborers respond to different types of forest disturbance and stand characteristics is important for predicting the response of forest communities to changes in the disturbance regime, and for designing restoration and management efforts that maximize the ecological services provided by woodborers.

Larval woodborers mature in 1 or more years depending on environmental conditions (Kariyanna and others 2017), feeding within the cambium during early development and later tunneling into sapwood and heartwood. Within trees colonized by bark beetles, there is some evidence that bark beetles and woodborers compete for phloem (Coulson and others 1976, Foelker and others 2018) and that woodborers consume bark beetles during the larval stage (Dodds and others 2001). Adults emerge and fly during the warmer months, using chemical cues to seek out recently dead or weakened trees (Kelsey and Joseph 2003, Miller 2006). Some woodborers locate burned trees by sensing heat and/or smoke (Schmitz and others 1997, Schütz and others 1999). Females deposit eggs in bark crevices, under bark scales, or in small cut niches, and have been observed to avoid oviposition where bark beetle activity is high (Gardiner 1957).

Research on woodboring beetles has concentrated primarily on native species that cause damage to wood products (Álvarez and others 2015) or exotic and invasive species that disrupt entire ecosystems (Aukema and others 2010, 2011). Much less is known about how native woodboring beetles colonize and use trees damaged by fire and primary bark beetles, and how woodborers respond to the timing and severity of disturbance, forest composition and structure, host tree attributes, and interspecific competition (Brin and Bouget 2018, Costello 2013, Costello and others 2011). To inform forest management strategies designed to maintain processes dependent on woodborers, we characterized woodborer activity in 16 sites representing 11 wildfires and five BBOs. Project objectives were as follows: (1) trap

adult beetles to identify and quantify the species of woodboring beetles inhabiting post-wildfire stands and bark beetle-impacted stands; (2) sample beetle larvae to identify and quantify the species of woodboring beetles colonizing fire-killed conifers and unburned bark beetle-killed conifers (primarily yellow pine [*Pinus* spp.] and true fir [*Abies* spp.]); (3) in burned areas, determine if the level of woodborer colonization and activity is associated with the severity of fire injury, tree species, tree diameter, stand-level burn severity, seasonal timing of the fire, and the number of years post-fire; (4) in unburned, beetle-killed areas, determine whether black-backed woodpeckers use bark beetle-killed stands in elevated densities compared to surrounding forest; (5) relate woodboring beetle activity to observed patterns of black-backed woodpecker occupancy and foraging habitat selection; and (6) use the above information to help guide the formulation of forest restoration and salvage logging treatments that effectively address the needs of woodpecker prey species.

METHODS

As detailed in Ray and others (2019), during 2015–2016 we surveyed 11 burned and five BBO sites within Sierran mixed conifer and eastside pine forests in the greater Sierra Nevada region, using a plot-within-transect design. Burned sites were selected using U.S. Department of Agriculture Forest Service, Region 5 Vegetation Burn Severity data (USDA Forest Service, Region 5 2018) and represented a range of fire ages (1–8 years post-burn) and ignition dates (July 5–September 13). Bark beetle outbreak sites were identified as areas of high tree mortality occurring in the 2–3 years prior to 2016, using the 2015 Region 5 Aerial Detection Survey data layer (USDA Forest Service, Region 5 2015). Within each site, transect placement was stratified by two tree size classes and three levels of burn severity: small (15–28-cm diameter at breast height [d.b.h.]) or large (>28-cm d.b.h.) tree size classes adapted from the California Wildlife Habitat Relationships classification system (California Department of Fish and Game 2005), and low, moderate, or high burn severity classes according to the Relative Differenced Normalized Burn Ratio (RdNBR). Each 100-m transect consisted of three variable-radius plots (VRPs) with centers at 0, 50, and 100 m. We sampled up to 12 transects per site, for a total of 159 transects and 477 VRPs. Each VRP was centered on a panel trap for adult beetles. To avoid attraction bias, traps were unbaited and positioned at least 2 m from the closest tree. Traps were visited every 2 weeks during an 8-week trapping period.

Adult activity per plot was defined as the number of captures per trap visit for each woodboring beetle taxon analyzed. Larval woodborer activity was measured in bark quadrats (15 cm × 15 cm) on the north and south sides of up to six (mean ± standard error [SE] = 5.19 ± 0.09) snags central to each VRP.

Larval activity per quadrat ranged 0–4 and was defined as the number of quarter-quadrats containing signs characteristic of any woodboring beetle larvae (Furniss and Carolin 1977). Bark quadrats were also sampled for

bark beetle presence, bark condition, and char depth class (Ryan 1982). Snags containing bark quadrats were scored for several characteristics including species, char height, d.b.h., percent needles retained, and woodpecker sign.

Woodpecker foraging activity per snag ranged 0–6 and was defined as the number of strata containing excavations or flaked bark characteristic of woodpecker foraging, where strata (n = 6) were the top, middle, and bottom thirds of the north- and south-facing sides of each snag. In each VRP, we also recorded all tree species, live tree basal area (BA), and snag BA.

Each of the three response variables defined above (adult activity, larval activity, or woodpecker foraging activity) was related to potential predictor variables (as suggested in objectives 1–5) using generalized linear mixed-effects models, including nested random effects of site, transect, plot, and snag as appropriate to account for the spatial dependence among samples and (for adult models) repeated measures at each trap. Null models (random effects only) and alternative models of each response were ranked using an information criterion (AIC_c or, for over-dispersed Poisson models of adult activity, $QAIC_c$; Burnham and Anderson 2002). Data from burned sites were modeled separately to assess effects of burn severity and timing not applicable in BBO sites.

RESULTS

We identified 10,412 adult insect captures belonging to six families, including 1,718 Buprestidae and 1,277 Cerambycidae. The most frequently captured buprestids were *Cypriacis aurulenta* (n = 466), *Melanophila consputa* (n = 200), and *Chalcophora angulicollis* (n = 193), while *Xylotrechus longitarsus* (n = 190), *Monochamus obtusus* (n = 89), and *Ortholeptura valida* (n = 88) were most frequent among cerambycids. Larval activity was evident mainly from galleries, frass/boring dust, and exit/transit holes. These indirect signs were sufficient for distinguishing larval woodborers from other taxa but often insufficient for differentiating woodborers by family due to intermingled galleries of unrelated taxa and deterioration of the inner bark and sapwood interface on older snags.

Patterns of adult woodborer activity varied by taxon (Ray and others 2019). The activity of adult buprestids was significantly higher at burned than BBO sites, according to null models fitted for each analysis (fig. 9.1A). Adding a fixed effect of burn severity class showed that buprestid activity also increased significantly with moderate and high RdNBR (fig. 9.1B). The five most highly ranked models of adult buprestid activity in burned sites included significant (α = 0.05, p <0.05) linear and quadratic effects of ignition date indicating a peak in adult activity at fires ignited mid-season, along with a significant decline in activity with fire age, and significant positive effects of snag BA and char height in the VRP. In BBO sites, the top-ranked model of adult buprestid activity included a significant negative effect of live tree BA, suggesting buprestids were most attracted to areas with few surviving trees, a pattern upheld by the second-ranked model, which included a significant positive effect of bark beetle

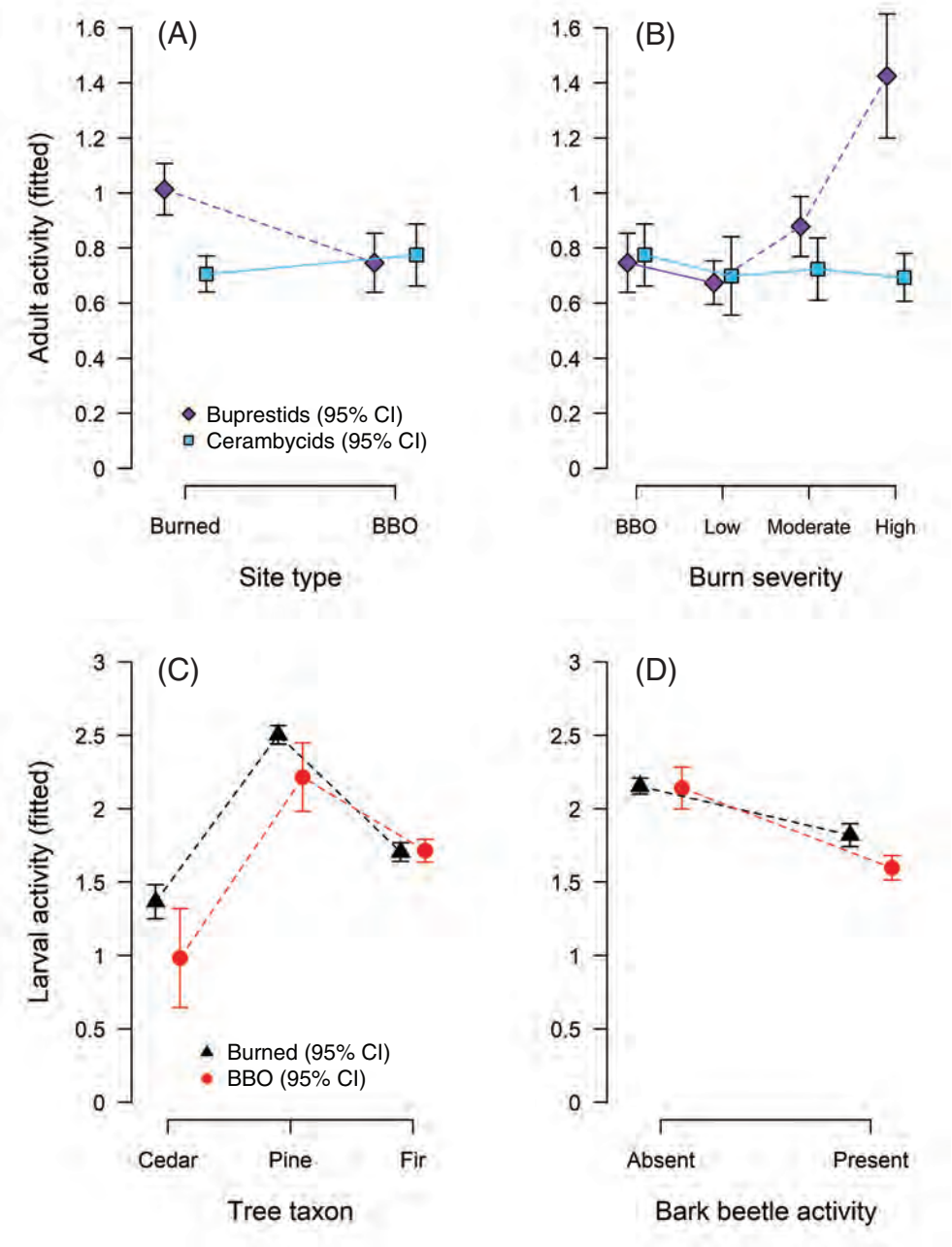

Figure 9.1—Fitted mean woodborer activity and 95-percent confidence interval (CI) from mixed-effects models, showing apparent effects of disturbance type (A) and severity (B) on adult buprestid activity (abundance index), and apparent effects of tree taxon (C) and localized bark beetle sign (D) on larval woodborer activity. Within each panel, lines join results for a given taxon, and solid lines join means that do not differ significantly. In (A), adult datasets from two taxa and two site types were each fit to a null model accounting for nested random effects of site, transect, and plot. In (B), a fixed effect of burn severity was added to the null model of data from burned sites for comparison with unburned (BBO) sites. In (C) and (D), larval data from two site types were each fit to a model with nested random effects of site, transect, and tree plus one fixed effect of host tree taxon (C) or bark beetle activity (D).

activity. In contrast, cerambycid activity was not explained by metrics of disturbance intensity. The top-ranked model of adult cerambycid activity in burned sites was the null model, and the top three models in BBO sites (only weakly supported relative to the null model) included significant negative effects of incense-cedar dominance, number of broken-topped trees, and mean d.b.h. across the VRP.

Larval woodborer activity also responded less to disturbance type and severity than to stand and tree characteristics. Significant differences in larval activity by host tree taxon were much greater than any differences by disturbance type (fig. 9.1C). We also found evidence for negative effects of bark beetle activity on larval woodborer activity in both burned and BBO sites (fig. 9.1D). The top-ranked models of larval activity in both burned and BBO sites included significant negative effects of bark beetle sign presence within the bark quadrat. Other significant effects in supported models of larval activity in burned sites included positive effects of smaller trees, southern bark aspects, and yellow pine species as the host tree taxon, and (like adult buprestids in burned sites) negative effects of linear and quadratic ignition date. In BBO sites, other significant effects in supported models suggested higher larval activity in more advanced stages of an outbreak, such as negative effects of percent needles retained (Ray and others 2019).

Woodpecker foraging activity was found on a greater proportion of snags in burned sites (95 percent confidence interval = 0.63–0.71) than BBO sites (0.50–0.62), and on a greater proportion of the sampling strata within each snag in burned sites (0.43–0.51) than in BBO sites (0.29–0.41). Regardless of disturbance type—but especially in burned sites—models of woodpecker foraging activity that included a fixed effect of larval woodborer activity ranked higher than null models of woodpecker foraging activity ($\Delta AIC_c > 2$), and the fitted effect of larval activity was significantly positive in these models.

DISCUSSION

Given the potential for ecological and economic impacts of many woodborer species, characterizing woodborer responses to stand conditions could help guide the management of disturbed forests. Post-disturbance forest management often involves multiple objectives, such as recovering the economic value of dead trees (Eklund and others 2009), mitigating hazards associated with disturbance, facilitating reforestation (Bohlman and others 2016, Collins and Roller 2013), reducing fuel levels and the risk of type conversion (Coppoletta and others 2016), and providing a diversity of wildlife habitats (White and others 2016). Achieving these objectives might be facilitated by manipulating woodborer impacts on woody fuel decomposition, nutrient cycling, and succession as well as the availability of woodboring larvae as prey for other species. The range of woodborer responses we observed suggests that managing for a diversity of disturbance types and severity will support a diverse woodborer community.

The relationships we found broadly support results or hypotheses from previous research on these taxa, such as taxon-specific differences in woodborer response to burn severity, apparent competition between woodborer and bark beetle larvae, and woodpecker response to larval woodborers as a prey resource. We also found preliminary evidence that diurnal warming of the cambium might enhance larval growth and activity on the south sides of smaller diameter trees, and that woodborer dispersal might coincide with the middle of the fire season, such that fires ignited early or late in the season will be colonized by fewer woodborers. If the latter result proves to be general, the current trend toward a longer fire season (Balch and others 2017) might not translate into larger populations of woodboring beetles. However, the relationships we found should be investigated for generality in other regions and across a diversity of fire ages and outbreak sites, to facilitate inferences currently constrained by the naturally high covariance and spatial clustering in values of key predictor variables.

CONCLUSIONS

Our results suggest a dynamic process of local initiation and accumulation of woodborer activity that likely leads to temporal trends in the faunal communities supported by larvae and adults as prey and agents of tree decomposition. Woodboring beetle activity at our study sites was often similar between burned stands and unburned stands damaged by bark beetles but varied dramatically with stand composition, burn severity, and bark beetle activity in each type of disturbance, suggesting management interventions that might effectively promote successional processes and provide prey for wildlife species like the black-backed woodpecker. Effects of these processes on snag longevity and woodpecker activity should be further explored to inform management of disturbed forest stands.

For more information, contact: Chris Ray, cray@birdpop.org.

LITERATURE CITED

Álvarez, G.; Ammagarahalli, B.; Hall, D.R. [and others]. 2015. Smoke, pheromone and kairomone olfactory receptor neurons in males and females of the pine sawyer *Monochamus galloprovincialis* (Olivier) (Coleoptera: Cerambycidae). Journal of Insect Physiology. 82: 46–55.

Aukema, J.E.; Leung, B.; Kovacs, K. [and others]. 2011. Economic impacts of non-native forest insects in the continental United States. PLOS ONE. 6: e24587.

Aukema, J.E.; McCullough, D.G.; Von Holle, B. [and others]. 2010. Historical accumulation of nonindigenous forest pests in the continental United States. BioScience. 60: 886–897.

Balch, J.K.; Bradley, B.A.; Abatzoglou, J.T. [and others]. 2017. Human-started wildfires expand the fire niche across the United States. Proceedings of the National Academy of Sciences. 114: 2946–2951.

Bentz, B.J.; Régnière, J.; Fettig, C.J. [and others]. 2010. Climate change and bark beetles of the Western United States and Canada: direct and indirect effects. BioScience. 60: 602–613.

Bohlman, G.N.; North, M.; Safford, H.D. 2016. Shrub removal in reforested post-fire areas increases native plant species richness. Forest Ecology and Management. 374: 195–210.

Brin, A.; Bouget, C. 2018. Biotic interactions between saproxylic insect species. In: Ulyshen, M.D., ed. Saproxylic insects. Zoological monographs 1. Chamonix: Springer: 471–514. Chapter 14.

Burnham, K.P.; Anderson, D.R. 2002. Model selection and multi-model inference: a practical information-theoretic approach. 2d ed. New York: Springer-Verlag. 488 p.

California Department of Fish and Game. 2005. California Wildlife Habitat Relationships (CWHR), version 8.1 [now updated to version 9]. Sacramento, CA: California Department of Fish and Game. https://wildlife.ca.gov/Data/CWHR. [Date accessed: April 30, 2019].

Collins, B.M.; Roller, G.B. 2013. Early forest dynamics in stand-replacing fire patches in the northern Sierra Nevada, California, USA. Landscape Ecology. 28: 1801–1813.

Coppoletta, M.; Merriam, K.E.; Collins, B.M. 2016. Post-fire vegetation and fuel development influences fire severity patterns in reburns. Ecological Applications. 26: 686–699.

Costello, S.L. 2013. Emergence of Buprestidae, Cerambycidae, and Scolytinae (Coleoptera) from mountain pine beetle-killed and fire-killed ponderosa pines in the Black Hills, South Dakota, USA. The Coleopterists Bulletin. 67(2): 149–154.

Costello, S.L.; Negrón, J.F.; Jacobi, W.R. 2011. Wood-boring insect abundance in fire-injured ponderosa pine. Agricultural and Forest Entomology. 13: 373–381.

Coulson, R.N.; Mayyasi, A.M.; Foltz, J.L.; Hain, F.P. 1976. Interspecific competition between *Monochamus titillator* and *Dendroctonus frontalis*. Environmental Entomology. 5: 235–247.

Dodds, K.J.; Graber, C.; Frederick, M. [and others]. 2001. Intraguild predation by larval Cerambycidae (Coleoptera) on bark beetle larvae (Coleoptera: Scolytidae). Environmental Entomology. 30: 17–22.

Eklund, A.; Wing, M.G.; Sessions, J. 2009. Evaluating economic and wildlife habitat considerations for snag retention policies in burned landscapes. Western Journal of Applied Forestry. 24: 67–75.

Foelker, C.J.; Parry, D.; Fierke, M.K. 2018. Biotic resistance and the spatiotemporal distribution of an invading woodwasp, *Sirex noctilio*. Biological Invasions. 20: 1991–2003.

Furniss, R.L.; Carolin, V.M. 1977. Western forest insects. Misc. Publ. 1339. Washington, DC: U.S. Department of Agriculture Forest Service. 654 p.

Gardiner, L.M. 1957. Deterioration of fire-killed pine in Ontario and the causal wood-boring beetles. Canadian Entomology. 98: 241–263.

Kahl, T.; Arnstadt, T.; Baber, K. [and others]. 2017. Wood decay rates of 13 temperate tree species in relation to wood properties, enzyme activities and organismic diversities. Forest Ecology and Management. 391: 86–95.

Kariyanna, B.; Mohan, M.; Gupta, R. 2017. Biology, ecology and significance of longhorn beetles (Coleoptera: Cerambycidae). Journal of Entomology and Zoology Studies. 5: 1207–1212.

Kelsey, R.G.; Joseph, G. 2003. Ethanol in ponderosa pine as an indicator of physiological injury from fire and its relationship to secondary beetles. Canadian Journal of Forest Research. 33: 870–884.

Kitzberger, T.; Falk, D.A.; Westerling, A.L.; Swetnam, T.W. 2017. Direct and indirect climate controls predict heterogeneous early-mid 21st century wildfire burned area across western and boreal North America. PLOS ONE. 12: e0188486. doi:10.1371/journal.pone.0188486.

Lowell, E.C.; Cahill, J.M. 1996. Deterioration of fire-killed timber in southern Oregon and northern California. Western Journal of Applied Forestry. 11: 1251–30.

Miller, D.R. 2006. Ethanol and (-)-α-pinene: attractant kairomones for some large wood-boring beetles in Southeastern U.S.A. Journal of Chemical Ecology. 32: 779–794.

Murphy, E.C.; Lehnhausen, W.A. 1998. Density and foraging ecology of woodpeckers following a stand-replacement fire. Journal of Wildlife Management. 62: 1359–1372.

Ray, C.; Cluck, D.R.; Wilkerson, R.L. [and others]. 2019. Patterns of woodboring beetle activity following fires and bark beetle outbreaks in montane forests of California, USA. Fire Ecology. 15: 21.

Ryan, K.C. 1982. Techniques for assessing fire damage to trees. In: Lotan, J.E., ed. Fire—its field effects: proceedings of the 1982 joint fire council meeting. Missoula, MT and Pierre, SD: The Intermountain Fire Council and The Rocky Mountain Fire Council: 1–10.

Schmitz, H.; Bleckmann, H.; Mürtz, M. 1997. Infrared detection in a beetle. Nature. 386: 773–774.

Schütz, S.; Weissbecker, B.; Hummel, H.E. [and others]. 1999. Insect antenna as a smoke detector. Nature. 398: 298–299.

Siegel, R.B.; Bond, M.L.; Howell, C.A. [and others], eds. 2018. A conservation strategy for the black-backed woodpecker (*Picoides arcticus*) in California—version 2.0. Point Reyes Station, CA: The Institute for Bird Populations and California Partners in Flight. 66 p.

U.S. Department of Agriculture (USDA) Forest Service, Region 5. 2018. Vegetation Burn Severity data. https://www.fs.usda.gov/detail/r5/landmanagement/gis/?cid=stelprd3805100. [Date accessed: March 25, 2015].

U.S. Department of Agriculture (USDA) Forest Service, Region 5. 2015. R5 Aerial Detection Survey (ADS) data. https://www.fs.usda.gov/Internet/FSE_DOCUMENTS/stelprd3845073.zip. [Date accessed: April 1, 2016].

White, A.M.; Manly, P.N.; Tarbill, G.L. [and others]. 2016. Avian community responses to post-fire forest structure: implications for fire management. Animal Conservation. 19: 256–264.

ACKNOWLEDGMENTS

This research presented in this report was supported in part through the project "Forest Health Monitoring and Assessment" of Cost Share Agreement 18-CS-11330110-026 (June 15, 2018 through October 31, 2019) and the project "Forest Health Monitoring, Analysis, and Assessment" of Cost Share Agreement 19-CS-11330110-027 (May 23, 2019 through September 22, 2020) between North Carolina State University (this institution is an equal opportunity provider) and the U.S. Department of Agriculture Forest Service, Southern Research Station, Asheville, NC. This research was supported by funds provided by the U.S. Department of Agriculture Forest Service, Southern Research Station, Asheville, NC.

The editors and authors of this report thank the following for their reviews and constructive comments: Chris Asaro, Chandler Barton, Jennifer Costanza, John Coulston, Robbie Flowers, Denita Hadziabdic-Guerry, Joshua Halman, Dennis Haugen, Linda Haugen, Frank Krist, Philip Marshall, Karen Ripley, Todd Schroeder, Beth Schulz, Tom Smith, Rob Trickel, Kayanna Warren, and Denys Yemshanov.

AUTHOR INFORMATION

Sections 1 and 2, Forest Health Monitoring Research

Mark J. Ambrose, Research Assistant, North Carolina State University, Department of Forestry and Environmental Resources, Raleigh, NC 27695.

Erin M. Berryman, Quantitative Ecologist, Cherokee Nation Technologies, Fort Collins, CO 80526.

Julie C. Canavin, Research Assistant, North Carolina State University, Department of Forestry and Environmental Resources, Raleigh, NC 27695.

William M. Christie, Biological Scientist, U.S. Department of Agriculture Forest Service, Southern Research Station, Eastern Forest Environmental Threat Assessment Center, Asheville, NC 28804.

John W. Coulston, Supervisory Research Forester, U.S. Department of Agriculture Forest Service, Southern Research Station, Blacksburg, VA 24060.

Frank H. Koch, Research Ecologist, U.S. Department of Agriculture Forest Service, Southern Research Station, Eastern Forest Environmental Threat Assessment Center, Research Triangle Park, NC 27709.

Steven P. Norman, Research Ecologist, U.S. Department of Agriculture Forest Service, Southern Research Station, Eastern Forest Environmental Threat Assessment Center, Asheville, NC 28804.

Jeanine L. Paschke, Geographic Information Systems Analyst, Cherokee Nation Technologies, Fort Collins, CO 80526.

Kevin M. Potter, Research Professor, North Carolina State University, Department of Forestry and Environmental Resources, Raleigh, NC 27695.

Daniel R. Cluck, Entomologist, U.S. Department of Agriculture Forest Service, Forest Health Protection, Susanville, CA 96130.

Matthew Ginzel, Professor, Purdue University, West Lafayette, IN 47907.

Christine A. Howell, Research Program Manager-Ecosystem Function and Health, U.S. Department of Agriculture Forest Service, Pacific Southwest Research Station, Albany, CA 94710.

Jennifer Juzwik, Research Plant Pathologist, U.S. Department of Agriculture Forest Service, Northern Research Station, St. Paul, MN 55108.

Melanie Moore, Biological Technician, U.S. Department of Agriculture Forest Service, Northern Research Station, St. Paul, MN 55108.

Chris Ray, Research Ecologist, The Institute for Bird Populations, Point Reyes Station, CA 94956.

Sarah C. Sawyer, Regional Wildlife Ecologist, U.S. Department of Agriculture Forest Service, Pacific Southwest Region, Vallejo, CA 94592.

Rodney B. Siegel, Executive Director, The Institute for Bird Populations, Point Reyes Station, CA 94956.

Gina L. Tarbill, Research Fellow, U.S. Department of Agriculture Forest Service, Pacific Southwest Research Station, Davis, CA 95618.

Angela M. White, Research Wildlife Biologist, U.S. Department of Agriculture Forest Service, Pacific Southwest Research Station, Davis, CA 95618.

Robert L. Wilkerson, Staff Biologist, The Institute for Bird Populations, Point Reyes Station, CA 94956.

Geoffrey Williams, Ph.D. Student, Purdue University, West Lafayette, IN 47907.

Potter, Kevin M.; Conkling, Barbara L., eds. 2020. Forest health monitoring: national status, trends, and analysis 2019. Gen. Tech. Rep. SRS-250. Asheville, NC: U.S. Department of Agriculture, Forest Service, Southern Research Station. 189 p.

The annual national report of the Forest Health Monitoring (FHM) program of the Forest Service, U.S. Department of Agriculture, presents forest health status and trends from a national or multi-State regional perspective using a variety of sources, introduces new techniques for analyzing forest health data, and summarizes results of recently completed Evaluation Monitoring projects funded through the FHM national program. In this 19th edition in a series of annual reports, national survey data are used to identify recent geographic patterns of insect and disease activity. Satellite data are employed to detect geographic patterns of forest fire occurrence. Recent drought and moisture surplus conditions are compared across the conterminous United States. Data collected by the Forest Inventory and Analysis (FIA) program are employed to detect regional differences in tree mortality. Twenty years of national Insect and Disease Survey data are used to provide a retrospective medium-term analysis of insect and disease damage to forests across the United States. A new measure is described for detecting forest disturbance using high-frequency satellite data. Two recently completed Evaluation Monitoring projects are summarized, addressing forest health concerns at smaller scales.

Keywords—Change detection, drought, fire, forest health, forest insects and disease, tree canopy, tree mortality.

Scan this code to submit your feedback, or go to www.srs.fs.usda.gov/pubeval.

A copy of this report is available for download at www.srs.fs.usda.gov/pubs/.

Please direct inquiries about the availability of hard copies to pubrequest@fs.fed.us. Number of copies is limited to two per person.

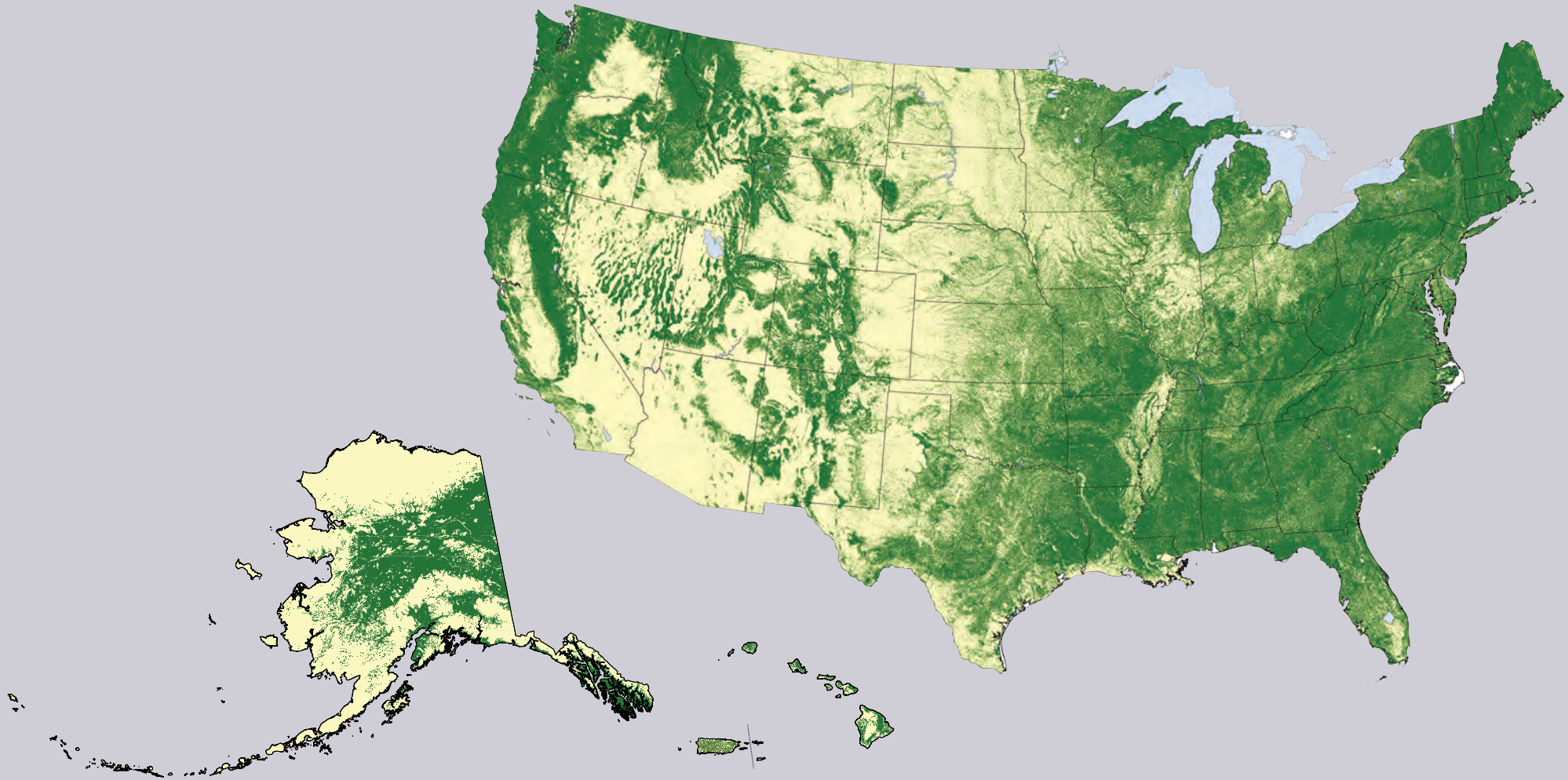

Forest Health Monitoring: National Status, Trends, and Analysis 2019

2020